Optimization
of Fischer-Tropsch Plant

A thesis submitted to The University of Manchester for the degree

of

Doctor of Philosophy

in

the Faculty of Engineering and Physical Sciences

Hyun-Jung Lee

2010

SCHOOL OF CHEMICAL ENGINEERING AND ANALYTICAL SCIENCE

ACKNOWLEDGEMENTS

LIST OF CONTENTS

Word count : 58131 words

LIST OF TABLES

LIST OF FIGURES

Optimization of Fischer-Tropsch Plant

ABSTRACT

Fischer-Tropsch synthesis is the technology for converting fuel feedstocks such as natural gas and coal into transportation fuels and heavy hydrocarbons. There is scope for research and development into integrated processes utilising synthesis gas for the production of a wide range of hydrocarbons. For this purpose there should be strategies for the development of Fischer-Tropsch processes, which consider both economic and technological feasibilities.

The aim of this study was to optimize Fischer Tropsch Plants in order to produce gasoline and gas oil by investigating the benefits of recycling & co-feeding of unconverted gas, undesired compounds, and lighter hydrocarbons over iron-based catalysts in order to save on capital and operating costs. This involved development of FT models for both two-phase and three-phase reactors. The kinetic parameters for these models were estimated using optimization with MATLAB fitting to experimental data and these models were then applied to ASPEN HYSYS flowsheets in order to simulate nine different Fischer-Tropsch plant designs.

The methodology employed involved qualitative modelling using Driving Force Analysis (DFA) which indicates the necessity of each compound for the Fischer-Tropsch reactions and mechanism. This also predicts each compounds influence on the selectivity of different products for both two-phase and three-phase reactors and for both pure feeding and co-feeding arrangements. In addition, the kinetic models for both two-phase and three-phase reactor were modified to account for parameters such as the size of catalyst particles, reactor diameter and the type of active sites used on the catalyst in order to understand and quantify their effects. The kinetic models developed can describe the hydrocarbon distributions consistently and accurately over large ranges of reaction conditions (480-710K, 0.5-2.5MPa, and H_2/CO ratio: 0.5-2.5) over an iron-based catalyst for once-through processes. The effect of recycling and co-feeding on the iron-based catalyst was also investigated in the two reactor types. It was found that co-feeding unwanted compounds to synthesis gas increases the production of hydrocarbons. This recycling and co-feeding led to an increase in H_2/CO feed ratio and increased selectivity towards C_5^+ products in addition to a slightly increased production of light hydrocarbons (C_1-C_4). Finally, the qualitative model is compared with the quantitative models for both two-phase and three-phase reactors and using both pure feeding and co-feeding with the same reactor conditions. According to the detailed quantitative models developed, in order to maximize hydrocarbon production pressures of 2MPa, temperatures of 450K and a H_2/CO feed ratio of 2:1 are required.

The ten different Fischer-Tropsch plant cases were based on Fischer-Tropsch process. FT reactor models were built in ASPEN HYSYS and validated with real FT plant data. The results of the simulation and optimization supported the proposed process plant changes suggested by qualitative analysis of the different

components influence. The plants involving recycling and co-feeding were found to produce higher quantities of gasoline and gas oil. The proposed heuristic regarding the economic scale of the optimized model was also evaluated and the capital cost of the optimized FT plant reduced comparison with the real FT plant proposed by Gerard. Therefore, the recycling and co-feeding to FT reactor plant was the best efficiency to produce both gasoline and gas oil.

DECLARATION

No portion of the work referred to in the thesis has been submitted in support of an application for another degree or qualification of this or any other university or other institute of learning.

Hyun-Jung Lee

September 2010

COPYRIGHT STATEMENT

i. The author of this thesis (including any appendices and/or schedules to this thesis) owns any copyright in it (the "Copyright") and she has given The University of Manchester the right to use such Copyright for any administrative, promotional, educational and/or teaching purposes.

ii. Copies of this thesis, either in full or in extracts, may be made **only** in accordance with the regulations of the John Rylands University Library of Manchester. Details of these regulations may be obtained from the Librarian. This page must form part of any such copies made.

iii. The ownership of any patents, designs, trade marks and any and all other intellectual property rights except for the Copyright (the "Intellectual Property Rights") and any reproductions of copyright works, for example graphs and tables ("Reproductions"), which may be described in this thesis, may not be owned by the author and may be owned by third parties. Such Intellectual Property Rights and Reproductions cannot and must not be made available for use without the prior written permission of the owner(s) of the relevant Intellectual Property Rights and/or Reproductions.

iv. Further information on the conditions under which disclosures, publication and exploitation of this thesis, the Copyright and any Intellectual Property Rights and/or Reproductions described in it may take place is available from the Head of the School of Chemical Engineering and Analytical Science.

NOMENCLATURE

A	Proportionality constant
C_i	Installed cost [$]
C_{im}	Cost of the installed module
C_{rj}	The capital cost of referred unit j at its referred size
C_t	Price of target year [$]
C_r	Price of reference year [$]
D_E	Effective dispersion coefficient
D_e	Effective diffusivity
D_G	Gas phase dispersion coefficient
D_m	Molecular diffusivity
D_r	Reactor diameter [m]
Ea	Activation energy [KJ/mol]
E_{cg}	Activation energy for chain growth [KJ/mol]
E_{met}	Activation energy for methane formation [KJ/mol]
E_p	Activation energy for paraffin formation [KJ/mol]
E_o	Activation energy for olefin formation [KJ/mol]
E_w	Activation energy for WGS reaction [KJ/mol]
F_c	The cost for common support system [$]
H	Henry's constant
K	Equilibrium constant
K_1	Equilibrium constant of the elementary reaction 2.64 for FTS [bar^{-1}]
K_2	Equilibrium constant of the elementary reaction 2.65 for FTS [bar^{-1}]
K_3	Equilibrium constant of the elementary reaction 2.74 for FTS [bar^{-1}]
K_4	Equilibrium constant of the elementary reaction 2.66 for FTS [bar^{-1}]
K_5	Equilibrium constant of the elementary reaction 2.78 for FTS [bar^{-1}]

N	Maximum carbon number of the hydrocarbons involved
P	Plant cost [$]
P(n)	Paraffin containing n carbons [mol]
P=(n)	Olefin containing n carbons [mol]
P_{CO}	Partial pressure of carbon monoxide [MPa]
P_{H2}	Partial pressure of hydrogen [MPa]
P_{H2O}	Partial pressure of water [MPa]
P_e	The Peclet number
P_r	Catalyst particle radius [m]
R	Ideal gas constant [J/molK]
R(n)	Alkyl propagating species containing n carbons [mol]
R"(n)	Alkenyl propagating species containing n carbons [mol]
R_{FTS}	Overall Fischer-Tropsch reaction rate [mol/g_{cat} h]
$SA'_1 SA'_2 SA'_3$	Catalyst parameters of active sites θ for the two-phase model
$SA'_{E1} SA'_{E2} SA'_{E3}$	Catalyst parameters of active sites θ and σ for experimental data
Tc	Total capital investment [$]
U	Average velocity
U_G	Space Velocity [1/s]
V_o	Total flow rate [m^3/s]
Z_{rs}	The size of a unit in step s used for calculation basis
c	Exponential factor of carbon number dependence
f_z	Multiplier used in the model for sensitivity analysis on plant capacity
i_f	Installation factor
k	rate constant [mol/h]
k_{cg}	rate constant of chain growth [mol/g s bar]
k_{co}	rate constant of CO_2 formation[mol/g s bar]
k_p	rate constant of paraffin formation [mol/g s bar]

k_o	rate constant of olefin formation [mol/g s bar]
k_{-o}	rate constant of olefin re-adsorption reaction [mol/g s bar]
k_i	Initiation rate constant for the alkyl mechanism [MPa^{-1}]
k_{i2}	Initiation rate constant for the alkenyl mechanism [mol/h]
k_p	Propagation rate constant for alkyl mechanism [h/mol]
k_{p2}	Propagation rate constant for alkenyl mechanism [h/mol]
k_{par}	Termination rate constant for alkyl mechanism yielding paraffin [MPa^{-1}h^{-1}]
k_{olef}	Termination by β-elimination rate constant for alkyl mechanism [h^{-1}]
k_{olef2}	Termination rate constant for alkenyl mechanism [h^{-1}]
k_{met}	Methane formation rate constant[MPa^{-1}h^{-1}]
k_{et}	Ethane formation rate constant [MPa^{-1}h^{-1}]
k_{O2}	Ethylene formation rate constant [h/mol]
k_t	Termination rate constant [mol/h]
m_f	Module factor
$m_{out\ i,s}$	Mass flow rate of component i leaving each step s
o	Fraction of offsite facilities with respect to plant cost
r	Overall rate [mol/h]
r_z	Size ratio
w	Fraction of working capital with respect to plant cost
w_n	Weight fraction of chains [-]
m_n	Mole fraction of hydrocarbon [-]

Greek letters

α	Chain growth probability factor
θco	Fractional surface coverage
θ	The activation site for primary FT reaction and secondary reaction of the participation into the chain growth of 1-olefins

η	The effectiveness factor
φ	Thiele modulus
λ	Active coefficient of ethene comparing to other olefins
σ	The active site for the secondary hydrogenation reaction of 1-olefins
ψ	The active site for the WGS reaction

Subscripts

exp	Experimental value
h	Hydrogenation reaction
m	Methane
n	Carbon number
o	Olefins
p	Chain propagation step
t	Termination step

ABBREVIATIONS

ASF	Anderson-Schulz-Flory
BBL	Barrel
BPD	Barrels per Day
CEPCI	Chemical engineering plant cost index
DFA	Driving Force Analysis
FBR	Fixed Bed Reactor
FTS	Fischer-Tropsch Synthesis
GHSV	Gas Hourly Space Velocity
GTL	Gas-To-Liquids
HTFT	High Temperature Fischer-Tropsch
ISBL	In Side Battery Limits
LHHW	Langmuir-Hinshelwood-Hougen-Watson
LTFT	Low Temperature Fischer-Tropsch
MMSCFD	Million Standard Cubic Feet per Day
PFR	Plug flow reactor
POX	Partial oxidation
RDS	Rate determining step
RKS	Redlich Kwong Soave equation
ROI	Return on Investment
SD	Surface Diffusion
SBR	Slurry Bed Reactor
SMDS	Shell Middle Distillate Synthesis
SPD	Slurry phase distillation
SR	Side Reaction
SSPD	Slurry Bubble Column Reactor
VLE	Vapour Liquid Equilibrium
WGS	Water Gas Shift

GLOSSARY

MATLAB   a mathematics computer software

Aspen HYSYS   a simulation package

BRIST   a qualitative modelling methodology

Dedicated to

my dearest parents and brother

1

Introduction: Fischer-Tropsch Process

1.1 OVERVIEW

There has been significant interest in the development of technologies for converting fuels like natural gas and coal into more readily transportable liquid fuels at reasonable operating conditions. One important method for producing to liquid fuels is Fischer-Tropsch synthesis (FTS).

The reaction of synthesis gas consisting of hydrogen and carbon monoxide, over an iron catalyst to form hydrocarbon and oxygenated products was discovered by German scientists, Fischer.F and H.Tropsch working at the Fuel Research Laboratories of the Kaiser Wilhelm Institute for Kohlenforschung in the 1920's (F.Fischer and H.Tropsch 1923). This reaction was used by Hans Fischer and Franz Tropsch to make fuels during World War II and they spent the next several years attempting to increase the yield of hydrocarbons. However, Germany was not alone in its efforts to commercialize the Fischer-Tropsch synthesis and there has been continued interest world-wide in Fischer-Tropsch technology ever since. The US Bureau of Mines began to study this process in the late 1920's (Anderson 1984) and continued with development work for more than forty years. In particular, studies carried out during the 1940's resulted in the development of a widely accepted overall kinetic model and detailed models of chemical selectivity. The Bureau of Mines' efforts focused on the use of fused iron catalysts, but also included evaluation of precipitated iron and cobalt catalysts. Several facilities are continuing to study the iron-based Fischer-Tropsch synthesis (Bechtel 1990; Shell 2001). Current research interests focus on the development of slurry reactor

processes, which offer excellent temperature control, high single-pass conversion, and flexible operating conditions. Slurry reactor research, including new catalyst development, is also ongoing at SASOL (South African State Oil) and in Germany and Japan (Gerard 1999).

There are currently three main points of consideration, concerning the Fischer-Tropsch process. Firstly, there is the mechanism of the Fischer-Tropsch reaction, the details of which are still not fully understood. In addition, from the perspective of chemical engineering, there is the design and scale-up of the commercial Fischer-Tropsch synthesis reactor and plant in which studies of the kinetic models play an important role. To reach the ideal performance of the Fischer-Tropsch process, an accurate comprehensive kinetic model which can describe the product distribution of Fischer-Tropsch synthesis is required. Lastly, there is the economic point of view, and potential processes are required to be operated on a large scale. Fischer-Tropsch(FT) process developers typically constructed FT plant costing in the order of $400M (Davis 2005). Vosloo pointed out that, in order to make the GTL technology more cost effective, the focus must be on reducing both the capital and operating cost of the Fischer-Tropsch plant (Vosloo 2001).

These developments of the Fischer-Tropsch process are the result of work carried out by many industrial and research institutes interested in the process including those exploiting the process commercially. For example, although SASOL and Shell have experience using their Fischer-Tropsch technologies on commercial scale for several years, the Fischer-Tropsch process is still subject to further development. EXXON has also proven its technology in pilot plants and is ready to practice it on commercial scale (Eisenberg et al., 1998) and Williams Energy, Syntroleum, Statoil, and Rentech each claim to have their own technologies (Wilson and Carr, 1999; Benham and Bohn, 1999). FT fuels will lessen the dependence on foreign oil and reduce environmental impacts. Also, due to the high quality of the transportation fuels derived from the Fischer-Tropsch process, the product oil should fetch a higher price than crude oil-derived fuels. At crude oil prices of $16-18 per barrel it was estimated that the FT-derived oil could fetch $22-25 per barrel (Jager 1997).
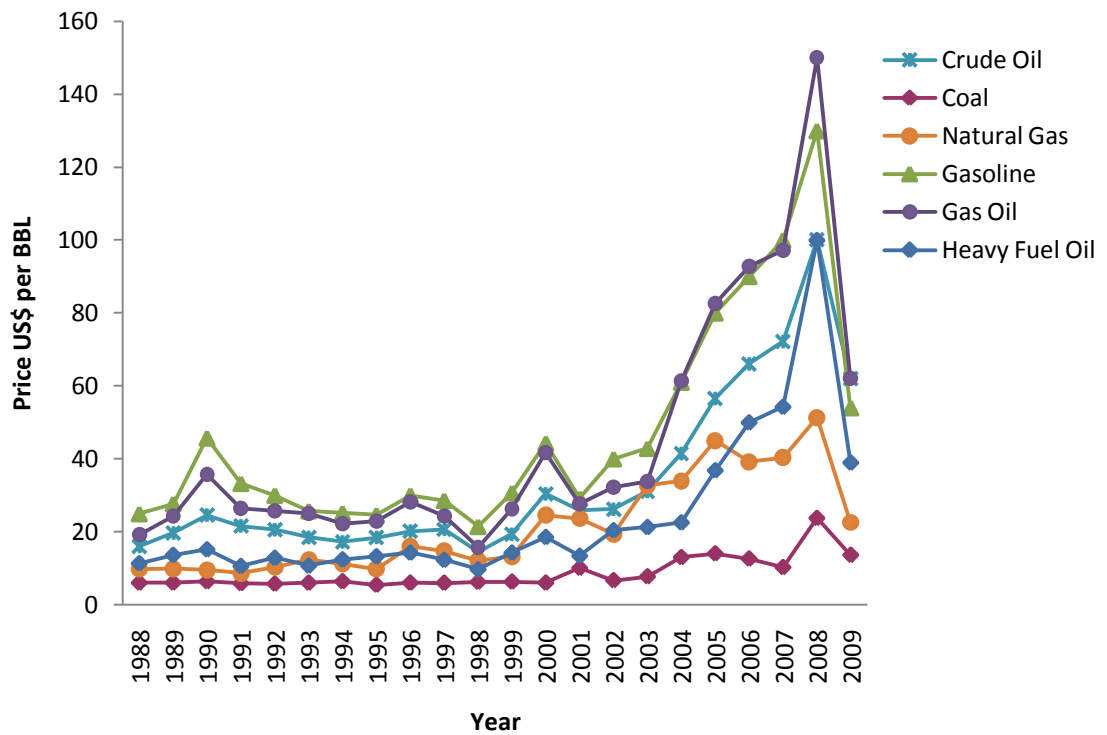
FIGURE 1.1 Product prices of Oil and Gas (BP 2010)

An overview of oil prices from 1988 to 2009 is given in Figure 1.1 (BP 2010). These prices are shown to rapidly increase after 2002 and reached a peak in 2008. There is also a small increase in 1990 when Iraq invaded Kuwait and the oil prices showed a slight decline due to the Asian financial crisis at end of 1990s. The prices then rapidly increased due to the influence of the invasion of Iraq in 2003. From this data it can be seen that there is only a small gap between the prices of crude oil feedstock and gasoline or gas oil products. So, if gasoline and gas oil are produced using crude oil as feedstock, the plant yields little profit due to the high cost of the crude oil. However, this data also suggests that natural gas could be considered as a promising feed material because it is less expensive than crude oil. Even though coal is the cheapest feedstock as shown in Figure 1.1, the capital and operating costs of the reforming unit for coal are more expensive than those for natural gas and crude oil. The most striking observation to emerge from this data comparison is that the price of natural gas is much lower than the prices of both gasoline and gas oil as shown in Figure 1.1. Therefore, to maximize profits, this analysis implies that natural gas should be used as feedstock and this should be used to produce gasoline and gas oil.

The high demand for inexpensive feedstocks causes increasing prices of those in industry but also encourages research to further develop the Fischer-Tropsch process. Many companies have successfully launched Fischer-Tropsch process technology on a commercial scale.

Company	Scale [KBBL/Day]	Actual Capital Cost	Year	Connected Capital Cost (2009) [STD 45KBBL/Day]	Comments
Shell	12.5	$850 M	1993	$4671.8 M	SMDS process
Bechtel	8.8	$415 M	1996	$3048.9 M	Combined cycle plant
SASOL	20	$550 M	1998	$1742.4M	GTL, Slurry phase reactor
Joint venture (Qatar Petroleum & SASOL)	34	$900 M	2006	$1307.6 M	GTL complex Liquid production No hydrocracking
Joint venture (Qatar Petroleum & SASOL)	130	$3600 M	2010	$1246.2 M	GTL facility SPD process

TABLE 1.1   Comparison of Capital Costs in commercial FT plant (Gerard 1999)
* US$ STD in present

Table 1.1 compares the capital costs of FT plants for a number of different companies. The capital cost is also calculated for a standard 45K BBL per day according to the equation of Plant Cost Indices Data (refer to Appendix A) in order to compare the different plants. In 1993, Shell started up the Shell Middle Distillate Synthesis (SMDS) process that produced heavy paraffins in multitubular trickle bed reactors at a plant based in Bintulu, Malaysia. The plant converts natural gas by non-catalytic partial oxidation. Unfortunately this plant also had high capital costs due to the multitubular reactor design and the high costs of using many tubes. In 1996, Gerald et al. reported the design and economics of a commercial FT plant using natural gas as the feedstock by Bechtel Corporation in San Francisco, USA. Also, SASOL in 1998 used the new complex; gas to liquid (GTL) plant based on the Slurry Phase Distillate Process (SSPD) technology from SASOL. The synthesis gas of the plant is produced with coal gasifiers. As mentioned earlier, the price of coal is

cheaper than other feedstocks but, the process of coal gasification is quite expensive, meaning the capital cost of the SASOL plant is quite high. In another modern GTL facility, Qatar petroleum and SASOL are working together in a joint venture using a Slurry Phase Distillate (SPD) process. Unlike the other places mentioned, Qatar has 15.2 billion barrels of proven oil reserves, so in addition to exporting most of their crude oil to Asia, Qatar Petroleum (Oil & Gas Journal) also develops GTL plants such as the Fischer-Tropsch plant. As shown in Table 1.1, the capital cost of whole FT plant is gradually decreasing when compared at the same plant scale(45K BBL per day); however the capital cost of an FT plant is still expensive and complex. According to Clarke (Clark 1951), "The FT route has the potential to become a major processing route, but built on the back of the existing refinery and therefore using existing facilities, infrastructure and technologies to keep costs down." Therefore, reducing the cost of the Fischer-Tropsch process will have a large impact on the economics. Choi et al. (Choi, Kramer et al. 1996) gives a capital cost breakdown of the three individual process sections for a 45K BBL per day FT plant in Figure 1.2.
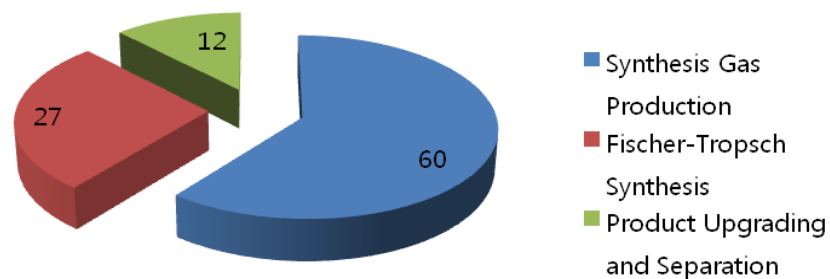
FIGURE 1.2   The capital cost breakdown of a general Fischer-Tropsch plants (Choi, Kramer et al. 1996; Vosloo 2001).

1.2 FISCHER-TROPSCH PROCESS

The Fischer-Tropsch synthesis process collectively refers to the process of converting synthesis gas into liquid hydrocarbons using a metal catalyst. The FTS process can be used to produce liquid transportation fuels such as gasoline, diesel and other chemicals.

The standard Fischer-Tropsch plant process involves three main sections, namely: synthesis gas production, Fischer-Tropsch synthesis and product upgrading and separation. High value added products are usually obtained by upgrading the FT products with well established refinery processes, such as hydrocracking and isomerisation. Figure 1.3 shows a block diagram of the overall Fischer-Tropsch plant configuration. These are described in more detail below.

Synthesis Gas Production

Coal

Natural Gas

Gasifier ← Steam O$_2$ → Partial Oxidation

Steam Reforming

Synthesis gas cooling Purification

Fischer-Tropsch Synthesis

Steam Reforming

Fischer-Tropsch Synthesis

Steam

Oxygenates

Product Recovery

Fuel Gas (LPG)

C$_2$H$_4$

C$_3$H$_6$

Product Stream & Upgrading

Hydrocarbon Upgrading:

-. Hydrocracking

-. Isomerization

Pentene/hexane

Naphtha

Diesel

Waxes

FIGURE 1.3 Overall process scheme of a Conventional Fischer-Tropsch plant

As can be seen from Figure 1.3, there are FT processes using both natural gas or coal as feedstock and many countries have large reserves of cheap gas or coal which can be converted into high value liquid products.

Synthesis gas production and product upgrading rely on established technologies. Synthesis gas manufacturing is widely applied in the production of methanol and ammonia. Future developments are expected in the field of catalytic partial oxidation and in membrane techniques for oxygen purification (venkatarama et al., 2000). Product upgrading processes originate directly from the refining industry and are highly optimized.

The FT process could be improved in several areas to reduce the costs. The production of a range of compounds indicates that the synthesis might be used to supply several chemical feedstocks, but it also requires extensive product upgrading and separation system for the product stream.

Reflecting on the FT process, the high investment costs of the whole process, in the absence of special circumstances requires negative value feedstock to achieve attractive overall economics. Low quality residual oil, of course, has a low or even negative value. As can be seen from the Figure 1.1, the price of crude oil is close to that of the products and there is only little profit giving a low value to the residual oil which could become negative if the processing becomes too expensive. In addition, because of the expensive coal gasifiers involved in the synthesis gas production unit, the capital costs are quite large in spite of the low price of the coal feedstocks due to the costs associated with materials handling. The product upgrading and separation section also has high capital costs and requires a big investment because a hydrogen production facility is required to supply hydrogen and because high hydrogen partial pressure is required in this unit. To reduce the high capital cost of the whole process, many researchers (Carlson and Daniel 1989; Sie and Krishna 1999; Peter, Diane et al. 2006; Schweitzer and Viguie 2009) have presented new process methods for reducing costs such as recycling system to reformer and co-feeding of unreacted CO and H_2.

In regard to the operating cost for the whole process, the main areas of energy loss from the process are the synthesis gas production and synthesis gas conversion sections. The reformer combination is responsible for about 45% and

the Fischer-Tropsch section for about 50% of the energy losses from the plant. Approximately 50% of the energy loss from the Fischer-Tropsch plant is due to condensing of the reaction water produced by the Fischer-Tropsch reaction and the balance results from the inefficiency with which energy is recovered from the relatively low pressure steam.

Consequently, the capital and operating cost of synthesis gas production and product upgrading & separation systems are extremely expensive. Therefore, any cost reduction in both feed stream production and upgrading of the product stream is most beneficial and will have a large impact on the economics. A high selectivity of the FT process to desired products is of utmost importance to the overall economics. Although the Fischer-Tropsch plant has been optimized for some applications, from the economical points of view opportunities do exist to decrease the capital and operating costs by re-optimizing the Fischer-Tropsch process. In order to have the greatest impact on the economics of the process, proposed change should be made in areas that decrease the capitals and operating costs of synthesis gas production and upgrading & separation units and improving the thermal efficiency of the plant as a whole.

1.2.1 SYNTHESIS GAS PRODUCTION

Synthesis gas is a mixture that contains various amounts of CO and H_2, which can be produced by gasifying feedstocks at high temperatures. Common feedstocks are natural gas (80%) on the one hand, and naphtha and coal (20%) on the other.

Three basic methods of converting a feed stream into synthesis gas exist, i.e. reforming, partial oxidation, and catalytic partial oxidation. In all cases, a near to equilibrium synthesis gas mixture is obtained where the H_2/CO ratio can be adjusted via the water gas shift reaction. The most important reactions for methane are:

$$\text{Steam reforming} \qquad CH_4 + H_2O \leftrightarrow CO + 3H_2 \qquad (1.1)$$

$$\text{Partial oxidation} \qquad CH_4 + 0.5O_2 \leftrightarrow CO + 2H_2 \qquad (1.2)$$

$$\text{Water gas shift reaction} \qquad CO + H_2O \leftrightarrow CO_2 + H_2 \qquad (1.3)$$
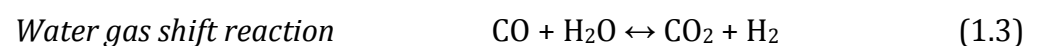
In reforming, the feed stream is passed over a Ni-based catalyst together with H_2O and/or CO_2 at high temperature (1073-1173K) and medium pressure (10-30bar). Steam reforming and autothermal reforming hold the leading positions among commercial processes in synthesis gas production for the synthesis of methanol and ammonia.

The partial oxidation process involves an intimate coupling of several complex chemical reactions which produce synthesis gas. The mechanism is an exothermic reaction that consists of a number of steps reacting the carbon feedstock with oxygen. This reaction has a number of advantages: it has a quick response time, high reaction efficiency and can generate hydrogen without a catalyst. Nevertheless, the disadvantages of this process are that it requires a high operating temperature and a high fuel/air ratio for the combustion reaction to proceed, and at the end of reaction (Jin 2004). The synthesis gas from industrial partial oxidation has a low H_2/CO ratio ($H_2/CO=0.5-2$) (Kamm, Charleston et al. 1979).

In Catalytic partial oxidation the catalyst takes over the function of the flame in partial oxidation. The advantages of catalytic partial oxidation of methane over steam reforming of methane are the low exothermicity of the process and the high reaction rates, leading to significantly smaller reactors. Although catalytic partial oxidation is a promising process for the production of H_2-rich gas for small scale fuel-cell applications, it is still awaiting a commercial breakthrough (De Smet, 2000).

It can be seen from the data in Figure 1.2 that the major component of the FTS process is the synthesis gas production unit which represents 60 percent of whole plant cost. Therefore, reducing the cost of synthesis gas product unit should significantly decrease the overall process capital cost.

1.2.2 FISCHER-TROPSCH SYNTHESIS

The primary Fischer-Tropsch reactions are represented in the following equations,

$$nCO + (2n + 1)H_2 = C_nH_{2n+2} + nH_2O \tag{1.4}$$

$$nCO + 2nH_2 = C_nH_{2n} + nH_2O \tag{1.5}$$

$$C_nH_{2n} + H_2O = C_nH_{2n+2}O \qquad (1.6)$$
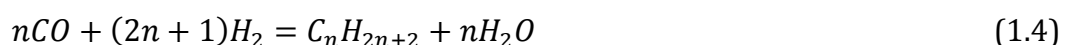
Equation 1.4 relates to the production of paraffins and Equation 1.5 to the production of olefins. Alcohol products (Eq. 1.6) can also be formed either as by-products or as main product depending on the catalytically active metal and the pressure. In addition to these reactions, there are also some side reactions. Catalyst selectivity, synthesis gas composition and process conditions govern the product distribution and the limit of the paraffinic chain length. In addition, the Fischer-Tropsch reactions are highly exothermic. Therefore, the heat generated by the reaction needs to be removed rapidly in order to avoid temperature increases which would result in the undesired formation of high levels of methane and light hydrocarbons. Also, in extreme cases high temperatures can lead to catalyst deactivation due to coking and sintering and catalyst disintegration due to Boudouard carbon deposition (Eq. 1.7) (Dry 1981).

$$2CO \rightarrow C + CO_2 \qquad (1.7)$$

The mix of products depends on reactor temperature, pressure, feed gas composition (H_2 to CO ratio), and the types of catalysts and promoters used. Depending on the types and quantities of FT products desired, either low (473-513K) or high temperature (573-623K) synthesis is used with either a cobalt or iron catalyst respectively. Low temperature synthesis yields high molecular weight waxes while high temperatures produce gasoline and low molecular weight olefins such as ethylene and propylene. <u>Production of gasoline products is highest under conditions of high temperatures using an iron catalyst in a fixed fluid bed reactor</u> and the theoretical maximum conversion for carbon is 48% of the synthesis gas for a once-through system. Production of diesel fractions is maximized in a slurry reactor using low temperatures and a cobalt catalyst with maximum yield of about 40% (Dry 1996).

The most active metals for the Fischer-Tropsch synthesis are iron, cobalt and ruthenium (Anderson 1984; Schulz 1995). Iron catalysts generally consist of precipitated iron, which is promoted with potassium and copper to obtain a high activity and selectivity, and the catalysts formed are also active for the water-gas shift reaction. Cobalt catalysts are usually supported on metal oxides due to the higher cobalt price and better catalyst stability. The water gas shift activity of Co-

based catalysts is low and water is the main oxygen containing reaction product. Ruthenium catalysts are the most active Fischer-Tropsch catalysts. A high molecular weight wax is obtained at reaction temperatures as low as 423K. However, the high price of ruthenium excludes its application on industrial scale and the use of Ru-based catalysts for the Fischer-Tropsch synthesis is limited to academic studies.

Fischer-Tropsch reactor designs have focused on heat removal and temperature control. Insufficient heat removal leads to localized overheating which causes high carbon deposition and subsequent deactivation of the catalyst. The fixed bed tubular reactor design has been used for many years and contains many tubes filled with iron catalyst immersed in boiling water for heat removal. The water bath temperature is maintained in the reactor by controlling the pressure. Synthesis gas is introduced into the top of the reactor that is operated at 20-30bar and at an operating temperature of 473-623K. Additional temperature control is achieved by using high gas velocities and gas recycling. Another reactor design, the low temperature slurry reactor is a three-phase reactor consisting of a solid catalyst suspended and dispersed in a high thermal capacity liquid (often the FTS wax product). Synthesis gas is bubbled through the liquid phase achieving contact with the catalyst while also keeping the catalyst particles dispersed. Slurry reactors are optimized at low temperatures for FTS wax production with low methane production. Compared to other reactors, liquid slurry bed reactors have better temperature control, lower catalyst loading and significantly lower catalyst attrition rates. The improved isothermal conditions in slurry bed reactors allows for higher average reactor temperatures leading to excellent conversion of synthesis gas to products. Compared with multi-tubular fixed bed reactors, slurry reactors have lower pressure differences across the reactor resulting in lower costs. However, any poisons in the synthesis gas will affect all of the catalyst in the reactor, whereas in a fixed tube design, they will primarily affect only the catalyst near the gas inlet. These slurry reactors are beginning to be used in commercial applications.

1.2.3 PRODUCT STREAM AND UPGRADING

As the product mix exits from a standard FTS reactor, it contains a wide range of olefins (alkenes, C_nH_{2n}), paraffins (alkanes, C_nH_{2n+2}), oxygenated products (i.e., alcohols, aldehydes, acid and ketones), and aromatics with water as a by-product. The product stream can also be defined as various fuel types: LPG (C_3-C_4), gasoline/naphtha (C_5-C_{12}), diesel fuel (C_{13}-C_{17}), and jet fuel (C_{11}-C_{13}; Kerosene). The definitions and conventions for the composition and the names of different fuel types are obtained from crude oil refining terminology. The products from FTS are higher value because diesel fuel, jet fuel, and gasoline are low in sulphur and aromatics. In addition, the FTS diesel fuel has a high cetane[1] number. The C_9-C_{15} olefins are very suitable for the production of biodegradable detergents, whereas the paraffins make excellent lubricants. These products of the Fischer-Tropsch process are based on industrial materials suitable for e.g. food applications, cosmetics & medicines. High selectivities towards fuels are obtained through hydrocracking[2], which is a selective process converting heavy hydrocarbons into lights hydrocarbons in the C_4-C_{12} range with small amounts of C_1-C_3. This directly produces a high quality gas oil (high cetane index, low sulphur content, low aromatics) and kerosene (high paraffin content), which are very suitable as blending components to upgrade lower quality stock. The linearity of the Fischer-Tropsch naphtha is a drawback for gasoline production. The naphtha is therefore better used as feedstock for the petrochemical industry. Its high paraffin content makes the naphtha an ideal cracker feedstock for ethylene and propylene production.

Product selectivity can be improved using multi-step processes to upgrade the FTS products. Upgrading involves a combination of hydrotreating, hydrocracking, and hydroisomerization in addition to product separation. Where, hydrotreating involves adding hydrogen and a catalyst to remove impurities like nitrogen, sulphur, and aromatic hydrocarbons. Hydrocracking is a catalytic

---

[1] Cetane: Is actually the measure of a fuel's ignition delay; the time period between the start of injection and the start of combustion (ignition) for the fuel. In a particular diesel engine, higher cetane fuels will have shorter ignition delay periods than lower cetane fuels. Cetane numbers are only used for relatively light distillate diesel oils.
[2] Hydrocracking: the process whereby complex hydrocarbons are broken down into light hydrocarbons by the breaking of carbon-carbon bonds in the precursors.

cracking process assisted by an elevated partial pressure of hydrogen gas and hydroisomerization involves the addition of hydrogen and a catalyst to drive isomerization processes.

As mentioned above, most upgrading units are considered to produce desired hydrocarbons, however the products from the Fischer-Tropsch synthesis will typically comprise hydrocarbons, waxes, alcohols, and undesired products such as unreacted synthesis gas and lighter hydrocarbons. These undesirable products can be recirculated to the reformer or to the Fischer-Tropsch reactor. This recycling process is one method of upgrading and it increases the synthesis gas yield. Additionally, recirculated olefins and alcohols in the Fishcer-Tropsch reactor feed will readsorb and form longer chain compounds. This can also lead to higher overall conversions (Raje and Inga 1997). The recycling process can be characterized by the feed location where the undesired compounds from C_1 to C_4 are recycled to: either used as co-feed to the Fischer-Tropsch reactor, or else converted to synthesis gas.

1.3   THESIS STRUCTURE

This thesis consists of eight chapters, starting with this first chapter, which introduces the background to the research and includes objectives and framework of this study.

In chapter 2, relevant literature on the reactions and kinetics of the Fischer-Tropsch synthesis are reviewed, followed by its processes and a discussion on its special characteristics. This literature review is focused on the major aspects of the Fischer-Tropsch mechanism which are discussed in detail. Chapter 3 describes the qualitative modelling of the Fischer-Tropsch reactions for both two-phase and three-phase reactors. Chapter 4 presents the development process for a Fischer-Tropsch plant. Firstly, the Fischer-Tropsch reactor models are proposed using MATLAB, the mathematical programming language. The Base case models for kinetic modelling of the Fischer-Tropsch synthesis over an iron based catalyst and, the influence of these different cases modelled on the product selectivity and the different reaction kinetics obtained are presented in this chapter. Furthermore, these case models developed for the Fischer-Tropsch synthesis are used to predict the product selectivity for simulations of co-feeding over an iron based catalyst. Next, the plant processes are modelled and simulated using the ASPEN HYSYS computer simulation tool. The results and discussions for modelling and simulation of Fischer-Tropsch synthesis are presented in Chapter 5 and 6, respectively. The economic impacts of the Fischer-Tropsch simulation models considered in Chapter 6 are evaluated in Chapter 7. Finally, the conclusions of this study and recommendations for further research are presented in Chapter 8.

2

Literature Review: Fischer-Tropsch Synthesis

2.1 FISCHER-TROPSCH MECHANISMS

A considerable quantity of literature has been published on the Fischer-Tropsch reaction mechanism. These studies, however, have not fully understood the reaction mechanism of the Fischer-Tropsch synthesis. The major problem describing the Fischer-Tropsch reaction kinetics is the complexity of its reaction mechanism and the large number of species involved. Despite of this complexity, there have been several attempts made to investigate the Fischer-Tropsch reaction mechanism; the earliest mechanism proposed by Fischer and later refined by Rideal (Rideal 1939) involved surface carbides[3]. The progressive work of Fischer and Tropsch in the 1920s showed that hydrocarbon chain formation proceeds via the stepwise addition of one carbon atom at a time. Over the past 20 years a great deal more information has become available describing the application of various sophisticated surface analytical techniques and experiments. The general consensus from these experiments has been that carbene (-CH$_2$) species are involved in the chain growth mechanism with CO insertion accounting for the formation of oxygenates (Sachtler 1984; Bell 1988). There are many apparently different mechanisms reported (Dry 1981; Dry 1990). Since Anderson's research in 1956, most studies have assumed a simple polymerization reaction for the hydrocarbons yield. It is widely accepted that the Fischer-Tropsch reaction is

---

[3] Carbides: a compound of carbon with a weaker electronegative element. Carbides are important industrially; for example calcium carbide is a feedstock for the chemical industry and iron carbide, Fe$_3$C (cementite), is formed in steels to improve their properties.

based on polymerization of methylene units, which was originally proposed by Fischer and Tropsch (Fischer and Tropsch 1923). Another widely accepted theory maintains that the initiation of the Fischer-Tropsch reaction involves the adsorption and dissociation of CO on to catalyst sites. The absorbed and dissociated CO on the catalyst surface reacts with hydrogen to form the surface methyne and methylene which are the monomers of the overall polymerization reaction (Fernandes 2005). Generally, two major mechanisms have been proposed for the Fischer-Tropsch reactions.

Through the dissociation of CO and H_2 and the formation of water, the Fischer-Tropsch reaction follows the steps of a polymerization reaction (Spath and Dayton 2003; Fernandes 2005): (1) chain initiation, (2) chain growth, (3) chain termination, (4) re-adsorption and (5) water shift gas (WGS) reaction.

2.1.1   CHAIN INITIATION

Table 2.1 shows the primary reaction mechanisms for both adsorption and hydrogenation of the Fischer-Tropsch synthesis. Chain initiation is through both associative and dissociative adsorption of CO (Reaction 2.1 in Table 2.1). Hydrogen molecules react either in molecular state or via dissociative adsorption (2.3). CH-s(Monomer-s refers to the adsorbed species) is formed through the combination of C-s and H-s and similarly CH_2-s is formed by combining H-s and CH-s and so on with CH_3-s is formed using CH_2-s and H-s.

The diagram accompanying the carbide mechanism proposed by Schulz and Beck et al in 1988 included only a single bond for each carbon atom. However, carbon has four electrons available to form covalent chemical bonds, so the figure by Schulz and Beck et al. is modified to give four carbon bonds (Schulz, Beck et al. 1988). The mechanism emerged from the investigation of Eliason and Bartholomew determining the kinetics of deactivation of Fe and Fe-K catalysts for fixed bed reactor as a two-phase reactor. The CH_3-s formation mechanism including Eqn. 2.1-2.5 proposed by Eliason and Bartholomew(1999) is similar to the mechanism proposed by Schulz and Beck et al.(1988) except for reaction 2.4.

	mechanisms	no.
	$-C \equiv O \longrightarrow$ $\overset{C \equiv O}{\big\vert}$	(2.1)
Carbide mechanism (Schulz, Beck et al. 1988)	$\overset{C \equiv O}{\big\vert} \longrightarrow \overset{=C - O}{\big\vert}$	(2.2)
	$H\text{-}H \longrightarrow \overset{H \; H}{\big\vert \; \big\vert}$	(2.3)
	$\overset{C}{\big\Vert} + \overset{H}{\big\vert} \longrightarrow \overset{C\,H}{\big\Vert} + \overset{H}{\big\vert} \longrightarrow \overset{C\,H_2}{\big\vert}$	(2.4)
CH$_3$-s formation (Eliason and Bartholomew 1999)	$\overset{C\,H_2}{\big\Vert} + \overset{H}{\big\vert} \longrightarrow \overset{C\,H_3}{\big\vert}$	(2.5)
Formate mechanism (Wang and Ma 2003)	$-C \equiv O + \overset{H}{\big\vert} \longrightarrow \overset{\overset{H}{\big\vert}}{\underset{\big\vert}{C} =O}$	(2.6)

Table 2.1 Chain initiation mechanisms for the Fischer-Tropsch synthesis.

In addition, the formate mechanism of Yi-Ning Wang et al.(2003) was systematically developed including detailed kinetics and was indicated that rate expressions for FTS reactions are based on the carbide polymerization mechanism and for the WGS reaction the expression is based on the formate[4] mechanism (2.6). The reaction 2.6 is the important monomer to convert oxygenates such as alcohols and acids. Jun Yang and AN Fernandes assumed that the rate determining steps are steps 2.1-2.4. Therefore, the adsorption mechanisms of hydrogen and carbon monoxide are included in chain initiation step and the monomers of -CH$_2$ and -CH$_3$ are also regarded as mechanisms of chain initiation. In addition, the formate mechanism from Yi-Ning Wang et al. should be considered the first monomer for the production of oxygenates.

---

[4] Formate: the ion CHOO$^-$ or HCOO$^-$ (formic acid minus one hydrogen ion)

2.1.2 CHAIN GROWTH

Chain growth continues through the addition of methylene units to give alkyl intermediates or through the addition of alkyl species, R-CH₂.

Reaction 2.7 of Schulz and Beck et al.(1988) is based on the monomer -CH₂. Chain growth of Yi-Ning Wang et al.(2003a) only has a formation of ethylene(2.8 and 2.9) and Jun Yang et al. (2004a) proposed that the ethyl chains form (2.10 and 2.11) and that leads to produce two types of olefins-s and paraffins-s to grow hydrocarbon chain(2.12) in Table 2.2. The alkyl mechanism from AN Fernandes(2005) does not form ethylene because the propagation species that could form ethylene, $-CH_2 - CH_3$, has a stable methyl group $(-CH_3)$ at the end of the chain that will not donate one of its hydrogens in order to generate the double bond between the two carbons of the propagating species. This problem does not affect longer alkyl propagation species such as propyl groups chains, $-CH_2 - CH_2 - CH_3$, which have a less stable intermediate $-CH_2 -$ that can more easily donate its hydrogen to form a double bond resulting in an olefin $(CH_2 = CH - CH_3)$.

	mechanisms	no.
Carbide mechanism (Schulz, Beck et al. 1988)		(2.7)
Carbide polymerization mechanism (Wang and Ma 2003)		(2.8)
		(2.9)

Jun Yang (Yang 2004)

$$CH_2- \;\; + \;\; CH_2- \;\; \longrightarrow \;\; \begin{array}{c} CH_2- \\ | \\ CH_2 \end{array} \tag{2.10}$$

$$CH_2- \;\; + \;\; C_nH_{2n}- \;\; \longrightarrow \;\; \begin{array}{c} C_nH_{2n}- \\ | \\ CH_2 \end{array} \tag{2.11}$$

$$C_nH_{2n}- \;\; + \;\; H \;\; \longrightarrow \;\; \begin{array}{c} C_nH_{2n+1} \\ | \\ CH_2 \end{array} \tag{2.12}$$
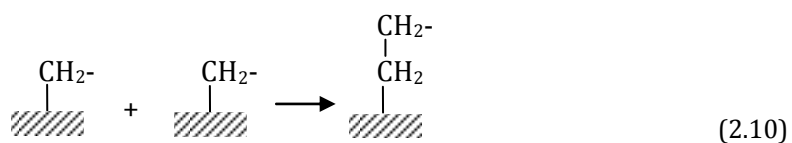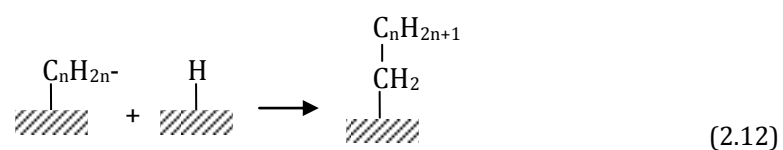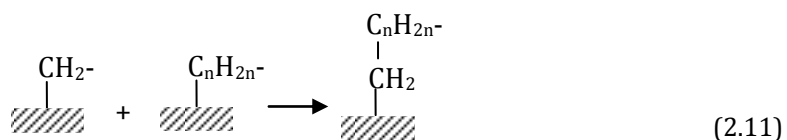
Polymerization (Fernandes 2005)

$$R \;\; + \;\; CH_2- \;\; \longrightarrow \;\; CH_2- R \tag{2.13}$$

$$CH_2 \;\; + \;\; CH \;\; \longrightarrow \;\; \begin{array}{c} CH_2 \\ \| \\ CH \end{array} \;\; + \;\; H \;\; H \;\; \longrightarrow \;\; R \tag{2.14}$$

$$\begin{array}{c} CH_2 \\ \| \\ CH \;\; CH_2 \end{array} \longrightarrow \begin{array}{c} CH_2 \\ \| \\ C\,H \\ | \\ C\,H_2 \end{array} \longrightarrow \begin{array}{c} CH_3 \\ | \\ C\,H \\ \| \\ C\,H \end{array} \longrightarrow \begin{array}{c} R \\ | \\ C\,H \\ \| \\ C\,H \end{array} \tag{2.15}$$

$$\begin{array}{c} R \\ | \\ C\,H \\ \| \\ C\,H \end{array} \longrightarrow \begin{array}{c} R \\ | \\ C\,H \\ \| \\ C\,H \;\; CH_2 \end{array} \longrightarrow \begin{array}{c} CH- R \\ | \\ C\,H \\ \| \\ C\,H_2 \end{array} \tag{2.16}$$

$$\begin{array}{c} R \\ | \\ C\,H_2 \\ | \\ C\,H \\ \| \\ CH \end{array} \tag{2.17}$$

Bo-Tao et al.(2006)

$$CH_3 \ + \ CH_2 \ \longrightarrow \ C\,H_2CH_3 \ + \ CH_2 \ \cdots \ \left[R \right]_n \qquad (2.18)$$

$$\begin{array}{c} \overset{H}{\underset{|}{C}} =O \ + \ CH_2 \\ \overset{|}{C} =O \ + \ CH_3 \end{array} \longrightarrow \ C\,OCH_3 \ + \ CH_2 \ \cdots \ \left[COR \right]_n \qquad (2.19)$$
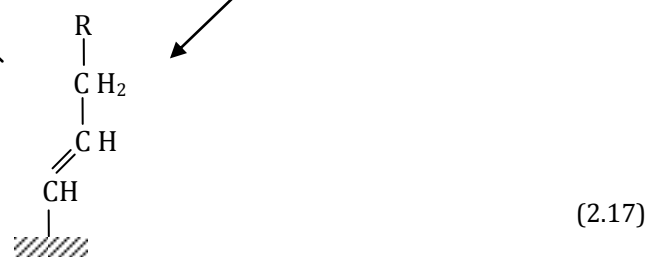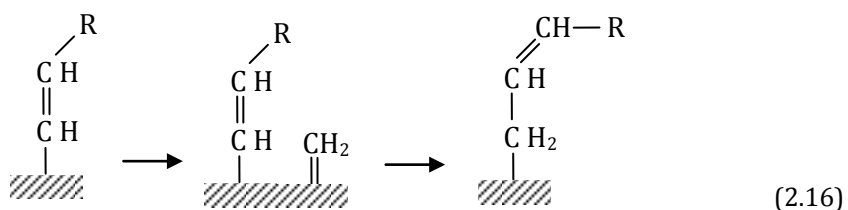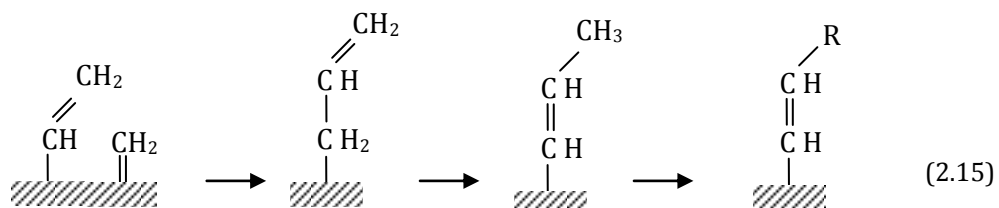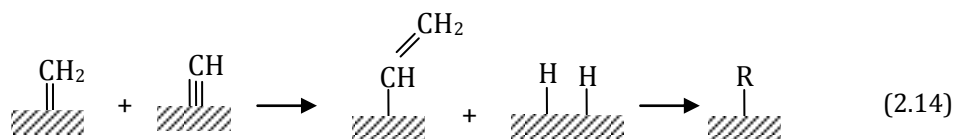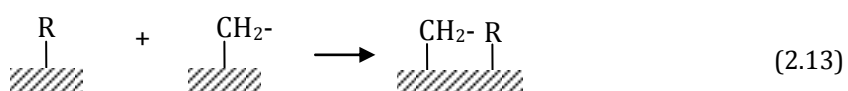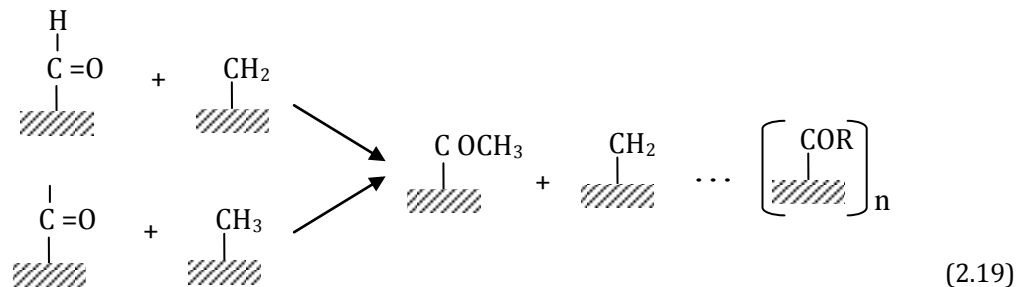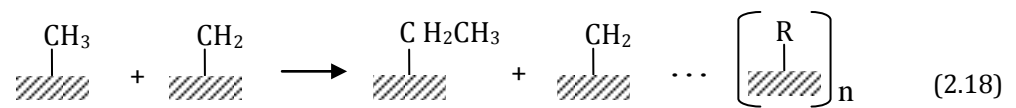
Table 2.2 Chain growth mechanisms for the Fischer-Tropsch synthesis. (*R means $C_nH_{2n+1}(n\geq1)$).

In addition, Bo-Tao et al.(2006) proposed a kinetic model including the hydrocarbon and oxygenate formation reactions with the water gas shift (WGS) reaction over an Fe-Mn catalyst. Oxygenates can be produced when CO-s is not dissociated into C-s and O-s, however if C-s and O-s are produced from CO-s, they will almost certainly lead to the production of hydrocarbon via polymerization. Against mentioned above, the interesting feature in this kinetics model is that the kinetic expressions for paraffins, olefins, alcohols and acids were derived on the basis of CH_2 insertion alkyl mechanism as shown in Table 2.2. They assumed that the FTS and WGS reactions occur on two different active sites on the catalyst. This is the same assumption made by Jun Yang et al. in their model. However, the hydrocarbon and oxygenate formation reactions are considered to occur on the same active sites. As can be seen in Table 2.2, oxygen atoms are not desorbed and this leads to the production of oxygenates (unlike the other mechanisms mentioned). Additionally, adsorbed hydrogen atoms and also hydrogen gas are converted into paraffins and alcohols, respectively, while the desorption of hydrogen atoms and hydroxyl groups leads to the production of olefins and acids. The chain growth is proposed two monomers (CH_2-s or CH_3-s) to lead higher hydrocarbons. However, the CH_2-s monomer is also included to convert CH_3-s. Therefore, both of them should be regarded the proposed mechanism. Moreover,

the oxygenates mechanism from Bo-Tao Teng et al. should be also considered to production total hydrocarbons.

2.1.3 CHAIN TERMINATION

Chain termination can occur via one of two processes, hydrogenation to form either paraffins or olefins. Thus one may visualize the formation of C2+ hydrocarbons as a polymerization process in which the methylene group act as the monomer and the alkyl groups are the active centres for chain growth.

The alkenyl mechanism from AN Fernandes(2005) does not form ethylene because the initiated chain $-CH = CH_2$ would have to be attacked by a surface hydrogen in order to form ethylene, but the termination mechanism for the alkenyl theory does not include reactions with hydrogen and according to the β-elimination mechanism no ethylene can be formed. The chain termination step is to give olefins or a reduction by surface hydride to give paraffins (2.20 and 2.21). Unlike presented above, his mechanism is focused on the reaction of hydrogen with the surface carbon atoms leading to the formation of methyne and methylene, which are the monomer units of the overall polymerization reaction. Jun Yang et al. also proposed the mechanisms of methane termination (2.22), paraffins(2.23) and olefins termination(2.24). These three reactions are usually considered as the chain termination steps. Also, Bo-Tao Teng et al. proposed that CHO-s with H_2 or OHs lead to CH_3OH and CHOOH, respectively (2.25 and 2.26). In addition, CH_3-species with CH_2- species and CO-s species lead to produce hydrocarbons (2.27) and oxygenates(2.28), respectively.

	mechanisms	no.
FN Fernandes (Fernandes 2005)		(2.20)
		(2.21)
Jun Yang (Yang 2004)		(2.22)
		(2.23)
		(2.24)
Bo-Tao et al.(2006)		(2.25)
		(2.26)
		(2.27)
		(2.28)

Table 2.3 Chain termination mechanisms for the Fischer-Tropsch synthesis.

For the primary reaction included the chain initiation, growth and termination, to describe the main products which have substantial variation in carbon number and product type, Anderson was the first to introduce a kinetic model for the Fischer-Tropsch reaction (Anderson 1956). According to Anderson, the product distribution of hydrocarbons can be described for primary reactions by the Anderson-Schulz-Flory (ASF) equation:

$$m_n = (1 - \alpha)\alpha^{n-1} \tag{2.29}$$

With m_n the mole fraction of a hydrocarbon with chain length n and the chain growth probability factor α independent of n. α determines the total carbon number distribution of the FT products. The chain growth probability (α) for a CH_2 monomer insertion to a hydrocarbon chain is defined as the ratio of the propagation rate (k_p) and the sum of the propagation and termination (k_t) rates.

$$\alpha = \frac{k_p}{k_p + k_t} \tag{2.30}$$

It was also empirically established that α is generally independent of the chain size (Anderson 1984). A high α value implies a high yield of heavy hydrocarbons, whereas a low α value implies there will be a greater production of lighter hydrocarbons. The range of α depends on reaction conditions and catalyst type. Dry (1982) reported typical ranges of α on Ru, Co, and Fe catalysts of: 0.85-0.95, 0.70-0.80, and 0.50-0.70, respectively. More recent references report Co catalysts with chain growth factors between 0.85-0.95 (Sie 1998). Figure 2.1 shows the distribution of hydrocarbons, as a function of the probability of chain growth (α).
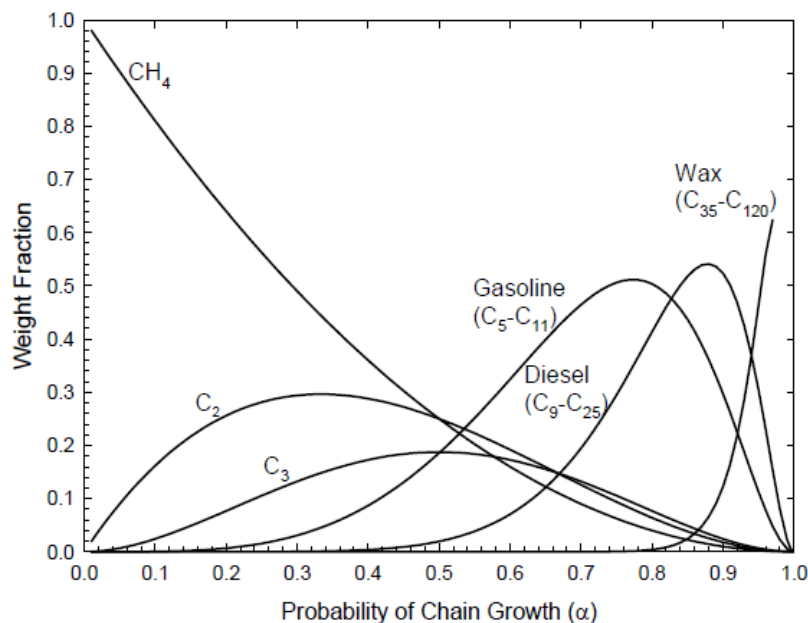
FIGURE 2.1 Weight Factor as a function of probability of chain growth (α)

2.1.4 RE-ADSORPTION

The most important secondary reaction is re-adsorption of olefins resulting in initiation of chain growth processes. It is possible that the re-adsorption of olefins is followed by hydrogenation to paraffins.

Hydrogenation of olefins is inhibited by CO suggesting competitive adsorption of olefins and CO for the same catalytic sites. Schulz (Schulz 1995) mentioned secondary hydrogenation as the most important process for the selectivity of the Fischer-Tropsch products on iron catalysts. They concluded that hydrogenation increases with higher carbon number due to increased adsorption strength. The secondary reaction steps involving olefins are hydrogenation to give paraffins, isomerisation, cracking, insertion into growing chains, re-adsorption and initiation of hydrocarbon chains. These steps are shown in Table 2.4 in a mechanism presented by Schulz et al. for re-adsorption of olefins followed by hydrogenation. In addition, Madon et al.(Madon, S.C et al. 1991) assumed there to be a dominant surface reaction mechanism starting with olefins which are adsorbed to give an intermediate, which is converted into a 2-σ intermediate and then a 1-σ intermediate and implication of the σ-complex is that paraffins can dehydrogenate back to olefins. The incomplete hydrocarbon chains also cause

steric hindrance for chain growth at the penultimate carbon atom. The absence of a steric hindrance for the shortest chains is the reason for the low C_2 production.

The re-adsorption and secondary reactions of olefins were taken into account, and deviations of hydrocarbon distribution could therefore be quantitatively described (Yang 2004). The deeper information about the olefin to paraffin ratio has not been intrinsically described at this stage, leaving room for further improvements in models considering the transportation enhanced re-adsorption and secondary reactions of olefins.

	mechanisms	no.
Secondary reactions of olefins (Schulz 1995)		(2.31)
Secondary reaction (Madon, S.C et al. 1991)		(2.32)
Bo-Tao et al.(2006)		(2.33)

Table 2.4 Re-adsorption mechanisms for the Fischer-Tropsch synthesis (*R means $C_nH_{2n+1}(n\geq1)$).

Many studies around olefin re-adsorption models have been developed mainly to account for the increase of secondary reactions with olefin chain length. Selectivities towards olefins compared with all the hydrocarbon products are appreciable in the C_2-C_{15} hydrocarbon range. The selectivity and yields of total hydrocarbons, light olefins and linear-olefins decrease considerably with increasing reaction times and higher CO conversions for synthesis gas (Raje and Davis 1997). A kinetic model is described by Fernandes (Fernandes 2005) who used the data reported by Raje and Davis (Raje and Davis 1997), including a good collection of data for Fischer-Tropsch reactions over an iron-based catalyst. Many

theories have focused on secondary chain growth of readsorbed olefins whilst Fernandes used with a dual mechanism of chain growth. Furthermore, the reactions were modelled with industrially relevant reaction conditions and the kinetic model was used to describe the product distribution from C_1 to C_{20} in order to obtain the optimum conditions for diesel, kerosene and gasoline production (Fernandes 2005). This model of a three-phase reactor was built with a number of basic assumptions suggested by AN Fernandes. He proposed a kinetic model that covers the important physicochemical phenomena in the FT reactions. A set of differential equations as well as equations based on mass and population balances is derived.

2.1.5 WATER SHIFT GAS(WGS) REACTION

Several mechanisms for the WGS reaction are proposed in the literature. Single studies of the WGS reaction over supported iron shift catalysts suggest the appearance of formate species. A mechanism based on a reactive formate intermediate is shown in Table 2.5 (Rethwisch and Dumesic 1986; Graaf and Winkelman 1988; Lox and Froment 1993). The formate species can be formed by the reaction between a hydroxy species or water and carbon monoxide in the gas phase or in the adsorbed state. The hydroxy intermediate can be formed by the decomposition of water. The formate intermediate is reduced to adsorbed or gaseous carbon dioxide. Rofer-De Poorter (Poorter 1981) suggested that a mechanism with direct oxidation of adsorbed or gas-phase CO to CO_2 (Sachtler 1982; Rethwisch and Dumesic 1986; Vandenbussche 1996) is more plausible in conjunction with the Fischer-Tropsch synthesis on iron catalysts. The oxygen intermediate can be formed from the dissociation of water. Direct oxidation of CO proceeds via a regenerative or redox mechanism where H_2O oxidizes the surface with the formation of H_2 and CO subsequently reduces the surface with the formation of CO_2 (Rethwisch and Dumesic 1986). Rethwisch and Dumesic (Rethwisch and Dumesic 1986) studied the WGS reaction on several supported and unsupported iron oxide and zinc oxide catalysts. They suggested that the WGS reaction over unsupported magnetite proceeds via a direct oxidation mechanism, while all supported iron catalysts operate via a mechanism with formate species due to limited change of oxidation state of the iron cations.

The proposed mechanism includes the WGS from Eliason and Bartholomew(1999) that considered the five steps (2.34-2.38)of WGS. According to Eliason and Bartholomew, the iron based catalyst had selectivities for hydrocarbons that were higher and CO_2 selectivities lower than typical iron catalysts due to their high iron and low oxide contents(Eliason and Bartholomew 1999).

	mechanisms	no.
Water and CO_2 Selectivities (Eliason and Bartholomew 1999)	$O- + H \longrightarrow OH$	(2.34)
	$OH + H \longrightarrow H_2O$	(2.35)
	$O- + H\text{-}H \longrightarrow H_2O$	(2.36)
	$=C\text{-}O + H_2O \leftrightarrow -CO_2 + H\ H$	(2.37)
	$=C\text{-}O + =C\text{-}O \longrightarrow C + CO_2$	(2.38)
Water formation (Wang and Ma 2003)	$\overset{H}{C}=O + H\text{-}H \longrightarrow \overset{H}{C}= + H_2O$	(2.39)

Table 2.5 Water shift gas reaction mechanisms for the Fischer-Tropsch synthesis

The water shift gas reactions (2.34-39) proposed by Eliason and Bartholomew(1999) were considered the part of Fischer-Tropsch mechanisms (Lox and Froment 1993). Cs species of Reaction 2.38 with iron based catalyst leads to produce iron carbide (Fe_3C). The WGS reaction mechanism is also similar with mechanism proposed by Schulz and Beck et al.(1988).

2.1.6   DISCUSSIONS OF PUBLISHED MECHANISMS

As presented in Table 2.1 and 2.2 the elementary mechanisms by Yi-Ning Wang et al. were based on the FT mechanism originally proposed by Lox and Froment (Lox and Froment 1993) which was extended by introducing the reverse step of olefin desorption. However, the Lox and Froment model fails to account for the effects of olefin re-adsorption, which has been proven to be a significant factor influencing selectivity, nevertheless the kinetics model proposed by Lox and Froment has an approach which is close to the fundamentals of FTS kinetics. The model from Yi Ning Wang Et al. (2003) is unlike some other mathematical modeling studies on Fisher-Tropsch fixed bed reactors which have been reported by other authors (Bub and Baerns 1980; Jess, Popp et al. 1999). This is important because typical industrial FTS processes with fixed bed reactors normally produce products ranging from methane to wax and catalyst pores fill with a stagnant phase formed by the waxy products. However, unlike the other models, this is regarded as a detailed model which deals with the intraparticle diffusion effect (Wang, Xu et al. 2003). This model may be useful for FT processes that produce hydrocarbon across the overall range of carbon number; however, the study fails to consider the production of specific ranges of hydrocarbons.

According to AN Fernandes(2005), as with the alkyl mechanism, only propylene and higher olefins can be formed by the alkenyl mechanism. This alternative mechanism for ethylene production and the impossibility of ethylene production from alkyl and alkenyl mechanisms can explain the low molar fraction of ethylene in the product distribution. The polymerization model reported by Fernandes described both mass balance and formation rate for both the alkyl and the alkenyl mechanisms; while the model is not considered to produce oxygenates products and is based on once-through process without recycling and co-feeding. Additionally, he did not consider the effects of active sites on catalyst and sizes of particle and reactor diameter and re-adsorption reaction. Therefore, the model might be optimized to discuss the above effects with modifying rate expressions.

The isothermal kinetics of the Fischer-Tropsch synthesis over a Fe-Cu-K spray-dried catalyst were studied in a spinning basket reactor by Guo and Liu(2006). Their kinetic model for hydrocarbon formation was derived on the

basis of a simplified carbide mechanism to reduce the number of parameters. The mechanism proposed by Guo and Liu(2006) includes equations introduced above (Guo and Liu 2006). The simulation results indicated that the simplified model could fit the experimental data. The formation rate constants for both methane and ethane were evaluated separately, however, the calculated quantities of olefins fitted well with experimental data while, the calculated quantities of paraffins did not fit well with experimental data. Therefore, the simplified model from Guo and Liu(2006) is an appropriate choice for calculating olefin production rates.

The kinetic model developed by Jun Yang et al. (2004a) is accurate only for the cases excluding the diffusivity and solubility factors so, the model is only considered for two-phase reactors with two active sites on the catalyst. For the kinetic model, the overall FTS reactions can be simplified as a combination of FTS reactions and the WGS reaction. Active sites for the above reactions in FTS are still not clear, especially in the cases of iron catalysts. This is because of the fact that the iron based catalysts starting from oxide precursors have been experimentally proven to have complex phase transfer during the reduction as well as synthesis operation.

2.2   FISCHER-TROPSCH KINETICS

In the past decades, many models of three-phase reactors have been studied and published as a single phase model. Slurry bed columns for FTS have been first commercialized by SASOL in the 1980s and the three-phase models were first investigated starting in earnest by Van der Laan who modelled the FTS using an Fe catalyst in 1999. Van der Laan established a model where olefin re-adsorption depends on chain length because of the increasing solubility of long chain hydrocarbons in the liquid phase (Laan and Beenackers 1999). More recently, a new product characterization model has been proposed for iron-based low-temperature Fischer-Tropsch synthesis by F. Gideon Botes (Botes 2007). He proposed a model which can successfully describe the olefin and paraffin distributions in the C_{3+} range (excluding methane and ethane) which is attributed to the inclusion of olefins re-adsorption and secondary reactions, mainly including chain growth to higher hydrocarbons and hydrogenation to the corresponding paraffins. In addition, he reported that the chain length dependent effects can only be ascribed to olefin reincorporation if the propensity for secondary reactions increases with an increasing carbon number. The reasons for this proposed dependency of secondary reactions on chain length include: slower diffusion of longer molecules through catalyst pores, higher concentration of heavier olefins in the liquid phase because of an increase in solubility with longer chain length, stronger physisorption of longer molecules on the catalyst surface and variations in reactor residence times because of the different solubilities in the liquid phase (Botes 2007). However, this model suffers from some limitations at low temperature conditions. Schulz et al. developed an olefin reincorporation model based mainly on chain length that is dependent on the product solubilities, but their model was compared to a very limited number of experimental products which was not enough to evaluate the olefin mass transfer effects.

The kinetics models of both Jun Yang et al. for two-phase and AN Fernandes for three-phase reactors are considered in detail. According to Jun Yang et al., the rates of formation of paraffins and olefins with n carbons can thus be written as

$$dP(1)/dt = k_{met}[CH_3s][Hs_1] = k_{met}K_5[CH_2s][Hs]^2/[s] \qquad (2.40)$$

$$dP(n)/dt = k_p[C_nH_{2n+1}s][Hs] = \frac{k_pK_5[C_nH_{2n}s][Hs]^2}{[s]} \quad (\boldsymbol{n \geq 2}) \tag{2.41}$$

$$dP^=(n)/dt = k_o[C_nH_{2n}s] - k_{-o} P_{C_nH_{2n}}[s] \quad (\boldsymbol{n \geq 2}) \tag{2.42}$$

Equation 2.43 gives chain growth factor for carbon number n.

$$\alpha_n = \frac{[C_nH_{2n}s]}{[C_{n-1}H_{2n-2}s]} = \frac{k_{CG}K_4 \frac{P_{H_2}^2 P_{CO}}{P_{H_2O}}[s]}{k_{CG}K_4 \frac{P_{H_2}^2 P_{CO}}{P_{H_2O}}[s] + k_pK_5K_2P_{H_2}[s] + k_o(1 - \beta_n)}$$

$$(n \geq 2) \tag{2.43}$$

$$\alpha_A = \frac{k_{CG}[CH_2s]}{k_{CG}[CH_2s] + k_pK_5K_2P_{H_2}[s] + k_o} = \frac{k_{CG}K_4 \frac{P_{H_2}^2 P_{CO}}{P_{H_2O}}[s]}{k_{CG}K'_3 \frac{P_{H_2}^2 P_{CO}}{P_{H_2O}}[s] + k_pK_5K_2P_{H_2}[s] + k_o}$$

$$\tag{2.44}$$

The re-adsorption factors for 1-olefin with carbon number n (n≥2) are defined as follows:

$$\beta_n = \frac{k_{-o}}{k_o} \left\{ \frac{P_{C_nH_{2n}}}{\left[\alpha_A^{n-1}K_4 \frac{P_{H_2}^2 P_{CO}}{P_{H_2O}} + \frac{k_{-o}}{k_{CG}K_4 \frac{P_{H_2}^2 P_{CO}}{P_{H_2O}}[s] + k_pK_5K_2P_{H_2}[s] + k_o} \times \sum_{i=2}^n \alpha_A^{i-2} P_{C_{(n-i+2)}H_{2(n-i+2)}} \right]} \right\}$$

$$(n \geq 2) \tag{2.45}$$

$$\frac{dP(1)}{dt} = k_{met}K_2K_5K_4 \frac{P_{H_2}^3 P_{CO}}{P_{H_2O}}$$

$$/[1 + \sqrt{K_2P_{H_2}} + K_1P_{CO} + K_4 \frac{P_{H_2}^2 P_{CO}}{P_{H_2O}} + K_1K_3P_{CO}P_{H_2} + K_5K_4K_2^{0.5} \frac{P_{H_2}^{2.5} P_{CO}}{P_{H_2O}}$$

$$+ K_4 \frac{P_{H_2}^2 P_{CO}}{P_{H_2O}} (1 + K_5\sqrt{K_2P_{H_2}}) \sum_{i=2}^n \prod_{j=2}^i (\alpha_j)]^2$$

$$\tag{2.46}$$

$$\frac{dP(n)}{dt} = k_p K_2 K_5 K_4 \frac{P_{H_2}^3 P_{CO}}{P_{H_2O}} \prod_{j=2}^{i} \alpha_j$$

$$/[1 + \sqrt{K_2 P_{H_2}} + K_1 P_{CO} + K_3' \frac{P_{H_2}^2 P_{CO}}{P_{H_2O}} + K_1 K_3 P_{CO} P_{H_2} + K_2 K_5 K_4 \frac{P_{H_2}^{2.5} P_{CO}}{P_{H_2O}}$$

$$+ K_4 \frac{P_{H_2}^2 P_{CO}}{P_{H_2O}} (1 + K_5 \sqrt{K_4 P_{H_2}}) \sum_{i=2}^{n} \prod_{j=2}^{i} (\alpha_j)]^2$$

$$(2.47)$$

$$\frac{dP^=(n)}{dt} = k_o (1 - \beta_n) K_4 \frac{P_{H_2}^2 P_{CO}}{P_{H_2O}} \prod_{j=2}^{i} \alpha_j \, /[1 + \sqrt{K_2 P_{H_2}} + K_1 P_{CO} + K_4 \frac{P_{H_2}^2 P_{CO}}{P_{H_2O}}$$

$$+ K_1 K_3 P_{CO} P_{H_2} + K_2 K_5 K_4 \frac{P_{H_2}^{2.5} P_{CO}}{P_{H_2O}} + K_4 \frac{P_{H_2}^2 P_{CO}}{P_{H_2O}}$$

$$+ K_5 \sqrt{K_2 P_{H_2}}) \sum_{i=2}^{n} \prod_{j=2}^{i} (\alpha_j)]$$

$$(2.48)$$

The rates of formation of paraffins and olefins with carbon number n are thus demonstrated in Eqs. (2.46)-(2.48) (Fernandes 2005).

parameter	value	parameter	value
K_{CG}	7.88×10^3 mol/g.s.bar	k_{CO}	3.42 mol/g.s.bar$^{1.5}$
E_{CG}	75.52 KJ/mol	E_W	58.43 KJ/mol
k_{met}	2.01×10^6 mol/g.s.bar	K_W	2.76×10^{-2} bar$^{-0.5}$
E_{met}	97.39 KJ/mol	$K_{2.1}$	2.59 bar^{-1}
k_p	1.10×10^6 mol/g.s.bar	$K_{2.2}$	1.21bar^{-1}
E_p	111.48 KJ/mol	$K_{2.19}$	1.67×10^{-3} bar^{-1}
k_o	8.79×10^3 mol/g.s	$K_{2.20}$	8.34×10^{-2}
E_o	97.37 KJ/mol	$K_{2.24}$	0.10
k_{-o}	2.77×10^{-5} mol/g.s.bar		

TABLE 2.6 Values of the parameters for the mechanism FT proposed Jun Yang (2004).

The rate constants and ativation energies of the best model are listed in Table 2.6 and the rate is little faster than other literature (Guo and Liu 2006; Jie Chang et al. 2007).

In the kinetic model of AFN Fernandes, methane, ethane and ethylene are formed by reactions that do not involve a propagation step, therefore, their mass balances are given by different equations than those for higher carbon numbers.

$$\frac{dP(1)}{dt} = k_{met} * [-H] * R(1)$$

(2.49)

$$\frac{dP(2)}{dt} = k_{et} * [-H] * R(2)$$

(2.50)

$$\frac{dP^{=}(2)}{dt} = k_{o2} * [-CH_2] * [-CH_2]$$

(2.51)

The mass balance for a propagation species, R(n), is affected by the propagation of the species and termination by β-hydride elimination and reduction. R(n) is formed by propagation of an R(n-1) species and is consumed by its own propagation to form an R(n+1) species and to form paraffins (P(n)) or olefins ((P$^{=}$(n)) with *n* carbons in their chain leading to Eq (2.52):

$$\frac{dR(n)}{dt} = k_p * [-CH_2] * R(n-1) - k_p * [-CH_2] * R(n) - k_{olef} * R(n) - k_{par} * [-H] * R(n)$$

(2.52)

In a polymerization process such as the FTS the lifetime of a propagation species with *n* carbons in its chain (R(n)) is very short, and these species are being formed and consumed constantly. This effect leads to an almost constant concentration of R(n) in any location, so that its concentration can be considered constant for modelling purposes. If this quasi-steady state is applied to all propagation species, the derivative term becomes null and the concentrations of the propagating species are given by:

$$R(n) = \frac{k_p * [-CH_2] * R(n-1)}{k_p * [-CH_2] + k_{par} * [-H] + k_{olef}}$$

(2.53)

The formation of a propagating species occurs through the reaction of methylene with a surface hydride yielding a starting chain, which is followed by propagation:

$$\frac{dR(1)}{dt} = k_i * [-CH_2][-H] - k_p * [-CH_2] * R(1)$$

(2.54)

Applying the quasi-steady state to the initiation step, one obtains the following equation:

$$R(1) = \frac{k_i * [-CH_2][-H]}{k_p * [-CH_2]} = \frac{k_i * [-H]}{k_p}$$

(2.55)

The mass balances for alkenes and olefins are affected only by termination of the propagating chains leading to the formation of paraffins and olefins:

$$\frac{dP(n)}{dt} = k_{par} * [-H] * R(n)$$

(2.56)

$$\frac{dP^=(n)}{dt} = k_{olef} * R(n)$$

(2.57)

The mass balance for a propagating species in the alkenyl mechanism is affected by propagation and termination by reduction. A propagating species, $R''(n)$, is formed by propagation of an $R''(n-1)$ species and is consumed by its own propagation to form an $R''(n+1)$ species and an olefin $P^=(n)$ with n carbons in its chain.

$$\frac{dR''(n)}{dt} = k_{p2} * [-CH_2] * R''(n-1) - k_{p2} * [-CH_2] * R''(n) - k_{olef2} * R''(n)$$

(2.58)

If the quasi-steady state is applied to this process, the derivative term becomes null and the concentration of the propagating species is given by:

$$R^{''}(n) = \frac{k_{p2} * [-CH_2] * R^{''}(n-1)}{k_{p2} * [-CH_2] + k_{olef2}}$$

$$(2.59)$$

The rate of initiation is given by:

$$\frac{dR^{''}(2)}{dt} = k_i * [-CH_2][-CH] - k_{ps} * [-CH_2] * R^{''}(2)$$

$$(2.60)$$

Applying the quasi-steady state to the initiation step, one obtains the following equation:

$$R^{''}(2) = \frac{k_{i2} * [-CH_2][-CH]}{k_{p2} * [-CH_2]} = \frac{k_{i2} * [-CH]}{k_{p2}}$$

$$(2.61)$$

The mass balances for olefins are affected only by termination leading to:

$$\frac{dP^{=}(n)}{dt} = k_{olef2} * R^{''}(n)$$

$$(2.62)$$

Ethylene if formed by the reaction of two methylene species $(-CH_2)$ rather than termination of $R(2)$ or $R^{''}(2)$ species.

$$\frac{dP^{=}(2)}{dt} = k_{o2} * [-CH_2] * [-CH_2]$$

$$(2.63)$$

So far in the literature there have been a number of mechanism and kinetic models for Fischer-Tropsch synthesis in both two-phase and three-phase reactors. Two of these models were chosen as appropriate kinetic models and called Base case model I for the two-phase reactor and Base case model II for the three-phase reactor, respectively. Base case models I and II will be used to model the effects of various operating conditions.

2.3 INFLUENCE OF PROCESS CONDITIONS
ON THE PRODUCT SELECTIVITY

The product selectivity is influenced by the process conditions. This section discusses the effect of process conditions, temperature, pressures of H_2 and CO, and residence time.

2.3.1 TEMPERATURE

Dictor and Bell reported that an increase of temperature results in a shift toward products with a lower carbon number on iron catalyst (Dictor and Bell 1986). Donnelly (Donnelly and Satterfield 1989) and other researchers (Anderson 1984; Dictor and Bell 1986) observed an increase of the olefin to paraffin ratio on iron catalysts with increasing temperature. However, Dictor and Bell (Dictor and Bell 1986) reported a decrease in the olefin selectivity with increasing temperature for unalkalized iron oxide powders. Dry observed that the fixed bed multi-tubular Arge reactors operate at low temperatures and produce waxes while the fluidized catalyst bed reactors operate at high temperatures to produce essentially low molecular weight olefins and gasoline (Dry 1990). Figure 2.2 shows that the higher temperature leads to higher light paraffins(C_1-C_7), and lower heavy paraffins (C_{15+}). Therefore, low temperatures are also preferable for the increased production of heavy olefins and high temperatures are preferable for increased production of light olefins as can be seen from the comparisons in Figure 2.2. Temperature effect on the distributions of C_9-C_{15} paraffins seems more complicated. In addition, the figure shows that the high temperature leads to higher light olefins(C_2-C_7) and lower heavy olefins(C_9-C_{26}). The olefins distributions from C8 to C15 at low temperature appear to be almost horizontal straight lines.
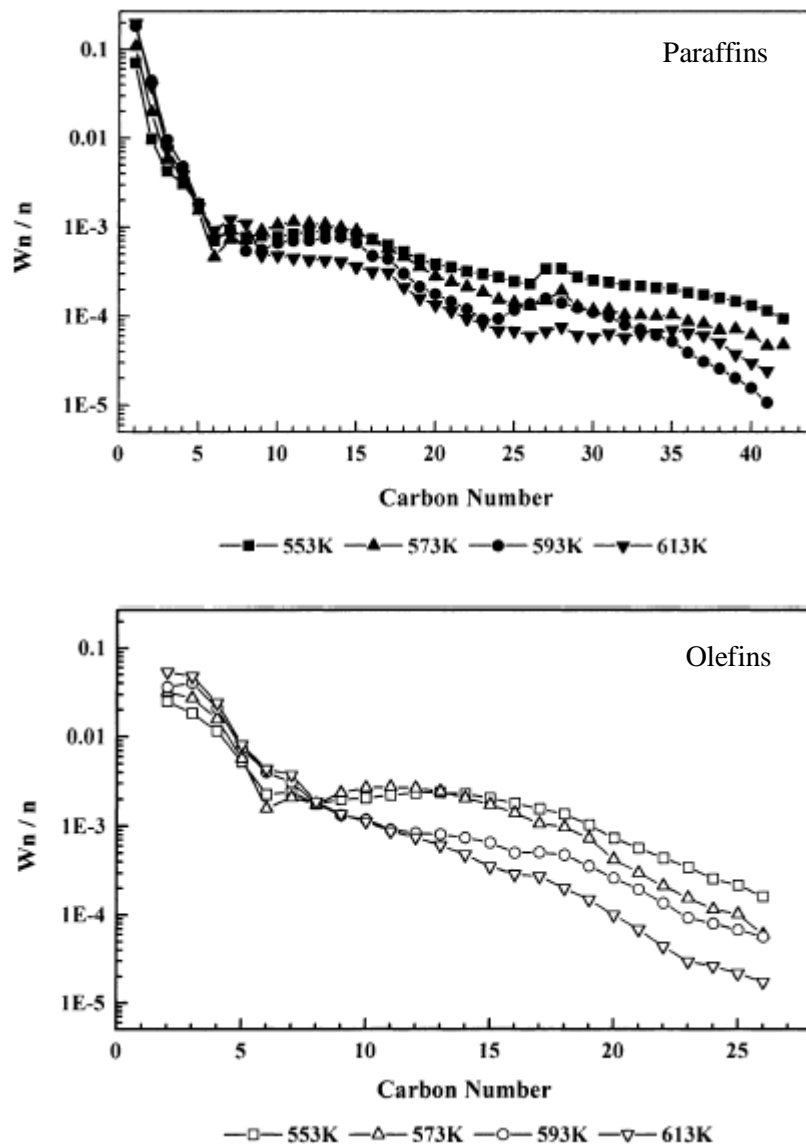
Figure 2.2 Influence of temperature on paraffin and olefin distributions from Yuan-Yuan Ji et al. ($H_2/CO=1.97$, 2.25MPa, 2000h^{-1})

Figure 2.3 shows the results that operating temperature is increased, the CO conversion is increased. In addition, for the reaction temperature at 633K, the total selectivity of light olefin products was higher than the other reaction temperatures under the same reaction conditions. In general, an increase in the reaction temperature leads to an increase in the catalytic performance furthermore; it has shown that the reaction temperature should not be too low.
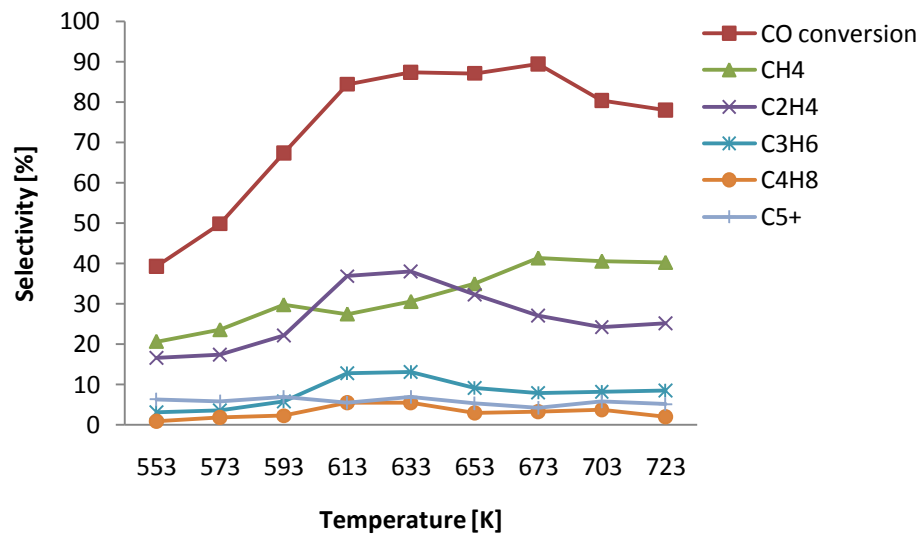
Figure 2.3 Influence of temperature on the selectivity for Fe-Mn-Al$_2$O$_3$ catalyst from Mirzaei AA et al. (H$_2$/CO=1, 0.1 MPa)

2.3.2 PRESSURE

At low total pressures, establishment of the thermodynamic equilibrium will proceed more slowly, while at equilibrium mainly paraffins are present. Most studies show that the product selectivity shifts to heavier products and to more oxygenates with increasing total pressure (Dry 1981).
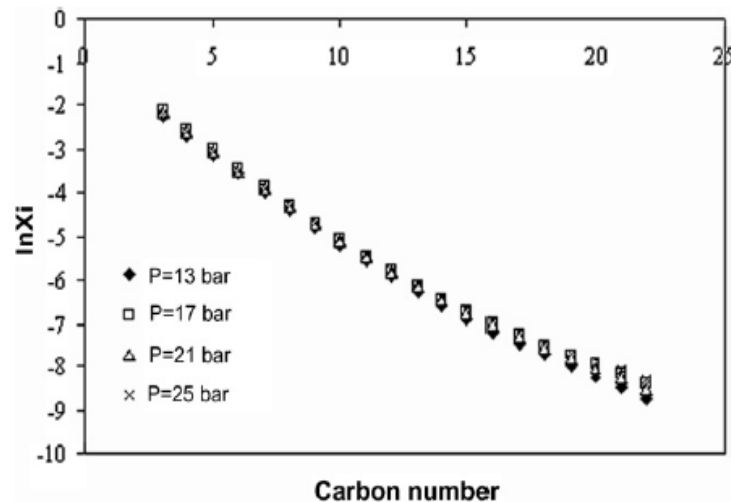
Figure 2.4 Influence of pressure on the carbon number distributions from AN Pour et al.(2004) (H$_2$/CO=1, 563K and GHSV[5]= 10NL/hg)

Xi: mole fractions of hydrocarbons

---

[5] GHSV: Gas Hourly Space Velocity

Chain length distributions shown in Figure 2.4 for different pressure from 1.3-2.5 MPa(13-25 bar), indicate that average carbon number of products is almost independent of reaction pressure.
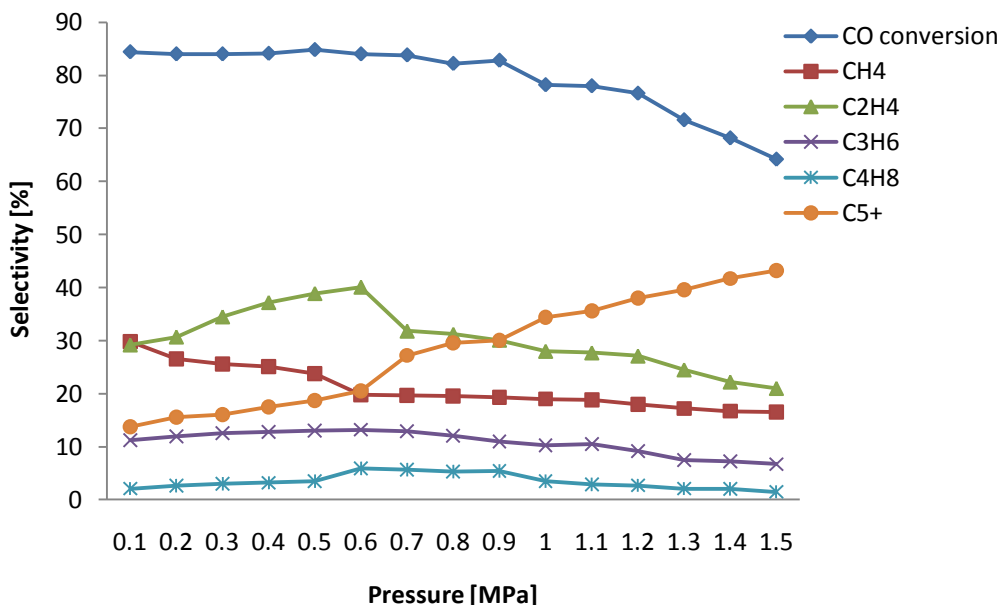
Figure 2.5 Influence of pressure on the selectivity for Fe-Mn-Al$_2$O$_3$ catalyst from Mirzaei AA et al.(2009) (H$_2$/CO=1, 0.1 MPa)

An increase in total pressure would generally result in condensation of hydrocarbons, which are normally in the gaseous state at atmospheric pressure. Higher pressures and higher carbon monoxide conversions would probably lead to saturation of catalyst pores by liquid reaction products (A. Griboval-Constant et al. 2002). It is apparent that increasing in total pressure in the ranges of 0.2–1.5MPa significantly increases the C$_{5+}$selectivity and leads to an increase to 43.2% at the pressure of 1.5 MPa. On the other hand, as can be seen on Figure 2.6 at the ranges of 0.1–0.6 MPa total pressures, no significant decreasing of CO conversion was observed, however, the light olefins selectivities were increased and the results indicate that at the total pressure of 0.6 MPa. The results also indicate that the CO conversion and the total selectivity with respect to C$_2$-C$_4$ light olefins were decreased as the total pressures are increased from 0.6 to 1.5 MPa. Hence because of high CO conversion, low CH$_4$ selectivity, and also higher total selectivity with respect to C$_2$-C$_4$ olefins at the total pressure of 0.6 MPa, this pressure was chosen as the optimum pressure.

2.3.3 H_2/CO FEED RATIO

Changing the H_2/CO ratio leads to different proportion of both adsorbed hydrogen and surface carbon. At lower ratio the hydrogenation activity will decrease resulting in higher olefin selectivity. Increasing H_2/CO ratios in the reactor results in lighter hydrocarbons and a lower olefin content (Donnelly and Satterfield 1989). Donnelly and Satterfield (Donnelly and Satterfield 1989) observed a decrease of the olefin to paraffin ratio from 6 to 1 by increasing the H_2/CO ratio from 0.3 to 4. Dry proved a relation between the methane selectivity and the factor $P_{H2}^{1/2}/(P_{CO} + P_{CO2})$ for alkaline-promoted fused iron catalysts in a fluidized-bed reactor. This indicates that CO_2 appears to play an important role. Increasing CO_2 pressures result in a decrease of the methane selectivity (Dry 1981).

Figure 2.6 shows the distributions of both paraffins and olefins. The olefin distributions have a slight declining tendency with the increase of the carbon number. It also shows that the lower H_2/CO ratio in feed leads to higher heavy olefins(C_{9+}) and lower light ones(C_2-C_7) and the lowest ratio in feed leads to the existence of a high amount of heavy olefins up to about C_{26}. In addition, it can be seen that all paraffin distribution curves sharply decline from C_1 to C_6, level off from C_7 till about C_{26}, increase at about C_{27}, and decline again from C_{28}. The figure reveals that a higher H_2/CO ratio in feed leads to higher light paraffins(C_1-C_8) and lower heavy ones(C_{26+}). The effect of H_2/CO ratio on the selectivity of paraffins with carbon number of C_{10}-C_{25} seems more complicated. Generally, the effect of H_2/CO ratio in feed on paraffins is less than on olefins.
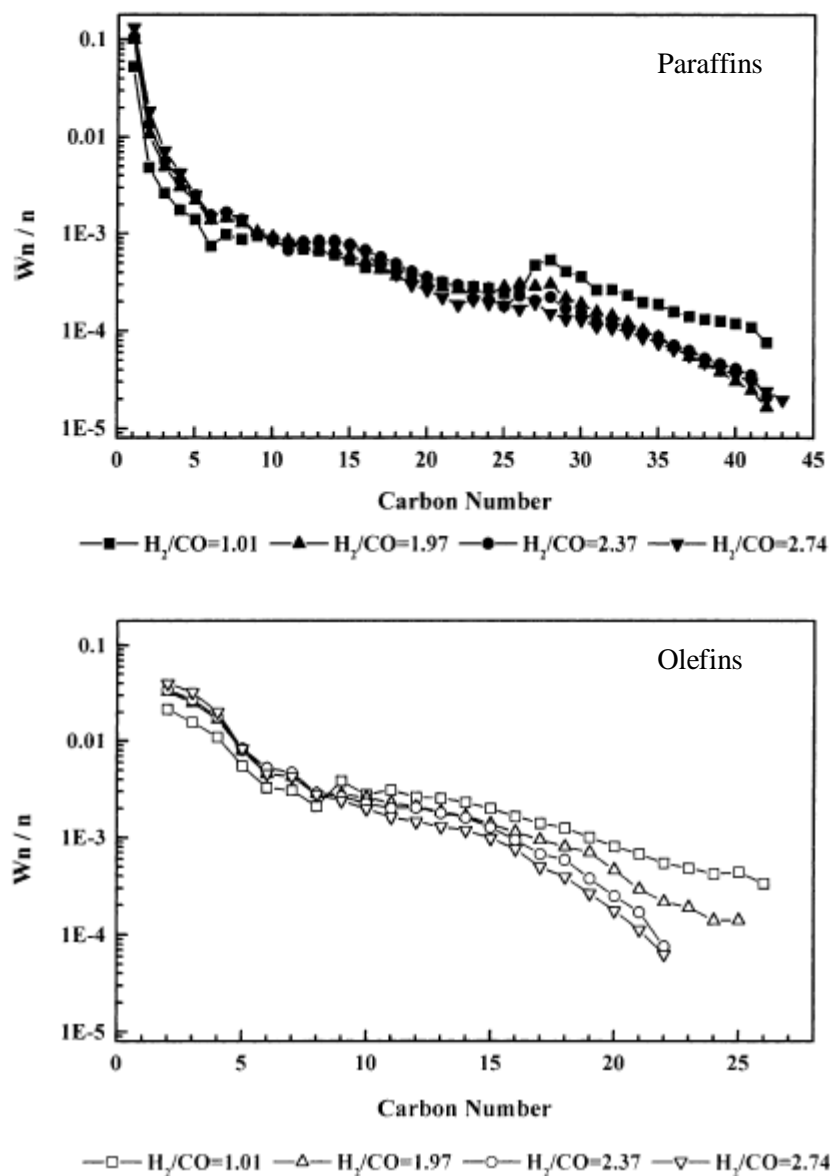
Figure 2.6 Influence of H_2/CO feed ratio on the paraffin and olefin distributions from Yuan-Yuan Ji et al. (573K, 2.25MPa, 7000h[-1])

Wn/n: weight fraction for carbon number n

Therefore, a low H_2/CO ratio in the feed is preferable for the increased production of heavy olefins and a high H_2/CO feed ratio is preferable for increased production of light olefins.
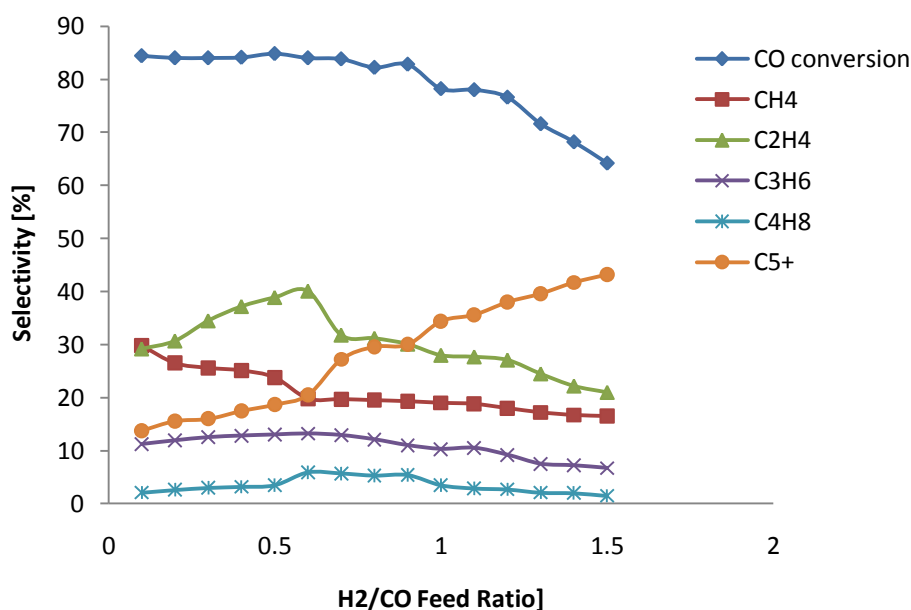
Figure 2.7 Influence of H_2/CO feed ratio on the selectivity for Fe-Mn-Al$_2$O$_3$ catalyst from Mirzaei AA et al.(2009) (H_2/CO=1, 0.1 MPa)

Figure 2.7 shows with H_2/CO feed ratio from 1 to 3, different selectivities with respect to light olefins were obtained. However, in the case of the H_2/CO=1, the total selectivity of light olefins products was higher and the CH$_4$ selectivity was lower than the other H_2/CO feed ratios under the same temperature and pressure condition.

2.3.4   SPACE VELOCITY

Space velocity in bed is increased such that CO conversion from 5-60% results in a drastic decrease of olefin to paraffin ratios due to enhanced secondary conversion of primary formed olefins. The isomerisation of 1-olefins to 2-olefins increased with increasing carbon numbers, possibly as a result of longer space velocity of higher molecular weight 1-alkenes. At lower space velocity, 1-alkene are hydrogenated or isomerized less than at higher space velocity because of the decrease in space velocity of the 1-alkenes (Yates and Satterfield 1992).
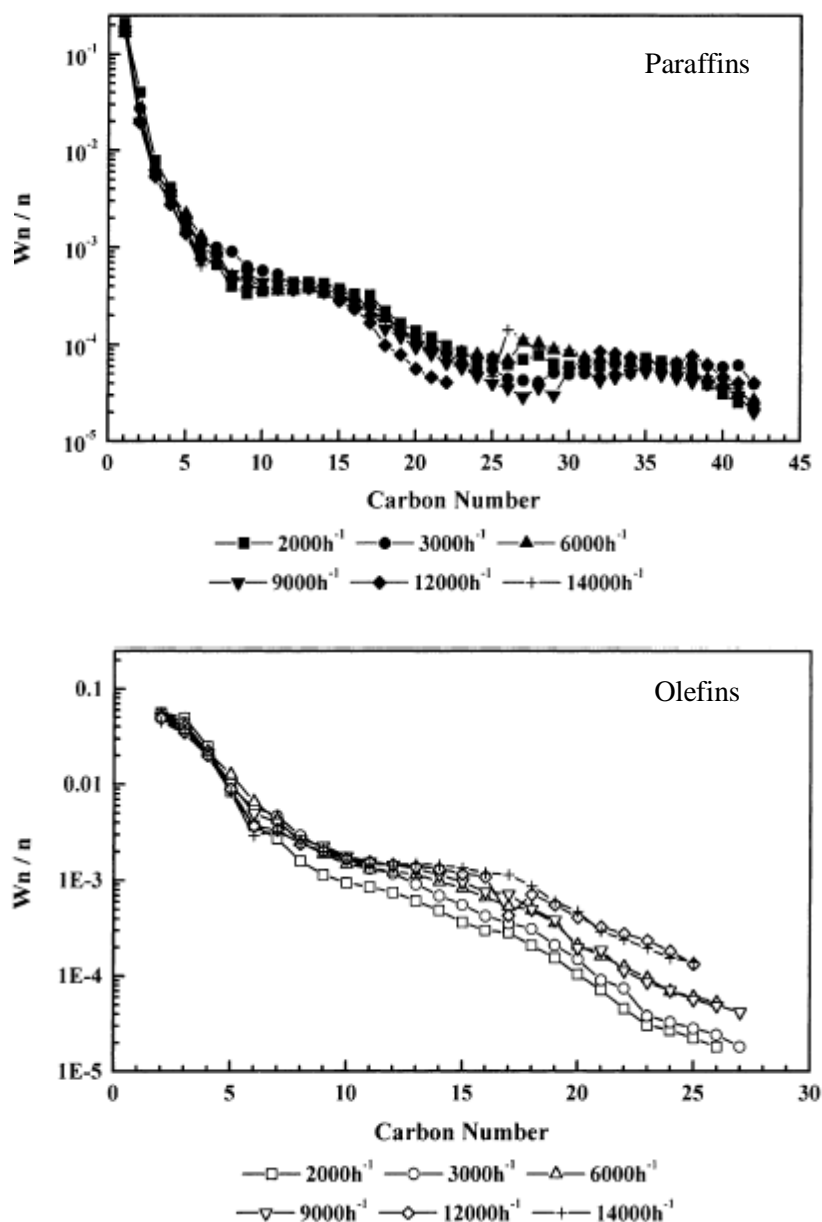
Figure 2.8 Influence of Space velocity on the paraffin and olefin distributions from Yuan-Yuan Ji et al (623K, $H_2/CO=1.97$, 2.25MPa)

The paraffins and olefins distributions under different space velocities are respectively illustrated in Figure 2.8. It is found from the figure that olefins (C_2-C_7) are nearly unchanged when space velocities are larger than 3000h^{-1}. However, higher space velocity leads to higher contents of heavy olefins (C_{8+}). At the lowest space velocity, the contents of olefins larger than C_7 are significantly lower compared with those at higher space velocities. With the increase of space velocity., olefin distributions over C_9-C_{15} gradually become horizontal lines. In addition, C_1-C_{27} paraffins slightly decrease with the increase of space velocity, especially at low

space velocity. For the paraffins above C_{27} the distributions become more complicated. Generally, the effect of space velocity on paraffins is less than on olefins.

2.3.5   CATALYST CONSIDERATION

Iron and cobalt based catalysts are known to be very effective Fischer-Tropsch catalysts for the synthesis of long chain hydrocarbons from synthesis gas. Ruthenium also produces paraffins however, this produces much more methane, while at low temperatures and high pressures it is selective towards high molecular waxes(Iglesia, Reyes et al. 1993). Co and Fe are by far, the main ones with these particular attributes. The characteristics of these catalysts are given in Table 2.7.

Catalyst	Typical Conditions	Product	Advantage	Disadvantage	Reference
Co-based	T=543K, P=8.5MPa, $H_2/CO=2$	Higher alcohols	- To give higher selectivity for any specific product - To be partially compensated with high product selectivity - To provide long-chain hydrocarbons (mainly paraffinic products)	- High capital cost	P. Chaumette, 1995
Fe-based	T=503K, P=2.5MPa, $H_2/CO=1.8$	C_2-C_4	- To be preferred due to cheap catalyst - To be the most suitable metal to catalyse the formation of lower olefins - To have remarkable electronic properties and preliminary catalytic properties		G. Henrici, 1976

TABLE 2.7 Characteristics of Co-based and Fe-based catalysts as Fischer-Tropsch catalysts

The iron-based catalyst caused the high water gas shift activity to be flexible towards the H_2/CO feed ratio of the synthesis gas. At high temperature (613K), Fe-based catalysts are selective for light olefins with a low selectivity towards methane. This only seems possible with Fe-based catalysts, making them unique in this respect. The application of Fe-based catalysts in the production of heavy wax is limited (Adrianus 2001). Bukur et al. studied several reducing gases in a fixed bed and concluded that activation in CO led to catalysts with higher initial activity and better selectivity towards higher hydrocarbons than H_2 activated catalysts (Bukur, Nowicki et al. 1995).

Iron catalysts for the Fischer-Tropsch synthesis generally consist of precipitated irons, which are promoted with K, Ru and Cu to obtain a high activity and selectivity, and with Al_2O_3 and SiO_2 added as structural stabilizers. These promoters have an important influence on activity. According to Eliason and Bartholomew (1999), the Fe-K catalyst had selectivities for hydrocarbons that were higher and CO_2 selectivities lower than typical iron catalysts due to their high iron and low oxide contents and the values of the propagation probability were low for Fe and about the same for Fe-K relative to those reported for Fe FT catalysts (Eliason and Bartholomew 1999). Senzi Li et al proposed that K, Ru and Cu promoters increased steady-state FTS rates, and the number of COs present after activation and FTS (Senzi and Sundaram 2002). In addition, iron-based catalysts are prepared by activation protocols that favour the nucleation of small Fe carbide crystallites and inhibit sintering of oxide catalyst precursors[6] during synthesis and activation. Iron catalyst is active and is highly likely to be present intermediate between FeC and FeO. Iron catalysts react with oxygen in the air to form various oxide and hydroxide compounds; the most common are iron(II) oxide, iron(III) oxide, and iron(II, III) oxide. (Greenwood, Norman N. and Earnshaw, A. , 1997):

$$FeC_2O_4 \rightarrow FeO + CO + CO_2 \qquad (2.64)$$

---

[6] Precursor: a compound that participates in the chemical reaction that produces another compound

The iron(III) oxide can be produced by the reaction (2.65-2.67). At about 200℃, the iron(III) hydroxide converts in Fe_2O_3.

$$2Fe + 3/2\ O_2 + H_2O \leftrightarrow 2\ FeO(OH) \tag{2.65}$$

$$2FeO(OH) \leftrightarrow Fe_2O_3 + H_2O \tag{2.66}$$

$$2Fe + 3CO_2 \leftrightarrow Fe_2O_3 + 3CO \tag{2.67}$$

The iron(II,III) oxide(Fe_3O_4)can be prepared by reduction of Fe_2O_3 with hydrogen(2.68) and CO (2.69) as below reaction:

$$3Fe_2O_3 + H_2 \rightarrow 2Fe_3O_4 + H_2O \tag{2.68}$$

$$3Fe_2O_3 + CO \rightarrow 2Fe_3O_4 + CO_2 \tag{2.69}$$

In addition, Fe_3O_4 can be prepared by the reaction of pure iron and water (2.70) and reduction of Fe_2O_3 (2.71) and disproportionation because FeO is thermodynamically unstable below 575℃ (2.72).

$$2Fe + 4H_2O \leftrightarrow Fe_3O_4 + 4\ H_2 \tag{2.70}$$

$$3Fe_2O_3 + 1/2\ O_2 \leftrightarrow 2Fe_3O_4 \tag{2.71}$$

$$4FeO \rightarrow Fe + Fe_3O_4 \tag{2.72}$$

(A)   (B)
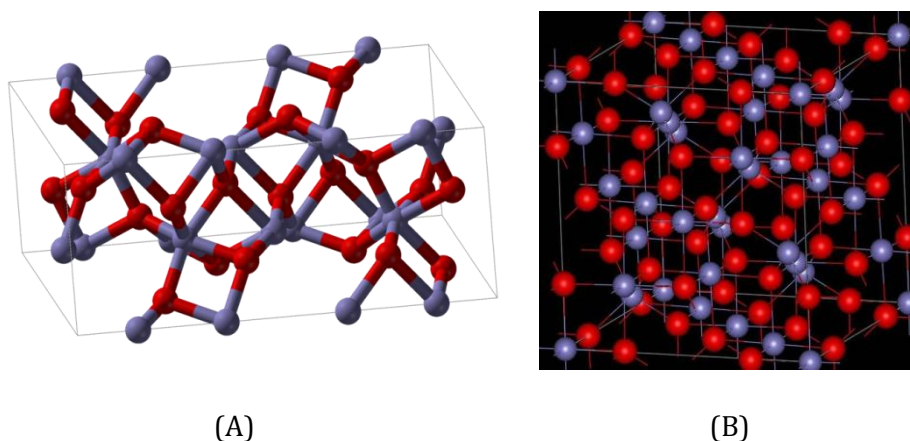
FIGURE 2.9 Structures of Iron(III) oxide(Fe_2O_3)(A) and Magnetite(Fe_3O_4)(B).

Iron carbide is a chemical compound of iron and carbon and can also be prepared by the reaction 2.73. As can be seen from the Figure 2.10, it has an orthorhombic crystal structure and is a hard material. HH Storch and N. Golumbic(1951) indicated that the higher iron carbides were active catalysts, frequently more

active than similar non-carburized catalyst. In addition, Cs species of Reaction 2.35 might lead to produce FeC_x as mentioned above. The structure is shown in Figure 2.10.

$$xC + Fe \leftrightarrow FeC_x \qquad\qquad\qquad (2.73)$$
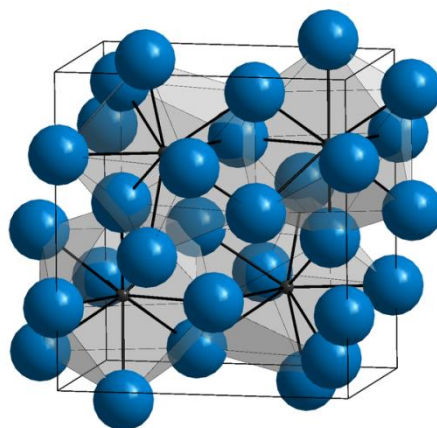
FIGURE 2.10 Structures of iron carbide (FeC_x).

Senzi Li et al.(2001) proposed that the contacting of Fe oxide precursors with synthesis gas(H_2/CO mixtures) leads to structural and chemical changes and to the formation of the active sites required for the Fischer-Tropsch synthesis (FTS). The activation of these precursors occurs via reduction to Fe_3O_4 followed by carburization to form FeC_x. They report that Fe_2O_3 converts to Fe_3O_4, and subsequently to FeC_x more rapidly than for the unpromoted Fe oxide. The conversion provides sites for H_2 dissociation, which leads to adsorbed hydrogen species that reduce Fe_2O_3 to Fe_3O_4. According to Senzi and Sundaram (2002), concentration of Fe_3O_4 precursors increased for initial times and decreased after initial times. However, FeC_x concentration continuously increased for FT reactions. This means that Fe_3O_4 precursors are active to initiation reaction such as adsorption of hydrocarbons. Also, Fe_3O_4 is formed, which are active for the water gas shift reaction and controlled oxidation of Fe_3O_4 is used to produce Fe_2O_3. FeC_x precursors are active to produce hydrocarbon by re-adsorption and Fe_2O_3 precursors are active to dissociation of H_2 and CO. As be seen from Figure 2.10, a large number of carbon atoms provide opportunities to contact monomers, which are compounds to affect the chain growth to produce the higher hydrocarbon. These precursors provide higher surface areas, a higher CO conversion by increasing CO binding sites, and shorter diffusion distances for oxide carbide

transformations. The iron-based catalyst with the precursors produces significantly low CH_4 and CO_2 selectivities. According to their report, Fe_3O_4 to FeC_x precursors are sufficient for the formation of the required active sites. The active sites are formed during activation by favoring the nucleation of smaller Fe_3O_4 and FeC_x domains as Fe_2O_3 precursors and these convert to active catalysts with synthesis gas.

The existence of diffusion limitations inside catalyst particles has been reported (Anderson, RB et al. 1952; Lox 1987) but the evidence is in general of a qualitative nature and is rather limited compared to the abundance of literature available on other aspects of the Fischer-Tropsch process. The theory of particle size effect was based on the assumption that the catalyst metal particle of a certain size led to a strict maximum chain length of the produced hydrocarbons (Nijs and Jacobs 1980). In addition, it has long been known that the finer particles contain more Boudouard carbon, more iron carbide and less iron oxide than the courser particles (Dry 1981). In addition, Lox (Lox 1987) studied the occurrence of concentration gradients of synthesis gas in larger particles of this porous catalyst which had been predicted on theoretical grounds; the experimental data, however, did not permit quantitative interpretation of the particle size effects observed. Generally, a good catalyst for liquid phase FTS reaction must be with large pores to reduce the pore diffusion resistance. On the other hand, the large surface area of catalyst support is favourable to increase metal dispersion, leading to high CO conversion of the supported FT metal catalysts. Unfortunately, a higher surface area means a smaller pore size, and the stronger pore resistance. Furthermore, the shape and size of the pore can affect the reaction pathways (Iglesia, Reyes et al. 1991). Bolian Xu et al. proposed that the smaller metal particle gave higher metal surface area and higher surface catalytic activity. On the contrary, the large particle catalyst had lower surface activity (Bolian and Yining 2005). In other words, the smaller particle catalysts have a greater external surface area, and hence a greater rate constant per mass of catalyst with comparing a larger particle catalysts. Post and co-researchers (Post, Hoog et al. 1989) conducted a study with a number of iron and cobalt catalysts, in which they have evaluated the effects of catalyst particle size and pore diameter on rates of carbon monoxide and hydrogen conversion. Intraparticle diffusion can be a limiting factor for the overall reaction

rate due to particle size. Studies with porous iron catalysts under conditions which ruled out external mass transfer effects have confirmed the occurrence of diffusion limitation and made it plausible that diffusion of reactants and product molecules through liquid-filled pores is the determining factor in intraparticle transport of mass. For Fischer-Tropsch catalysts with the usual chemical activities this means that intraparticle diffusion starts to play a role for particle diameters greater than about 0.5 mm. Intraparticle diffusion is therefore an important factor to be taken into account in choosing catalyst particle size and shape for a fixed-bed Fischer-Tropsch process, in addition to pressure drop and heat transfer consideration (Sie and Krishna 1999).

The effect of particle size on reaction rate can be quantified using the well-known relation between effectiveness factor and the Thiele modulus. The effectiveness factor is defined as the ratio between observed rate constant and the intrinsic rate constant. The diffusion constant appearing in the Thiele modulus should be considered as an apparent effective diffusivity of hydrogen, based on gas-phase concentrations, to be used in combination with the current kinetic expression.

Most studies have proposed that the primary reaction and secondary reactions as mentioned above were considered to be on only one active site of the catalyst (Anderson 1984; Donnelly 1985; Guo and Liu 2006; Botes 2007; Wang and Wang 2007). However, Jie Chang et al. in 2007 have published three kinds of reactions that take place on separate active sites of a catalyst. These three active sites were named site θ, site σ and site ψ, respectively (Jie., Liang. et al. 2007). As shown in Figure 2.11, the primary olefins are considered to be able to re-adsorb onto the catalyst surface, and then re-enter as propagation species on site θ. In addition, it is possible to hydrogenate directly to produce paraffins on site σ. The difference between the model proposed by Jun Yang et al. and that proposed by Jie Chang et al. is a number of active sites; the former model was considering two active sites, θ and ψ, and the latter model was developed three active sites, θ, σ, and ψ.

Secondary hydrogenation:

$C_nH_{2n} + H_2 \rightarrow C_nH_{2n+2}$

Primary olefins:

$nCO + 2nH_2 \rightarrow C_nH_{2n} + nH_2O$

WGS reaction:

$CO + H_2O \leftrightarrow CO_2 + H_2$

Re-enter propagation:

$C_nH_{2n} \rightarrow C_{n+1}$ Propagation species

Active site θ

Active site σ

Active site ψ

Fe-Cu-K-SiO$_2$

Primary propagation:

$nCO + 2n+1H_2 \rightarrow C_nH_{2n+2} + nH_2O$

Feed gas: CO + H$_2$
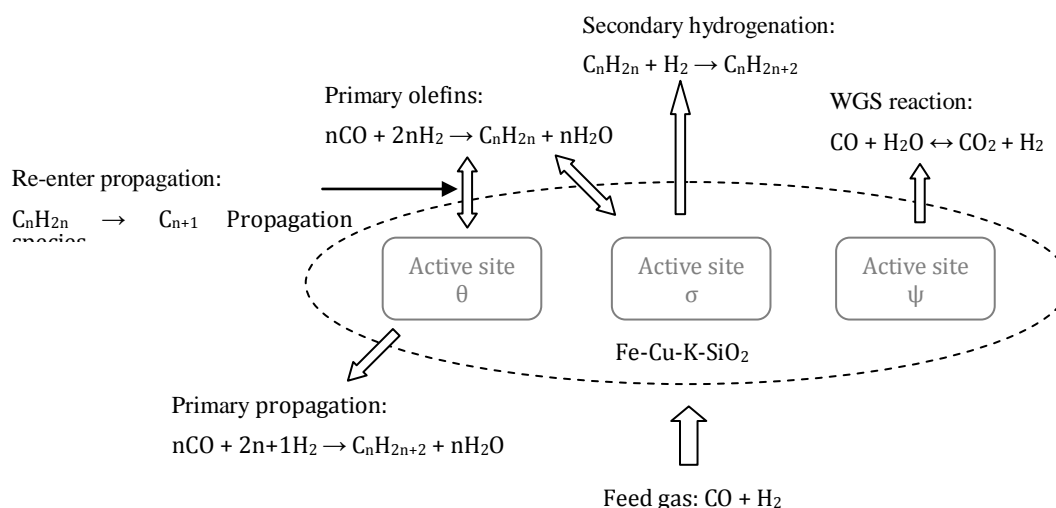
FIGURE 2.11 Kinetic scheme of FTS, secondary hydrogenation reaction, and WGS on Fe-Cu-K-SiO$_2$ Catalyst (Source: Jie Chang, 2007)

Jie Chang et al. suggested that active sites θ and σ are responsible for paraffins primary and olefin primary & secondary reaction, respectively, while Jun Yang et al. considered that both paraffin and olefin primary reactions occurred at the θ active site. Considering the active sites on catalyst, the rate expressions for hydrocarbon formation may predict quite well the experimental data. All the previously mentioned models suffer from some serious weaknesses; however Jun Yang et al. point out that the kinetic parameters were evaluated by the global optimization on Fe-Mn catalyst and their model focuses on re-adsorption and secondary reaction of olefins in the reactor modeling. In addition, there are known to be two types for FTS of uniformly distributed active sites respectively for primary, secondary and WGS reactions on the catalyst surface (Yang 2004).

The water gas shift reaction is considered on site ψ. Several researchers have suggested that the magnetite (Fe$_3$O$_4$) is the most active site for the WGS reaction on iron catalysts (Newsome 1980; Zhan and Schrader 1985; Lox and Froment 1993; Rao, Huggins et al. 1995). Rao and Huggins (Rao, Huggins et al. 1995) studied the iron phases of Fe-Cu-K-SiO$_2$ and found that the changes of magnetite phase corresponded to the WGS reaction activity. Lox (Lox and Marin 1988) showed that Fe$_3$O$_4$ coexists with various iron carbides on the catalyst during synthesis gas reactions. It is generally assumed that the WGS reaction and the Fischer-Tropsch reaction proceed using different active sites. The development of

a kinetic model with the assumption that the primary paraffins and olefins react on separate active sites may well improve the prediction of product selectivities and in particular, it may able to account for the primary olefins re-entering the carbon chain growth.

Schulz and Claeys (Schulz and Claeys 1995) illustrate that co-feeding of olefins generally results in unchanged or decreased methane selectivity. The chain growth for the formation of a C_1 species is generally negligible at Fischer-Tropsch reaction conditions. Chain initiation by co-feed olefins is widely observed in literature (Hanlon and Satterfield 1988). Hanlon and Satterfield (Hanlon and Satterfield 1988) observed an increased selectivity of C_{3+} hydrocarbons with addition of ethylene on an Fe-K catalyst. Likewise, addition of 1-butene or 1-hexene resulted in a minor increase of the yield of high molecular products, suggesting olefins to act as chain initiators. Addition of ethylene and ethanol also resulted in a lower methane selectivity because the hydrogenation of olefins on the catalyst was decreased by ethanol and ethylene on catalyst surface according to Hanlon and Satterfield (Hanlon and Satterfield 1988). Addition of olefins and ethanol resulted in a change of the chain growth factor. The termination reaction is generally accepted as the most important secondary reaction of 1-olefins. As such, it controls the probability of chain termination giving an olefin product, leading to a higher chain growth probability and higher paraffin selectivity. Furthermore, the re-adsorption of olefins becomes more effective with increasing chain length (Gerard 1999). This results in a curved product distribution, in which the selectivity towards heavy products is higher than expected from the ASF distribution (Eqn. 2.30). Insertion of co-feed olefins was considered by many authors (Hanlon and Satterfield 1988; Iglesia, Reyes et al. 1993) and is known to reverse the chain termination step to olefins which increases the chain growth probability and decreases the olefin content of the products. Liu et al. (2008) investigated the effect of co-feeding CO_2 on the catalytic properties of an iron-based catalyst. They found that the co-feeding CO_2 can significantly increase the water formation rate and that it does not influence the hydrocarbon formation rate significantly. Moreover, Hilmen et al. (Hilmen, Schanke et al. 1999) also described co-feeding of water, however they focused on deactivation of cobalt-based catalyst with co-feeding of water during Fischer-Tropsch synthesis under specific condition.

Li et al also observed a decrease in CO conversion by co-feeding of water (Li, Y et al. 2002). Patzlaf et al. (Patzlaf, Liu et al. 2002) studied the effects of 1-alkene re-adsorption and secondary chain growth on the product distribution of FTS on iron catalyst by co-feeding of 1-alkenes. In general, co-feeding of water is used to test the deactivation of cobalt-based catalyst; otherwise co-feeding is only limited to particular components like only CO_2.

2.3.6 REACTOR CONSIDERATION

The mechanisms mentioned above are developed for both two-phase and three-phase reactors. The designs of a Fixed-bed and slurry-bed reactor of Fischer-Tropsch synthesis require a careful balance between conversion, pressure, activation, mass and energy transfer. The two-phase reactors such as the fixed-bed reactor has low conversion per pass and the three-phase reactor, slurry bed reactor has a higher conversion per pass. The development of rate expressions for the conversion of CO to Fischer-Tropsch products and for the WGS reaction over a precipitated iron catalyst for fixed-bed reactor as a two-phase reactor based on realistic reactors is reported by many researchers (Bub and Baerns 1980; Bukur, Patel et al. 1990; Eliason and Bartholomew 1999; Yang 2004; Davis 2005). The slurry bubble column is a kind of the three-phase reactor, where the catalyst is kept in a liquid suspension with synthesis gas bubbling through it.
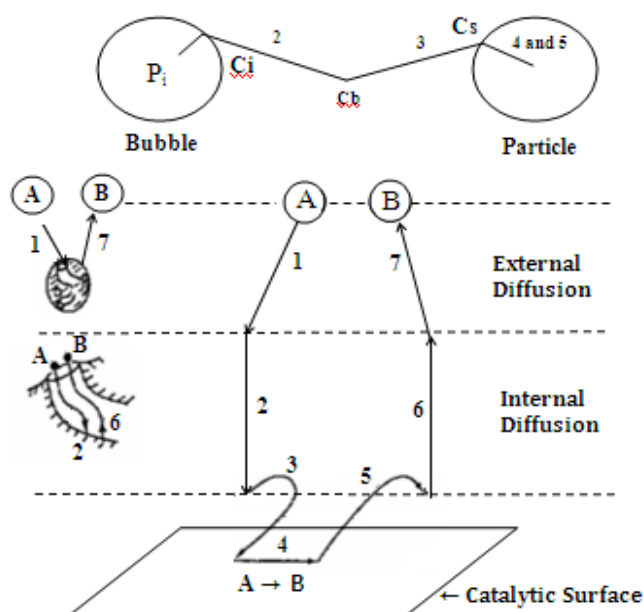
FIGURE 2.12 Gas-Liquid-Solid Contact in a Three-phase Reactor (Hopper 1982)

Figure 2.12 shows the mechanism of three phase reactions. Gaseous reactant A reacts with non-volatile liquid reactant B on solid catalyst sites and the three phase reaction proceeds through the following seven steps:

(1)   Mass transfer of component A from bulk gas to gas-liquid interface

(2)   Mass transfer of component A from gas-liquid interface to bulk liquid

(3)   Mass transfer of A and B from bulk liquid to catalyst surface

(4)   Intra particle diffusion of species A and B through the catalyst pores to active sites.

(5)   Adsorption of one or both of the reactant species on catalyst active sites

(6)   Surface reaction involving at least one or both of the adsorbed species

(7)   Desorption of products, (the reverse of the forward steps)

However, the three-phase reactor needs to have an internal cooling system and is more expensive than the two-phase reactor. This study deals with both reactors in order to consider economic comparison and performance comparison (Satterfield and Huff 1985). The three-phase reactor is attracting more and more interest because of its advantages relative to other reactor types. The basic reaction and kinetics are the same for both two-phase and three-phase reactors, with the only difference being the mass transfer and any effects that the solubility of the species in the liquid phase has on the surface concentrations. In fact, three phases are involved in this reaction where the gas phase (synthesis gas) is the reactant, the liquid phase (mixture of linear paraffins) is the reaction products and the solid phase is the catalyst on which the reaction occurs as shown in Table 2.9. However, the challenges of this reactor type are the required catalyst separation from the liquid products and the highly demanding scale-up (Wang and Wang 2007). Additionally, because the reactions in question are highly exothermic, cooling coils are provided in the reaction zone, contacting the liquid phase with cooling medium, normally in the form of steam generation.
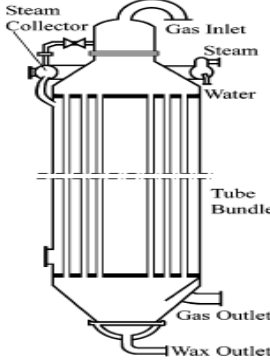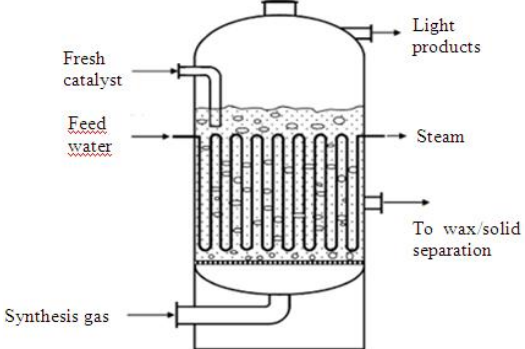
A primary difference is the preferred conversion level. The slurry reactor, because of its superficial velocity limitation, fits best into the high conversion end

of the scale where the recycling to fresh feed ratio is low, the only limitation of mass transfer being that due to back mixing (Yang, Kim et al. 2010). The fixed-bed reactor of the quenched or intercooled variety requires a high recycling ratio to limit the temperature rise, but even the externally cooled, tubular design requires a high mass velocity to achieve good heat transfer characteristics. A recycling to fresh feed ratio of at least 2 is preferred with pressure drop being the limiting factor.

Cooling surface requirement in a slurry reactor is less than a quarter that in a tubular fixed-bed reactor. This is partially because the heat transfer film coefficient is improved but also because a higher ΔT is permissible between reactants and coolant. In the tubular fixed-bed reactor, hydrogen content of the gas improves the heat transfer coefficient significantly, another reason why that reactor may not be a good choice for very low H_2/CO ratio gases.

Increasing pressure has significant advantages for either type of reactor, regardless of its effect on kinetics or equilibrium. At lower pressure, more slurry reactors are required because of the superficial velocity limitation. In the fixed-bed case, the limitation on superficial velocity is pressure drop. The higher the pressure, the higher the permissible superficial velocity, so there is a double advantage. A high mass velocity is required for good heat transfer and this can more readily be achieved at high pressure. Higher pressure will permit a higher recycling ratio to be used without causing an increase in compressor horsepower. In either case, the vessel must be designed for the higher pressure but in the fixed-bed case the shell thickness is set by steam pressure rather than reaction pressure so there is less of an effect on cost.

The Table 2.8 described the comparison on fixed bed reactor and slurry bed reactor.

Reactor Model	Fixed-Bed Reactor	Slurry Bed Reactor
Definitions	Gas or liquid reactants flow over a fixed bed of catalysts	Liquid is agitated by means of the dispersed gas bubbles. Gas bubble provides the momentum to suspend the catalyst particles.
Classification	Heterogeneous - Catalytic Two Phase (Gas-Catalyst or Liquid-Catalyst)	Heterogeneous - Catalytic Three Phase (Gas-Liquid-Catalyst)
Types		
Advantages	-. The fluid flow regimes approach plug flow, so high conversion can be achieved. -. Pressure drop is low -. Owing to the high hold-up there is better radial mixing and channelling is not encountered. -. High catalyst load per unit of reactor volume	-. Ease of heat recovery and temperature control -. Ease of catalyst supply and regeneration process -. Low intra-particle resistance -. High external Mass transfer rate (Gas-Liquid and Liquid Solid)
Disadvantages	-. The intra-particle diffusion resistance is very high. -. Comparatively low Heat and mass transfer rates -. Catalyst replacement is relatively hard and requires shut down.	-. Axial mixing is very high -. Catalyst separation may require filtration. -. High liquid to solid ratio may promote liquid side reactions -.Low catalyst load.
Cost		Low construction and operation cost

TABLE 2.8 Comparisons on FBR and SBR

2.4 OVERALL FISCHER-TROPSCH PROCESS

This section presents the overall Fischer-Tropsch process which includes Fischer-Tropsch reactors based on the kinetics of the two-phase and three-phase models (as mentioned at Section 2.2). The Fischer-Tropsch process studies should not consider only the kinetic models but also the development of the FT reactor. For example, the addition of recycling and co-feeding could give a higher production rate of hydrocarbons than a pure feed operation. The recycling here is to circulate both unconverted synthesis gas and water (which are recovered with a separation unit) to the synthesis gas preparation unit or to the Fischer-Tropsch reactor. In addition, the co-feeding is a process where undesirable by-products are passed through the Fischer-Tropsch reactor which leads to the increased production of paraffins and oxygenates through secondary reactions. The effects of co-feeding have been discussed by a number of authors (deKlerk 2006; Gaube and Klein 2008). Consequently, the Fischer-Tropsch process can be considered using both co-feeding of unreacted reactants and recycling of undesirable products such as CO_2 and lighter hydrocarbons over iron-based catalysts. The Fischer-Tropsch products from an upgrading unit are transportation fuels such as gasoline and diesel (Seo, Oh et al. 2000; Davis 2005) and to date, there has been no development of FT reactors integrated with an upgrading facility. The light, saturated hydrocarbon product gases such as methane and ethane that can be used neither as chemical feedstocks nor as transportation fuels. Hence, the selectivity towards these gases and other undesirable components in the hydrocarbon products should be minimized. In addition, a recycling process to synthesis gas is operated in Fischer-Tropsch plants in order to increase the overall synthesis gas conversion because the plants operate at low conversion (Peter, Diane et al. 2006).

J Gaube showed that the co-feeding of alcohols leads to an increased rate of hydrocarbon formation (Gaube and Klein 2008), and P. Mukoma pointed out that the objective of the recycling process is to achieve higher reactor productivity using higher synthesis gas flow rates (Peter, Diane et al. 2006). The most important reason for operating a recycling process is to reduce capital and operating costs and the objective of recent developments in Fischer-Tropsch

plants has been to reduce costs. PJ Kuchar reported that co-processing of light hydrocarbons can be a cost effective way to achieve the optimum gasoline production (Kuchar, Bricker et al. 1993).

There are three distinct recycling and co-feeding options: recycling to the reforming unit, recycling to the FT reactor or to use normal FT reactors in series.

In one of the first studies of this type, Daniel (Daniel 1989) investigated a process for recycling condensates from a hydrocarbon or alcohol synthesis back to the steam reformer. The condensates consisted here of water and organic compounds such as alcohols and hydrocarbons. Arno de Klerk (deKlerk 2006) proposed that the product yield can be increased by recycling some of the by-products from the process and co-feeding into the reformer producing more synthesis gas (Figure 2.13).
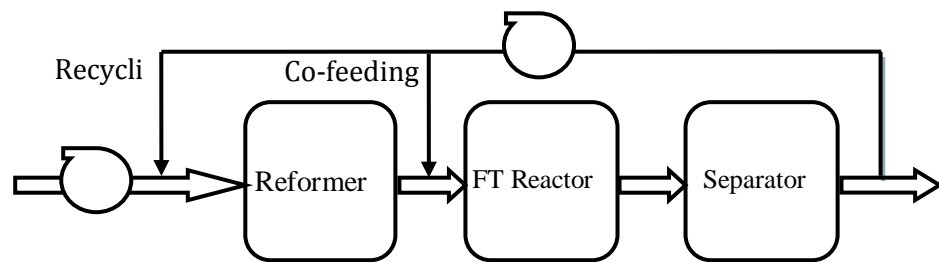
FIGURE 2.13 A schematic diagram of Recycling and Co-feeding to reformer

Additionally, Peter et al. (Peter, Diane et al. 2006) suggested that it is possible to evaluate two processes, the once-through process and the process recycling and co-feeding into the reformer that produces synthesis gas, and their efficiencies. It is observed that, for a fixed production rate of liquid fuels at 100% conversion, the carbon efficiency for the process with recycle stream is higher than that of the once-through process for all values of α.The results presented in Figure 2.14 show that, the maximum carbon efficiency for both processes is the same, at 85%, achieved at the highest α value (α=1), at which no lighter gases are produced. It is thus possible to achieve the same carbon efficiency using either of the two processes; however, carbon efficiency values achieved in the process with a recycling stream at lower α values will only be achievable at higher α values in a once-through process. At α = 0.35-0.85, there is a big difference in the value of

carbon efficiency obtained in the two processes at the same α values. However, at α = 0.95-1, it is apparent that it does not matter what process configuration is used to achieve this α value, because very similar carbon efficiencies can be achieved either way (Peter, Diane et al. 2006).
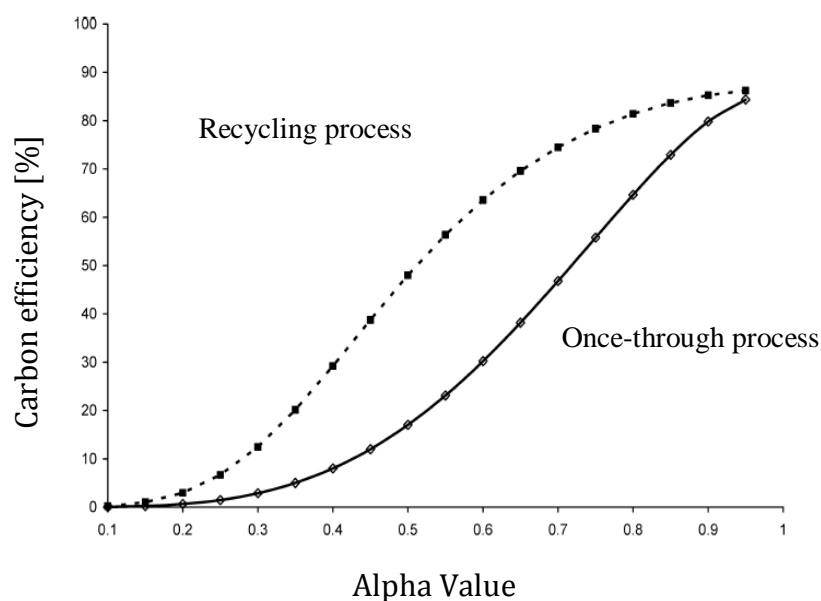
FIGURE 2.14 Comparison of carbon efficiencies at different α values in once-through and recycling processes at 100% conversion. (Peter, Diane et al. 2006)

Any decrease in the rate of CO conversion affects the carbon efficiency of the once-through process negatively. Because this analysis is based on the production of a fixed amount of hydrocarbons, in a once-through process, any amount of carbon lost through unconverted synthesis gas that was produced at great material and energy costs must be compensated for by an increase in the feed materials required to maintain the production rate. In a recycling process to reformer, the unreacted synthesis gas in the recycling loop that joins the feed stream improves the amount of hydrocarbon products and, hence, does not affect the overall conversion and carbon efficiency. Although there is an energy cost to recycling and reforming, this is small, compared to the cost of material lost in the once-through process (Peter, Diane et al. 2006). They note that if we regard all C_{5+} products as being equally valuable, they would like to operate both once-through and the recycling process at the highest possible α value.

Exxon Research and Engineering Company investigated a process for recycling and purifying condensate from a hydrocarbon to the Fisher-Tropsch reactor (Exxon 1990) in order to increase the product yield. The Fischer-Tropsch reactor was investigated by Rafael et al. that lowers the average molecular weight of the hydrocarbon liquids inside the reactor, and more preferably by recycling a portion of low-molecular weight hydrocarbon products back into the reactor. Lowering the molecular weight of the hydrocarbon liquids inside the reactor increase the mass transfer and solubility, and diffusivity of the reactants in the hydrocarbons present (Rafael, A et al. 2003). In principle, the recycling compounds can be sent to a Fischer-Tropsch reactor. Schematic diagram of recycling and co-feeding to FT reactor is shown in Figure 2.15.
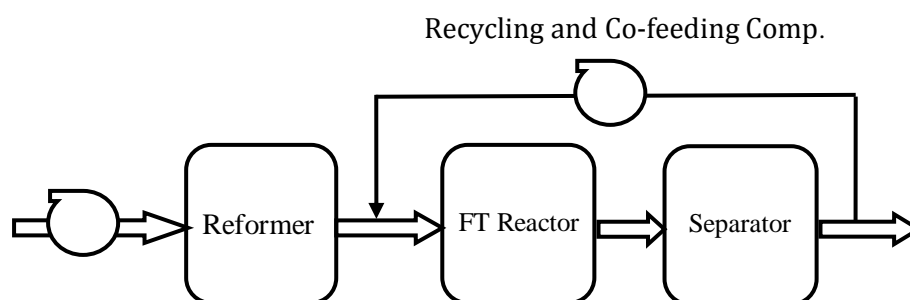
FIGURE 2.15 Schematic diagram of Recycling and Co-feeding to Fischer-Tropsch reactor

The third choice of using reactors in series (especially if the same volume reactors are to be used) is complicated by the fact that additional fresh synthesis gas might have to be added to the synthesis gas that is leaving the previous reactor to obtain the required feed rate. The series reactors provide a number of practical reasons for using two or more small reactors rather than one large reactor. Temperature control is better in smaller reactors and inter stage cooling can be used. It is often advantage to mix and match reactors. Raje and Davis (1997) concluded that processes utilizing a series of reactors achieve CO conversions of over 90%. In other words, higher overall synthesis gas conversions can be achieved by using FT reactors in series; however, this process would have disadvantages including increased design and engineering cost. In addition, the recycling process to series Fischer-Tropsch reactor was investigated by Ajoy P Raje

and Burtron H. Davis (Raje and Davis 1997). The results inferred that the yield of products can be significantly enhanced by a lower single-pass reactor CO conversion with recycling of unconverted synthesis gas or by using reactors in series.
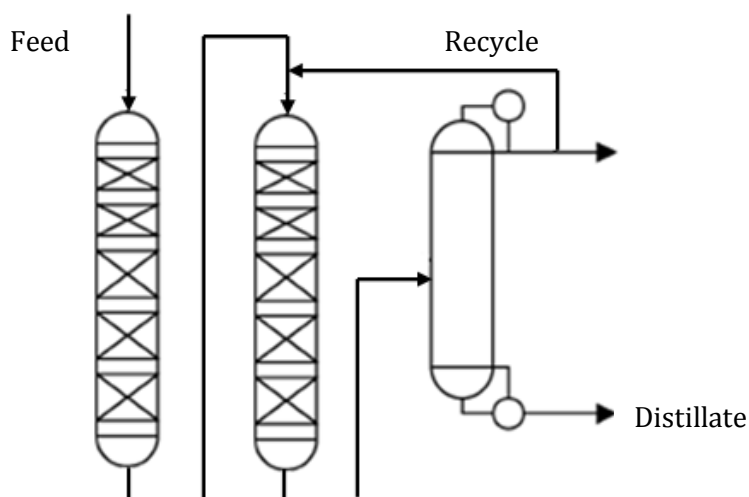
FIGURE 2.16 Recycling operation for distillate production by AP Raje and Burtron.

Figure 2.16 shows recycling operation using two reactors. They considered two reactors with equal sizes and catalyst loadings. The first reactor is single-pass reactor and the second reactor operated with recycling. The recycling reactor can process more than double the volume of synthesis gas per weight of iron and produces twice as much hydrocarbon as the single-pass reactor. Further, the yields of intermediate range linear alkenes are increased by the use of recycling (Raje and Davis 1997). The research that was investigated by Arno de Klerk, gives a strong indication that it can be worked to improve distillate yield beyond 70% by a recycling process. This is contrary to what is known from tetramer-mode[7] operation as feed. The tetramer-mode operation is same process with normal FT once-through process. This limitation on distillate yield, however, has indeed been found commercially, where one of the SASOL Synfuels refineries in South Africa is operated in such a mode (deKlerk 2006). He found that changing the reactor configuration from tetramer-mode to split-mode[8] had no effect in terms of reactor productivity. These modes of reactor are referred Figure 2.17 and 2.18,

[7] Tetramer-mode: formation of four sub-units
[8] Split-mode: division of more than one

respectively. Both modes of operation resulted in the same production rate of distillate per mass of catalyst, 0.23 and $0.22kg_{distillate}/kg_{catalyst}h$, suggesting that the overall distillate yield is dependent on catalyst contact time as well (deKlerk 2006). Moreover, deKlerk proposed that it is difficult to manage heat energy in the first reactor and the same principle can be applied to other mixture of short chain olefins, but it will be quantitatively different.
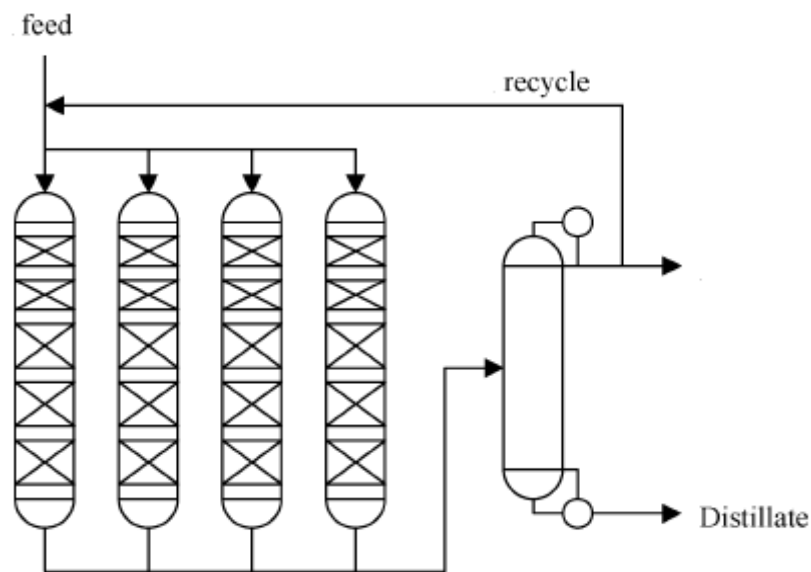
FIGURE 2.17 Recycling (tetramer-mode) operation for distillate production (deKlerk 2006)
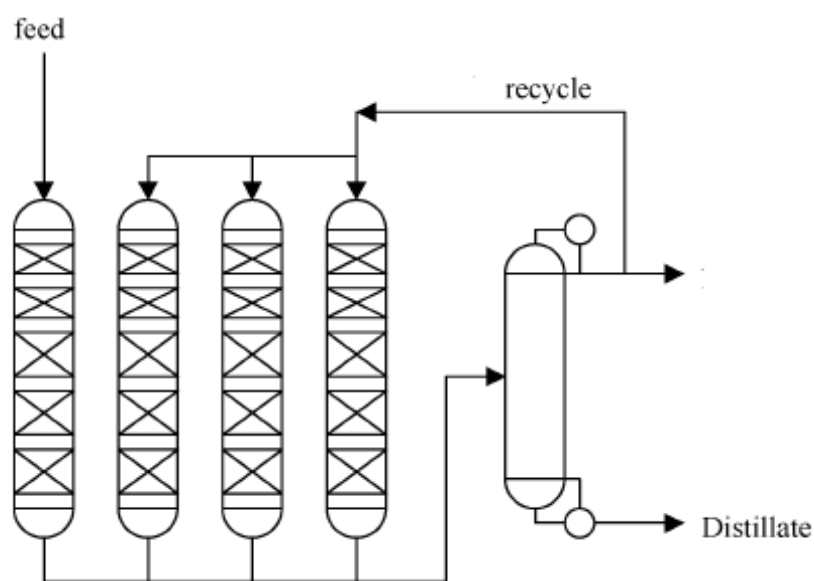
FIGURE 2.18 Separate processing (split-mode) operation for distillate production (deKlerk 2006)

Among other things, Arend and Joris reported the optimisation of multi-stage slurry Fischer-Tropsch process (Arend and Joris 2007). Each of the stages may comprise more than one slurry bubble column in parallel. As can be seen from the Figure 2.19, the gaseous product stream of the first stage is fed, after a condensing stage for condensing heavy components and optionally water, to the second stage and so on for further stages. It is mentioned that a portion of the unreacted gas of a stage may be recycling back to mix with the inlet gas of that stage.
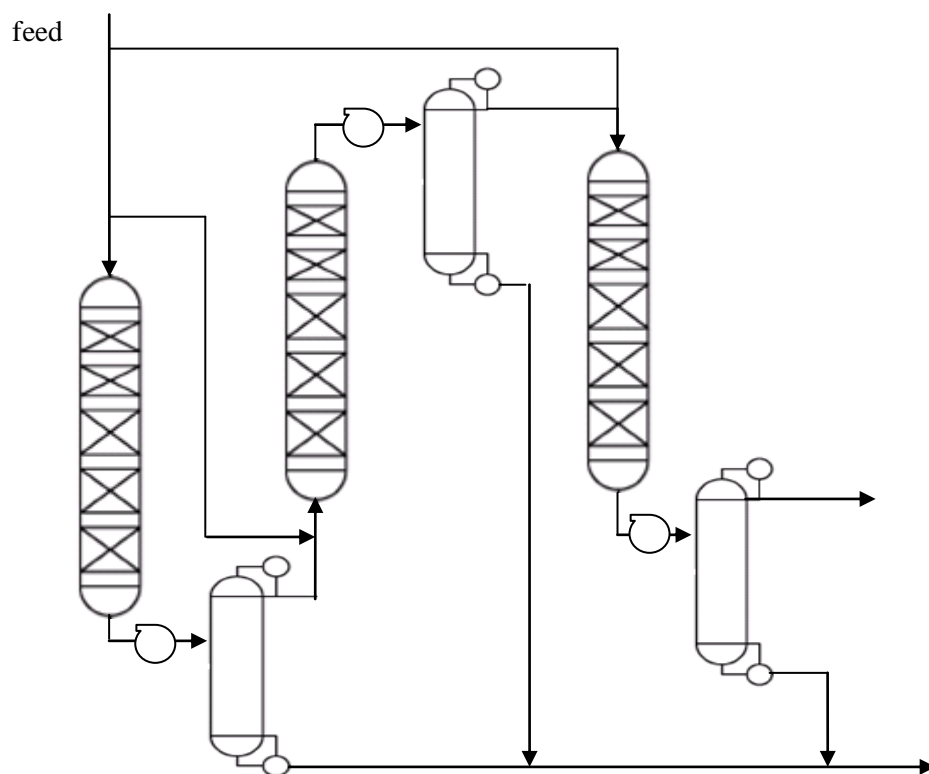
FIGURE 2.19 Multi-stage slurry Fischer-Tropsch separate process

The inert produced in a stage, such as paraffins (C_1-C_4) and CO_2, will slow the reaction in the following stage. Furthermore, recycling of tail gas over a stage will cause a build up of inert which were already present in the feed gas to that stage, such as for example nitrogen. A two-stage Fischer-Tropsch process is described wherein a first synthesis gas having a H_2/CO ratio in the range of 1.4 to 1.75 is fed to a first Fischer-Tropsch synthesis reactor, a second synthesis gas is recovered from the effluent of the first reactor and mixed with a third synthesis gas having a H_2/CO ratio of at least 2.0 and the blended second and third synthesis gas is fed

into a second Fischer-Tropsch reactor. In order to compensate for the decreased yield in a second stage Fischer-Tropsch reactor due to inert build up, one could:

(1)   increase the temperature in the second stage; or

(2)   increase the pressure in the second stage.

In case of the consideration for multi-stage reactor (Arend and Joris 2007), to increase the pressure in second stage compressors or the like are required which may not be economically viable and so increasing the temperature in the second stage is deemed the more viable solution. A problem, however, with the increased temperature in the second stage is the increase in unwanted CO_2 production and a lower C_{5+} selectivity. The total carbon monoxide conversion in a multi-stage Fischer-Tropsch reactor system is typically greater than 80%, and often exceeds 90%. In addition, the productivity in the second stage reactor was lower than in the first stage reactor. The ratio of the amount of carbon monoxide is lower in the second stage compared to the first stage. Therefore, they proposed that in order to obtain productivity in the second stage, the stage reactor preferably contains a catalyst with a shorter diffusion path length than that of the first stage reactor such as catalyst particles with a smaller diameter or of a different shape.

2.5 SUMMARY

The reaction mechanisms of the Fischer-Tropsch synthesis are not yet fully established. Further research should concentrate on development of mechanistic rate expressions based on reliable mechanism. However, the reaction mechanisms of Fischer-Tropsch synthesis consists of several steps; primary reactions of chain initiation and chain propagation, secondary reactions of hydrogenations, water-shift-gas reaction, re-adsorption. The WGS reaction is important for iron catalyst at low H_2/CO ratios. Only a few authors reported on the WGS kinetics on iron catalysts under FT conditions. Therefore, development of WGS kinetic expressions from intrinsic kinetic experiments requires additional research.

The reaction conditions and some of the characteristics for both the two-phase and three-phase reactors of the above discussed authors are summarized in Table 2.15. As mentioned above, the model proposed by SA Eliason et al. fails to obtain correct rate constants and does not consider oxygenated hydrocarbons with propagation only through the addition of CH_2 species. The model by developed Yi-Ning Wang et al. also has a number of limitations. It was developed for the study of heavier hydrocarbons and considered only hydrocarbons produced by the primary reactions. Therefore, it is not an appropriate kinetic model for the production of diesel and gasoline as mentioned in Chapter 1 and it would be difficult to estimate the carbon distribution without considering the WGS. Moreover, Yuan-Yuan Ji failed to account for the effect of olefin re-adsorption and Xiaohui Guo et al. developed the model further using a simplified carbide mechanism; however the predicted carbon distributions did not fit well with experimental data. In addition, the study by Bo-tao Teng et al. might have been much more useful if they had considered CH_2 insertion in addition to the alkyl and alkenyl mechanisms focusing on primary and secondary reactions. However, the interesting point is that the experimental distributions of paraffins, olefins, alcohols and acids were considered when developing the kinetics model. In contrast to other authors, the proposed mechanism and model of Jie Chang et al. was developed with consideration for active sites on the catalyst for primary, secondary and WGS reactions. Subsequently Jun Yang et al. developed re-adsorption and secondary reaction models with the kinetics of chain growth and termination and most importantly,

they combined FTS and WGS into their model. Finally, the model proposed by AN Fernandes considered the polymerization kinetics of Fischer-Tropsch reactions on an iron based catalyst using alkyl and alkenyl mechanisms acting together to give hydrocarbon chain growth (Fernandes 2005). However, the model might have been much more persuasive if he had adopted the oxygenate formation proposed by Bo-Tao Teng. Furthermore, Jie Chang's model would have been more useful for finding the influences of catalyst surface if the three-phase model had been modified to account for the effects of various reaction conditions such as particle size, active sites on the catalyst and the reactor size. Considering all these models and their limitations the most promising are, the kinetic models by Jun Yang et al. and AN Fernandes which could be developed further to account for effects such as catalyst type and product distributions for both alcohols and acids which are not considered in their models.

Finally, the adsorption of both CO and H_2 (2.74, 2.75 and 2.76) are included in the proposed mechanism because the above mentioned mechanisms are considered to be the first step of the Fischer-Tropsch synthesis and their adsorption leads on to the side reactions, the formation of hydrocarbons and the water gas shift reaction. In the chain initiation steps, reactions including the formation of both methylene and methyl are also considered in the mechanism (2.77-2.80). This is because polymerization kinetics is based on the monomers of methyl and methylene. Furthermore, methanation, chain growth, hydrogenation and dehydrogenation should also be included to further develop the proposed mechanism. As mentioned above, the Fe_3O_4 and Fe_2C_3 precursors on active sites θ, σ and ψ provide higher surface areas and a higher CO conversion. The iron-based catalyst with the precursors produces significantly lower CH_4 and CO_2 selectivities than pure Fe-catalysts. However, Fe_2O_3 should be produced by controlled oxidation of Fe_3O_4 because Fe_3O_4 provides active sites for the water gas shift reaction. Iron carbide and iron oxide which provide higher active sites on the catalyst, are conversed by Fe. Fe_3O_4 provides active sites, θ and ψ, for hydrocarbon production and water gas shift reaction, respectively. FeC_x also provides active site σ for re-adsorption.

Table 2.9 shows a summary of the proposed FT reactions on site θ. and Table 2.10 shows the general secondary hydrogenation on site σ which was proposed by Jie Chang et al. The accepted mechanism for the water gas shift reaction on catalyst site ψ is summarized in Table 2.11 and Table 2.12 provides the catalyst specific reactions of Fe_2O_3, Fe_3O_4 and FeC_3.

	Primary reaction on site θ
Adsorption	
2.74	$CO + s_\theta \leftrightarrow COs_\theta$
2.75	$COs_\theta + s_\theta \leftrightarrow Cs_\theta + Os_\theta$
2.76	$H_2 + 2s_\theta \leftrightarrow 2Hs_\theta$
Surface reactions	
Chain initiation	
2.77	$Cs_\theta + Hs_\theta \leftrightarrow CHs_\theta + s_\theta$
2.78	$CHs_\theta + Hs_\theta \leftrightarrow CH_2s_\theta + s_\theta$
2.79	$CH_2s_\theta + Hs_\theta \leftrightarrow CH_3s_\theta + s_\theta$
2.80	$CH_3s_\theta + s_\theta \leftrightarrow CH_2s_\theta + 1/2H_2$
Oxygenate formation	
2.81	$COs_\theta + 2Hs_\theta \leftrightarrow CHOHs_\theta$
2.82	$COs_\theta + Hs_\theta \leftrightarrow CHOs_\theta + s_\theta$
2.83	$CHOs_\theta + Hs_\theta \leftrightarrow CHOHs_\theta + s_\theta$
2.84	$CHOHs_\theta + H_2 \leftrightarrow CH_2s_\theta + H_2O$
2.85	$CHOHs_\theta + Hs_\theta \leftrightarrow CH_2OHs_\theta + s_\theta$
Methanation	
2.86	$CH_3s_\theta + Hs_\theta \rightarrow CH_4 + 2s_\theta$
Chain growth	
2.87	$C_nH_{2n+1}s_\theta + CH_2s_\theta \rightarrow C_{n+1}H_{2n+3}s_\theta + s_\theta$
Hydrogenation to paraffins	
2.88	$C_nH_{2n+1}s_\theta + Hs_\theta \rightarrow C_nH_{2n+2} + 2s_\theta$
β-Dehydrogenation to olefins	
2.89	$C_nH_{2n+1}s_\theta \leftrightarrow C_nH_{2n} + Hs_\theta$

TABLE 2.9 Primary elementary reactions for Fischer-Tropsch synthesis on catalyst active site θ

	Secondary reaction on site σ
2.90	$CO + s_\sigma \leftrightarrow COs_\sigma$
2.91	$C_nH_{2n} + Hs_\sigma \leftrightarrow C_nH_{2n+1}s_\sigma$
2.92	$C_nH_{2n+2} + 2s_\sigma \rightarrow C_nH_{2n+1}s_\sigma + Hs_\sigma$

TABLE 2.10 Secondary reactions for Fischer-Tropsch synthesis on catalyst active site σ

	Primary reaction on site ψ
Water formation	
2.93	$CO + s_\psi \leftrightarrow COs_\psi$
2.94	$Os_\psi + Hs_\psi \leftrightarrow HOs_\psi + s_\psi$
2.95	$HOs_\psi + Hs_\psi \rightarrow H_2O + 2s_\psi$
2.96	$Os_\psi + H_2 \rightarrow H_2O + s_\psi$
2.97	$H_2O + s_\psi \leftrightarrow H_2Os_\psi$
2.98	$COs_\psi + H_2Os_\psi \leftrightarrow CO_2\ s_\psi + H_2s_\psi$
2.99	$2COs_\psi \rightarrow Cs_\psi + CO_2\ s_\psi$
2.100	$CO_2 + s_\psi \leftrightarrow CO_2\ s_\psi$

TABLE 2.11 Primary elementary reactions for Fischer-Tropsch synthesis on catalyst active site ψ

	Catalyst specific reactions	Operation conditions
Fe		
2.101	$2Fe + O_2 \rightarrow 2FeO$	
Fe$_2$O$_3$ (active site θ)		
2.102	$2Fe + 3/2\ O_2 + H_2O \rightarrow 2\ FeO(OH)$	200 ℃
2.103	$2FeO(OH) \rightarrow Fe_2O_3 + H_2O$	
2.104	$2Fe + 3CO_2 \leftrightarrow Fe_2O_3 + 3CO$	
Fe$_3$O$_4$ (active sites θ, ψ)		
2.105	$2Fe + 4H_2O \leftrightarrow Fe_3O_4 + 4\ H_2$	
2.106	$4FeO \rightarrow Fe + Fe_3O_4$	575 ℃
2.107	$3Fe_2O_3 + H_2 \rightarrow 2Fe_3O_4 + H_2O$	
2.108	$3Fe_2O_3 + CO \rightarrow 2Fe_3O_4 + CO_2$	
2.109	$2Fe_3O_4 + 1/2\ O_2 \leftrightarrow 3Fe_2O_3$	
FeC$_x$ (active sites σ)		
2.110	$X\ C + Fe \leftrightarrow FeC_x$	207 ℃

TABLE 2.12 Catalyst specific reactions for Fe-based catalysts.

The product distribution of the FTS shows significant deviations from the Anderson-Schulz-Flory distribution on iron catalyst. The ASF product distribution is changed by the occurrence of secondary reactions. Due to high CO and H_2O pressures present at FTS conditions, insertion of olefins appears to be the most important secondary reaction. The rates of these secondary reactions increase exponentially with chain length. Table 2.13 and 2.14 show the general influences of the process conditions on the selectivity and reaction conditions for mentioned models, respectively.

Parameter	Chain length	Olefin selectivity	Alcohol selectivity	Carbon deposition	Methane select.
Temperature	↓	*	↓	↑	↑
Pressure	↑	*	↑	*	↓
H_2/CO	↓	↓	↓	↓	↑
Residence Time	*	↑	↑	*	↓
Conversion	*	↓	↓	↑	↑
Iron Catalyst	↑	↑	↑	↑	↓

TABLE 2.13 Selectivity in Fischer-Tropsch synthesis by process conditions

Increase ↑ with increasing parameter, complex relation *

	Mechanism and Kinetics Models							
Conditions	SA Eliason et al.	Jie Chang	Yi-Ning Wang et al.	Yuan-Yuan Ji	Jun Yang et al.	Xiaohui Guo et al.	Bo-Tao Teng et al.	AN Fernandes
Reactor Type	FBR	SBR	FBR	FBR	FBR	SB	SBR	SBR
Catalyst	Fe, Fe-K	Fe-Cu-K-SiO$_2$	Fe-Cu-K	Fe-Mn	Fe-Mn	Fe-Cu-K	Fe-Mn	Fe-Cu-K-SiO$_2$
Temperature[K]	473-513	523	493-542	573	556	523K	533-573K	523-563K
Pressure[MPa]	1	1.45	1.09-3.09	2.25	2.51	1.09-2.45MPa	1.1-2.6MPa	1.0-2.5MPa
H$_2$/CO Ratio	1-3	0.67	0.98-2.99	1.97	2.62	0.60-1.99	0.67-2.05	0.67-1.5
characteristics	-consideration of WGS -failure to obtain rate constant -no oxygenated hydrocarbons -only propagation by adding CH$_2$ species.	-consideration of active sites(θ, σ and ψ) on catalyst - focused on secondary reaction	-higher hydrocarbon consideration (Wax) -industrial conditions operating	-failure to account for the effect of olefin re-adsorption	-re-adsorption and secondary reactions -consideration for both chain growth and termination. -combination of FTS and WGS	-Quasi-equilibrium and rate determining steps -rate constants: independent of carbon number -simplied carbide mechanism -not good fit with experimental data	-The olefin re-adsorption and secondary reactions are included in the derivation of the comprehensive kinetics model -The hydrocarbon and oxygenate formation reactions: on the same sites -All intermediates on the catalyst surface: quasi-steady state	-primary and secondary reaction -Polymerization kinetics of both alkyl and alkenyl mechanisms -systematic consideration of the carbon number dependence for the secondary reactions of primary 1-olefins -no consideration of WGS

TABLE 2.14   Reaction conditions and characteristics for the models

2.6 OBJECTIVES OF THE RESEARCH

The problem to be dealt with in this thesis is the lack of accurate models for hydrocarbon distributions and Fischer-Tropsch reaction kinetics and the reduction of capital and operating costs for scale up of industrial FT plant.

The main aim of this research is to investigate alternative process schemes in order to reduce the overall production costs, because Fischer-Tropsch plant typically installed the cost of \$400M (Davis 2005) as mentioned in Chapter 1. To minimise operating cost of Fischer-Tropsch plant and to produce transportation fuels, the Fischer-Tropsch plant is designed in order to increase system efficiency. The chosen product is gasoline(C_4-C_8) and gas oil (C_9-C_{20}) which is desirable because the prices of gasoline and gas oil are rapidly increasing and the plant should yield a lot of profit using natural gas as feedstocks as shown in Figure 1.1. In addition, these products are easily converted into other chemical compounds and optimized as part of the overall FTS. The detailed objectives of the research are as below:

- Determine optimal manufacturing process of Fischer-Tropsch synthesis

- Identify and determine kinetic models using experimental data

- Investigate alternative FT processes

- Determining optimal process conditions for different reactor designs

- Evaluate the economic impacts of the different options considered

The Fischer-Tropsch mechanism in both two-phase and three-phase reactors is proposed respectively and FT reaction is modelled qualitatively and analyzed. Also, both the two-phase and three-phase reactors with an iron based catalyst are modelled quantitatively with kinetic models developed and modified to define the influences of operational conditions on product distribution as mentioned in Section 2.3. The models developed should also include a mechanistic model of olefin re-adsorption and kinetics describing chain growth and termination on the different catalyst active sites proposed by Jie Chang et al. (See Table 2.10-2.12). The optimal process conditions from the kinetic models for both

two-phase and three-phase reactors are applied to FT plant and these models should be evaluated and validated with experimental data from literature reviews and used for various processes including both once-through and recycling & co-feeding processes without any upgrading units to increase the system efficiency and reduce operating costs as mentioned in Section 2.4. Determining the effect of co-feeding and the final fate of the paraffins C_1-C_4, and olefins C_2-C_4 recycling is the biggest challenge. The validated kinetic models for the reactor are to be applied to overall Fischer-Tropsch plant in order to predict the product distributions from the process.

Lastly, the proposed various FT plants for optimal conditions will allow the process to be evaluated considering the possibility of applying this data to real commercial plants which will provide the basis for Fischer-Tropsch plant design and scale-up in the near future.

3

Driving Force Analysis(DFA)

The Driving Force Analysis (DFA) methodology is one of a set of tools developed by BRITEST (www.britest.co.uk). BRITEST was established in the late 1990s as a joint industry and academic collaboration focused on the research and application of new methodologies for process and manufacturing design. The tools aim to create innovative whole process solutions by inspiring a step change in the way processes in the chemistry-using industries are designed and operated. The DFA methodology has been applied successfully to reaction and product formulation processes across the fine chemicals sector. Benefits from the methodology include: (I) better understanding of process and complex technical issues (II) better, more efficient plant design (III) reduced risk through knowledge sharing (IV) capturing and retention of process knowledge. The methodology of whole process design thinking can achieve: (a) reactions in minutes, not hours (b) Smaller, more flexible plant, (c) sustainable chemical processing.

3.1 DEVELOPMENT OF DRIVING FORCE ANALYSIS

Two analysis tools are used for rate processes, the Transformation Map and the Driving Force Table. The Transformation Map simply not only shows all reactions of transformations but also presents rate processes and the reversibility or irreversibility of transformations. The Driving Force Table is designed for each reactions of the Fischer- Tropsch synthesis. The first column of the tables indicates all materials involved in the Fischer-Tropsch reactions, such as products and catalysts. The reactions are divided into main primary reactions and side reaction such as H_2O formation and CO_2 formation. The end of the first column also contains factors that may affect the kinetics such as temperature, pressure, solvent polarity, ionic strength, Heat of reaction and reaction time. The Driving Force Table is easy and fast to analyze the kinetics and conversion as mentioned the various factors that affect that of Fischer-Tropsch reactions. The Table 3.1 presents the convention for showing effect of increase in a concentration and reaction using the Driving Force Analysis.

The conditions, the end part of first column, show the effect of positive or negative changes in the conditions on the kinetics. For example, temperature "+" or "-" represents a greater or lesser variation. The reaction time is the underlying reaction rate potential for rate-limiting mass transfer.

According to the explanation of the table development, it was carried out DFA that indicated analysis of each compounds' necessity for the Fischer-Tropsch reaction and mechanism, and understood the influence of selectivity products on the reaction both two-phase and three-phase mechanism for the pure feed and co-feed. The reactants and products included in each reaction were reported whether they are a positive effect or not, and it was evaluated which compounds are desired or not in the Fischer-Tropsch synthesis from DFA. The results of the DFA should be summarised to provide the focus for the experiments and later analysis.

Convention	Description
+	a 1st order reactant or an increase in the condition variable causes an increase in the reaction rate
++	a 2nd order reactant or a large positive effect for a condition variable
*	Product from an irreversible reaction. (has no effect on reaction and its presence is not required)
0	a zero order reactant. The variable shows no effect, but must be present.
-	For a moderate negative effect. (1st order for reverse reaction)
--	For a strong negative effect (2nd order for reverse reaction)
?	If there is doubt then a "?" should be used
F	<10 sec. To completion, Equivalent to a first order rate constant k of the order $1\text{-}10s^{-1}$. Examples include hydrogenations, oxidations, unhindered halogenations etc..
M	$10\text{-}10^3$ secs. First order k of $10^{-2}\text{-}1$ s^{-1}. E.g. esterifications, hindered halogenations etc..
S	$10^3\text{-}10^5$ secs. To completion, $k=10^{-4}\text{-}10^{-2}$ s^{-1}. E.g. hindered esterifications, isomerisations, substitutions.
VS	$>10^5$ secs. To completion, $k<10^{-4}$ s^{-1}. Hindered substitutions, some molecular rearrangements etc..

TABLE 3.1   Convention of Driving Force Analysis

3.2 DRIVING FORCE ANALYSIS FOR TWO-PHASE

The section is represented the driving force table of two-phase for pure feed and co-feed. The Figure 3.1 shows the transformation map for synthesis gas conversion of two-phase FTS. It illustrates the transformation on one active site from synthesis gas adsorption to chain growth and termination reactions.

Tables 3.2-3.4 illustrate, for parafins, olefins and olefins plus oxygenates, the two-phase FT reactions in both pure and co-feed arrangements. The desired reactions and processes are shown to the left of the vertical doublet in each table whilst the right hand portions show the undesirable processes. The shaded columns represent co-feeding. The co-feed compounds are unreacted reactant, H_2 and CO, H_2O, light hydrocarbons (C_1-C_4) and CO_2. The driving force analysis is carried out on the assumption that these compounds are totally recycled to the reactor.
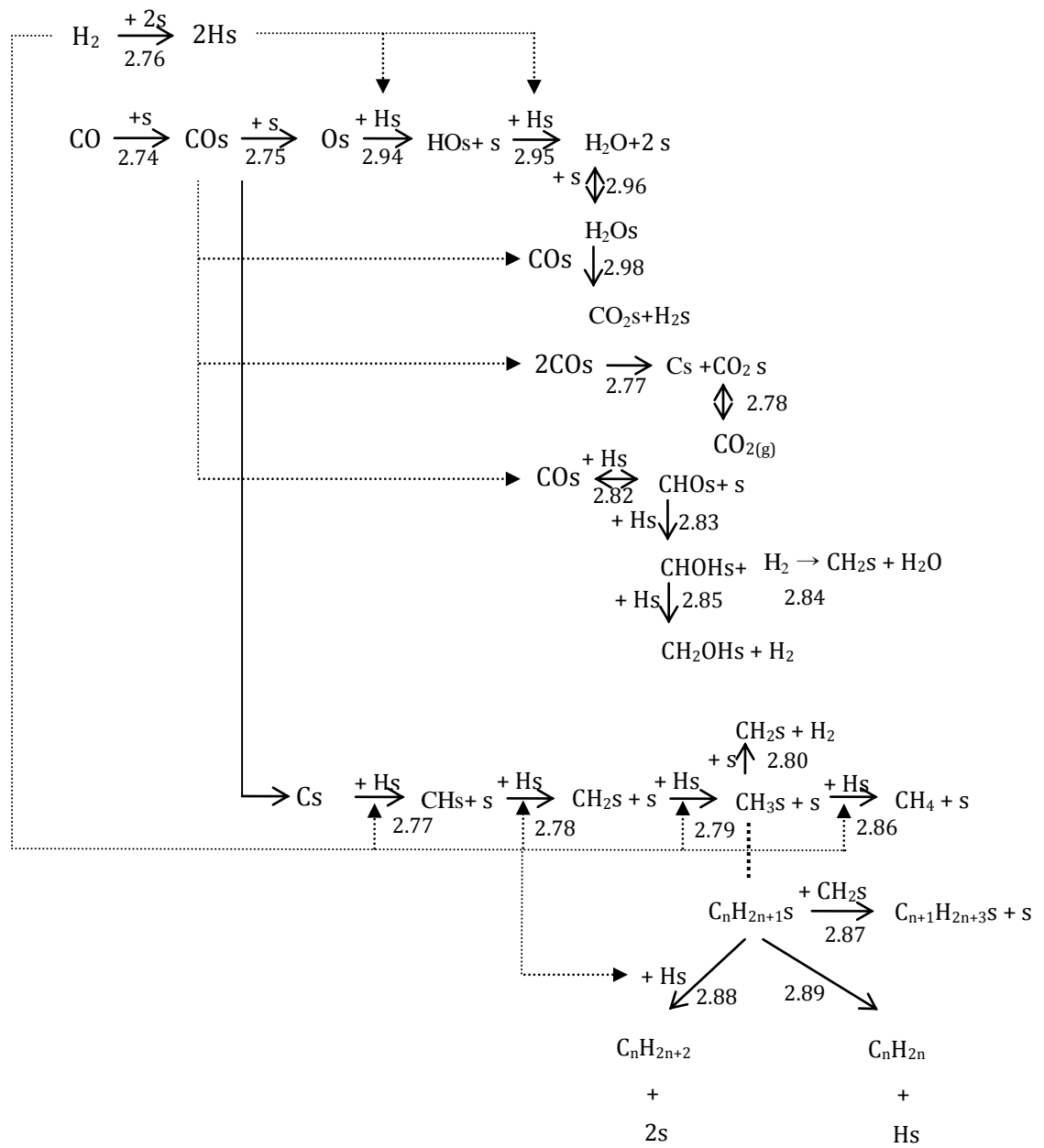
FIGURE 3.1 Transformation Map for synthesis gas conversion of two-phase FTS

Table 3.2-3.4 illustrated the driving force and they are represented desired product from Fischer-Tropsch synthesis for three active sites on the catalyst, respectively.

For all driving force table, Hs addition in order to increase chain growth of hydrocarbon causes high heat in reactor because the Fischer-Tropsch reaction is exothermic reaction. Therefore the FT reactor should be able to remove heat and easily control high heat. As mentioned in Reactor consideration section, in the tubular fixed bed reactor, hydrogen content of the gas improves the heat transfer coefficient more significantly than a slurry reactor, and given the need to remove heat, the ideal equipment would seem to be another heat exchanger reactor. Furthermore, oxygenates may be produced from reaction of COs and H_2, and addition of Hs lead to produce more oxygenates. However, oxygenates with H_2 could be also produced CH_2s monomer via reactions 2.81, 2.82 and 2.85. Also high concentration of CHs, CH_2s and CH_3s is better because of the opportunity of chain growth. The more it is high concentration of C_4H_9s, C_5H_{11}s and so on, the more the best C_5 to C_{20} would be produced. However, CH_3s may seem to have no direct influence on production higher hydrocarbon because of Methanation of reaction 2.86, CH_3s react with Hs leads production of CH_4 that is undesired product. Especially, CH_2s of chain initiation 2.83-2.84 and chain growth 2.85 is one of favorable compounds having a strongly positive influence to increase carbon number as previously reported in Table 2.10. On active site θ, another one of the strongest influence is C_nH_{2n+1}s; the compound is reactant of chain growth via the reaction 2.87, hydrogenation to paraffins via the reaction 2.88, and β-Dehydrogenation to olefins in Table 2.10. In addition, on active site σ, the olefin products produces as primary products could be readsorbed as C_nH_{2n+1}s monomer via the reaction 2. 92 and paraffin products could be also transformed as C_nH_{2n+1}s monomer in Table 2.10. Some of reaction could be carried out continuously because continuous operation would be suitable, e.g., even though a constant amount of synthesis gas is converted to CHs, CH_2s and CH_3s, the limited Hs could not continued to grow chain. Therefore, desired reactants such as Hs and Cs should be continuously supplied to carry out the production of high hydrocarbons. From this reason, it is useful to involve the plug flow reactor as continuous process. Finally, a lot of catalyst surface positively affected to produce higher hydrocarbon

and easily transfer heat that is caused by reaction. On the other hand, it is negative effect to be compounds of Os and COs because they lead to water formation based on the reactions 2.94 and 2.95. Moreover, HOs and H_2O in side reaction 2.96 and 2.97 must also have a bad effect from water formation. These are general effects for each monomer to produce higher hydrocarbon.

They have something in common for two-phase that it would like low concentration H_2O in accordance with water formation and side reaction. Also low concentration CO at high temperature is better. Furthermore, the concentration of Hs and Cs is concluded to be better in high and CHs and CH_2 s are also desired to be high concentration. However, paraffins of CH_4, C_2H_6s, C_3H_8s and C_4H_{10}s and olefin of C_2H_5s, C_3H_7s, and C_4H_{11}s would be like low concentration and these compounds have to operate recycling and co-feeding to reactor. The shadow columns are involved to recycling reactions. The DFA is shown the same rate progress, provided that the reactions of recycling compounds are more active.

Table 3.2 shows that the desired product is paraffin rather than other compounds such as olefins and oxygenates. To achieve high production of paraffins, the adsorption of H_2 and CO is more active and CH_2s and CH_3s (C_nH_{2n+1}s) monomers should be produced rather than other monomers according to the reactions 2.77-2.79. Table 3.3 shows that the olefins are desired product rather than paraffins and oxygenates. Like analysis of paraffins productions, the adsorption of H_2 and CO is produced rather than other compounds. The reaction 2.77 should be also encouraged because the olefins are produced by dehydrogenation of C_nH_{2n+1}s as reaction 2.88. The consideration of olefins and oxygenates as desired products are presented in Table 3.4. Oxygenates offer beneficial gasoline blending properties and reduce CO emissions because of low atmospheric reactivity. It also provides for more complete combustion of gasoline. The catalyst is not useful to produce olefins and oxygenates except adsorption of H_2 and CO. COs, Hs and HOs are proper monomers, and CH_2s is negative effect to achieve oxygenates.

Concentration \ Reactions	$CO + \theta \leftrightarrow CO\,\theta$	$CO\,\theta + \theta \leftrightarrow C\,\theta + O\,\theta$	$H_2 + 2\,\theta \leftrightarrow 2H\,\theta$	$C\,\theta + H\,\theta \leftrightarrow CH\,\theta + \theta$	$CH\,\theta + H\,\theta \leftrightarrow CH_2\,\theta + \theta$	$CH_2\,\theta + H\,\theta \leftrightarrow CH_3\,\theta + \theta$	$CH_3\,\theta + \theta \leftrightarrow CH_2\,\theta + H\,\theta$	$C_nH_{2n+1}\,\theta + CH_2\,\theta \to C_{n+1}H_{2n+3}\,\theta + \theta$	$C_nH_{2n+1}\,\theta + H\,\theta \leftrightarrow C_nH_{2n+2} + 2\,\theta$	$CO + \sigma \leftrightarrow CO\,\sigma$	$C_nH_{2n+1}\,\sigma + H\,\sigma \leftrightarrow C_nH_{2n+2} + 2\,\sigma$	$CO\,\theta + H_2 \leftrightarrow CHOH\,\theta$	$CO\,\theta + H\,\theta \leftrightarrow CHO\,\theta + \theta$	$CHO\,\theta + H\,\theta \leftrightarrow CHOH\,\theta + \theta$	$CHOH\,\theta + H_2 \leftrightarrow CH_2\,\theta + H_2O$	$CHOH\,\theta + H\,\theta \leftrightarrow CH_2OH\,\theta + \theta$	$CH_3\,\theta + H\,\theta \to CH_4 + 2\,\theta$	$C_nH_{2n+1}\,\theta \leftrightarrow C_nH_{2n} + H\,\theta$	$C_nH_{2n+1}\,\sigma \leftrightarrow C_nH_{2n} + H\,\sigma$	$CO + \psi \leftrightarrow CO\,\psi$	$O\,\psi + H\,\psi \to HOs + \psi$	$HO\,\psi + H\,\psi \to H_2O + 2\,\psi$	$O\,\psi + H_2 \to H_2O + \psi$	$H_2O + \psi \leftrightarrow H_2O\,\psi$	$CO\,\psi + H_2O\,\psi \leftrightarrow CO_2\,\psi + H_2\,\psi$	$2CO\,\psi \to C\,\psi + CO_2\,\psi$	$CO_2 + \psi \leftrightarrow CO_2\,\psi$
Description	DS	Dis	Dis	CI	CI	CI	CI	CG	HG	DS	HG	CI	CI	CI	CI	CI	MT	DH	DH	DS	WF	WF	WF	WF	WF	SR	SR
Reaction no.	2.74	2.75	2.76	2.77	2.78	2.79	2.80	2.87	2.88	2.90	2.92	2.81	2.82	2.83	2.84	2.85	2.86	2.89	2.91	2.93	2.94	2.95	2.96	2.97	2.98	2.99	2.100
Active site θ	+	+	++	-	-	-	+	*	*			-	-		-	*	-										
Active site σ										+	*								-								
Active site ψ																				+	*	*	*	+			+
C θ		-		+																							
O θ		-																									
O ψ																					+		+				
CO θ	-	+										+	+														
CO σ										-																	
CO ψ																				-						+	++
CO (g)	+								+											+							
CO$_2$ ψ																									-	*	-
CO$_2$ (g)																											+
H θ			--	+	+	+	-		+				+	+		+	+										
H σ											+																
H ψ																					+	+					
H$_2$ ψ																										-	
H$_2$ (g)		+										+			+								+				
HO ψ																					*	+					
H$_2$O ψ																								-		+	
H$_2$O (g)															-							*	*	+			
CH θ				-	+																						
CH$_2$ θ					-	+	-	+							-												
CH$_3$ θ						-	+										+										
CH$_4$ (g)																	*										
CHO θ													-	+													
CHOH θ												-		-	+	+											
CH$_2$OH θ																-											
C$_n$H$_{2n+1}$																		-	-								
C$_n$H$_{2n+1}$ θ								+	+									+									
C$_n$H$_{2n+1}$ σ											+								+								
C$_n$H$_{2n+2}$ (g)									*		*																
C$_{n+1}$H$_{2n+3}$ θ								*																			
T $_{rate}$	-	+	-	+	+	+	+	+	-	-	-	+	+	+	+	+	+	+	+	-	-	+	+	-	+	-	-
Pressure	+	+	+	-	-	-	+	+	-	+	-	+	+	+	+	+	-	-	-	+	-	-	-	+	-	-	+
Heat of reaction	+/o	+	+/o	+	+	+	+	+	+	+/o	+	+	+	+	o	+	+/o	+	+	+/o	+	+/o	+/o	+/o	+/o	+	+/o
Reaction Time	-	+	-	-	-	-	+	-	-	-	-	-	-	-	+	--	-	-	-	-	+	--	+	-	+	+	-

TABLE 3.2 Driving Forces Analysis of Paraffins Production as desired product in two-phase for pure feed and co-feed

Concentration / Reactions	$CO + \theta \leftrightarrow CO\,\theta$	$CO\,\theta + \theta \leftrightarrow C\,\theta + O\,\theta$	$H_2 + 2\theta \leftrightarrow 2H\,\theta$	$C\,\theta + H\,\theta \leftrightarrow CH\,\theta + \theta$	$CH\,\theta + H\,\theta \leftrightarrow CH_2\,\theta + \theta$	$CH_2\,\theta + H\,\theta \leftrightarrow CH_3\,\theta + \theta$	$CH_3\,\theta + \theta \leftrightarrow CH_2\,\theta + H\,\theta$	$C_nH_{2n+1}\,\theta \leftrightarrow C_nH_{2n} + H\,\theta$	$C_nH_{2n+1}\,\sigma \leftrightarrow C_nH_{2n} + H\,\sigma$	$CO\,\theta + H_2 \leftrightarrow CHOH\,\theta$	$CO\,\theta + H\,\theta \leftrightarrow CHO\,\theta + \theta$	$CHO\,\theta + H\,\theta \leftrightarrow CHOH\,\theta + \theta$	$CHOH\,\theta + H_2 \leftrightarrow CH_2\,\theta + H_2O$	$CHOH\,\theta + H\,\theta \leftrightarrow CH_2OH\,\theta + \theta$	$CH_3\,\theta + H\,\theta \rightarrow CH_4 + 2\theta$	$C_nH_{2n+1}\,\theta + CH_2\,\theta \rightarrow C_{n+1}H_{2n+3}\,\theta + \theta$	$C_nH_{2n+1}\,\theta + H\,\theta \leftrightarrow C_nH_{2n+2} + 2\theta$	$CO + \sigma \leftrightarrow CO\,\sigma$	$C_nH_{2n+1}\,\sigma + H\,\sigma \leftrightarrow C_nH_{2n+2} + 2\sigma$	$CO + \psi \leftrightarrow CO\,\psi$	$O\,\psi + H\,\psi \rightarrow HOs + \psi$	$HO\,\psi + H\,\psi \rightarrow H_2O + 2\psi$	$O\,\psi + H_2 \rightarrow H_2O + \psi$	$H_2O + \psi \leftrightarrow H_2O\,\psi$	$CO\,\psi + H_2O\,\psi \leftrightarrow CO_2\,\psi + H_2\,\psi$	$2CO\,\psi \rightarrow C\,\psi + CO_2\,\psi$	$CO_2 + \psi \leftrightarrow CO_2\,\psi$
Description	DS	Dis	Dis	CI	CI	CI	CI	DH	DH	CI	CI	CI	CI	CI	MT	CG	HG	DS	HG	DS	WF	WF	WF	WF	WF	SR	SR
Reaction no.	2.74	2.75	2.76	2.77	2.78	2.79	2.80	2.89	2.91	2.81	2.82	2.83	2.84	2.85	2.86	2.87	2.88	2.90	2.92	2.93	2.94	2.95	2.96	2.97	2.98	2.99	2.100
Active site θ	+	+	++	-	-	-	+	-			-	-		-	*	*	*										
Active site σ									-									+	*								
Active site ψ																				+	*	*	*	+			+
$C\,\theta$		-		+																							
$O\,\theta$		-																									
$O\,\psi$																					+		+				
$CO\,\theta$	-	+								+	+																
$CO\,\sigma$																		-									
$CO\,\psi$																				-					+	++	
$CO\,(g)$	+																	+		+							
$CO_2\,\psi$																									-	*	-
$CO_2\,(g)$																											+
$H\,\theta$			--	+	+	+	-				+	+		+	+		+										
$H\,\sigma$																			+								
$H\,\psi$																					+	+					
$H_2\,\psi$																									-		
$H_2\,(g)$		+								+			+										+				
$HO\,\psi$																					*	+					
$H_2O\,\psi$																								*	*		
$H_2O\,(g)$													-									*	*	+			
$CH\,\theta$				-	+																						
$CH_2\,\theta$					-	+	-						-			+											
$CH_3\,\theta$						-	+								+												
$CH_4\,(g)$															*												
$CHO\,\theta$											-	+															
$CHOH\,\theta$										-		-	+	+													
$CH_2OH\,\theta$														-													
C_nH_{2n+1}								-	-																		
$C_nH_{2n+1}\,\theta$								+								+	+										
$C_nH_{2n+1}\,\sigma$									+										+								
$C_nH_{2n+2}\,(g)$																	*		*								
$C_{n+1}H_{2n+3}\,\theta$																*											
T_{rate}	-	+	-	+	+	+	+	+	+	+	+	+	+	+	+	+	-	-	-	-	-	+	+	-	+	-	-
Pressure	+	+	+	-	-	-	+	-	-	+	+	+	+	+	-	+	-	+	-	+	-	-	+	-	-	-	+
Heat of reaction	+/o	+	+/o	+	+	+	+	+	+	+	+	+	o	+	+	+/o	+	+/o	+	+/o	+	+/o	+/o	+/o	+/o	+	+/o
Reaction Time	-	+	-	-	-	-	+	-	-	-	-	-	+	-	--	-	-	-	-	-	+	--	+	+	-	+	-

TABLE 3.3 Driving Forces Analysis of Olefins Production as desired product in two-phase for pure feed and co-feed

Reactions / Concentration	$CO + \theta \leftrightarrow CO\,\theta$	$CO\,\theta + \theta \leftrightarrow C\,\theta + O\,\theta$	$H_2 + 2\,\theta \leftrightarrow 2H\,\theta$	$C\,\theta + H\,\theta \leftrightarrow CH\,\theta + \theta$	$CH\,\theta + H\,\theta \leftrightarrow CH_2\,\theta + \theta$	$CH_2\,\theta + H\,\theta \leftrightarrow CH_3\,\theta + \theta$	$CH_3\,\theta + \theta \leftrightarrow CH_2\,\theta + H\,\theta$	$CO\,\theta + H_2 \leftrightarrow CHOH\,\theta$	$CO\,\theta + H\,\theta \leftrightarrow CHO\,\theta + \theta$	$CHO\,\theta + H\,\theta \leftrightarrow CHOH\,\theta + \theta$	$CHOH\,\theta + H_2 \leftrightarrow CH_2\,\theta + H_2O$	$CHOH\,\theta + H\,\theta \leftrightarrow CH_2OH\,\theta + \theta$	$C_nH_{2n+1}\,\theta \leftrightarrow C_nH_{2n} + H\,\theta$	$C_nH_{2n+1}\,\sigma \leftrightarrow C_nH_{2n} + H\,\sigma$	$CH_3\,\theta + H\,\theta \rightarrow CH_4 + 2\,\theta$	$C_nH_{2n+1}\,\theta + CH_2\,\theta \rightarrow C_{n+1}H_{2n+3}\,\theta + \theta$	$C_nH_{2n+1}\,\theta + H\,\theta \leftrightarrow C_nH_{2n+2} + 2\,\theta$	$CO + \sigma \leftrightarrow CO\,\sigma$	$C_nH_{2n+1}\,\sigma + H\,\sigma \leftrightarrow C_nH_{2n+2} + 2\,\sigma$	$CO + \psi \leftrightarrow CO\,\psi$	$O\,\psi + H\,\psi \rightarrow HOs + \psi$	$HO\,\psi + H\,\psi \rightarrow H_2O + 2\,\psi$	$O\,\psi + H_2 \rightarrow H_2O + \psi$	$H_2O + \psi \leftrightarrow H_2O\,\psi$	$CO\,\psi + H_2O\,\psi \leftrightarrow CO_2\,\psi + H_2\,\psi$	$2CO\,\psi \rightarrow C\,\psi + CO_2\,\psi$	$CO_2 + \psi \leftrightarrow CO_2\,\psi$
Description	DS	Dis	Dis	CI	CI	CI	CI	CI	CI	CI	CI	CI	DH	DH	MT	CG	HG	DS	HG	DS	WF	WF	WF	WF	WF	SR	SR
Reaction no.	2.74	2.75	2.76	2.77	2.78	2.79	2.80	2.81	2.82	2.83	2.84	2.85	2.89	2.91	2.86	2.87	2.88	2.90	2.92	2.93	2.94	2.95	2.96	2.97	2.98	2.99	2.100
Active site θ	+	+	++	-	-	-	+		-	-		-			*	*	*										
Active site σ														-				+	*								
Active site ψ																				+	*	*	*	+			+
$C\,\theta$		-		+																							
$O\,\theta$		-																									
$O\,\psi$																					+		+				
$CO\,\theta$	-	+						+	+																		
$CO\,\sigma$																		-									
$CO\,\psi$																				-					+	++	
$CO\,(g)$	+																	+		+							
$CO_2\,\psi$																									-	*	-
$CO_2\,(g)$																											+
$H\,\theta$			--	+	+	+	-		+	+		+			+		+										
$H\,\sigma$																			+								
$H\,\psi$																					+	+					
$H_2\,\psi$																									-		
$H_2\,(g)$			+					+			+												+				
$HO\,\psi$																					*	+					
$H_2O\,\psi$																								*	+		
$H_2O\,(g)$											-											*	*	+			
$CH\,\theta$				-	+																						
$CH_2\,\theta$					-	+	-				-					+											
$CH_3\,\theta$						-	+								+												
$CH_4\,(g)$															*												
$CHO\,\theta$									-	+																	
$CHOH\,\theta$								-		-	+	+															
$CH_2OH\,\theta$												-															
C_nH_{2n+1}													-	-													
$C_nH_{2n+1}\,\theta$																+	+										
$C_nH_{2n+1}\,\sigma$																			+								
$C_nH_{2n+2}\,(g)$																	*		*								
$C_{n+1}H_{2n+3}\,\theta$																*											
T_{rate}	-	+	-	+	+	+	+	+	+	+	+	+	+	+	+	+	-	-	-	-	-	+	+	-	+	-	-
Pressure	+	+	+	-	-	-	+	+	+	+	+	+	-	-	-	+	-	+	-	+	-	-	+	-	-	-	+
Heat of reaction	+/o	+	+/o	+	+	+	+	+	+	+	o	+	+	+	+/o	+	+	+/o	+	+/o	+	+/o	+/o	+/o	+/o	+	+/o
Reaction Time	-	+	-	-	-	-	+	-	-	-	+	-	-	-	--	-	-	-	-	-	-	+	--	+	-	+	-

TABLE 3.4 Driving Forces Analysis of Production of olefins and oxygenates as desired product in two-phase for pure feed and co-feed

3.3 DRIVING FORCE ANALYSIS FOR THREE-PHASE

The section was analyzed the driving force of three-phase for pure feed and co-feed. Figure 3.2 presents the transformation map that captured all transformations and rate processes based on the Table 2.10-2.12 of the Fischer-Tropsch synthesis. The driving force diagram that corresponds to the data is shown in Table 3.5-3.7. Like the driving force table of two-phase, the table indicates that left part of doublet is desired process and right part of that is undesired process to produce high hydrocarbon and the shadow column is correspond to co-feeding.

General effects of each reaction are as previously reported at the section of two-phase because basic reactions and kinetics are the same for two-phase and three-phase. However, the different is only the mass transfer and the solubility of the species in the liquid phase has on the surface concentrations. Therefore, the driving force table added a condition of solvent polarity to analyze the effect of solubility of the species in the liquid phase. The positive reaction of three-phase process is high concentration of H_2, however, the concentration of CO, CO_2, H_2O, C_nH_{2n+2} ($n \leq 4$, CH_4, C_2H_6, C_3H_8 and C_4H_{10}), and C_nH_{2n} ($n \leq 4$, C_2H_4, C_3H_6, and C_4H_8) is lower in order to decrease the unwanted process' production. Additionally, gas phase of these products affects better than liquid phase. This is important to minimize the concentration of the compounds to satisfy the aims of this research.

H₂(*l*)

$\Updownarrow$3.2

H₂(*g*) $\xrightarrow[2.76]{+\,2s}$ 2Hs

H₂O(*g*)

$\Updownarrow$3.6

CO(*l*) $\xrightarrow[2.74]{+s}$ COs $\xrightarrow[2.75]{+\,s}$ Os $\xrightarrow[2.94]{+\,Hs}$ HOs+ s $\xrightarrow[2.95]{+\,Hs}$ H₂O(*l*) + 2 s

$\Updownarrow$3.1

CO(*g*)

$+\,s\ \Updownarrow2.97$

H₂Os

+CO $\downarrow$2.98

CO₂s+H₂s

2COs $\xrightarrow{2.77}$ Os +CO₂ s

$\Updownarrow$ 2.78

CO₂(*g*) $\xrightarrow{3.7}$ CO₂(*l*)

COs $\underset{2.82}{\overset{+\,Hs}{\rightleftharpoons}}$ CHOs+ s

+ Hs$\downarrow$2.83

CHOHs+ H₂ → CH₂s + H₂O

+ Hs$\downarrow$2.85   2.74

CH₂OHs + H₂

CH₂s + H₂   CH₄(*g*)

+ s$\uparrow$ 2.80 $\Updownarrow$3.4

Cs $\xrightarrow[2.77]{+\,Hs}$ CHs+ s $\xrightarrow[2.78]{+\,Hs}$ CH₂s + s $\xrightarrow[2.79]{+\,Hs}$ CH₃s + s $\xrightarrow[2.86]{+\,Hs}$ CH₄(*l*)+ s

CₙH₂ₙ₊₁s $\xrightarrow{+\,CH_2s}$ Cₙ₊₁H₂ₙ₊₃s + s

+ Hs $\swarrow$2.88   2.89 $\searrow$

CₙH₂ₙ₊₂ (*g*) $\underset{3.3}{\Longleftrightarrow}$ CₙH₂ₙ₊₂ (*l*)   CₙH₂ₙ(*l*) $\underset{3.5}{\Longleftrightarrow}$ CₙH₂ₙ(*g*)

+   +

2s   Hs
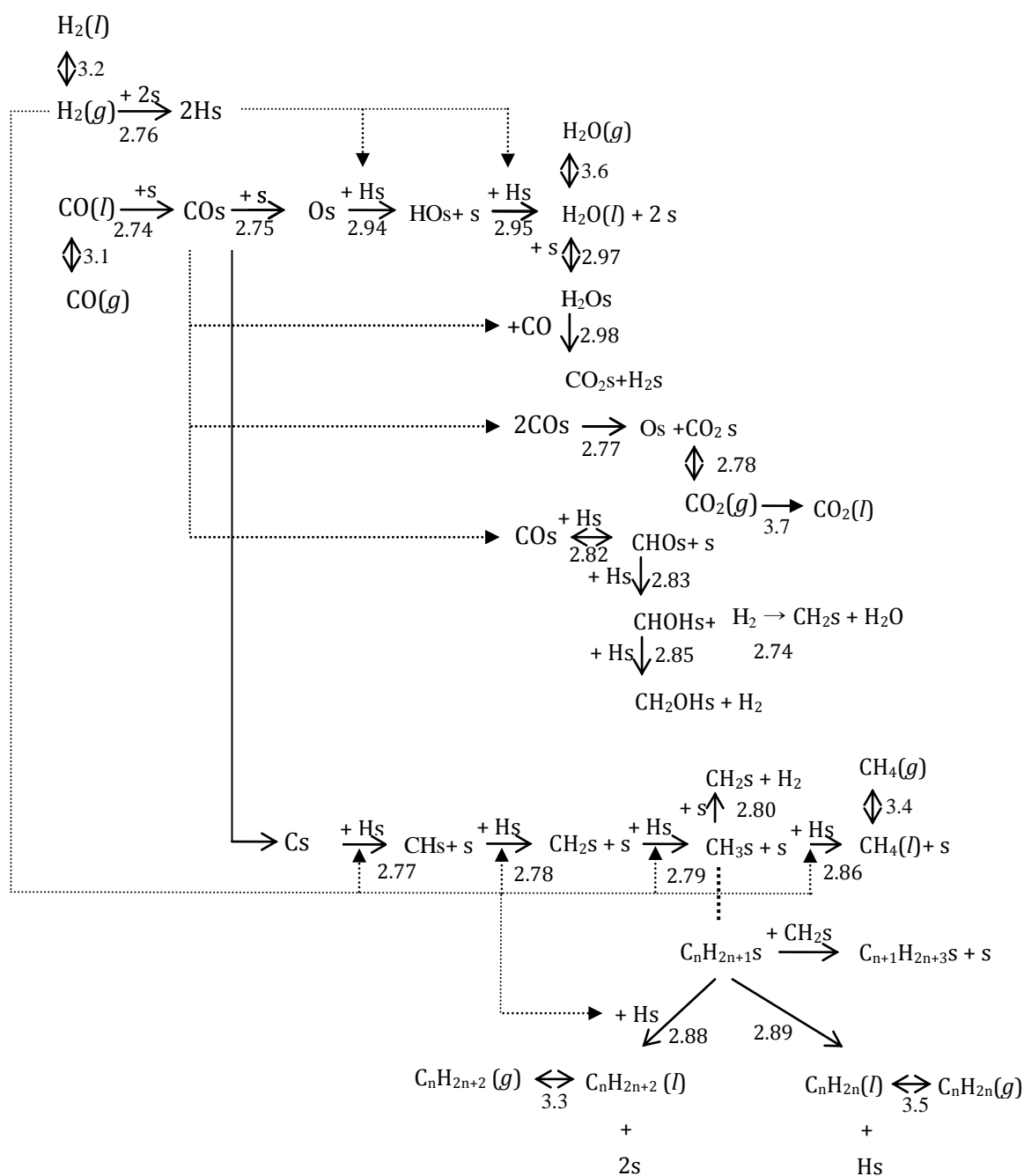
FIGURE 3.2 Transformation Map for synthesis gas conversion of three-phase

Concentration \ Reactions	$CO + \theta \leftrightarrow CO\,\theta$	$CO(g) \leftrightarrow CO(l)$	$CO\,\theta + \theta \leftrightarrow C\,\theta + O\,\theta$	$H_2 + 2\theta \leftrightarrow 2H\,\theta$	$H_2(g) \leftrightarrow H_2(l)$	$C\,\theta + H\,\theta \leftrightarrow CH\,\theta + \theta$	$CH\,\theta + H\,\theta \leftrightarrow CH_2\,\theta + \theta$	$CH_2\,\theta + H\,\theta \leftrightarrow CH_3\,\theta + \theta$	$CH_3\,\theta + \theta \leftrightarrow CH_2\,\theta + H\,\theta$	$C_nH_{2n+1}\,\theta + CH_2\,\theta \rightarrow C_{n+1}H_{2n+3}\,\theta + \theta$	$C_nH_{2n+1}\,\theta + H\,\theta \leftrightarrow C_nH_{2n+2} + 2\theta$	$CO + \sigma \leftrightarrow CO\,\sigma$	$C_nH_{2n+1}\,\sigma + H\,\sigma \leftrightarrow C_nH_{2n+2} + 2\sigma$	$C_nH_{2n+2}(g) \leftrightarrow C_nH_{2n+2}(l)$	$CO\,\theta + H_2 \leftrightarrow CHOH\,\theta$	$CO\,\theta + H\,\theta \leftrightarrow CHO\,\theta + \theta$	$CHO\,\theta + H\,\theta \leftrightarrow CHOH\,\theta + \theta$	$CHOH\,\theta + H_2 \leftrightarrow CH_2\,\theta + H_2O$	$CHOH\,\theta + H\,\theta \leftrightarrow CH_2OH\,\theta + \theta$	$CH_3\,\theta + H\,\theta \rightarrow CH_4 + 2\theta$	$CH_4(g) \leftrightarrow CH_4(l)$	$C_nH_{2n+1}\,\theta \leftrightarrow C_nH_{2n} + H\,\theta$	$C_nH_{2n+1}\,\sigma \leftrightarrow C_nH_{2n} + H\,\sigma$	$C_nH_{2n}(g) \leftrightarrow C_nH_{2n}(l)\ (n \leq 4)$	$CO + \psi \leftrightarrow CO\,\psi$	$O\,\psi + H\,\psi \rightarrow HOs + \psi$	$HO\,\psi + H\,\psi \rightarrow H_2O + 2\psi$	$O\,\psi + H_2 \rightarrow H_2O + \psi$	$H_2O(g) \leftrightarrow H_2O(l)$	$H_2O + \psi \leftrightarrow H_2O\,\psi$	$CO + H_2O\,\psi \leftrightarrow CO_2\,\psi + H_2\,\psi$	$2CO \rightarrow C\,\psi + CO_2\,\psi$	$CO_2(g) \leftrightarrow CO_2\,\psi$	$CO_2(g) \leftrightarrow CO_2(l)$
Description	DS	PT	Dis	Dis	PT	CI	CI	CI	CI	CG	HG	DS	HG	PT	CI	CI	CI	CI	CI	MT	PT	DH	DH	PT	DS	WF	WF	WF	PT	WF	WF	SR	SR	PT
Reaction no.	2.74	3.1	2.75	2.76	3.2	2.77	2.78	2.79	2.80	2.81	2.88	2.90	2.91	3.3	2.81	2.82	2.83	2.84	2.85	2.86	3.4	2.89	2.92	3.5	2.93	2.94	2.95	2.96	3.6	2.97	2.98	2.99	2.100	3.7
Active site θ	+		+	++		-	-	-	+	*	*					-	-		-	*		-												
Active site σ												+	*										-											
Active site ψ																									+	*	*	*		+				+
C θ			-			+																												
O θ			-																															
O ψ																						+				+		+						
CO θ	-		+																															
CO σ												-																						
CO ψ																									-							+		++
CO (g)	+	+										+																			+			
CO (l)		-																																
CO₂ ψ																															-		*	-
CO₂ (g)																																+		+
CO₂ (l)																																		-
H θ				--		+	+	+	-		+					+	+		+	+														
H σ													+																					
H ψ																						+	+											
H₂ ψ																															-			
H₂ (g)															+			+														+		
HO ψ																						*	+											
H₂O ψ																														-	+			
H₂O (g)																		-									*	*	+	+				
H₂O (l)																													-					
CH θ						-	+																											
CH₂ θ							-	+	-	+								-																
CH₃ θ								-	+											+														
CH₄ (g)																				*	+													
CH₄ (l)																					-													
CHO θ																-	+																	
CHOH θ															-		-	+	+															
CH₂OH θ																			-															
CₙH₂ₙ (g)																								+										
CₙH₂ₙ (l)																								-										
CₙH₂ₙ₊₁																						-	-											
CₙH₂ₙ₊₁ θ										+	+											+												
CₙH₂ₙ₊₁ σ													+										+											
CₙH₂ₙ₊₂ (g)											*		*	+																				
CₙH₂ₙ₊₂ (l)														-																				
Cₙ₊₁H₂ₙ₊₃ θ										*																								
T rate	-	-	+	-	-	+	+	+	+	+	-	-	-	-	+	+	+	+	+	+	-	+	+	-	-	-	+	+	+	-	+	-	-	-
Pressure	+	+	+	+	+	-	-	-	+	+	-	+	-	+	+	+	+	+	+	-	-	+	-	-	+	+	-	-	-	-	-	+	+	+
Solvent polarity	+	+	+	-	-	-	-	-	-	-	-	+	-	-	o	o	o	o/+	o	-	-	-	-	-	-	+	+	+	+	+	+/o	-	-	-
Heat of reaction	+/o	o	+	+/o	o	+	+	+	+	+	+	+/o	+	o	+	+	+	o	+	+/o	o	+	+	o	+/o	+	+/o	+/o	o	+/o	+/o	+	+/o	o
Reaction Time	-	-	+	-	-	-	-	-	+	-	-	-	-	-	-	-	-	+	-	--	-	+	-	-	-	+	--	+	-	-	+	+	-	+

TABLE 3.5 Driving Forces Analysis of paraffins production as desired product in three-phase for pure feed and co-feed

Reactions / Concentration	$CO + \theta \leftrightarrow CO\theta$	$CO(g) \leftrightarrow CO(l)$	$CO\theta + \theta \leftrightarrow C\theta + O\theta$	$H_2 + 2\theta \leftrightarrow 2H\theta$	$H_2(g) \leftrightarrow H_2(l)$	$CO + H\theta \leftrightarrow CH\theta + \theta$	$CH\theta + H\theta \leftrightarrow CH_2\theta + \theta$	$CH_2\theta + H\theta \leftrightarrow CH_3\theta + \theta$	$CH_3\theta + \theta \leftrightarrow CH_2\theta + H\theta$	$C_nH_{2n+1}\theta \leftrightarrow C_nH_{2n} + H\theta$	$\Psi_vH_{2v+1}\sigma \leftrightarrow \Psi_vH_{2v} + H\sigma$	$C_nH_{2n}(g) \leftrightarrow C_nH_{2n}(l)\ (n \leq 4)$	$CO\theta + H_2 \leftrightarrow CHOH\theta$	$CO\theta + H\theta \leftrightarrow CHO\theta + \theta$	$CHO\theta + H\theta \leftrightarrow CHOH\theta + \theta$	$CHOH\theta + H_2 \leftrightarrow CH_2\theta + H_2O$	$CHOH\theta + H\theta \leftrightarrow CH_2OH\theta + \theta$	$CH_3\theta + H\theta \rightarrow CH_4 + 2\theta$	$CH_4(g) \leftrightarrow CH_4(l)$	$C_nH_{2n+1}\theta + CH_2\theta \rightarrow C_{n+1}H_{2n+3}\theta + \theta$	$C_nH_{2n+1}\theta + H\theta \leftrightarrow C_nH_{2n+2} + 2\theta$	$C_nH_{2n+2}(g) \leftrightarrow C_nH_{2n+2}(l)$	$CO + \sigma \leftrightarrow CO\sigma$	$C_nH_{2n+1}\sigma + H\sigma \leftrightarrow C_nH_{2n+2} + 2\sigma$	$CO + \psi \leftrightarrow CO\psi$	$O\psi + H\psi \rightarrow HOs + \psi$	$HO\psi + H\psi \rightarrow H_2O + 2\psi$	$O\psi + H_2 \rightarrow H_2O + \psi$	$H_2O(g) \leftrightarrow H_2O(l)$	$H_2O + \psi \leftrightarrow H_2O\psi$	$CO\psi + H_2O\psi \leftrightarrow CO_2\psi + H_2\psi$	$2CO\psi \leftrightarrow C\psi + CO_2\psi$	$CO_2 + \psi \leftrightarrow CO_2\psi$	$CO_2(g) \leftrightarrow CO_2(l)$
Description	DS	PT	Dis	Dis	PT	CI	CI	CI	CI	DH	DH	PT	CI	CI	CI	CI	CI	MT	PT	CG	HG	PT	DS	HG	DS	WF	WF	WF	PT	WF	WF	SR	SR	PT
Reaction no.	2.74	3.1	2.75	2.76	3.2	2.77	2.78	2.79	2.80	2.89	2.91	3.5	2.81	2.82	2.83	2.84	2.85	2.86	3.4	2.87	2.88	3.3	2.90	2.91	2.93	2.94	2.95	2.96	3.6	2.97	2.98	2.99	2.100	3.7
Active site θ	+		+	++		-	-	-	+	-				-	-		-	*		*	*													
Active site σ											-												+	*										
Active site ψ																									+	*	*	*		+			+	
C θ			-			+																												
O θ			-																															
O ψ																										+		+						
CO θ	-		+										+	+																				
CO σ																							-											
CO ψ																									-							+	++	
CO (g)	+	+																					+		+									
CO (l)		-																																
CO₂ ψ																															-	*	-	
CO₂ (g)				+																												+	+	
CO₂ (l)					-																													-
H θ				--		+	+	+	-					+	+		+	+			+													
H σ																								+										
H ψ																										+	+							
H₂ ψ																															-			
H₂ (g)				+									+			+												+						
H₂ (l)																																		
HO ψ																										*	+							
H₂O ψ																														-	+			
H₂O (g)																-										*	*	+	+					
H₂O (l)																													-					
CH θ						-	+																											
CH₂ θ							-	+	-							+				+														
CH₃ θ								-	+																									
CH₄ (g)																		+	*		+													
CH₄ (l)																			-															
CHO θ														-	+																			
CHOH θ													-		+	-	+																	
CH₂OH θ																	-																	
CₙH₂ₙ(g)												+																						
CₙH₂ₙ(l)												-																						
CₙH₂ₙ₊₁										-	-																							
CₙH₂ₙ₊₁ θ										+										+	+													
CₙH₂ₙ₊₁ σ											+													+										
CₙH₂ₙ₊₂ (g)																					*	+		*										
CₙH₂ₙ₊₂ (l)																						-												
Cₙ₊₁H₂ₙ₊₃ θ																				*														
T rate	-	-	+	-	-	+	+	+	+	+	+	-	+	+	+	+	+	+	-	+	-	-	-	-	-	-	-	-	+	+	+	-	+	-
Pressure	+	+	+	+	+	-	-	-	+	-	-	+	+	+	+	+	+	-	+	-	+	+	+	+	+	-	+	+	+	+	-	-	+	+
Solvent polarity	+	+	+	-	-	-	-	-	-	-	-	-	o	o	o	o/+	o	-	-	-	-	-	+	-	-	+	+	+	+	+	+/o	-	-	-
Heat of reaction	+/o	o	+	+/o	o	+	+	+	+	+	+	o	+	+	+	o	+	+/o	o	+	+	o	+/o	+	+/o	+	+/o	+	+/o	+	+/o	+/o	o	+/o
Reaction Time	-	-	+	-	-	-	-	-	+	-	-	-	-	-	-	+	-	--	-	-	-	-	-	-	-	+	--	+	-	-	+	+	-	+

TABLE 3.6 Driving Forces Analysis of olefins production as desired product in three-phase for pure feed and co-feed

Concentration \ Reactions	$CO + \theta \leftrightarrow CO\,\theta$	$CO(g) \leftrightarrow CO(l)$	$CO\,\theta + \theta \leftrightarrow C\,\theta + O\,\theta$	$H_2 + 2\,\theta \leftrightarrow 2H\,\theta$	$H_2(g) \leftrightarrow H_2(l)$	$CO + H\,\theta \leftrightarrow CH\,\theta + \theta$	$CH\,\theta + H\,\theta \leftrightarrow CH_2\,\theta + \theta$	$CH_2\,\theta + H\,\theta \leftrightarrow CH_3\,\theta + \theta$	$CH_3\,\theta + \theta \leftrightarrow CH_2\,\theta + H\,\theta$	$CO\,\theta + H_2 \leftrightarrow CHOH\,\theta$	$CO\,\theta + H\,\theta \leftrightarrow CHO\,\theta + \theta$	$CHO\,\theta + H\,\theta \leftrightarrow CHOH\,\theta + \theta$	$CHOH\,\theta + H_2 \leftrightarrow CH_2\,\theta + H_2O$	$CHOH\,\theta + H\,\theta \leftrightarrow CH_2OH\,\theta + \theta$	$C_nH_{2n+1}\,\theta \leftrightarrow C_nH_{2n} + H\,\theta$	$C_nH_{2n+1}\,\sigma \leftrightarrow C_nH_{2n} + H\,\sigma$	$C_nH_{2n}(g) \leftrightarrow C_nH_{2n}(l)\ (n \le 4)$	$CH_3\,\theta + H\,\theta \to CH_4 + 2\,\theta$	$CH_4(g) \leftrightarrow CH_4(l)$	$C_nH_{2n+1}\,\theta + CH_2\,\theta \to C_{n+1}H_{2n+3}\,\theta + \theta$	$C_nH_{2n+1}\,\theta + H\,\theta \leftrightarrow C_nH_{2n+2} + 2\,\theta$	$C_nH_{2n+2}(g) \leftrightarrow C_nH_{2n+2}(l)$	$CO + \sigma \leftrightarrow CO\,\sigma$	$C_nH_{2n+1}\,\sigma + H\,\sigma \leftrightarrow C_nH_{2n+2} + 2\,\sigma$	$CO + \psi \leftrightarrow CO\,\psi$	$O\,\psi + H\,\psi \to HOs + \psi$	$HO\,\psi + H\,\psi \to H_2O + 2\,\psi$	$O\,\psi + H_2 \to H_2O + \psi$	$H_2O(g) \leftrightarrow H_2O(l)$	$H_2O + \psi \leftrightarrow H_2O\,\psi$	$CO + H_2O\,\psi \leftrightarrow CO_2\,\psi + H_2\,\psi$	$2CO \to C\,\psi + CO_2\,\psi$	$CO_2 + \psi \leftrightarrow CO_2\,\psi$	$CO_2(g) \leftrightarrow CO_2(l)$
Description	DS	PT	Dis	Dis	PT	CI	CI	CI	CI	CI	CI	CI	CI	CI	DH	DH	PT	MT	PT	CG	HG	PT	DS	HG	DS	WF	WF	WF	PT	WF	WF	SR	SR	PT
Reaction no.	2.74	3.1	2.75	2.76	3.2	2.77	2.78	2.79	2.80	2.81	2.82	2.83	2.84	2.85	2.89	2.9	3.5	2.86	3.4	2.87	2.88	3.3	2.90	2.91	2.93	2.94	2.95	2.96	3.6	2.97	2.98	2.99	2.100	3.7
Active site θ	+		+	++		-	-	-	+		-	-		-	-			*		*	*													
Active site σ																-							+	*										
Active site ψ																									+	*	*	*		+			+	
C θ			-			+																												
O θ			-																															
O ψ																										+		+						
CO θ	-		+							+	+																							
CO σ																							-											
CO ψ																									-						+	++		
CO (g)	+	+																					+		+									
CO (l)		-																																
CO₂ ψ																																-	*	-
CO₂ (g)																																+	+	
CO₂ (l)																																		-
H θ				--		+	+	+	-		+	+		+				+			+													
H σ																								+										
H ψ																										+	+							
H₂ ψ																															-			
H₂ (g)				+						+			+															+						
H₂ (l)																																		
HO ψ																										*	+							
H₂O ψ																															-		+	
H₂O (g)													-														*	*		+				
H₂O (l)																														-				
CH θ						-	+																											
CH₂ θ							-	+	-				-							+														
CH₃ θ								-	+									+																
CH₄ (g)																		*	+															
CH₄ (l)																			-															
CHO θ											-	+																						
CHOH θ										-		-	+	+																				
CH₂OH θ														-																				
CₙH₂ₙ (g)																	+																	
CₙH₂ₙ (l)																	-																	
CₙH₂ₙ₊₁															-	-																		
CₙH₂ₙ₊₁ θ																				+	+													
CₙH₂ₙ₊₁ σ																+								+										
CₙH₂ₙ₊₂ (g)																					*	+		*										
CₙH₂ₙ₊₂ (l)																						-												
Cₙ₊₁H₂ₙ₊₃ θ																				*														
T_rate	-	-	+	-	-	+	+	+	+	+	+	+	+	+	+	+	-	+	-	+	-	-	-	-	-	-	-	-	-	+	+	+	-	-
Pressure	+	+	+	+	+	-	-	-	+	+	+	+	+	-	-	-	+	-	+	-	+	+	+	+	+	+	-	-	-	-	-	-	+	+
Solvent polarity	+	+	+	-	-	-	-	-	-	o	o	o	o/+	o	-	-	-	-	-	-	-	-	+	-	-	+	+	+	+	+	+/o	-	-	-
Heat of reaction	+/o	o	+	+/o	o	+	+	+	+	+	+	+	o	+	+	+	o	+/o	o	+	+	o	+/o	+	+/o	+	+/o	+/o	o	+/o	+/o	+	+/o	o
Reaction Time	-	-	+	-	-	-	-	-	+	-	-	-	+	-	-	-	-	--	-	-	-	-	-	-	-	-	-	+	--	+	-	-	-	+

TABLE 3.7 Driving Forces Analysis of olefins and oxygenates production as desired product in three-phase for pure feed and co-feed

3.4 RESULTS AND DISCUSSION

According the the DFA, high concentration of Hs and Cs affected positive effect to produce higher hydrocarbons. To achieve high concentration of Hs and Cs, adsorption of H_2 and CO is active, and changing the H_2/CO ratio could lead to different proportion of both adsorbed H_2 and Cs. However, the H_2/CO ratio can become undesirable elevated due to the WGS conversion, because the WGS conversion depends on the ratio. In addition, water gas shift reaction is sensitive to temperature and high temperature (T>523K) leads to a high WGS activity as mentioned in Chapter 2. To increase production of water, catalyst choice may be considered in order to produce water because water production of iron based catalyst is more active than that of cobalt based catalyst. Furthermore, high concentrations of CHs, CH_2s and CH_3s are desired because of the opportunity of chain production. To achieve high product selectivity of heavier hydrocarbons and oxygenates, total pressure should be increased and H_2/CO ratio should be decreased as mentioned in Chapter 2.

Additionally, gas phase of these products affects better than liquid phase. It is also evident from the table that there is potential for high catalyst surface to increase the yield of hydrocarbons and easily heat removal. Furthermore, continuous supply of reactants in each reaction such as Hs and Cs should be needed therefore; the plant process should be developed as a continuous reactor. As a result, a continuous plant involving the use of intensive mixers, heat exchanger reactors and phase separation would deliver the primary functions identified.

In addition, overall conversion is found to increase with an increase in liquid phase velocity because of increase liquid compounds by recycling process. Furthermore, the process may be sensitive to gas-liquid mass transfer coefficient from the analysis of three-phase process.

Variable	Chain length		Chain branching		Water formation	Olefin selectivity	Alcohol Selectivity	Carbon deposition	Methane Selectivity
	Gerard	This Work	Gerard	This Work	This Work	This Work	This Work	This Work	This Work
Temperature	↓	↓	↑	↑	↑	↑	↑	↓	↑
Pressure	↑	↑	↓	↓	↓	↑	↑	↑	↓
H_2/CO	↓	↓	↑	↑	↑	↑	↑	*	↑
Conversion	*	*	*	*	*	*	*	*	*
Residence time	*	↓	*	↓	*	↓	↓	↓	↓
Solvent polarity	*	↓	*	↑	↑	↑	↑	↑	↓
Catalyst									
Iron Cat.	↑	↑	↓	↓	↑	↑	↓	↑	↑

TABLE 3.8 Comparison with Gerard by operating conditions and catalyst modifications (Gerard (1999))

Table 3.8 shows the general influence of different process variables on the selectivity and comparison with Gerard result for the driving force analysis results with those qualified. The effect of temperature, partial pressures of H_2 and CO, H_2/CO ratio, residence time solvent polarity that are known to influence the FT synthesis will be discussed briefly. Simple analysis yields identical results and we can test these using quantitative modelling.
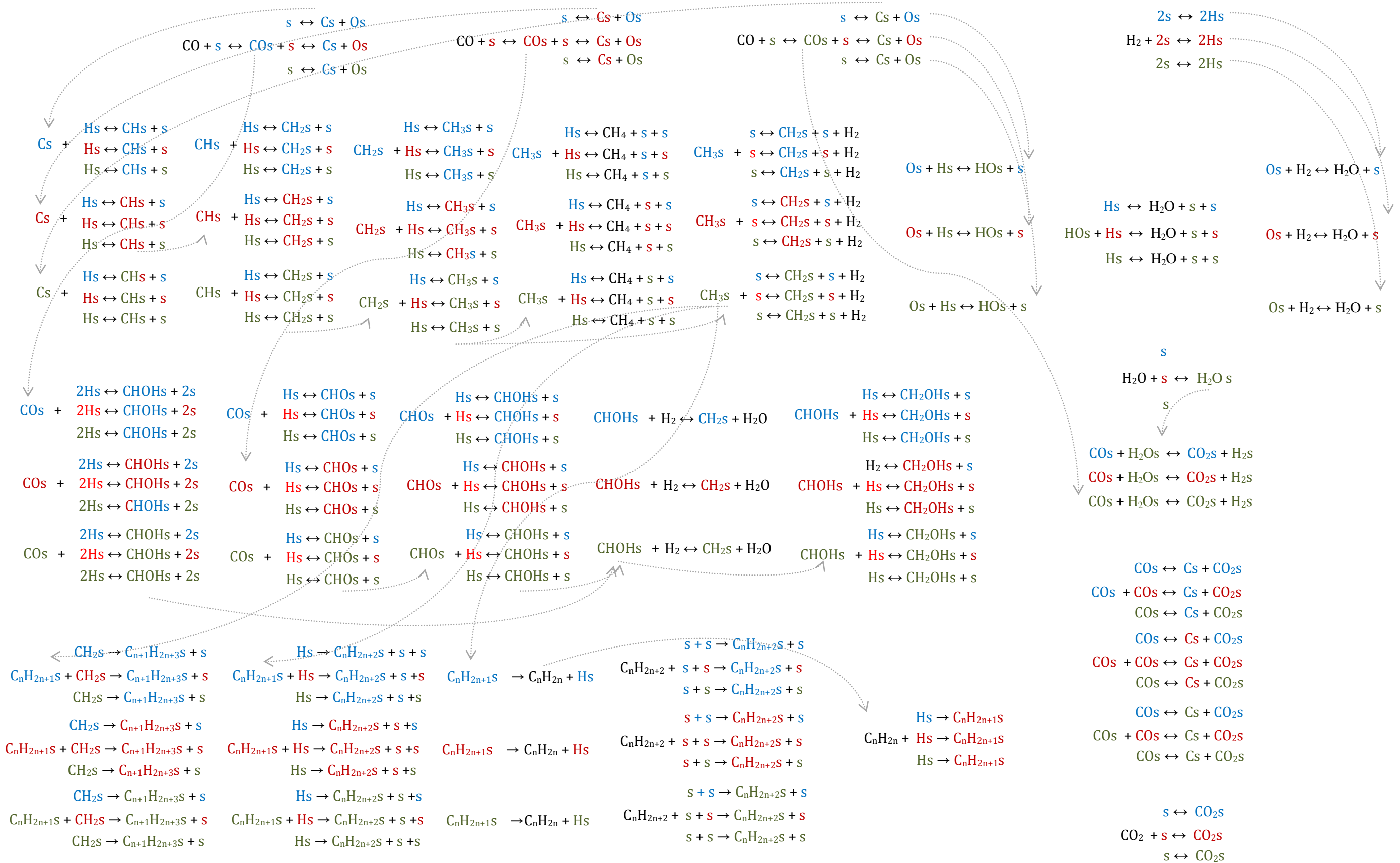
$$s \leftrightarrow Cs + Os \qquad s \leftrightarrow Cs + Os \qquad s \leftrightarrow Cs + Os \qquad 2s \leftrightarrow 2Hs$$
$$CO + s \leftrightarrow COs + s \leftrightarrow Cs + Os \qquad CO + s \leftrightarrow COs + s \leftrightarrow Cs + Os \qquad CO + s \leftrightarrow COs + s \leftrightarrow Cs + Os \qquad H_2 + 2s \leftrightarrow 2Hs$$
$$s \leftrightarrow Cs + Os \qquad s \leftrightarrow Cs + Os \qquad s \leftrightarrow Cs + Os \qquad 2s \leftrightarrow 2Hs$$

$$Cs + \begin{array}{l} Hs \leftrightarrow CHs + s \\ Hs \leftrightarrow CHs + s \\ Hs \leftrightarrow CHs + s \end{array} \quad CHs + \begin{array}{l} Hs \leftrightarrow CH_2s + s \\ Hs \leftrightarrow CH_2s + s \\ Hs \leftrightarrow CH_2s + s \end{array} \quad CH_2s + \begin{array}{l} Hs \leftrightarrow CH_3s + s \\ Hs \leftrightarrow CH_3s + s \\ Hs \leftrightarrow CH_3s + s \end{array} \quad CH_3s + \begin{array}{l} Hs \leftrightarrow CH_4 + s + s \\ Hs \leftrightarrow CH_4 + s + s \\ Hs \leftrightarrow CH_4 + s + s \end{array} \quad CH_3s + \begin{array}{l} s \leftrightarrow CH_2s + s + H_2 \\ s \leftrightarrow CH_2s + s + H_2 \\ s \leftrightarrow CH_2s + s + H_2 \end{array} \qquad Os + Hs \leftrightarrow HOs + s \qquad Os + H_2 \leftrightarrow H_2O + s$$

$$Cs + \begin{array}{l} Hs \leftrightarrow CHs + s \\ Hs \leftrightarrow CHs + s \\ Hs \leftrightarrow CHs + s \end{array} \quad CHs + \begin{array}{l} Hs \leftrightarrow CH_2s + s \\ Hs \leftrightarrow CH_2s + s \\ Hs \leftrightarrow CH_2s + s \end{array} \quad CH_2s + \begin{array}{l} Hs \leftrightarrow CH_3s + s \\ Hs \leftrightarrow CH_3s + s \\ Hs \leftrightarrow CH_3s + s \end{array} \quad CH_3s + \begin{array}{l} Hs \leftrightarrow CH_4 + s + s \\ Hs \leftrightarrow CH_4 + s + s \\ Hs \leftrightarrow CH_4 + s + s \end{array} \quad CH_3s + \begin{array}{l} s \leftrightarrow CH_2s + s + H_2 \\ s \leftrightarrow CH_2s + s + H_2 \\ s \leftrightarrow CH_2s + s + H_2 \end{array} \qquad \begin{array}{l} Hs \leftrightarrow H_2O + s + s \\ HOs + Hs \leftrightarrow H_2O + s + s \\ Hs \leftrightarrow H_2O + s + s \end{array} \qquad Os + H_2 \leftrightarrow H_2O + s$$

$$Cs + \begin{array}{l} Hs \leftrightarrow CHs + s \\ Hs \leftrightarrow CHs + s \\ Hs \leftrightarrow CHs + s \end{array} \quad CHs + \begin{array}{l} Hs \leftrightarrow CH_2s + s \\ Hs \leftrightarrow CH_2s + s \\ Hs \leftrightarrow CH_2s + s \end{array} \quad CH_2s + \begin{array}{l} Hs \leftrightarrow CH_3s + s \\ Hs \leftrightarrow CH_3s + s \\ Hs \leftrightarrow CH_3s + s \end{array} \quad CH_3s + \begin{array}{l} Hs \leftrightarrow CH_4 + s + s \\ Hs \leftrightarrow CH_4 + s + s \\ Hs \leftrightarrow CH_4 + s + s \end{array} \quad CH_3s + \begin{array}{l} s \leftrightarrow CH_2s + s + H_2 \\ s \leftrightarrow CH_2s + s + H_2 \\ s \leftrightarrow CH_2s + s + H_2 \end{array} \qquad Os + Hs \leftrightarrow HOs + s \qquad Os + H_2 \leftrightarrow H_2O + s$$

$$s$$
$$H_2O + s \leftrightarrow H_2Os$$
$$s$$

$$COs + \begin{array}{l} 2Hs \leftrightarrow CHOHs + 2s \\ 2Hs \leftrightarrow CHOHs + 2s \\ 2Hs \leftrightarrow CHOHs + 2s \end{array} \quad COs + \begin{array}{l} Hs \leftrightarrow CHOs + s \\ Hs \leftrightarrow CHOs + s \\ Hs \leftrightarrow CHOs + s \end{array} \quad CHOs + \begin{array}{l} Hs \leftrightarrow CHOHs + s \\ Hs \leftrightarrow CHOHs + s \\ Hs \leftrightarrow CHOHs + s \end{array} \quad CHOHs + H_2 \leftrightarrow CH_2s + H_2O \qquad CHOHs + \begin{array}{l} Hs \leftrightarrow CH_2OHs + s \\ Hs \leftrightarrow CH_2OHs + s \\ Hs \leftrightarrow CH_2OHs + s \end{array}$$

$$COs + H_2Os \leftrightarrow CO_2s + H_2s$$
$$COs + H_2Os \leftrightarrow CO_2s + H_2s$$
$$COs + H_2Os \leftrightarrow CO_2s + H_2s$$

$$COs + \begin{array}{l} 2Hs \leftrightarrow CHOHs + 2s \\ 2Hs \leftrightarrow CHOHs + 2s \\ 2Hs \leftrightarrow CHOHs + 2s \end{array} \quad COs + \begin{array}{l} Hs \leftrightarrow CHOs + s \\ Hs \leftrightarrow CHOs + s \\ Hs \leftrightarrow CHOs + s \end{array} \quad CHOs + \begin{array}{l} Hs \leftrightarrow CHOHs + s \\ Hs \leftrightarrow CHOHs + s \\ Hs \leftrightarrow CHOHs + s \end{array} \quad CHOHs + H_2 \leftrightarrow CH_2s + H_2O \qquad CHOHs + \begin{array}{l} H_2 \leftrightarrow CH_2OHs + s \\ Hs \leftrightarrow CH_2OHs + s \\ Hs \leftrightarrow CH_2OHs + s \end{array}$$

$$COs + \begin{array}{l} 2Hs \leftrightarrow CHOHs + 2s \\ 2Hs \leftrightarrow CHOHs + 2s \\ 2Hs \leftrightarrow CHOHs + 2s \end{array} \quad COs + \begin{array}{l} Hs \leftrightarrow CHOs + s \\ Hs \leftrightarrow CHOs + s \\ Hs \leftrightarrow CHOs + s \end{array} \quad CHOs + \begin{array}{l} Hs \leftrightarrow CHOHs + s \\ Hs \leftrightarrow CHOHs + s \\ Hs \leftrightarrow CHOHs + s \end{array} \quad CHOHs + H_2 \leftrightarrow CH_2s + H_2O \qquad CHOHs + \begin{array}{l} Hs \leftrightarrow CH_2OHs + s \\ Hs \leftrightarrow CH_2OHs + s \\ Hs \leftrightarrow CH_2OHs + s \end{array}$$

$$COs \leftrightarrow Cs + CO_2s$$
$$COs + COs \leftrightarrow Cs + CO_2s$$
$$COs \leftrightarrow Cs + CO_2s$$

$$C_nH_{2n+1}s + \begin{array}{l} CH_2s \rightarrow C_{n+1}H_{2n+3}s + s \\ CH_2s \rightarrow C_{n+1}H_{2n+3}s + s \\ CH_2s \rightarrow C_{n+1}H_{2n+3}s + s \end{array} \quad C_nH_{2n+1}s + \begin{array}{l} Hs \rightarrow C_nH_{2n+2}s + s + s \\ Hs \rightarrow C_nH_{2n+2}s + s + s \\ Hs \rightarrow C_nH_{2n+2}s + s + s \end{array} \quad C_nH_{2n+1}s \rightarrow C_nH_{2n} + Hs \quad C_nH_{2n+2} + \begin{array}{l} s + s \rightarrow C_nH_{2n+2}s + s \\ s + s \rightarrow C_nH_{2n+2}s + s \\ s + s \rightarrow C_nH_{2n+2}s + s \end{array}$$

$$COs \leftrightarrow Cs + CO_2s$$
$$COs + COs \leftrightarrow Cs + CO_2s$$
$$COs \leftrightarrow Cs + CO_2s$$

$$C_nH_{2n+1}s + \begin{array}{l} CH_2s \rightarrow C_{n+1}H_{2n+3}s + s \\ CH_2s \rightarrow C_{n+1}H_{2n+3}s + s \\ CH_2s \rightarrow C_{n+1}H_{2n+3}s + s \end{array} \quad C_nH_{2n+1}s + \begin{array}{l} Hs \rightarrow C_nH_{2n+2}s + s + s \\ Hs \rightarrow C_nH_{2n+2}s + s + s \\ Hs \rightarrow C_nH_{2n+2}s + s + s \end{array} \quad C_nH_{2n+1}s \rightarrow C_nH_{2n} + Hs \quad C_nH_{2n+2} + \begin{array}{l} s + s \rightarrow C_nH_{2n+2}s + s \\ s + s \rightarrow C_nH_{2n+2}s + s \\ s + s \rightarrow C_nH_{2n+2}s + s \end{array} \quad C_nH_{2n} + \begin{array}{l} Hs \rightarrow C_nH_{2n+1}s \\ Hs \rightarrow C_nH_{2n+1}s \\ Hs \rightarrow C_nH_{2n+1}s \end{array}$$

$$COs \leftrightarrow Cs + CO_2s$$
$$COs + COs \leftrightarrow Cs + CO_2s$$
$$COs \leftrightarrow Cs + CO_2s$$

$$C_nH_{2n+1}s + \begin{array}{l} CH_2s \rightarrow C_{n+1}H_{2n+3}s + s \\ CH_2s \rightarrow C_{n+1}H_{2n+3}s + s \\ CH_2s \rightarrow C_{n+1}H_{2n+3}s + s \end{array} \quad C_nH_{2n+1}s + \begin{array}{l} Hs \rightarrow C_nH_{2n+2}s + s + s \\ Hs \rightarrow C_nH_{2n+2}s + s + s \\ Hs \rightarrow C_nH_{2n+2}s + s + s \end{array} \quad C_nH_{2n+1}s \rightarrow C_nH_{2n} + Hs \quad C_nH_{2n+2} + \begin{array}{l} s + s \rightarrow C_nH_{2n+2}s + s \\ s + s \rightarrow C_nH_{2n+2}s + s \\ s + s \rightarrow C_nH_{2n+2}s + s \end{array}$$

$$s \leftrightarrow CO_2s$$
$$CO_2 + s \leftrightarrow CO_2s$$
$$s \leftrightarrow CO_2s$$

Figure 3.3 Transformation Map for active sites σ(blue), θ(red), and ψ(green) on the catalyst.

3.5   SUMMARY

The driving force analysis is provided easily understated of complex process and technology and efficient plant design, and reduced risk as early development of innovative process options. Moreover, the methodology can accomplish to save some time and area, sustainable chemical engineering through the driving force analysis.

This chapter presents the transformation map and driving force table of three-phase and two phase both pure feed and co-feed of Fischer-Tropsch synthesis as one of qualitative modelling. The results of this analysis show that high H_2/CO ratio is better due to high concentration of Hs and Cs caused the high chain growth and low water is positive effect. According to this analysis, heat exchanger reactor could be used to deliver the primary functions identified because the synthesis gas reaction is exothermic. Furthermore, high catalyst surface not only affected easily heat removal but also positive effect to grow chain.

The result of DFA is dependent on the increased ratio and pressure and changed catalyst and, it needs good mass transfer rate, high hydrocarbon surface, and high superficial velocity in order to enhance desired reaction performance.

From the analysis, comparing the Driving Force Analysis with simulation that has good impact on process design will discuss the conditions of Fischer-Tropsch in Chapter 5.

4

Fischer-Tropsch Reactor Model

4.1 DEVELOPMENT OF FISCHER-TROPSCH REACTOR MODEL

As above mentioned at Chapter 2, the two models were decided as basis models. The first, Base Case model I, was considered two-phase of Fischer-Tropsch reactor for pure feed systems. Base Case model II was simplified for three-phase reactor of Fischer-Tropsch synthesis. In addition, the two models need to modify and configuration of catalyst particle size, reactor diameter and space velocity.

In order to produce a specific product as transportation fuel, the operation conditions have significant influence upon the product distribution, hydrocarbons and oxygenates, therefore it is critically important to control the selectivity of the product (Raje and Davis 1997; Yang 2004; Guo and Liu 2006; Wang and Wang 2007; Wenping and Edwin 2007). This section was described to predict the results of kinetic model for Fischer-Tropsch synthesis to control the selectivity of the product before kinetic models and also to evaluate that the results are reasonable or not after completing the kinetic models. The kinetic modeling has to obey several restrictions: absence of internal and external temperature and mass gradients on catalyst particle size; isothermal operation of the reactor; constant total molar flow rate.

There were several challenges identified in Fischer-Tropsch synthesis such as temperature effect, sizing of catalyst and reactor and reaction parameters such as residence time and space velocity that are affected in Fischer-Tropsch synthesis. Moreover, the kinetic models were developed on various operating conditions both once-through and recycling & co-feeding for Fischer-Tropsch synthesis in reactors by MATLAB mathematic language.

4.1.1   THE PUBLISHED FISCHER-TROPSCH MODEL CONSIDERATIONS

(A)   CATALYST CHOICE

The three metals known to be most active for CO hydrogenation to hydrocarbons are Fe, Co and Ru. The choice between these metals is a complex one as it is influenced by several factors, e.g., cost, availability, desired product spectrum and required catalyst life-time and activity. It has been estimated that the entire available world stock of Ru would be needed to produce enough catalyst for a Fischer-Tropsch plant. On the other hand, if a relatively small capacity plant is required for the production of high quality Fischer-Tropsch waxes, the catalyst may be relevant. Workers at Johnson Matthey (Anderson, Griffin et al. 2003) have presented that a 0.3% Ru on Al_2O_3 gives a wax selectivity of 88% which is considerably higher than the 60% obtained with the iron based catalyst under similar conditions. The catalysts can also produce high yields of wax. Furthermore, Co loading is increased by the activity of supported cobalt catalysts and so some compromise between cost and activity is required. Cobalt catalysts could still be more than 10 times as expensive as the equivalent iron based catalysts. A much longer life, or higher activity would be required to justify its use (Dry 1990).

Additionally, the catalysts are generally poorly dispersed on metal oxide supports and Ru, Re, or Pt promoters are applied to prevent catalyst deactivation by carbon formation or oxidation. Compared to iron based catalysts, olefins tend more easily to reenter the chain growth process by re-adsorption on to Ru based catalyst, increasing the selectivity towards heavy hydrocarbons. Iron catalysts generally consist of precipitated iron, which is promoted with potassium and copper to obtain a high activity and selectivity. In addition, compared to other metal catalysts such as cobalt based and ruthenium catalysts for Fischer-Tropsch synthesis, an iron-based catalyst is distinguished by higher conversion and, selectivity to the lower olefins, and flexibility to the process parameters (Dry 1981; King, Cusumano et al. 1981). Typically, cheap iron based catalysts are active for the water gas shift reaction (Eq. 2.80 and 2.87 in Table 2.12). This high water gas shift activity makes these catalysts flexible towards the H_2/CO ratio of the synthesis gas; however, the water gas shift becomes more important as the CO conversion increases. For the iron based catalysts, the pressure can be varied over a wide range without having a significant impact upon the product distribution.

The effect of particle size on reaction rate can be quantified using the well-known relation between effectiveness factor, η, and the Thiele modulus, ϕ.

$$-r_s = \eta k * s \qquad (4.1)$$

The effectiveness factor for a first order reaction is

$$\eta = \frac{3}{\phi}\left(\frac{1}{tanh\phi} - \frac{1}{\phi}\right) \qquad (4.2)$$

For spherical particles (radius, P_r) and first-order kinetics, the Thiele modulus can be expressed as

$$\phi = \sqrt{\frac{\text{Pr}}{3}\left(\frac{k}{D_e}\right)} \qquad (4.3)$$

where k is the kinetic coefficient in 1/sec, and D_e is the effective diffusivity. The effective diffusivity, D_e appearing in the Thiele modulus, should be considered as Taylor dispersion equation (4.4). The effective diffusivity can be related to the Peclet number, based on the reactor diameter $d=2a$ and space velocity U_G.

$$D_e = D(1 + \frac{1}{192}P_e^2) \qquad (4.4)$$

where $P_e = dU_G/D$ is the Peclet number. The effect of Taylor dispersion is therefore more pronounced at higher Peclet numbers and reactor diameter. The diffusivity in the equation 4.4 is defined as

$$D = \frac{RT}{6\pi\mu P_r} \qquad (4.5)$$

Where μ is solution viscosity, gas constant, R, is 8.314 KJ/mol and T is temperature. On the whole therefore, Thiele Modulus (Eq. 4.3) is dependent on particle radius of catalyst, diffusivity coefficient and rate constant, and Thiele Modulus is defined as a function of effectiveness factor, η from Eq. 4.2. The effectiveness factor is involved as parameter of kinetic equations of Fischer-Tropsch synthesis and the effect of catalyst particle size could be predicted by the effectiveness factor.

As mentioned above, it is assumed that the primary and secondary reactions take place on separated catalyst sites, called as σ, θ, and site ψ, respectively. To apply the effect of catalyst active sites, the kinetic model is modified by introducing a parameter. Eq. 2.43, 2.44 and 2.45 of the two-phase model can be rewritten in the following form:

$$R_{CH_4,C} = k_{met} \frac{SA'_{E1}}{SA'_1} K_1 K_5 K_4 \frac{P_{H_2}^3 P_{CO}}{P_{H_2O}}$$

$$/[1 + \sqrt{K_2 P_{H_2}} + K_1 P_{CO} + K_4 \frac{P_{H_2}^2 P_{CO}}{P_{H_2O}} + K_1 K_3 P_{CO} P_{H_2} + K_5 K_4 K_4^{0.5} \frac{P_{H_2}^{2.5} P_{CO}}{P_{H_2O}}$$

$$+ K_4 \frac{P_{H_2}^2 P_{CO}}{P_{H_2O}} (1 + K_5 \sqrt{K_2 P_{H_2}}) \sum_{i=2}^{n} \prod_{j=2}^{i} (\alpha_j)]^2$$

$$(4.6)$$

$$R_{C_n H_{2n+2},C} = k_p \frac{SA'_{E2}}{SA'_2} K_2 K_5 K_4 \frac{P_{H_2}^2 P_{CO}}{P_{H_2O}} \prod_{j=2}^{i} \alpha_j$$

$$/[1 + \sqrt{K_2 P_{H_2}} + K_1 P_{CO} + K_4 \frac{P_{H_2}^2 P_{CO}}{P_{H_2O}} + K_1 K_3 P_{CO} P_{H_2} + K_5 K_4 K_2^{0.5} \frac{P_{H_2}^{2.5} P_{CO}}{P_{H_2O}}$$

$$+ K_4 \frac{P_{H_2}^2 P_{CO}}{P_{H_2O}} (1 + K_5 \sqrt{K_2 P_{H_2}}) \sum_{i=2}^{n} \prod_{j=2}^{i} (\alpha_j)]^2$$

$$(4.7)$$

$$R_{C_n H_{2n},C} = k_o \frac{SA'_{E3}}{SA'_3} (1 - \beta_n) K_4 \frac{P_{H_2}^2 P_{CO}}{P_{H_2O}} \prod_{j=2}^{i} \alpha_j / [1 + \sqrt{K_2 P_{H_2}} + K_1 P_{CO} + K_4 \frac{P_{H_2}^2 P_{CO}}{P_{H_2O}}$$

$$+ K_1 K_4 P_{CO} P_{H_2} + K_5 K_4 K_2^{0.5} \frac{P_{H_2}^{2.5} P_{CO}}{P_{H_2O}} + K_4 \frac{P_{H_2}^2 P_{CO}}{P_{H_2O}} (1$$

$$+ K_5 \sqrt{K_2 P_{H_2}}) \sum_{i=2}^{n} \prod_{j=2}^{i} (\alpha_j)]$$

$$(4.8)$$

Where

SA'_1, SA'_2 and SA'_3 : catalyst active surface areas of active site θ for the two-phase model

SA'_{E1}, SA'_{E2} and SA'_{E3}: catalyst active surface areas of active sites θ and σ for experimental data

For the three-phase reactor, the modified kinetic models with adopting the catalyst active sites are defined as follows:

$$\frac{dP(1)}{dt} = k_{met} \frac{SA_{E1}^{''}}{SA_1^{''}} *[-H]*R(1)$$

(4.9)

$$\frac{dP(2)}{dt} = k_{et} \frac{SA_{E2}^{''}}{SA_2^{''}} *[-H]*R(2)$$

(4.10)

$$\frac{dP^=(2)}{dt} = k_{o2} \frac{SA_{E3}^{''}}{SA_3^{''}} * [-CH_2] * [-CH_2]$$

(4.11)

$$\frac{dP(n)}{dt} = k_{par} \frac{SA_{E4}^{''}}{SA_4^{''}} * [-H] * R(n)$$

(4.12)

$$\frac{dP^=(n)}{dt} = k_{olef} \frac{SA_{E5}^{''}}{SA_5^{''}} * R(n) + k_{olef2} \frac{SA_{E6}^{''}}{SA_6^{''}} * R(n)^{''} + k_{-o} \frac{SA_{E7}^{''}}{SA_7^{''}} * R(n)^{''}$$

(4.13)

Where

$SA_1^{''}, SA_2^{''}, SA_3^{''}, SA_4^{''}, SA_5^{''}, SA_6^{''}$ and $SA_7^{''}$: catalyst parameters of active site θ for the three-phase model

$SA_{E1}^{''}, SA_{E2}^{''}, SA_{E3}^{''}, SA_{E4}^{''}, SA_{E5}^{''}, SA_{E6}^{''}$ and $SA_{E7}^{''}$: catalyst parameters of active sites θ and σ for experimental data

(B) CHOICE OF REACTOR

As mentioned in Chapter 2, various reactors have been developed by many research institutes and industrial companies; however there are still typical reactors such as fixed bed reactor and slurry bed reactor by reason of good temperature control, catalyst loading to higher conversions to products, and cheap cost. Therefore, the kinetic models of Fischer-Tropsch synthesis in this study were developed for both of them. For three phase reactor, liquid and gas phase dispersion coefficient should be considered in kinetic expressions. The kinetic expressions also were included parameters of reactor size and superficial velocity or flow rate to specify and apply in various conditions for both two-phae and three-phase reactors. All mentioned parameters applied in kinetic models were proposed as below section.

LIQUID PHASE DISPERSION COEFFICIENT

Various literature correlations for liquid phase dispersion in bubble column were compared by Wendt et al.(1984). The correlation proposed by Deckwer et al. (1974) provides a good estimate of the liquid phase dispersion coefficient.

$$D_L = 0.68 D_r^{1.4} U_G^{0.33} \qquad (4.14)$$

Where D_r: reactor diameter, [m] and U_G: gas superficial velocity [m/s]

$$U_G = \frac{v_o}{\pi D_r^2} \qquad (4.15)$$

Where V_o: total flow rate, [m³/s]

GAS PHASE DISPERSION COEFFICIENT

Only a few studies have investigated gas phase dispersion in bubble columns (Towell and Ackerman, 1972; Field and Davidson, 1980; Kawagoe et al., 199). Kawagoe et al. observed that the correlation of Towell and Ackerman provided a good estimate of the overall gas phase dispersion coefficient in bubble columns.

$$D_G = 20.0 D_r^2 U_G \tag{4.16}$$

EFFECTIVE DISPERSION COEFFICIENT

The relationship between liquid phase dispersion coefficient and gas phase dispersion coefficient is like as below equation:

$$D_E = \frac{D_G + \frac{C_L}{HC_G}D_L}{1 + \frac{C_L}{HC_G}} \tag{4.17}$$

Assuming mass transfer resistance is small, $C_G = HC_L$ at every point. The equation (4.18) simplifies to:

$$D_E = \frac{D_G + \frac{D_L}{H^2}}{1 + \frac{1}{H^2}} \tag{4.18}$$

Where, H: Henry's constant

This effectiveness factor for molecular diffusivity coefficient is:

$$D_E = D_m + \frac{D_r^2 u^2}{48 D_m} \tag{4.19}$$

Where, D_m : molecular diffusivity and U: average velocity

<u>OTHER PARAMETERS' CONSIDERATION</u>

The rates of expression for kinetic models both two-phase and three-phase model were demonstrated not only size of catalyst and reactor but also residence time or space velocity. This section proposes the other parameter's consideration. The flow rate of the gas stream through a reactor determines the length of time that the pollutants can be removed from the gas stream. This is termed the residence time or space velocity. These common equipment sizing parameters are defined mathematically.

The developed kinetic equations based on size of iron based catalyst, liquid & gas phase dispersion coefficient, size of both two phase and three phase reactor, and residence time or space velocity were prepared by MATLAB mathematics computer language. The two kinetic models were named as the Base case model I and II and the two models were performed not only once-through but also recycling & co-feeding. Figure 4.1 shows the model algorithm by MATLAB, and the MATLAB codes for the two models were referenced at Appendix B.

(C) TEMPERATURE EFFECT

The rate constant increases more strongly with temperature than the diffusivity. This could be interpreted by the diffusional behaviours of H_2 and CO and water, which are expressed in the kinetic equation. Diffusion coefficients of H_2 and CO are generally regarded to increase with temperature, while the diffusion coefficient of water that performs inhibition of reaction rate decreases with increasing temperature. By doing so, reaction rate will be increased more greatly than that of diffusion. As presented temperature effect in Section 2.3.1, lower hydrocarbons are produced at high temperature and olefins productions are obtained more than paraffins productions at high temperature. In other words, diffusion coefficient of the equations of 2.74, 2.75 and 2.76 in Table 2.9 increases with increasing temperature. It leads to shorter chains; mostly methane is produced as Eq. 2.86 in Table 2.9. Additionally, water formation of Eq. 2.93-2.97 is not vigorous due to a low diffusion coefficient at higher temperature. Furthermore, as the reaction temperature is increased, the CO conversion is increased. It means that the high CO conversion leads to produce more olefins than paraffin, an increase in the reaction temperature generally leads to an increase in the catalytic performance.

For these reasons the temperature parameter should be applied in kinetic equations. The only way to explain the relationship between temperature and the rate of a reaction was to assume that the rate constant depends on the temperature at which the reaction is run. The relationship obeyed the Arrhenius Equation.

4.1.2 THE MODIFIED FISCHER-TROPSCH MODEL

The equations for catalyst particle size, reactor diameter and space velocity as mentioned above are modified with methane, paraffins and olefins formation rate equations.

$$
R_{CH_4,C} = \eta * (k_{met} \frac{SA'_{E1}}{SA'_1} K_1 K_5 K_4 \frac{P_{H_2}^3 P_{CO}}{P_{H_2O}}
$$

$$
/[1 + \sqrt{K_2 P_{H_2}} + K_1 P_{CO} + K_4 \frac{P_{H_2}^2 P_{CO}}{P_{H_2O}} + K_1 K_3 P_{CO} P_{H_2} + K_5 K_4 K_4^{0.5} \frac{P_{H_2}^{2.5} P_{CO}}{P_{H_2O}}
$$

$$
+ K_4 \frac{P_{H_2}^2 P_{CO}}{P_{H_2O}} (1 + K_5 \sqrt{K_2 P_{H_2}}) \sum_{i=2}^{n} \prod_{j=2}^{i} (\alpha_j)]^2)
$$

$$(4.20)$$

$$
R_{C_n H_{2n+2},C} = \eta * (k_p \frac{SA'_{E2}}{SA'_2} K_2 K_5 K_4 \frac{P_{H_2}^2 P_{CO}}{P_{H_2O}} \prod_{j=2}^{i} \alpha_j
$$

$$
/[1 + \sqrt{K_2 P_{H_2}} + K_1 P_{CO} + K_4 \frac{P_{H_2}^2 P_{CO}}{P_{H_2O}} + K_1 K_3 P_{CO} P_{H_2} + K_5 K_4 K_2^{0.5} \frac{P_{H_2}^{2.5} P_{CO}}{P_{H_2O}}
$$

$$
+ K_4 \frac{P_{H_2}^2 P_{CO}}{P_{H_2O}} (1 + K_5 \sqrt{K_2 P_{H_2}}) \sum_{i=2}^{n} \prod_{j=2}^{i} (\alpha_j)]^2)
$$

$$(4.21)$$

$$
R_{C_n H_{2n},C} = \eta * (k_o \frac{SA'_{E3}}{SA'_3} (1 - \beta_n) K_4 \frac{P_{H_2}^2 P_{CO}}{P_{H_2O}} \prod_{j=2}^{i} \alpha_j / [1 + \sqrt{K_2 P_{H_2}} + K_1 P_{CO}
$$

$$
+ K_2 \frac{P_{H_2}^2 P_{CO}}{P_{H_2O}} + K_1 K_2 P_{CO} P_{H_2} + K_5 K_4 K_2^{0.5} \frac{P_{H_2}^{2.5} P_{CO}}{P_{H_2O}}
$$

$$
+ K_4 \frac{P_{H_2}^2 P_{CO}}{P_{H_2O}} \left(1 + K_5 \sqrt{K_2 P_{H_2}}\right) \sum_{i=2}^{n} \prod_{j=2}^{i} (\alpha_n)])
$$

$$(4.22)$$

In equation 4.22, re-adsorption term is $k_o \frac{SA'_{E3}}{SA'_3} (1 - \beta_n)$ and β_n can be calculated by equation 2.45 mentioned at Section 2.2.

For the three-phase reactor, the modified kinetic models with adopting the catalyst active sites are defined as follows:

$$\frac{dP(1)}{dt} = \eta * (k_{met} \frac{SA''_{E1}}{SA''_1} *[-H]*R(1))$$

$$(4.23)$$

$$\frac{dP(2)}{dt} = \eta * (k_{et} \frac{SA''_{E2}}{SA''_2} *[-H]*R(2))$$

$$(4.24)$$

$$\frac{dP^=(2)}{dt} = \eta * (k_{o2} \frac{SA''_{E3}}{SA''_3} * [-CH_2] * [-CH_2])$$

$$(4.25)$$

$$\frac{dP(n)}{dt} = \eta * (k_{par} \frac{SA''_{E4}}{SA''_4} * [-H] * R(n))$$

$$(4.26)$$

$$\frac{dP^=(n)}{dt} = \eta * (k_{olef} \frac{SA''_{E5}}{SA''_5} * R(n) + k_{olef2} \frac{SA''_{E6}}{SA''_6} * R(n)'' + k_{-o} \frac{SA''_{E7}}{SA''_7} * R(n)'')$$

$$(4.27)$$

Thiele Modulus (η) of Equations (4.20-27) are calculated by Equation (4.28).

$$\eta = \frac{3}{\sqrt{\frac{P_r}{3}\left(\frac{k}{\frac{RT}{6\pi\mu P_r}(1 + \frac{1}{192}\frac{dV^2}{D})}\right)}}\left\{\frac{1}{\tanh\left(\sqrt{\frac{P_r}{3}\left(\frac{k}{\frac{RT}{6\pi\mu P_r}(1 + \frac{1}{192}\frac{dV^2}{D})}\right)}\right)}\right.$$

$$\left. - \frac{1}{\sqrt{\frac{P_r}{3}\left(\frac{k}{\frac{RT}{6\pi\mu P_r}(1 + \frac{1}{192}\frac{dV^2}{D})}\right)}}\right\}$$

(4.28)

In addition, the three-phase FT model proposed by Jun Yang and Bo-Tao Teng(2006) was also modified some parameters mentioned above and the hydrocarbon production of the model compared with that of the three-phase FT model proposed by FN Fernandes(2005).

Model inputs

Pressure

Temperature

Inlet Synthesis gas flow rate

H_2/CO ratio and composition

Calculation of the liquid and gas compositions and flowrates

Kinetics Calculation

the reaction rate

Numerical resolution

Discretisation and numerical resolution of the main equations using the Ordinary Differential Equations using MATLAB

Calculation of Hydrocarbons compositions and flow-rate for co-feeding process

Recycling and Co-feeding

Model outputs

Conversion

Equilibrium time

Liquid water production

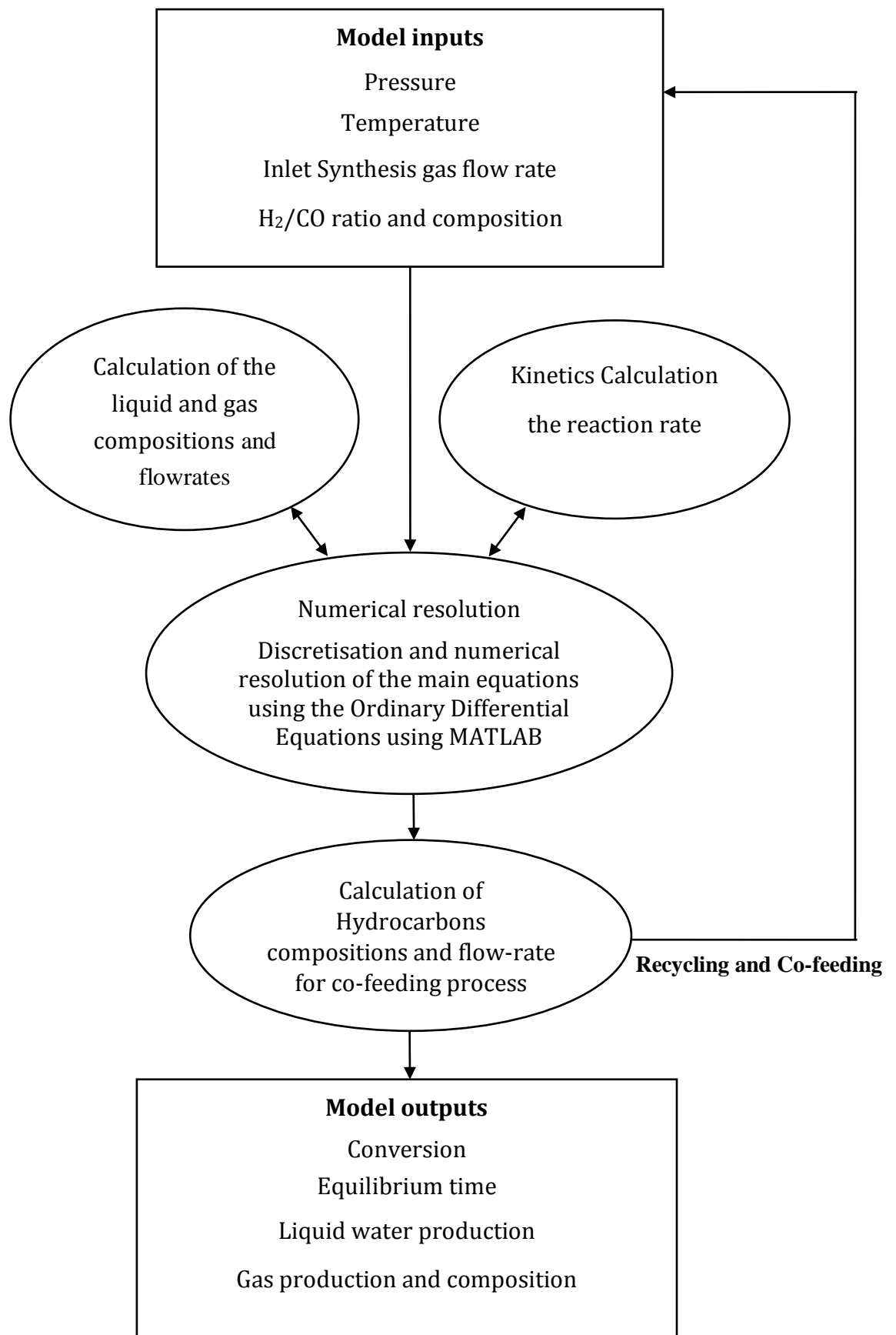Gas production and composition

FIGURE 4.1 Model algorithm of MATLAB

Iron based catalyst of Fischer-Tropsch synthesis form mostly hydrocarbon of straight chain type. As mentioned in Chapter 1, such products in the range of C_5 to C_{20} are of particular value as diesel and gasoline. By controlling reaction conditions such as temperature, pressure and H_2/CO ratio, low amounts of heavy wax products and methane are desired. Alkenes can be used as chemical feedstocks or can be reformed to gasoline in range of C_5 to C_{20}. Therefore, these results were presented the effects of reaction conditions on hydrocarbons distribution both paraffins and olefins in range of C_5 to C_{20}.

In order to find optimum reaction required to produce transportation fuels, FT reactor modelling was performed by MATLAB. The Base case model I and II mentioned at Section 2.2 were developed with considering the parameters such as temperature, size of catalyst and reactor and residence time (Eqs. 4.20-4.27). Many experimental data are optimized with Base case model I and II and the model are named the optimized Fischer-Tropsch model I and II, respectively. Data fitting of the optimized Fischer-Tropsch model is used the method of least squares. The best fit in the least-squares sense minimizes the sum of squared residuals, a residual being the difference between an observed value and the fitted value provided by a model. The least squares estimate of the model is given by,

$$\text{Error} = \sum_i (\text{Exp. Data}(i) - \text{Base Case Models}(i))^2 \tag{4.29}$$

Firstly, the optimized Fischer-Tropsch model was developed from the Base case model I and II for once-through reactor, and was also applied the recycling and co-feeding. In addition, productions of the alcohols and acids are also calculated by the optimized Fischer-Tropsch model.

4.2 THE MODIFIED FT MODEL FOR ONCE-THROUGH

4.2.1 BASE CASE MODEL I

The Base case model I was developed on two-phase reactor in based on the model from Jun Yang et al. using MATLAB.

The Base case model I was developed with consideration for size of catalyst and reactor and space velocity based on the data from Jun Yang (Yang 2004), was compared with other experimental distributions both paraffins and olefins. The other experimental works were established by Yuan-Yuan Ji (Ji, Xiang et al. 2001), Wenping Ma (Wenping and Edwin 2007), AN Pour (Pour, Zare et al. 2010) and DB Bukur (Bukur, Nowicki et al. 1995). Table 4.1 shows the reaction conditions of the experimental data on above authors.

	Jun Yang		Yuan-Yuan Ji	Wenping Ma	AN Pour	DB Bukur
	[a]	[b]				
Temperature[K]	556	585	573	553	563	523
Pressure[MPa]	2.51	3.02	2.25	2.01	1.7	1.48
H_2/CO feed ratio[-]	2.62	2.04	1.97	0.9	1.0	0.67
Space Velocity [m/Kg.cat.h]	$1.6*10^{-3}$	$3.2*10^{-3}$	7	3	13.28	3
Iron-based Catalyst	Fe-Mn	Fe-Mn	Fe-Mn	Fe-Cu-M-K/AC	Fe-Cu	Fe-Cu- K-SiO$_2$
diameter[m]	≈3e-4	≈3e-4	≈2.75e-4	≈5.95e-4	≈2.75e-4	≈3.75e-4
Reactor	Fixed-bed	Fixed-bed	Fixed-bed	Fixed-bed	Fixed-bed	Fixed-bed
diameter[m]	0.012	0.012	0.014	0.008	0.005	0.01

TABLE 4.1 The reaction conditions of Experimental data to compare with the Base Case Model I

Figure 4.2 and 4.3 show a comparison of experimental data and calculated product distributions and were predicted by the model FT III WGS of the research from Jun Yang et al. The ASF model (Figure 2.1) appears to give a strong deviation for the selectivity to hydrocarbons, lower to methane and higher to other hydrocarbons. From the figure below we can see that olefins selectivity predicted with the ASF type model was lower than paraffins selectivity, in contrast with the experimental results. The model product distributions were in good agreement with the experimental selectivity, and the deviation for methane was described fairly accurately.
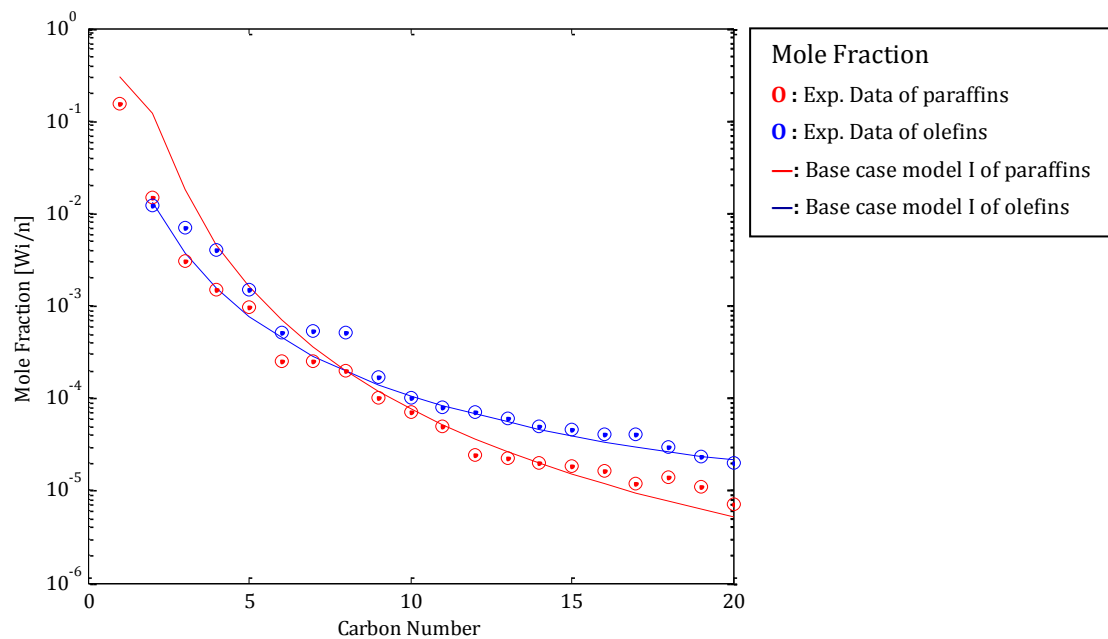
FIGURE 4.2 Comparison with the Base case model I and Experimental Data (a) from Jun Yang et al., Reaction condition: 556K, 2.51MPa, 2.62 H_2/CO Ratio, $1.6*10^{-3}$/Kg.cat.hr, $3*10^{-4}$m particle size and 0.012m reactor diameter.
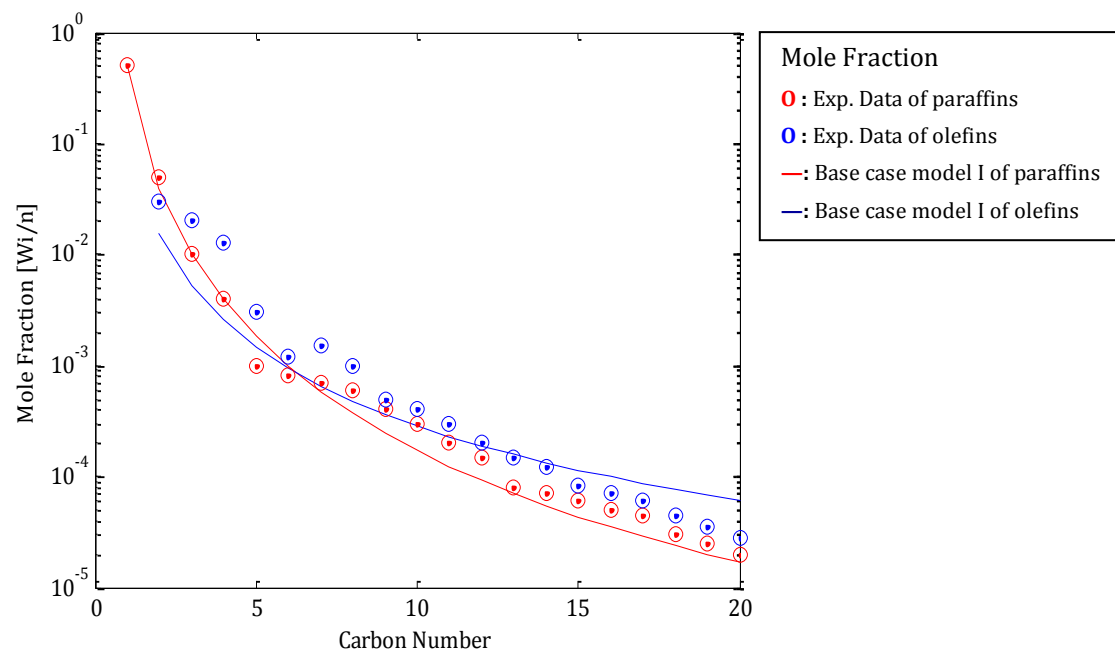
FIGURE 4.3 Comparison with the Base case model I and Experimental Data (b) from Jun Yang et al., Reaction condition: 585K, 3.02MPa, 2.04 H_2/CO Ratio, $3.2*10^{-3}$/Kg.cat.hr, $3*10^{-4}$m particle size and 0.012m reactor diameter.

Figure 4.2 and 4.3 presents the results obtained from the Base case model I and experimental data from Jun Yang et al. under each reaction conditions. The base case model I appeared to give a strong deviation for the selectivity to hydrocarbons, higher from C_1 to C_8 and good fit to above C_{9+}. As shown in these figures, the selectivities to olefins predicted with the Base case model I were higher than those to paraffins from C_1 to C_8, in contrast with the experimental results. The modelled product distributions were in good agreement with the experimental data in principle.
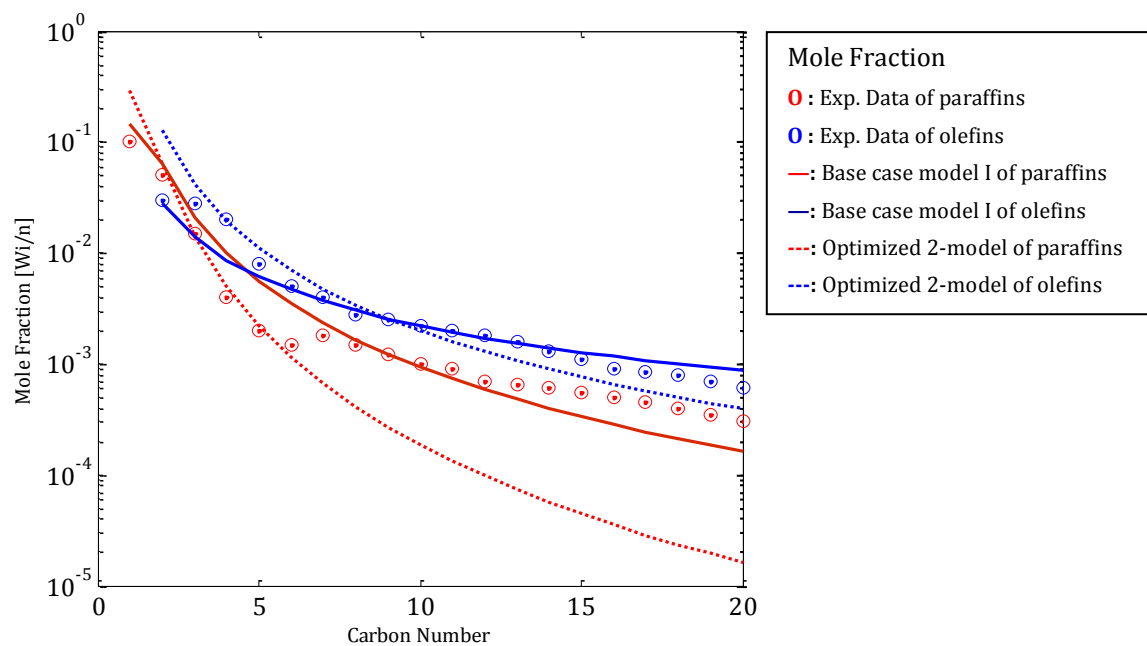
FIGURE 4.4 Comparison with the Base case model I and Experimental Data from Yuan-Yuan Ji et al., Reaction conditions: 573K, 2.25MPa, 1.97 H_2/CO Ratio, 7/Kg.cat.hr, $2.75*10^{-4}$m particle size and 0.014m reactor diameter..

The experimental data from Yuan-Yuan Ji indicate the product distributions over an industrial Fe-Mn catalyst under reaction conditions (573K, 2.25 MPa and 1.97 H_2/CO ratio) in an integral fixed bed reactor. As shown in Figure 4.4, the experimental data were presented constantly concentration both paraffins and olefins, and results of the Base case model I were apparent that methane concentration was high and olefins concentration were higher than those of paraffins even though the amounts of olefins from C_2 to C_5 were not good agreement with the Base case model I. What is interesting in this result is that olefins concentration was higher than paraffins concentration like the Base case model I. This result is in agreement with Kolbel et al. findings which higher selectivity of alkenes can be obtained on Fe-Mn catalysts than that of other hydrocarbons. Their experimental data was also same trend and in case of olefins,

the concentration of experimental data was agreed with the Base case model I at the range from C_6 to C_{20} without any optimization work. Error value of the Base case model I with experimental data was 6.79 and the site actives parameter on catalyst is shown in Table 4.2. Figure 4.4 reveals that in model, high light paraffins (C_1-C_8) are produced on 1.97 H_2/CO ratio, in other hand, the olefin distributions have a slight declining tendency leads to higher heavy olefins (C_{8+}) and lower light ones (C_2-C_7), and nearly horizontal lines of olefin distributions can be observed for the range from C_9 to C_{15}.

The Base case model I and experimental data from Wenping Ma et al. of overall hydrocarbon distributions over the Fe-Cu-M-K/Activated carbon(AC) were compared in Figure 4.5. The paraffins show a minimum around C_2-C_5, then a secondary maximum around C_8-C_{10}, followed by a monotonic decrease with the carbon number. 1-Alkenes are considered to be primary products of FTS as proposed by Wenping Ma et al. and they hypothesise that they can subsequently be hydrogenated to alkanes or be readsorbed on the catalyst surface to polymerize. The error value for optimization is 34 and the effect parameters of active sites are presented in Table 4.2. Even though activated carbon has a large surface area and pores ranging from the micro- to macrolevel, the hydrocarbon amounts of Wenping Ma et al. are lower than those of above experimental data from Yuan-Yuan Jie Chang et al. suggesting that AC-supported iron catalysts ase not useful to produce hydrocarbons and the catalyst might be need to promote with K, because for the selectivity of C_{5+} hydrocarbons, the K-catalyst is far superior to the AC-unpromoted catalyst.
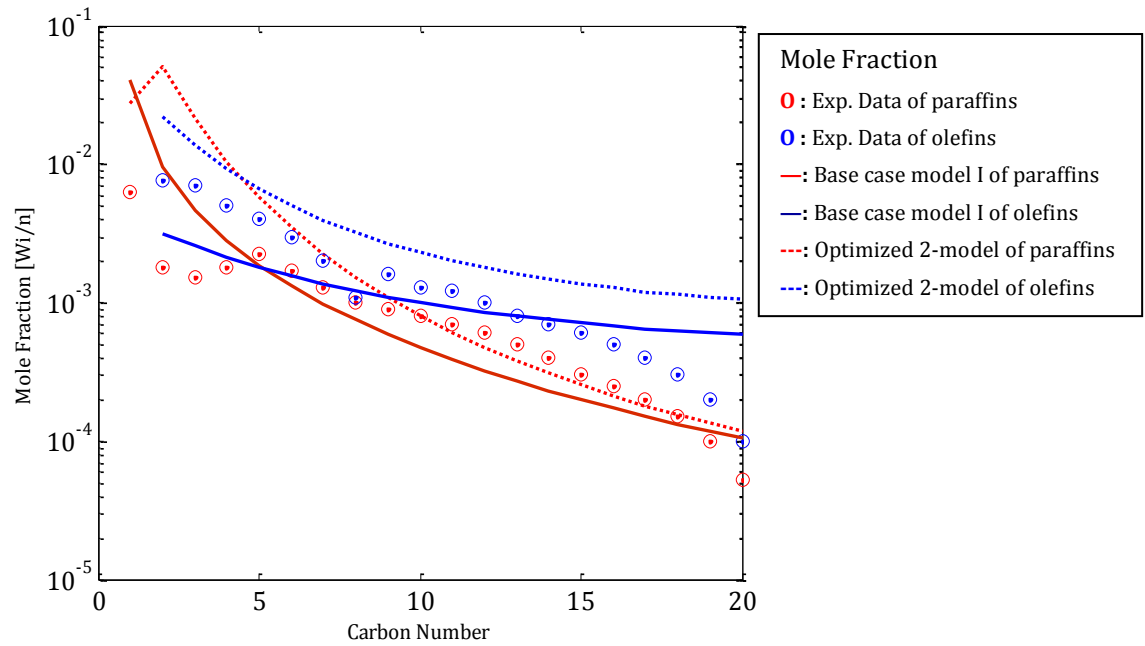
FIGURE 4.5 Comparison with the Base case model I and Experimental Data from Wenping Ma et al., Reaction condition: 553K, 2.01MPa, 0.9 H_2/CO Ratio, 3/Kg.cat.hr, $5.95*10^{-4}$m particle size and 0.008m reactor diameter.
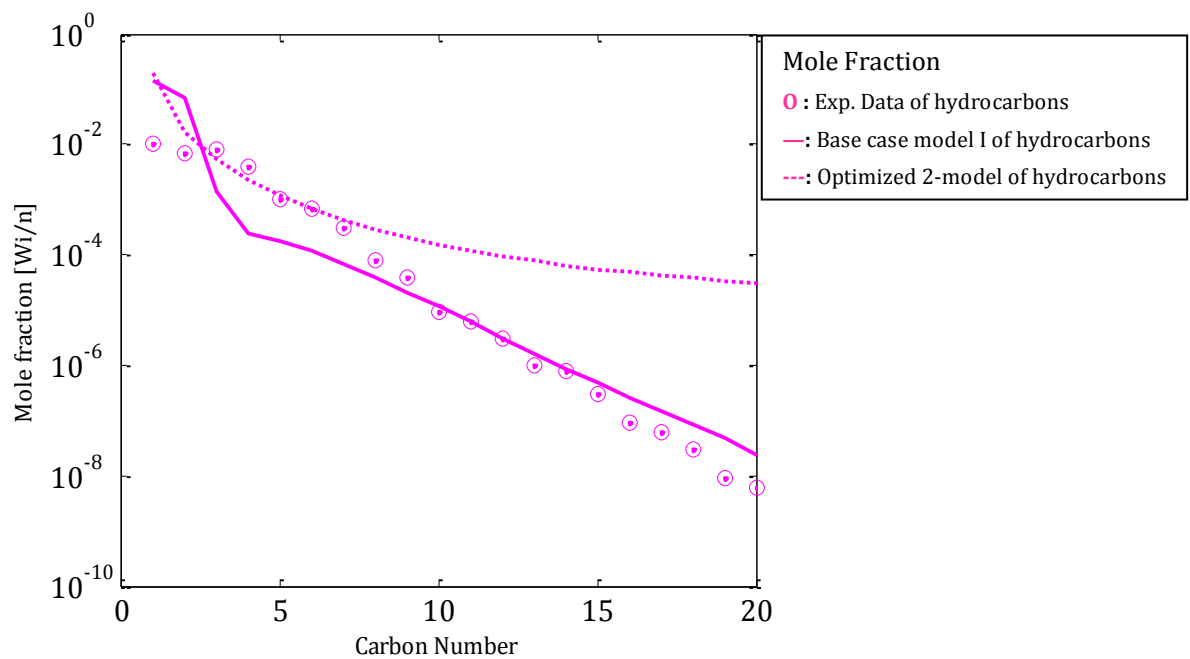
FIGURE 4.6 Comparison with the Base case model I and Experimental Data from AN Pour et al., Reaction condition: 563K, 1.7MPa, 1.0 H_2/CO Ratio, 13.28/Kg.cat.hr, $2.75*10^{-4}$m particle size and 0.005m reactor diameter..

Figure 4.6 shows total product distributions for both the models and experimental data from AN Pour et al. In Base case model I and optimized motel, the amounts of methane and ethane is higher than those of experimental data. The error value is 21.25 and the active sites parameter on catalyst is presented in Table 4.2. The reason that the error value is not good might be the lower CH_4 production.
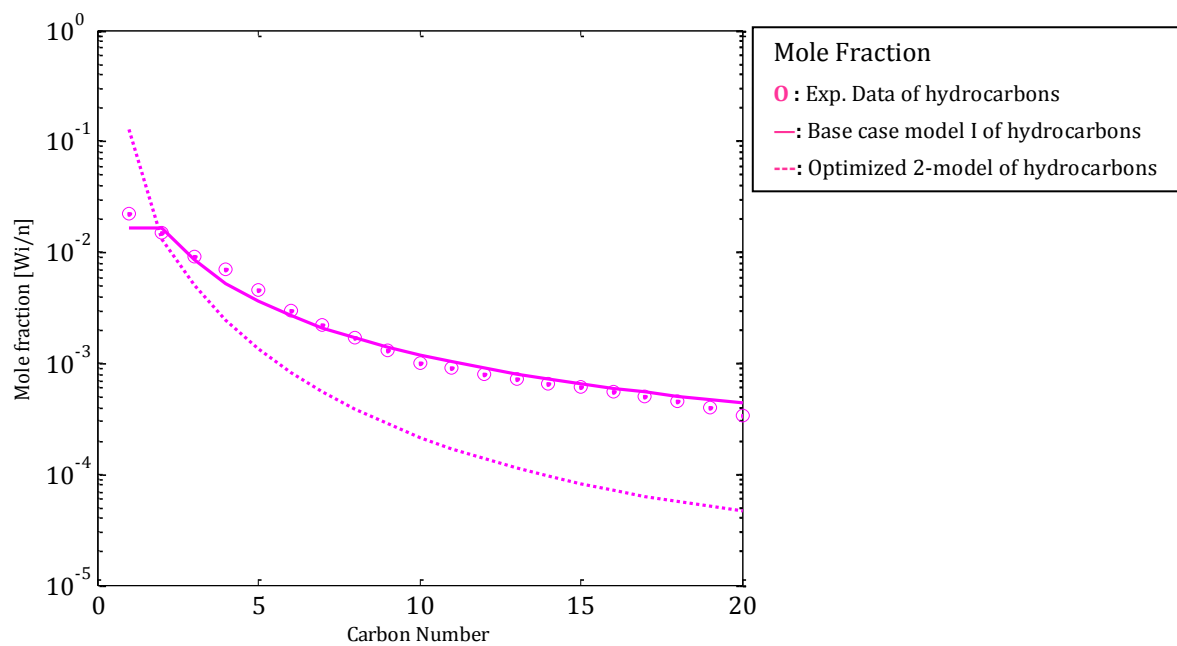
FIGURE 4.7 Comparison with the Base case model I and Experimental Data from DB Bukur et al., Reaction condition: 523K, 1.48MPa, 0.67 H_2/CO Ratio, 3/Kg.cat.hr, $3.75*10^{-4}$m particle size and 0.01m reactor diameter.

A total product distribution for both the models and experimental data from DB Bukur et al. is presented in Figure 4.7. The product distributions are good agreement with the Base case model I and optimized motel. The error value is 0.53 from (4.29) and active sites parameter on catalyst is presented in Table 4.2.

The rate equation for one active site of the catalyst should be expressed as 4.30, which defined the rate constants $k_{\sigma 1}$ and area $A_{\sigma 1}$ of σ active site on the catalyst.

$$r = [k_{\sigma 1} \cdot A_{\sigma 1}][C_{hydrocarbon}]$$

(4.30)

They are assumed that the active site on the catalyst is only one, σ_1 and fundamental rate constants, $k_{CG\,\sigma 1}$, $k_{met\,\sigma 1}$, $k_{p\,\sigma 1}$, $k_{o\,\sigma 1}$ and $k_{-o\,\sigma 1}$, on the catalyst are same for all workers. The active site effects which are calculated by equations for the four modified models shown in Table 4.3 are shown in Table 4.2.

	Kinetic parameters			Active sites values			
	Original model	Modified model		Yuan-Yuan Ji	Wenping Ma	AN Pour	DB Bukur
k_{CG}	2.84×10^9	3.49×10^8	$A_{CG\,\sigma 1}$	0.167	1.8×10^{-5}	8.7×10^{-6}	14.65
k_{met}	7.24×10^{11}	1.02×10^{14}	$A_{met\,\sigma 1}$	0.00057	0.0003	1.07×10^{-6}	0.0863
k_p	3.6×10^{11}	3.36×10^{13}	$A_{p\,\sigma 1}$	0.0063	3.5×10^{-5}	0.004	0.8112
k_o	3.16×10^9	3.19×10^{10}	$A_{o\,\sigma 1}$	8.4×10^{-5}	3.3×10^{-9}	2.3×10^{10}	1.37×10^{-8}
k_{-o}	9.972	3.9×10^3	$A_{-o\,\sigma 1}$	0.013	6.2×10^{-6}	9.17	0.04498

TABLE 4.2 The rate constants and active site A_{σ_1} effects for experimental data of two-phase.

The active site on the industrial Fe-Mn catalyst from Yuan-Yuan Ji is more active for chain growth and olefin readsorption reaction and one from Wenping Ma was not affected to react. In addition, according to the effect from AN Pour data, the active site for formation of paraffins and olefin readsorption is even more active than that for other formation. The active site from DB Bukur was 14.65 and is good for producing the higher hydrocarbon, because the chain growth is active at the site.

Yuan-Yuan Ji	$k_{CG_{Ji}} = k_{CG\,\sigma_1} \cdot A_{CG\,\sigma_{1Ji}}$
	$k_{met_{Ji}} = k_{met\,\sigma_1} \cdot A_{met\,\sigma_{1Ji}}$
	$k_{p\,Ji} = k_{p\,\sigma_1} \cdot A_{p\,\sigma_{1Ji}}$
	$k_{o\,Ji} = k_{o\,\sigma_1} \cdot A_{o\,\sigma_{1Ji}}$
	$k_{-o\,Ji} = k_{-o\,\sigma_1} \cdot A_{-o\,\sigma_{1Ji}}$
Wenping Ma	$k_{CG_{Ma}} = k_{CG\,\sigma_1} \cdot A_{CG\,\sigma_{1Ma}}$
	$k_{met\,Ma} = k_{met\,\sigma_1} \cdot A_{met\,\sigma_{1Ma}}$
	$k_{p\,Ma} = k_{p\,\sigma_1} \cdot A_{p\,\sigma_{1Ma}}$
	$k_{o_{Ma}} = k_{o\,\sigma_1} \cdot A_{o\,\sigma_{1Ma}}$
	$k_{-o\,Ma} = k_{-o\,\sigma_1} \cdot A_{-o\,\sigma_{1Ma}}$
AN Pour	$k_{CG_{AN}} = k_{CG\sigma_1} \cdot A_{CG\,\sigma_{1An}}$
	$k_{met_{AN}} = k_{met\,\sigma_1} \cdot A_{met\,\sigma_{1An}}$
	$k_{p_{AN}} = k_{p\,\sigma_1} \cdot A_{p\,\sigma_{1An}}$
	$k_{o_{AN}} = k_{o\,\sigma_1} \cdot A_{o\,\sigma_{1An}}$
	$k_{-o_{AN}} = k_{-o\,\sigma_1} \cdot A_{-o\,\sigma_{1An}}$
DB Bukur	$k_{CG\sigma_1} \cdot A_{CG\,\sigma_{1Db}}$
	$k_{met_{DB}} = k_{met\,\sigma_1} \cdot A_{met\,\sigma_{1Db}}$
	$k_{p_{DB}} = k_{p\,\sigma_1} \cdot A_{p\,\sigma_{1Db}}$
	$k_{o_{DB}} = k_{o\,\sigma_1} \cdot A_{o\,\sigma_{1Db}}$
	$k_{-o_{DB}} = k_{-o\,\sigma_1} \cdot A_{-o\,\sigma_{1Db}}$

TABLE 4.3 Equations of between rate constants and active site, σ for experimental data of two-phase.
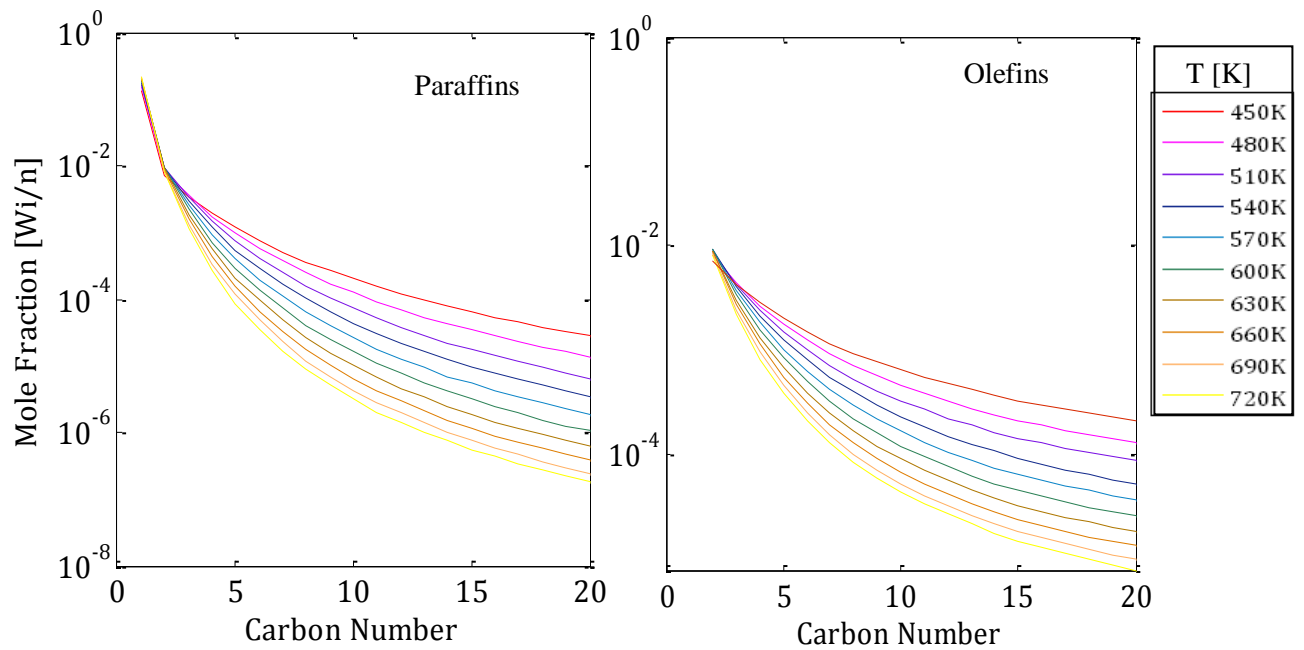
FIGURE 4.8 Carbon number distributions of temperature effect for the optimized two-phase FT Model; Reaction conditions: 1.0MPa, 1.0 H_2/CO Ratio and 0.4m/h

The paraffin and olefin distributions under different temperature in feed are illustrated in Figure 4.8. The figure shows that the high temperature leads to higher light paraffins (C_1-C_3) and lower heavy paraffins and olefins (C_4-C_{20}). These results are good agreement with the results from Yuan-Yuan Ji et al. (Figure 2.2). Higher temperature leads to higher light paraffins and lower heavy paraffins. The results are also evaluated with Figure 2.3 that operating temperature is increased, the selectivities of light hydrocarbons is increased however, and the selectivity of heavy hydrocarbons (C_{5+}) is decreased. According to the results, low temperatures are also preferable for the increased production of heavy olefins and high temperatures are preferable for increased production of light olefins as be seen the Figure 2.2, 2.3 and 4.8. In addition, these results are good agreement with analysis of driving force for two-phase reactor. At high temperature, production of paraffins hydrocarbons is lower than that of olefins hydrocarbons as shown in Table 3.8.

The gap between temperature 510K and 540K's hydrocarbon distributions is at its widest.
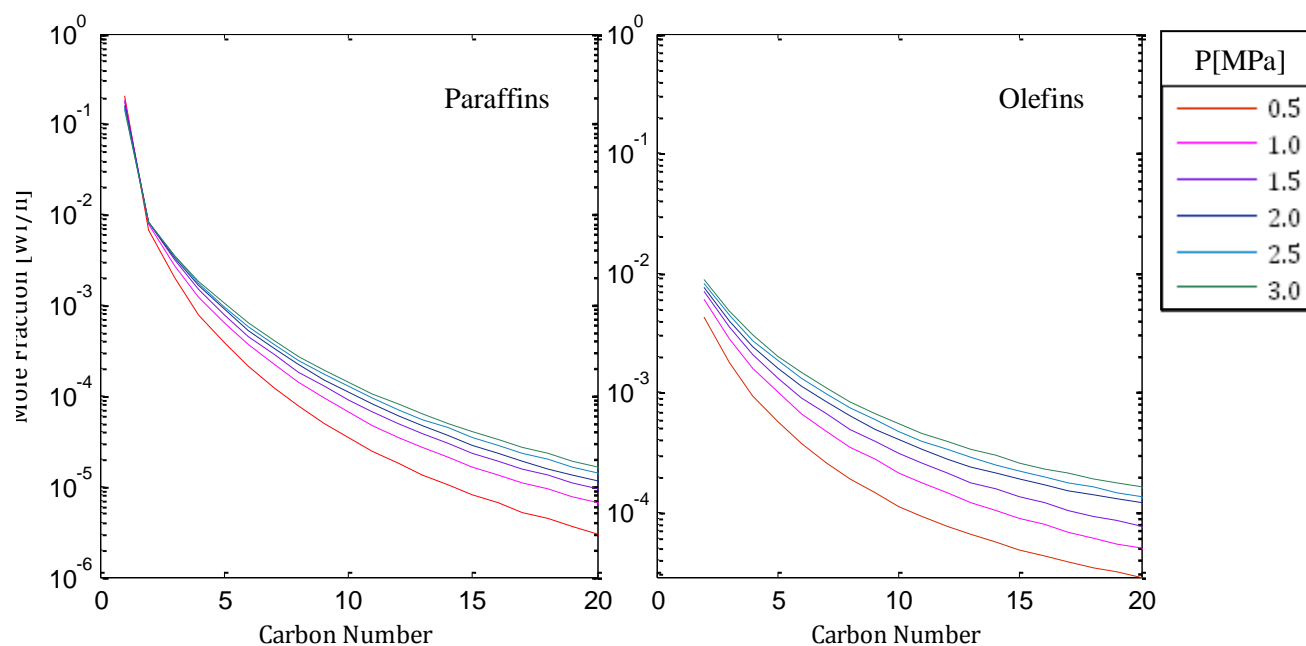
FIGURE 4.9 Carbon number distributions of pressure effect for the optimized two-phase FT; Reaction conditions: 510K, 1.0 H_2/CO Ratio and 0.4m/h.

Chain length distributions are shown in Figure 4.9 for different pressure from 0.5MPa to 3MPa, indicated that carbon number of products is almost independent to reaction pressure. The results agree with the results from AN Pour et al. as presented in Figure 2.4. However, both 0.5MPa and 1.0MPa mainly affect the carbon number distributions. In addition, low pressure leads to higher light paraffins, lower heavy paraffins and lower olefins. These results are also proven because CO conversion is decreased much at 1.0MPa and the selectivities of light hydrocarbons are very little change the all ranges of pressure. Furthermore, the C5+ selectivity of the range from 0.5MPa to 0.9MPa is bigger that that of the range from 1.0MPa to 1.5MPa as showed in Figure 2.5. According to the results, the low pressure(0.5-0.9MPa) leads to higher light paraffins (C_1-C_3) and lower heavy

paraffins and olefins (C_4-C_{20}). These results are good agreement with the results from AN Pour et al.(2004) and Mirzaei AA et al.(2009). In addition, these results are good agreement with analysis of driving force for two-phase reactor, which production of hydrocarbons is higher at high pressure as shown in Table 3.8.
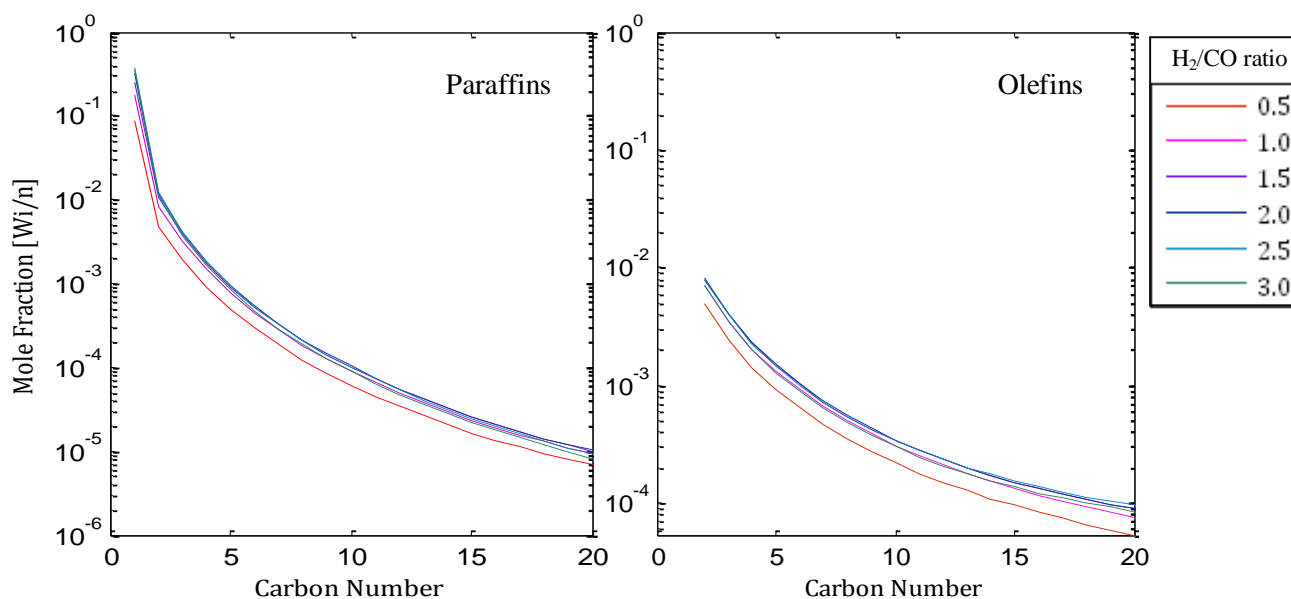
FIGURE 4.10 Carbon number distributions of H_2/CO feed ratio effect for the optimized two-phase FT Model; Reaction conditions: 510K, 1.5 MPa and 0.4m/h.

Figure 4.10 shows H_2/CO feed ratio effect on chain length distribution of iron catalyst at 510K and 1.0MPa. As can be seen, the carbon number of products has less of an effect of H_2/CO feed ratio and is decreased with increasing H_2/CO feed ratio except 3.0 H_2/CO feed ratio. According to the results, a high H_2/CO feed ratio is preferable for increased production of hydrocarbons. This has a good agreement that H_2/CO feed ratio has a small influence for carbon number distributions, however, it is obscured that production of light hydrocarbons lead to a high H_2/CO feed ratio.
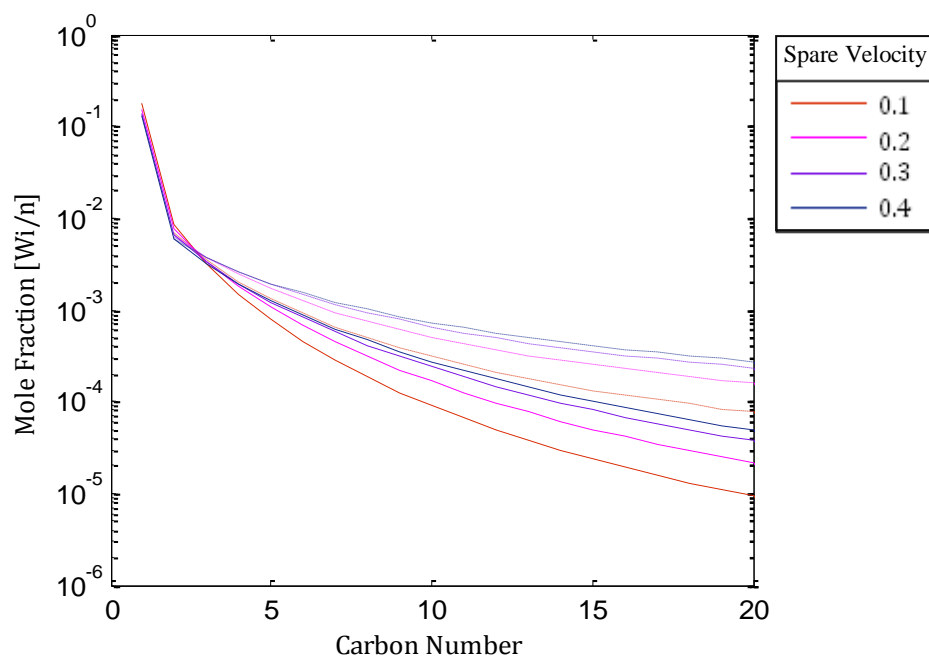
FIGURE 4.11 Carbon number distributions of Space velocity for the optimized two-phase FT Model; solid line(paraffins) and dotted line(olefins), Reaction conditions: 510K, 1.5MPa and 1.0 H_2/CO ratio.
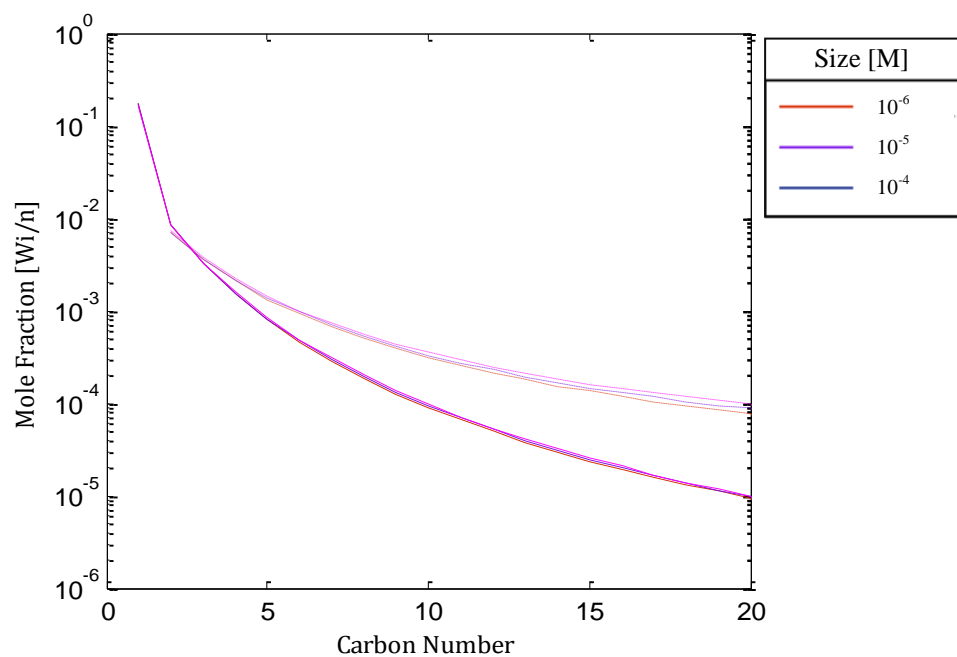
FIGURE 4.12 Carbon number distributions of Particle Size for the optimized two-phase FT Model; solid line(paraffins) and dotted line(olefins). 510K, 1.5MPa and 1.0 H_2/CO ratio.
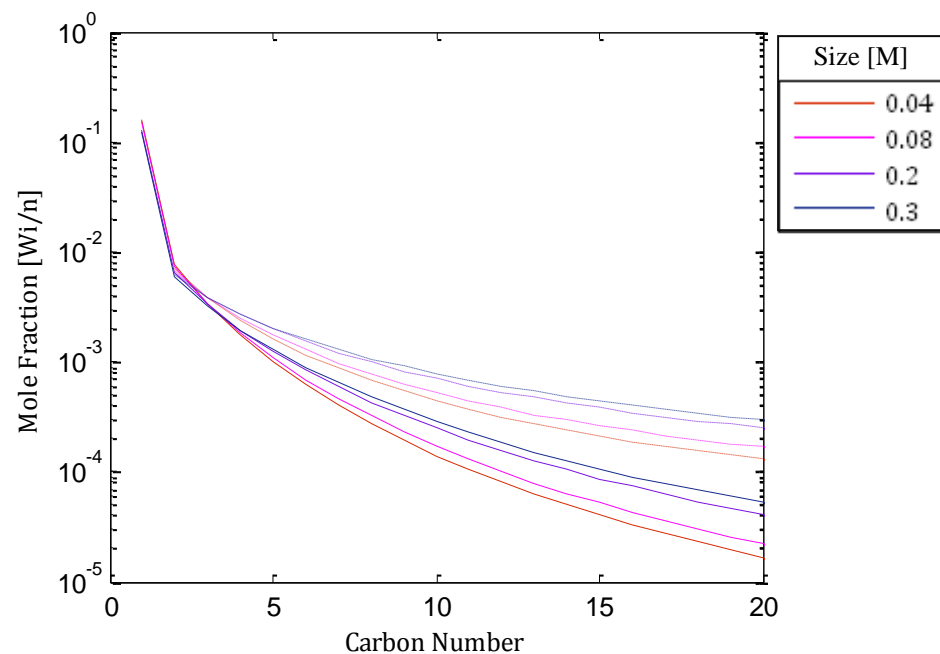
FIGURE 4.13 Carbon number distributions of reactor diameter for the optimized two-phase FT Model; solid line(paraffins) and dotted line(olefins). 510K, 1.5MPa and 1.0 H_2/CO feed ratio.

Figure 4.11 shows influence of space velocity on the paraffin and olefin distributions. Hydrocarbon products have a small change when space velocities are larger than 0.3. However, higher space velocity leads to higher products of hydrocarbon and light hydrocarbons slightly decrease with the increase of space velocity. Figure 4.12 shows carbon number distribution of the effect of particle size. This has a good agreement with the discussion by Iglesia et al.(1991). Namely, smaller particle catalysts have a greater external surface area, and hence a greater rate constant per mass of catalyst. Therefore, it is reasonable that a smaller particle catalysts lead to higher products of hydrocarbon. Carbon number distributions of reactor diameter are shown in Figure 4.13. Hydrocarbon distributions are also increased with increasing reactor diameter. It is supposed that higher reactor diameter is meant to increase the space velocity in the reactor. Increasing H_2/CO ratio and reaction temperature decrease the average carbon number of products.

4.2.2 BASE CASE MODEL II

As mentioned in Section 4.1, the Base case model II was developed on three-phase reactor by MATLAB. Most of all, both experimental data of AN Fernandes (Fernandes 2005) and the Base case model II for paraffins and olefins distributions under specific experimental condition (543K, 1.308 MPa and 1.0 H_2/CO ratio) were illustrated in Table 4.4.

	AN Fernandes et al. [a]	AN Fernandes et al. [b]	Gerard	Xiaohui Guo et al.	TJ Donnelly et al.	Liang Bai et al.
Temperature[K]	543	543	523	523	536	573
Pressure[MPa]	1.308	2.40	1.45	1.5	2.4	2.25
H_2/CO feed ratio[-]	1.0	0.7	0.67	1.99	0.7	2
Space Velocity [m/Kg.cat.hr]	0.3	0.3	3.6	2	0.034	2.51
Iron-based Catalyst	$Fe-K-SiO_2$	$Fe-K-SiO_2$	$Fe-Cu-K-SiO_2$	Fe-Cu-K	Fe-Cu	Fe-Mn
diameter[m]	≈3e-6	≈3e-6	≈4.4e-5	≈2.1e-4	≈0.7e-5	≈0.1e-5
Reactor						
diameter[m]	0.057	0.057	0.065	0.115	0.05	0.02
Height [m]	0.1	0.1	0.2	0.24	0.13	0.2
Volume[m³]	10^{-3}	10^{-3}	10^{-3}	$2*10^{-3}$	10^{-3}	10^{-3}

TABLE 4.4 Experimental conditions of the three-phase model
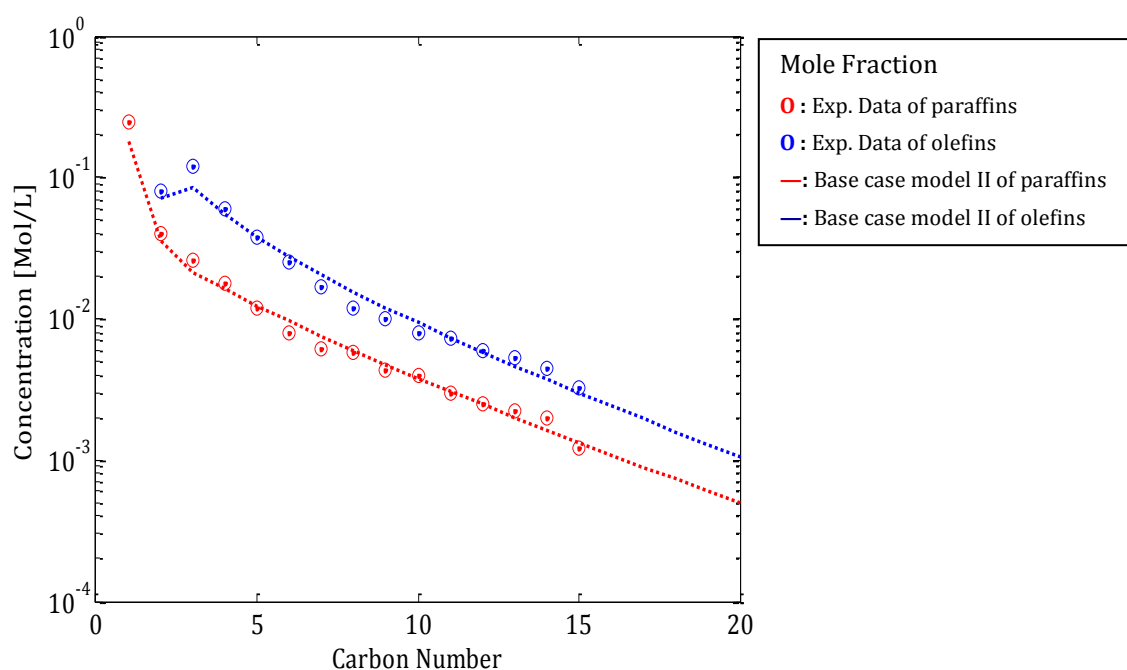
FIGURE 4.14 Comparison with the Base case model II and Experimental Data(a) from AN Fernandes et al., Reaction conditions: 543K, 1.308MPa, 1.0 H_2/CO Ratio, 0.3/Kg.cat.hr, $3*10^{-6}$m particle size and 0.057m reactor diameter.
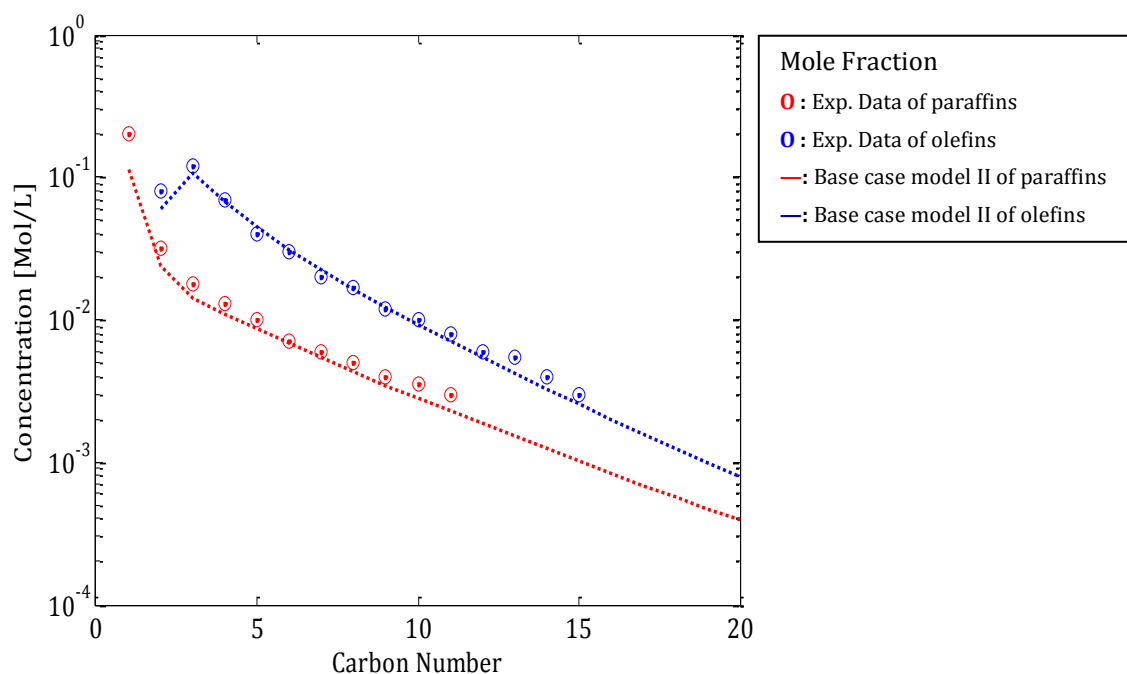
FIGURE 4.15 Comparison with the Base case model II and Experimental Data(b) from AN Fernandes et al., Reaction conditions: 543K, 2.40MPa, 0.7 H_2/CO Ratio, 0.3/Kg.cat.hr, $3*10^{-6}$m particle size and 0.057m reactor diameter.

The results for the dual mechanism; the alkyl mechanism and the alkenyl mechanism as provided by AN Fernandes, were in good agreement as shown in Figure 4.14 and 4.15. The predictions of product distributions both paraffin and olefin products described a satisfactory fitting with the experimental data. The predictions of product distributions both paraffin and olefin products described a satisfactory fitting with the experimental data.

The Base case model II can predict very well the deviation from the Anderson-Schulz-Flory distribution for both paraffins and olefins reducing the termination rate especially from methane towards butane, a range that showed greater ASF deviations. Ethylene was also in good agreement showing lower concentration than propylene. The relatively small amount of ethylene found, which appeared as a sharp dip at C_2 in the product distribution, could be explained by a different mechanism proposed for the formation of ethylene which could be directly formed by the reaction of two methylenes rather than by termination of C_2 chains.

The Base case model II was further validated against data from other literature reviews. Table 4.4 shows some experimental condition of Gerard et al., Xiaohui Guo et al., TJ Donnelly et al. and Liang Bai et al. under each condition. They had use of three-phase reactor in common. Figure 4.16 compares the experimental data on Gerard et al., and the Base case model II with optimized parameters. As can be seen from the Figure 4.16, the Base case model II was not in good agreement with the experimental data in overall range. It is surely the main cause of catalyst effects between the Base case model II and experimental data. The Base case model II used iron-based catalyst with promoters of K and SiO_2, while the experimental data from Gerard et al. were gained on Fe-Cu-K-SiO_2 catalyst. From the consideration of catalyst effects, the parameters of the effect are presented in Table 4.5 and the error that is the difference between the optimized three-phase model and experimental data is 4.20.

FIGURE 4.16 Comparison with the Base case model II and Experimental Data from Gerard et al., Reaction conditions: 523K, 3.2MPa, 2.0 H_2/CO Ratio, 3.6/Kg.cat.hr, $4.4*10^{-5}$m particle size and 0.065m reactor diameter.

It is apparent from the figure that the paraffin amount of the optimized three-phase model was in good fitting the range from C_2 to C_6, and C_{9+} selectivity of paraffins was little lower than that of olefins in the optimized three-phase model. However, it seems that the paraffins amounts is little higher than that of olefins in experimental data in range of C_{10}~C_{20}. The results indicate that it is reasonable the modification based on the olefin re-adsorption and its secondary hydrogenation because olefins concentration of experimental data is lower than one of paraffins. This is in comprehensive agreement with suggestion of Schulz and Claeys (Schulz 1995) as mentioned chapter 2 that the secondary reactions by the olefins distribution affect to increase chain length. It can be seen from the data in Table 4.2 that Cu promoter affected significantly the initiation rate constant both alkyl and akenyl mechanism, and termination by beta-elimination rate constant for alkyl mechanism.
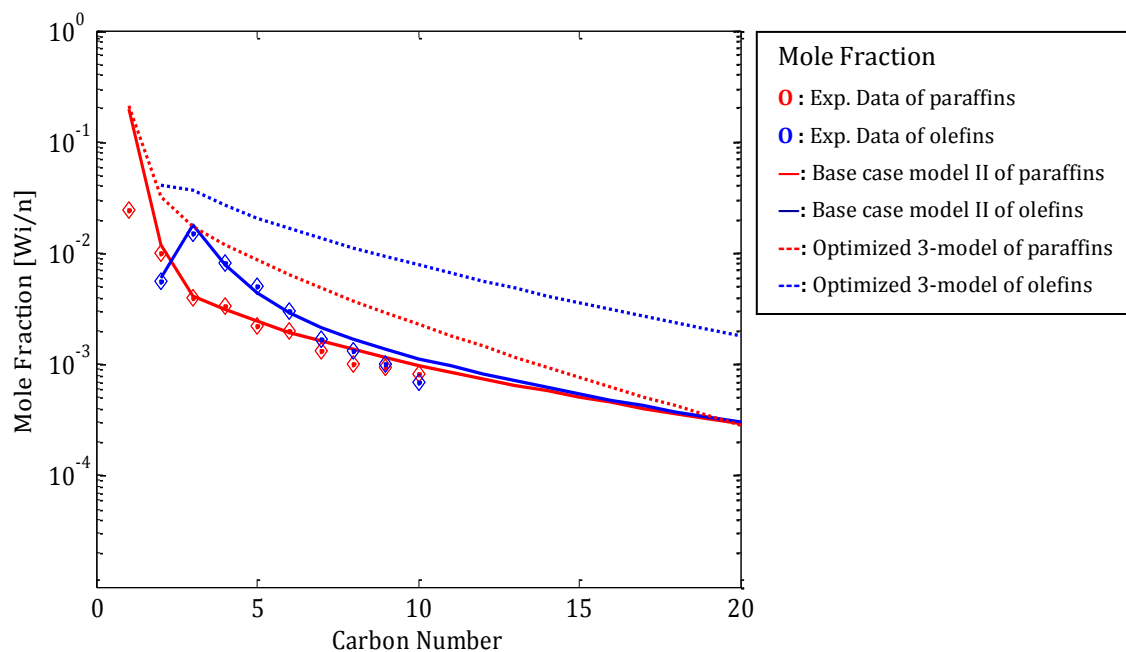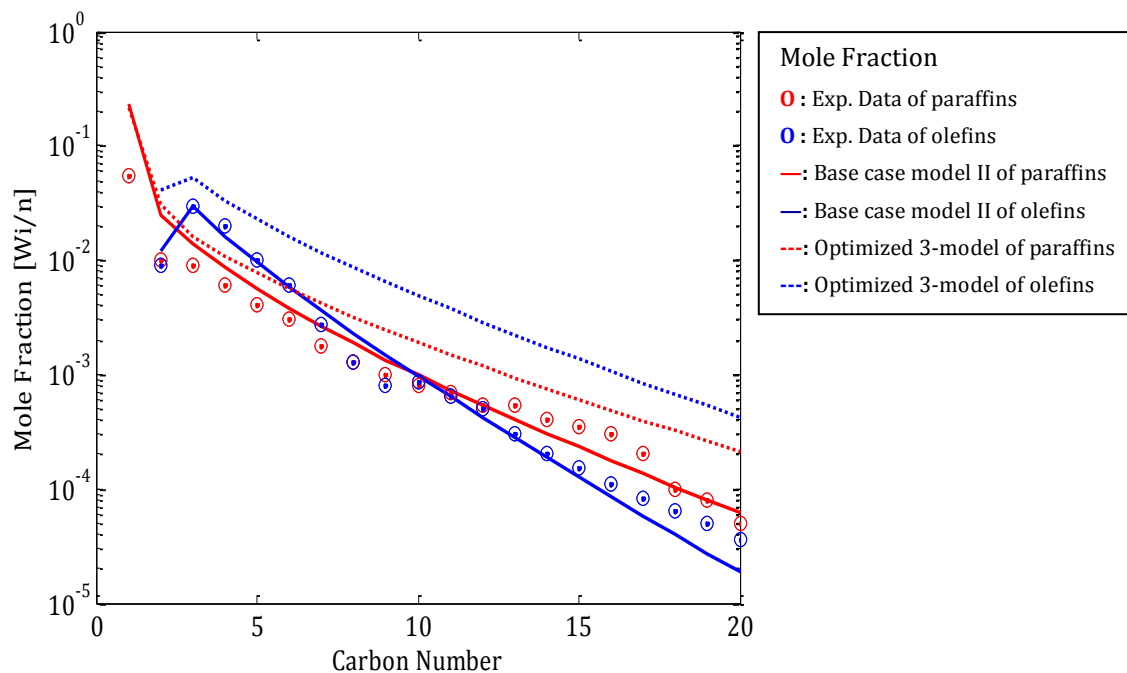
FIGURE 4.17 Comparison with the Base case model II and Experimental Data from Xiaohui Guo et al., Reaction conditions: 523K, 1.5MPa, 1.99 H_2/CO Ratio, 2/Kg.cat.hr, $2.1*10^{-4}$m particle size and 0.115m reactor diameter.

The comparison of experimental data and the Base case model II from Xiaohui Guo et al. are shown in Figure 4.17. Xiaohui Guo et al. carried out the kinetics of three-phase Fischer-Tropsch synthesis on Fe-Cu-K catalyst. The features are that the Base case model II indicates higher amount of paraffin and olefin than that of their experimental data and a high selectivity of olefins. This is agreement with Gerard that alkali-promoted iron catalysts have a high selectivity to olefins. It is also shown in these figures that the secondary reactions by the olefins affect to increase chain length and hydrogenation. To fit well with the experimental data, the Base case model II was optimized by consideration of catalyst active sites of σ_{Gu} and ψ_{Gu}. The model was found having the error value, 2.09 and Table 4.6 presents the catalyst parameters and rate constants obtained from the optimization of the Base case model II.

From the results, initiation rate constant of olefins should be increased to enhance the amount of paraffin and termination rate constant for alkenyl mechanism should be decreased. Ethylene formation rate constant should be also

increased. Data from Table 4.6 can be compared with the data in Table 4.2 which shows the catalyst with SiO_2 promoter is generally more active produced paraffins and olefins than that without the promoter. Formation rate constants both methane and ethane should be reduced because the amounts of them are little lower than that of the Base case model II.
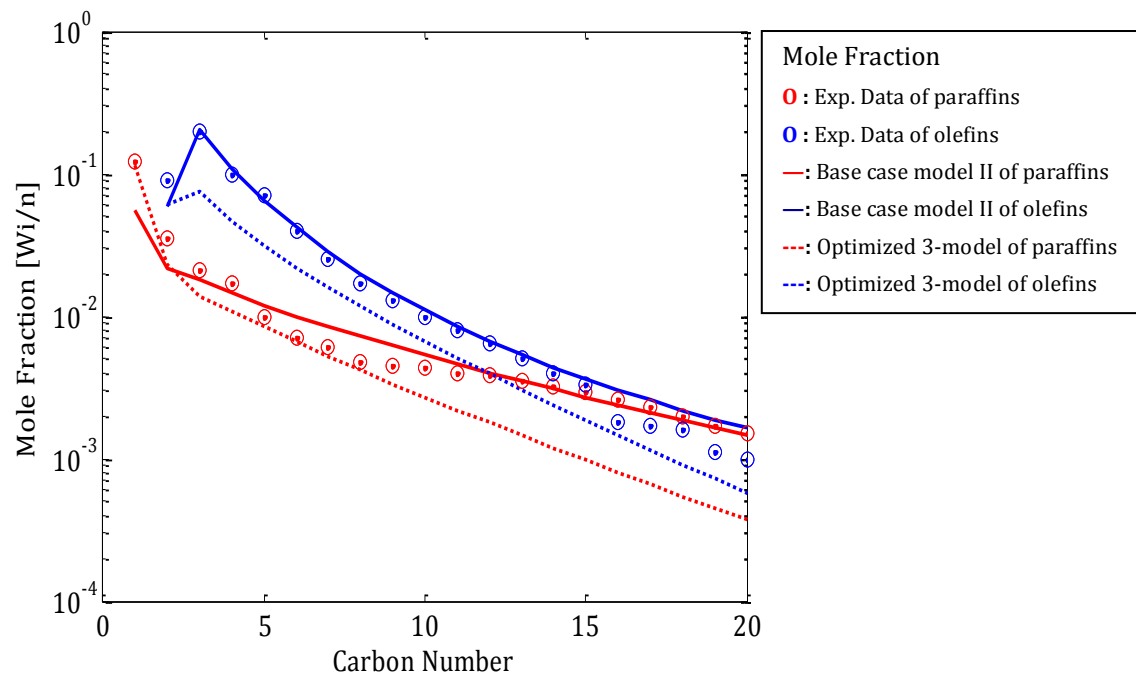
FIGURE 4.18 Comparison with the Base case model II and Experimental Data from TJ Donnelly et al., Reaction conditions 536K, 2.4MPa, 0.7 H_2/CO Ratio, 0.3/Kg.cat.hr, $3*10^{-6}$m particle size and 0.057m reactor diameter.

Figure 4.18 shows that a comparison of the Base case model II and experimental data applied FT conditions from TJ Donnelly et al. The paraffin amount of the Base case model II was also presented lower than that of experimental data and, it was found that the amount of olefin from C_{16} to C_{20} was little lower than that of paraffins. The optimized three-phase model had error 3.144 and the catalyst parameter and rate constant provides in Table 4.6. The amount of olefin from C_3 to C_{15} and paraffins from C_{13} to C_{20} described well fitting with their experimental data. The used catalyst Fe-Cu is more active to propagation both paraffins and olefins and termination of beta-elimination of paraffins. Unlike SiO_2 promoter, only Cu promoter was not active for formation of

methane and ethane, and initiation formation was also low selectivity in σ_{Tj} and ψ_{Tj}. In addition, the activation of θ_T was 1.5 times higher than that of θ from the Base case model II. However, above C_9 of olefin should be increased as rising propagation rate constant for alkenyl mechanism and paraffin from C_2 to C_{20} should be decreased, especially the range of C_2 to C_{11}.
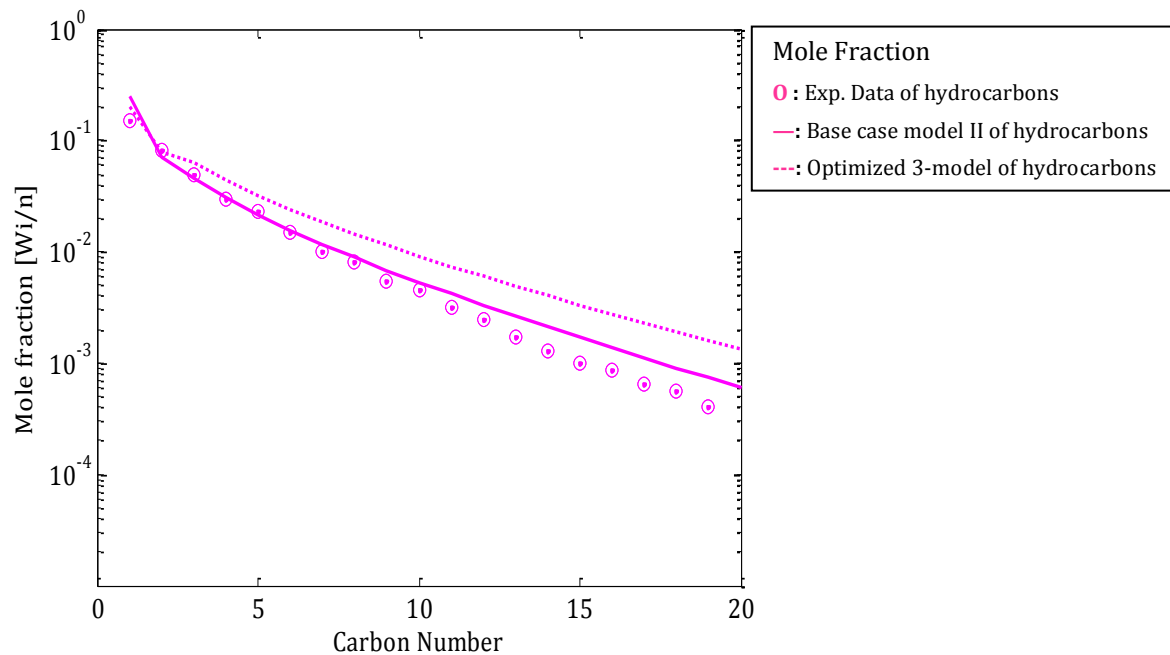
FIGURE 4.19 Comparison with the Base case model II and Experimental Data from Liang Bai et al., Reaction conditions: 573K, 2.25MPa, 2.0 H_2/CO Ratio, 2.5l/Kg.cat.hr, $1*10^{-6}$m particle size and 0.02m reactor diameter.

Lastly, the results of Liang Bai et al. (Bai, Xiang et al. 2002) are illustrated as shown in Figure 4.19. They considered the range from C_1 to C_{20} of hydrocarbons under operating conditions as described in Table 4.4. The amounts of the experimental data were also lower than that of the Base case model II like the results from Xiaohui Guo et al. The fitting as can be seen from Figure 4.19 was not good in the range of C_3 to C_9, however, the optimized three-phase model provided similar tendency with the results from Xiaohui Guo et al. Figure 4.19 shows the experimental data on Liang Bai et al., the Base Case model II, and optimized three-phase model. The methane and ethane amounts of experimental data were good fit with the Base case model II; however hydrocarbon amounts in range of C_3 to C_{20}

were not agreement with the Base case model II. To fit data, the catalyst active sites σ_{Li} and ψ_{Li} (σ_{Li}, ψ_{Li}: active sites from Liang Bai et al.) were considered and the optimized three-phase model of Liang Bai et al. was good agreements as error value 0.08. As can be seen from the Table 4.6, the termination of beta-elimination for olefins was very high active and ethane formation in Mn promoter of catalyst. In other words, σ_{Li} and ψ_{Li} is active to produce ethane compared to other promoters. Furthermore, the table presents that the rate constants of methane formation is higher than that of other paraffin products. The kinetic parameters also agree that high concentration of ethane complied with each experimental data.

The equation 4.30 for active site σ_1 on the catalyst had been applied to the three-phase model and the equations are shown in Table 4.5. They are assumed that the active site on the catalyst is only one, σ_1 and fundamental rate constants $k_{i2\,\sigma_1}$, $k_{i2\,\sigma_1}$, $k_{p\,\sigma_1}$, $k_{p2\,\sigma_1}$, $k_{par\,\sigma_1}$, $k_{olef\,\sigma_1}$, $k_{olef2\,\sigma_1}$, $k_{met\,\sigma_1}$, $k_{et\,\sigma_1}$ and $k_{o2\,\sigma_1}$, on the catalyst are same for all workers.

Gerard	TJ Donnely	Guo	Liang Bai
	$k_{i_{TJ}} = k_{i\,\sigma_1} \cdot A_{i\,\sigma_1\,Tj}$	$k_{i_{Guo}} = k_{i\,\sigma_1} \cdot A_{i\,\sigma_1\,Gu}$	$k_{i_{Liang}} = k_{i\,\sigma_1} \cdot A_{i\,\sigma_1\,Li}$
$k_{i_{Gerard}} = k_{i\,\sigma_1} \cdot A_{i\,\sigma_1\,Ge}$	$k_{i_{2TJ}} = k_{i_2\,\sigma_1} \cdot A_{i2\,\sigma_1\,Tj}$	$k_{i_{2\,Guo}} = k_{i_2\,\sigma_1} \cdot A_{i2\,\sigma_1\,Gu}$	$k_{i_{2\,Liang}} = k_{i_2\,\sigma_1} \cdot A_{i2\,\sigma_1\,Li}$
$k_{i_{2Gerard}} = k_{i_2\,\sigma_1} \cdot A_{i2\,\sigma_1\,Ge}$	$k_{p_{TJ}} = k_{p\,\sigma_1} \cdot A_{p\,\sigma_1\,Tj}$	$k_{p_{Guo}} = k_{p\,\sigma_1} \cdot A_{p\,\sigma_1\,Gu}$	$k_{p_{Liang}} = k_{p\,\sigma_1} \cdot A_{p\,\sigma_1\,Li}$
$k_{p_{Gerard}} = k_{p\,\sigma_1} \cdot A_{p\,\sigma_1\,Ge}$	$k_{p_{2TJ}} = k_{p_2\,\sigma_1} \cdot A_{p2\,\sigma_1\,Tj}$	$k_{p_{2\,Guo}} = k_{p_2\,\sigma_1} \cdot A_{p2\,\sigma_1\,Gu}$	$k_{p_{2Liang}} = k_{p_2\,\sigma_1} \cdot A_{p2\,\sigma_1\,Li}$
$k_{p_{2Gerard}} = k_{p_2\,\sigma_1} \cdot A_{p2\,\sigma_1\,Ge}$	$k_{par_{TJ}} = k_{par\,\sigma_1} \cdot A_{par\,\sigma_1\,Tj}$	$k_{par_{Guo}} = k_{par\,\sigma_1} \cdot A_{par\,\sigma_1\,Gu}$	$k_{par_{Liang}} = k_{par\,\sigma_1} \cdot A_{par\,\sigma_1\,Li}$
$k_{par_{Gerard}} = k_{par\,\sigma_1} \cdot A_{par\,\sigma_1\,Ge}$	$k_{olef_{TJ}} = k_{olef\,\sigma_1} \cdot A_{olef\,\sigma_1\,Tj}$	$k_{olef_{Guo}} = k_{olef\,\sigma_1} \cdot A_{olef\,\sigma_1\,Gu}$	$k_{olef_{Liang}} = k_{olef\,\sigma_1} \cdot A_{olef\,\sigma_1\,Li}$
$k_{olef_{Gerard}} = k_{olef\,\sigma_1} \cdot A_{olef\,\sigma_1\,Ge}$	$k_{olef2_{TJ}} = k_{olef2\,\sigma_1} \cdot A_{olef2\,\sigma_1\,Tj}$	$k_{olef2_{Guo}} = k_{olef2\,\sigma_1} \cdot A_{olef2\,\sigma_1\,Gu}$	$k_{olef2_{Liang}} = k_{olef2\,\sigma_1} \cdot A_{olef2\,\sigma_1\,Li}$
$k_{olef2_{Gerard}} = k_{olef2\,\sigma_1} \cdot A_{olef2\,\sigma_1\,Ge}$	$k_{met_{TJ}} = k_{met\,\sigma_1} \cdot A_{met\,\sigma_1\,Tj}$	$k_{met_{Guo}} = k_{met\,\sigma_1} \cdot A_{met\,\sigma_1\,Gu}$	$k_{met_{Liang}} = k_{met\,\sigma_1} \cdot A_{met\,\sigma_1\,Li}$
$k_{met_{Gerard}} = k_{met\,\sigma_1} \cdot A_{met\,\sigma_1\,Ge}$	$k_{et_{TJ}} = k_{et\,\sigma_1} \cdot A_{et\,\sigma_1\,Tj}$	$k_{et_{Guo}} = k_{et\,\sigma_1} \cdot A_{et\,\sigma_1\,Gu}$	$k_{et_{Liang}} = k_{et\,\sigma_1} \cdot A_{et\,\sigma_1\,Li}$
$k_{et_{Gerard}} = k_{et\,\sigma_1} \cdot A_{et\,\sigma_1\,Ge}$	$k_{o_{2TJ}} = k_{o_2\,\sigma_1} \cdot A_{o2\,\sigma\,Tj}$	$k_{o_{2\,Guo}} = k_{o_2\,\sigma_1} \cdot A_{o2\,\sigma_1\,Gu}$	$k_{o_{2Liang}} = k_{o_2\,\sigma_1} \cdot A_{o2\,\sigma_1\,Li}$
$k_{o_{2\,Gerard}} = k_{o_2\,\sigma_1} \cdot A_{o2\,\sigma_1\,Ge}$			

TABLE 4.5 Equations of between rate constants and active site, σ for experimental data of three-phase.

Kinetic parameters			Active sites of Experimental Data			
Original model	Optimized model		Gerard	TJ Donnely	Guo	Liang
k_i 0.4963	0.379	$A_{i\ \sigma 1}$	5.809	0.572	0.327	0.048
k_{i2} 8.054	3.726	$A_{i2\ \sigma 1}$	3.020	0.418	0.324	0.289
k_p 0.3530	0.214	$A_{p\ \sigma 1}$	0.108	1.772	4.061	0.291
k_{p2} 0.4206	0.308	$A_{p2\ \sigma 1}$	0.003	48.25	0.057	0.145
k_{par} 0.02314	0.0114	$A_{par\ \sigma 1}$	0.252	0.636	6.802	0.822
k_{olef} 0.003487	0.000077	$A_{olef\ \sigma 1}$	2.898	2.683	0.773	190.76
k_{olef2} 0.04792	0.02429	$A_{olef2\ \sigma 1}$	0.585	45.41	1.388	2.157
k_{met} 0.06386	0.0502	$A_{met\ \sigma 1}$	1.102	0.250	7.957	1.709
k_{et} 0.02421	0.01428	$A_{et\ \sigma 1}$	0.400	0.489	5.538	25.978
k_{o2} 0.09994	0.64441	$A_{o2\ \sigma 1}$	0.215	0.179	0.173	0.475

TABLE 4.6 The rate constants and active site, σ, effects for experimental data of three-phase.

Table 4.6 shows the effects of the active site for experimental data of four workders. The active site from Gerard is active for initiation of paraffins and termination by β-elimination of paraffins and active site from TJ is active for propagation and termination of olefins. In addition, Guo's active site on the catalyst is generally active for paraffins formation including methane and ethane and the active site from Liang data is even more active at termination by β-elimination of paraffins and ethane formation. These effects for three-phase model were larger value than those of two-phase model. The results are evaluated that active sites on the catalyst of three-phase model is more active than those of two-phase model.

The optimized three-phase FT model developed from the optimized rate constants should be applied to find the optimum conditions such as temperature, pressure, and H_2/CO ratio. The effects of temperature, pressure and H_2/CO ratio obtained are presented in Figure 4.20, 4.21 and 4.22, respectively.
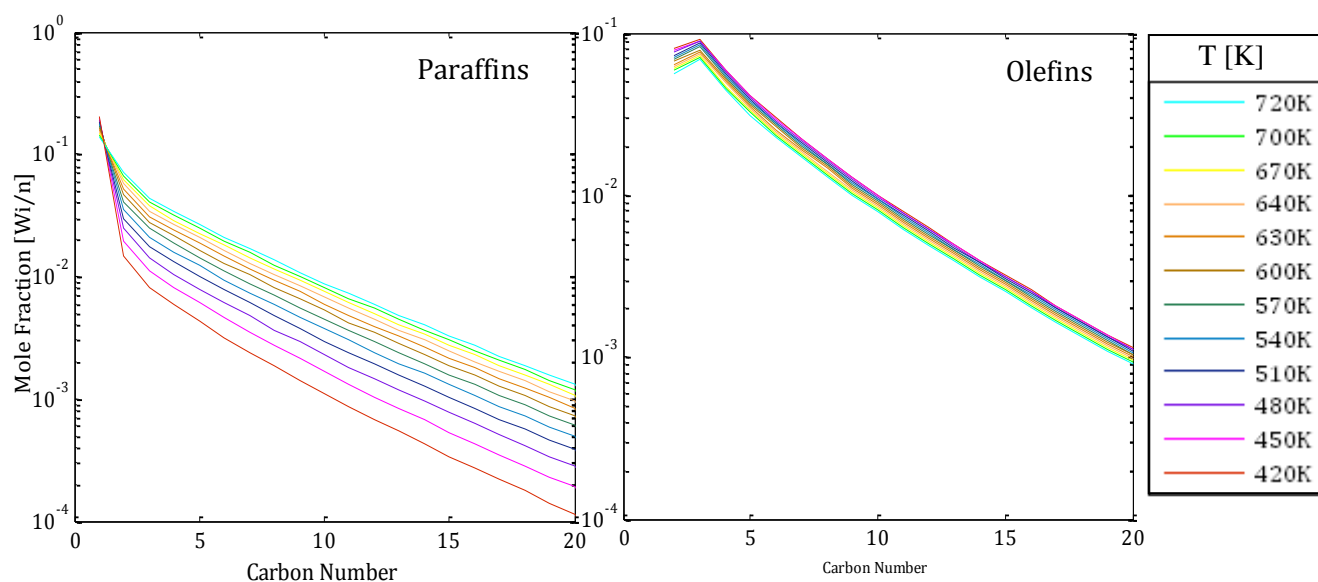
FIGURE 4.20 Hydrocarbons distribution of temperature effect for the optimized three-phase FT Model, Reaction conditions: 2.4 MPa and 1.0 H_2/CO ratio with different temperature.

The effect of temperature on the carbon number distribution was studied using the iron catalyst. From the Figure 4.20, the effect of temperature reveals that hydrocarbon concentration was increased at low temperature and concentration of paraffins was higher than that of olefins at overall temperature. Especially, the highest carbon number distributions were at 543K. In addition, according to product selectivity for a CH_2 monomer insertion to a hydrocarbon chain, the chain growth probabilities (α) of paraffins and olefins were about 0.93 and 0.92, respectively. As mentioned in Section 2.2, a high α value implies a high distribution of heavy hydrocarbons, therefore the chain growth probabilities calculated from the optimized FT three-phase model mean a greater production of heavy hydrocarbons. According to Dry, the range of α depends on catalyst type, for instance the typical range of α on iron based catalyst is about 0.7. However, α of

the optimized three-phase model was adjudged more dependent on reaction conditions. Therefore, the temperature 543K in high concentration both paraffins and olefins was chosen as the optimum operating temperature. In addition, these results could be compared with the driving force analysis. At high temperature, production of paraffins is higher while that of olefins is lower.
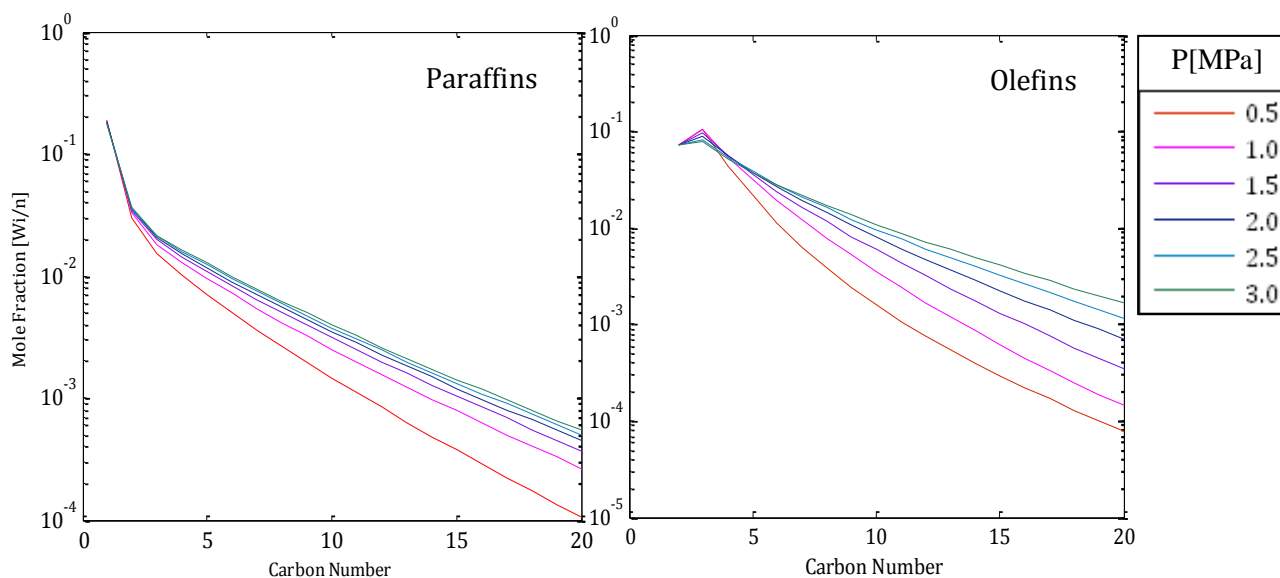
FIGURE 4.21 Hydrocarbon distributions of pressure effect for the optimized three-phase FT Model, Reaction conditions: 1.0 H_2/CO ratio and 540K temperature with different pressures.

Pressure is one of important parameters for the FT synthesis, which prefers to operate under high pressure. The effect of pressure on reaction is illustrated and pressures 0.5MPa~3.0MPa were considered on conditions of 1.0 H_2/CO ratio and different temperatures as shown in Figure 4.21. The figure illustrated that methane formation was higher than other hydrocarbons formation and the increase of pressure leads to decrease of hydrocarbons. With 1.0 H_2/CO, used in the model, the increase of pressure leads to the increase of CO conversion, causing the increase of hydrocarbons formation. The results of the pressure effect indicates that olefins hydrogenation at the high H_2/CO ratio is contributed on hydrocarbon formations over enhanced chain growth by increasing pressure. The single most striking observation to emerge from the results comparison was the low concentration of methane in spite of low concentration of hydrocarbons at 2MPa.

There is a thread of connection with the aim of this study to obtain low methane and higher olefin compounds. According to this result, the optimized three-phase FT model is required under optimum operating pressure 2MPa of the modified model. In addition, these results could be compared with the driving force analysis. The productions of both paraffins and olefins are higher at high pressure.
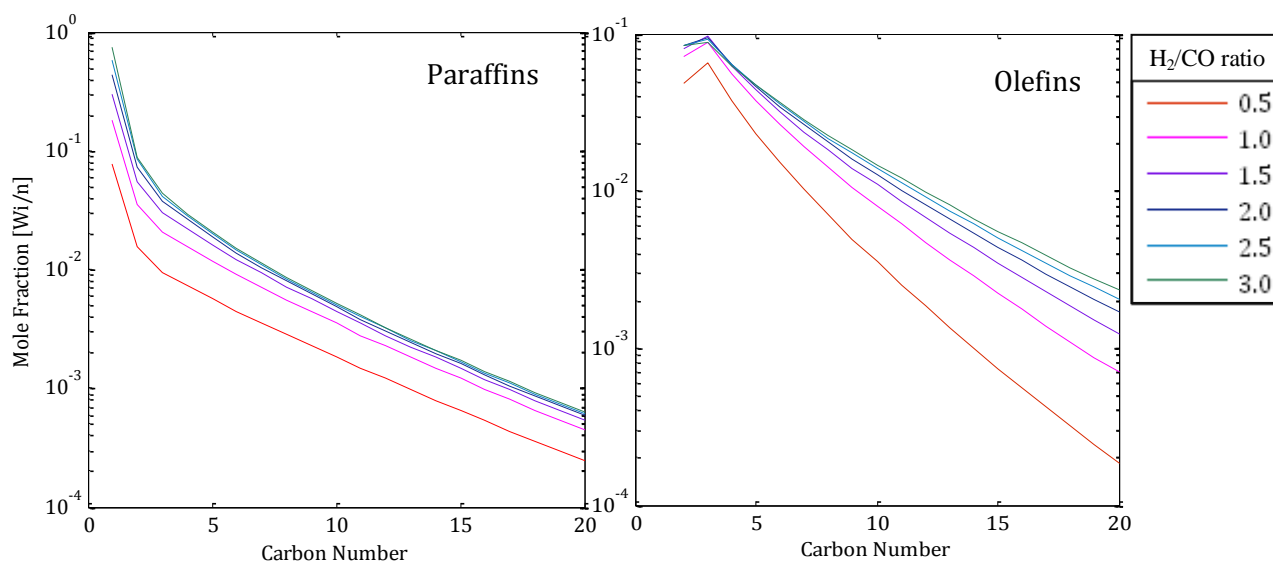
FIGURE 4.22 Hydrocarbons distributions of H_2/CO ratio effect for the optimized three-phase FT Model, Reaction conditions: 540K and 2.0 MPa with different H_2/CO ratio.

The results obtained from optimization of H_2/CO ratio were compared in Figure 4.22 on conditions of 543K and different pressures and H_2/CO ratio. The FT synthesis of three-phase operates to increase the formation of hydrocarbons in range of C_5 to C_{20}. Kolbel and Ralek (Kolbel and Ralek 1980) found that the operation of a large scale slurry reactor using an iron based catalyst produced with H_2/CO ration of 0.67, however chain growth of hydrocarbon is related to hydrogen amounts and it is possible to grow the hydrocarbons chain dependent on the hydrogen amounts. Therefore, the result reported by Kolbel and Ralek are not correct in this study. From the result, the satisfactory operation pressure is 2.0 H_2/CO ratio to produce heavy hydrocarbons.
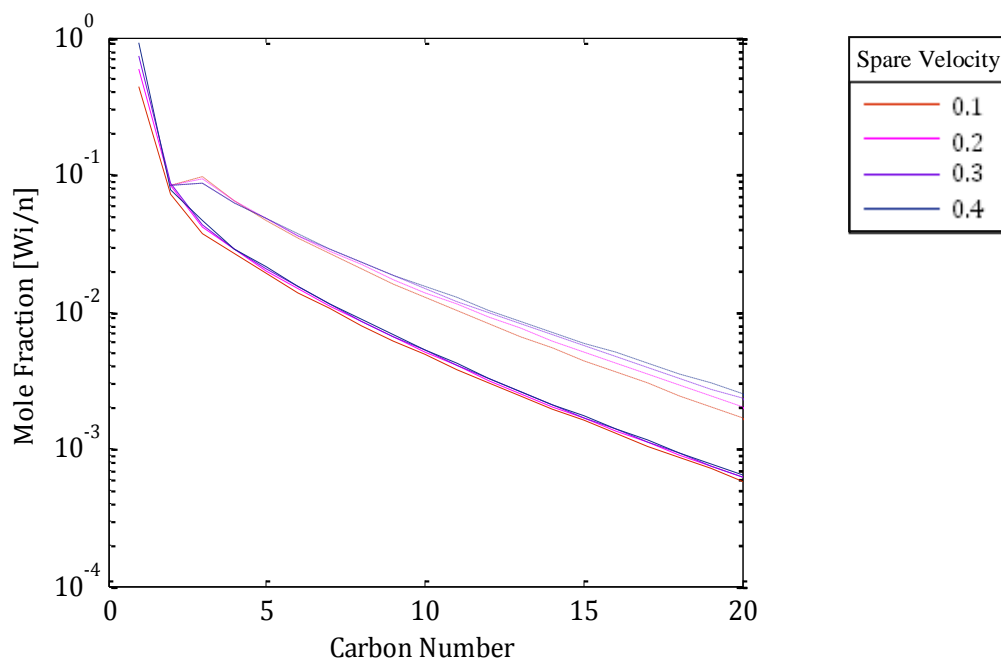
FIGURE 4.23 Hydrocarbons distributions of Space velocities effect for the optimized three-phase FT Model, Reaction conditions: 540K, 2MPa and 2.0 H_2/CO ratio.
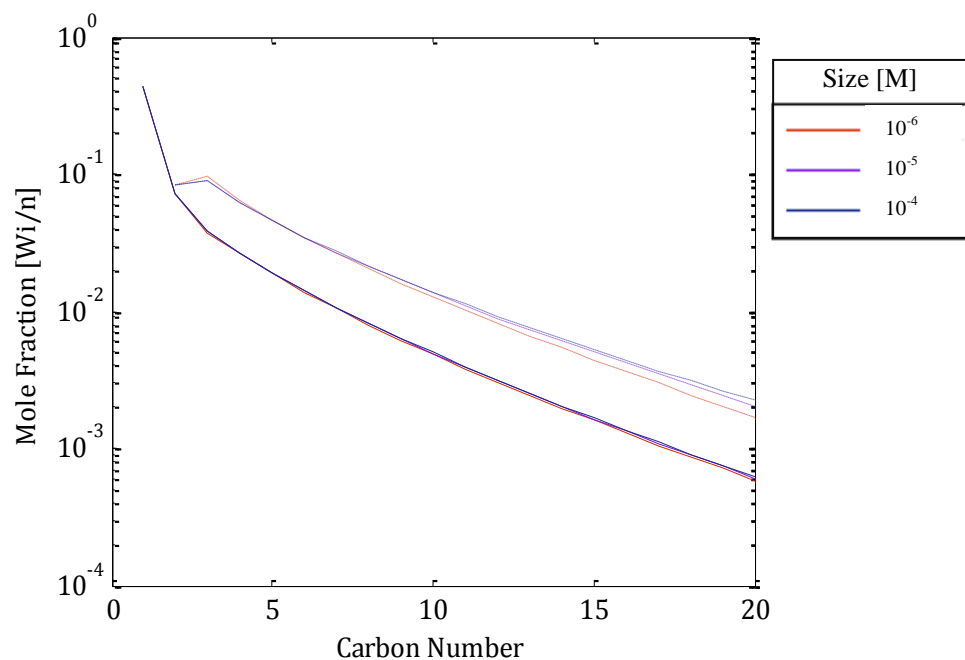
FIGURE 4.24 Hydrocarbons distributions of Catalyst Particle size effect for the optimized three-phase FT Model, Reaction conditions: 540K, 2MPa, 2.0 H_2/CO ratio and different particle size [m].
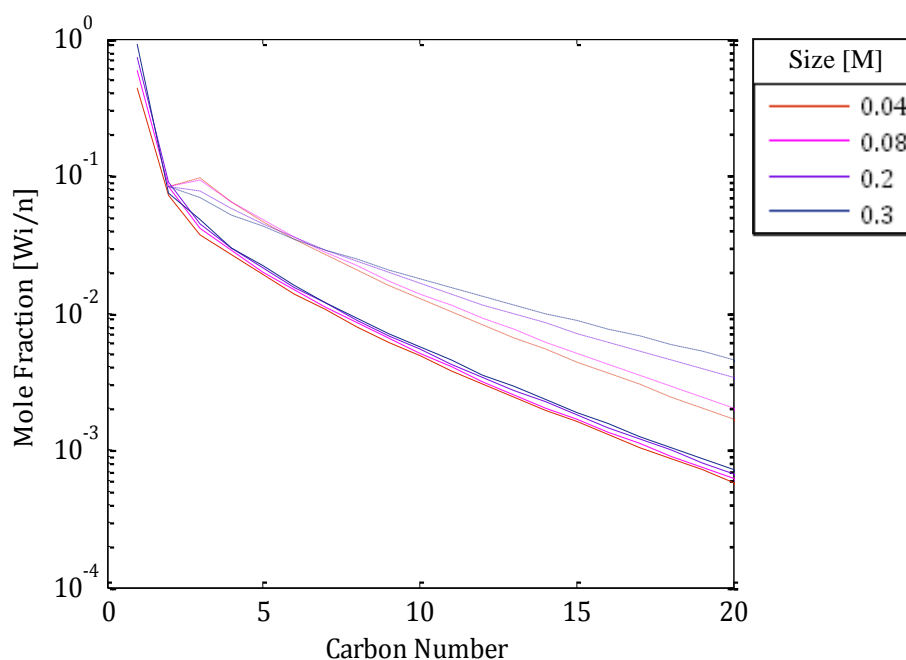
FIGURE 4.25 Hydrocarbons distributions of Reactor Diameter effect for the optimized three-phase FT Model, Reaction conditions: 543K, 2MPa, 2.0 H_2/CO ratio and different reactor diameter.

The optimized FT model mentioned in Section 4.2 was modified with consideration for formations of alcohols and acids. The kinetic expressions for these products were derived on the basis of CH_2 insertion alkyl mechanism, which were proposed by Bo-Tao et al. It was shown in Figure 4.28 that the distributions of paraffins, olefin, alcohol and acid in a logarithmic figure are almost similar before carbon number 10 and the formation of paraffins, olefins, alcohols and acids are indicated parallel competitive reactions. After carbon number 10, the olefins re-adsorption and secondary reactions were attributed to paraffins formation because the amount of olefin was decreased, while that of paraffin was increased with increasing carbon number. In addition, the results agree with the results of experimental data provided by Bo-Tao et al.
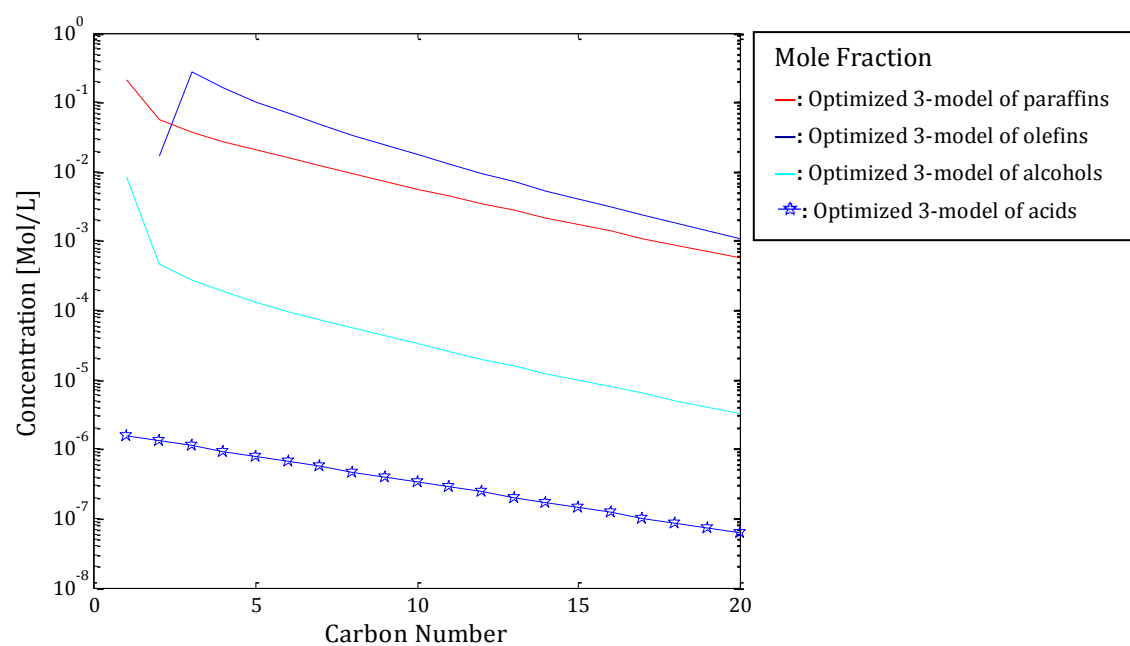
FIGURE 4.26 Hydrocarbons, alcohols and acids distributions for optimum conditions of the modified three-phase model Reaction conditions: 540K, 2MPa and 2.0 H_2/CO Ratio.

It was shown in Figure 4.26 that the slopes of paraffins, olefins, alcohols and acids distribution curve were almost similar. In addition, it was apparent from this figure that distributions of paraffins and olefins were higher than those of alcohols and acids. The results indicate that the formation of paraffin, olefins, alcohols and acids over the iron based catalyst are parallel competitive reactions. Oxygenates might readsorb over the catalyst surface and take part in the corresponding secondary reactions.

The optimized FT model mentioned in Section 4.2 was considered with co-feeding for lighter hydrocarbons. The Figure 4.27 and 4.28 show the paraffin and olefin distribution for the co-feeding process of 1-10 number, respectively. It can be seen from the data in the figures, the amount of olefins was higher than that of paraffin in once-through process, while the more it has co-feeding, and the amount of olefins was decreased, on the contrast that of paraffins was increased. The result implied that co-feed olefins lead to a higher chain growth probability and higher paraffin selectivity. Furthermore, the re-adsorption of olefin becomes more effective with increasing chain length. These results are strongly agreement with

many literatures, which are proposed by Hanlon and Satterfield, and Gerard et al so on.
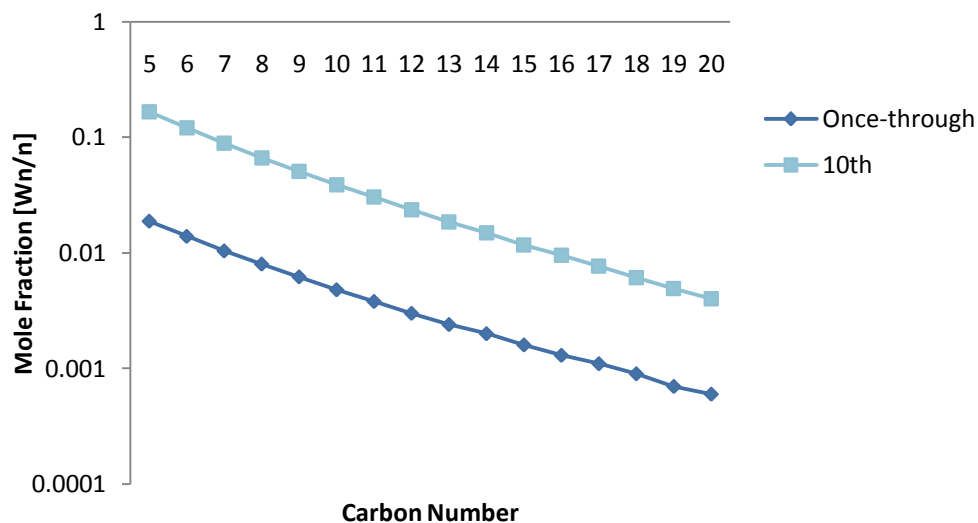
FIGURE 4.27 Paraffin distributions of Co-feeding with once-through for three-phase FT model, Reaction condition: 540K, 2MPa and 2.0 H_2/CO ratio.
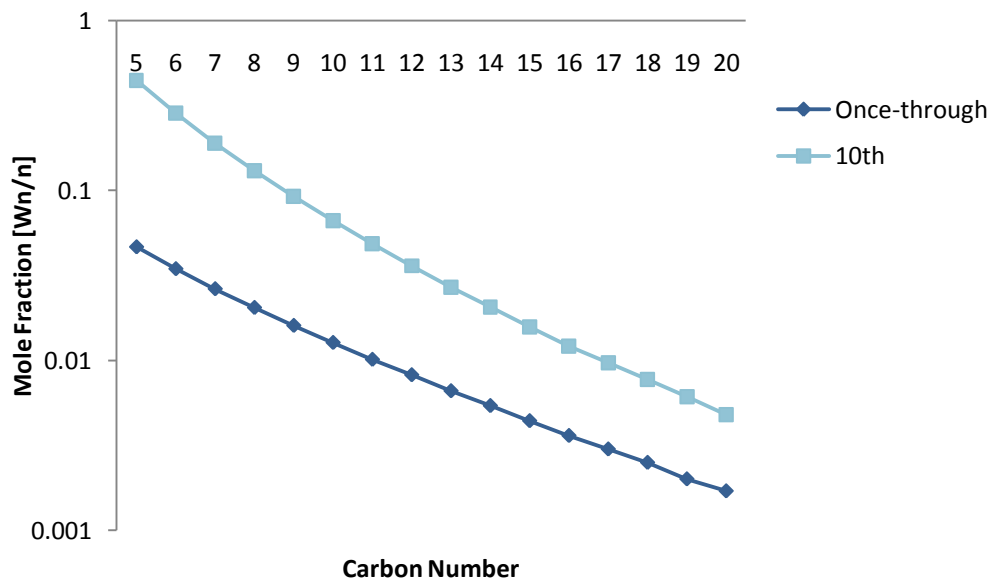
FIGURE 4.28 Olefin distributions of Co-feeding with once-through for three-phase FT model, Reaction condition: 540K, 2MPa and 2.0 H_2/CO ratio.

4.3 SUMMARY

The proposed process is to use of fuel gases fed directly into Fischer-Tropsch reactor as a form of co-feed. Therefore, the proposed Fischer-Tropsch process modelling was to first develop the Fischer-Tropsch reactor model in MATLAB, as a programming language. This study simulated the Base case model I & II and the models were optimized in terms of parameters and conditions by using MATLAB. Two developed simulation models were used as reference for this study. The first was developed by MATLAB in Fernandes et al. The second was developed by MATLAB in Jun Yang. Some assumptions were applied both to the base case. Additionally, two base models had proved to be feasible for representing mass balances of the targeted processes. These models were also capable for estimating the kinetic parameters. These models could therefore be used for observing behaviour of corresponding process configurations under varying circumstances. The objective of process optimization could be expanded to include other aspects of sustainability (e.g. minimum environmental impact and product marketability).

The kinetics model for both two-phase and three-phase reactor were developed based on the proposed reaction mechanism and modified with some parameters such as size effects of catalyst and reactor and active sites on iron based catalysts, and with consideration of formation of alcohols and acids to comprehend the effects of these parameters using MATLAB mathematics tool.

The considered kinetic models with sizes of catalyst and reactor, three active sites on catalyst, reactions of both primary and secondary reaction and polymerization of hydrocarbon were developed and compared with other experimental data under specific conditions. According to the results, the rate of hydrogenation increases with increasing chain length of the molecule. The research has been also suggested that alkenes are primary synthesis products while alkanes are formed by secondary hydrogenation of alkenes. In order to maximize hydrocarbon production, reaction conditions of the optimized two-phase model require pressure 1.5MPa and temperature 510K. Also H_2/CO ratio 1 produces on the desired hydrocarbon using iron-based catalyst. The reaction

conditions of the optimized three-phase model require 540K, 2MPa and H_2/CO ratio 2.

For co-feeding, the distributions of paraffins, olefin, alcohol and acid agree with real experimental data and the results implied that the formation of paraffins, olefins, alcohols and acids have parallel competitive reactions. Oxygenates might re-adsorb over the catalyst surface and take part in the corresponding secondary reaction.

The effect of co-feeding on the iron-based catalyst was investigated in the two reactor types. It was found that co-feeding unwanted compounds with synthesis gas did increase the production of hydrocarbons. The recycling and co-feeding led to an increase in feed ratios of C_5^+ selectivity and a slight increase of low carbon hydrocarbons.

5

Fischer-Tropsch Plant Model

5.1 DEVELOPMENT OF FISCHER-TROPSCH PLANT

The material in this section presents the simulation work for both the optimized three-phase FT model and two-phase FT model by ASPEN HYSYS and the code integration with MATLAB for simulation of the Fischer-Tropsch plant with recycling and co-feeding process. Most of all, ASPEN HYSYS as simulation tool were introduced a brief information and the simulation process were suggested not only two-phase and three-phase model but also once-through to FT reactor and recycling & co-feeding process of Fischer-Tropsch plant by spreadsheet of ASPEN HYSYS. Furthermore, parts of whole Fischer-Tropsch plant were proposed and optimized and the process was simulated to design, to observe, and to evaluate recycling effect and for Fischer-Tropsch plant with ASPEN HYSYS 2006.1.

5.1.1 SIMULATION SETUP:ASPEN HYSYS

ASPEN HYSYS is a commercially available process simulator for process analysis. It contains a rigorous thermodynamic and physical property database and provides comprehensive built-in process models, offering a convenient and time saving means for chemical process studies, including system modelling, integration and optimization. The original purpose of this software is for supporting the chemical engineering of crude oil refineries. Process components of the simulation were implemented in ASPEN HYSYS using standard, built-in unit operation modules and functions including all the components and functions contained in the process, such as pumps and compressors.

5.1.2 Developing Simulation Models

The model was simulated using the ASPEN HYSYS simulation programme that was interfaced with MATLAB for collecting the optimization results. The model in this study was used for simulations by adopting the data of the two reference models, i.e. the optimized three-phase FT model and two-phase FT model. Figure 5.1 shows overall flow sheet and presets a link between Fischer-Tropsch reactor's MATLAB codes for recycling and co-feeding to reformer or FT reactor.
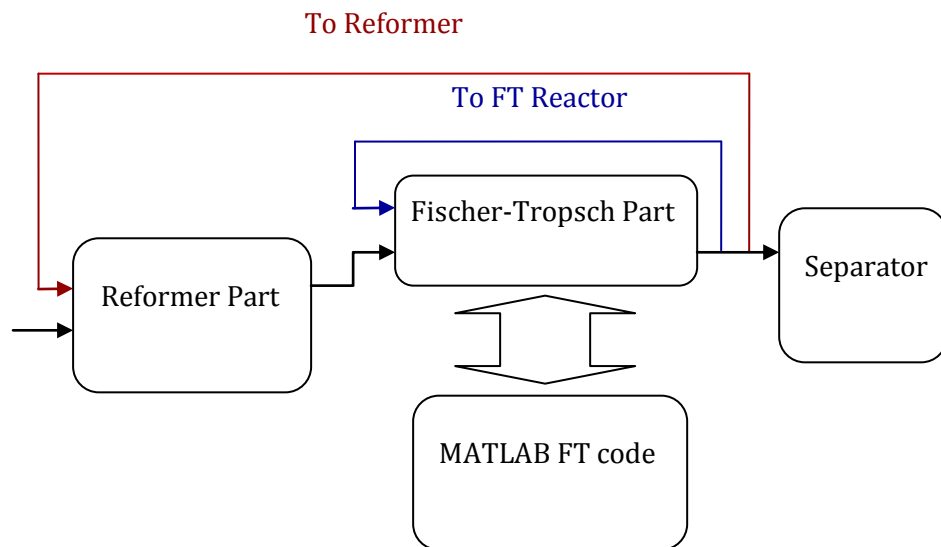
FIGURE 5.1 Fischer-Tropsch Process flow diagram integrated with FT reactor code of MATLAB

Assumptions of the simulation FT process considered as following. The process was steady state and isothermal and Input flow rate of natural gas in reformer part was constant. Furthermore, the process used FT synthesis catalyst that was composed of homogeneous catalyst and the catalyst was charged with constant void fraction of catalyst bed in FT reactor. Finally, catalytic poisoning effect of H_2S was neglected.

Next, it was required to utilize thermodynamic parameters which could be applied to fundamental equation of state for simulating a GTL process by ASPEN HYSYS. Many equations of state of varying complexity had been developed. No equation was sufficiently accurate to represent all real gases under all conditions.

In this simulation study, RKS (Redlich Kwong Soave) equation is utilized for calculating thermodynamic parameters in the model. RK (Redlich-Kwong) equation of state is interpreted with an extension of the more familiar Van der Waal's equation. The RK equation generally has application to binary components. It has good accuracy in volumetric and thermal properties between pure components and mixture; however it is tend to lower accuracy of VLE (Vapour Liquid Equilibrium) calculation in multi-components. Giorgio Soave (1972) modified the RK equation to extend its usefulness to the critical region and for use with liquids in order to make up for the weakness of RK state equation. Because FT process is composed of multi-components with vapour-liquid phase, RKS equation was selected as governing equation for simulating of FT process. With this adequate explanation, the RK equation was employed in this modified form in ASPEN HYSYS simulation.

5.1.3 SIMULATION PROCEDURE

This section presentes the process description for the Fischer-Tropsch plant that consists of three main process units; a reforming unit where natural gas or coal are converted into synthesis gas, a FTS unit where synthesis gas was converted into transportation fuel, and a separator as product upgrading unit. The simulation scheme of FT process in this study is in Figure 5.2.
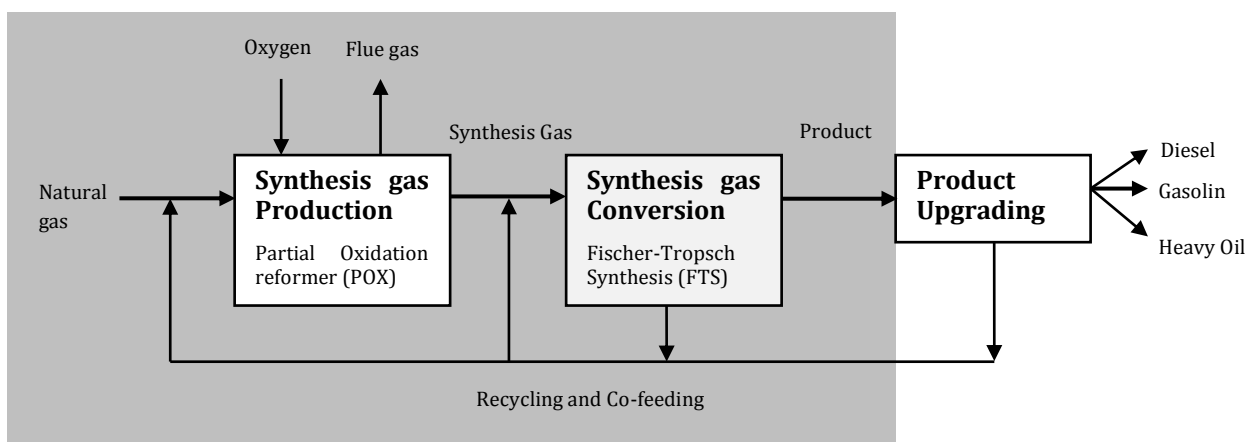
FIGURE 5.2 Schematic layout of a FT procession with highlighted area as the main focus of this study

The proposed FTS process was approached by one synthesis gas production unit flowsheet and ten sub-flowsheets of Fischer-Tropsch synthesis and production unit (Case A-J). These cases were applied to modified two-phase and also were considered with modified three-phase model based on Jun-Yang et al. because the modified three-phase model based on FN Fabiano was only considered polymerization. Therefore, as mentioned at Section 4.1.2 the three-phase model considered re-adsorption of olefins by Jun Yang and Bo-Tao Teng et al. applied to compare with amounts of higher hydrocarbons.

SYNTHESIS GAS PRODUCTION UNIT

The simulated PFD (Process Flow Diagram) of POX for the production of synthesis gas from natural gas is shown in Figure 5.3. The natural gas fed into the POX reformer together with preheated air was converted into synthesis gas. Heat from the POX reformer was recovered by Heat exchanger-1 to raise temperature of air feed stream, and unreacted air and synthesis gas were separated through the separator. Furthermore, the X-100 reactor was facilitated to separate synthesis gas from undesired compounds such as C_3H_8, O_2, CO_2, H_2S and N_2. Analysis was performed under specific conditions and the main process parameters were the H_2/CO ratio and energy efficiency of POX.
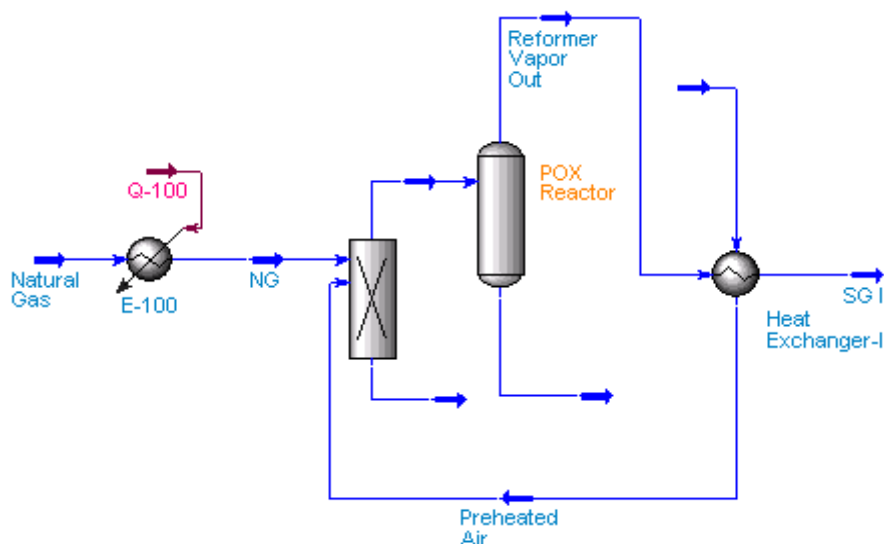
FIGURE 5.3 Simulated PFD of POX for the production of synthesis gas from natural gas.

A. ONCE-THROUGH TO FISCHER-TROPSCH REACTOR

Figure 5.4 shows the simulated PFD of FTS for the production of transportation fuel from synthesis gas with once-through FT reactor. The PFR reactor in ASPEN HYSYS was used for the Fischer-Tropsch reactor. The detailed kinetic models for iron-based catalyst were programmed in MATLAB as mentioned above section and complied as the optimized FT model for ASPEN HYSYS. The synthesis gas from reformer unit was increased the pressure through compressor to set up relevant pressure, and go through the FT reactor after setting the reaction temperature. Finally, the feed is separated water from hydrocarbon products. In order to understand the performance of the model, CO conversion, synthesis gas conversion and product distribution were analyzed for each flowsheet structure under specific conditions proposed by the optimized FT model.
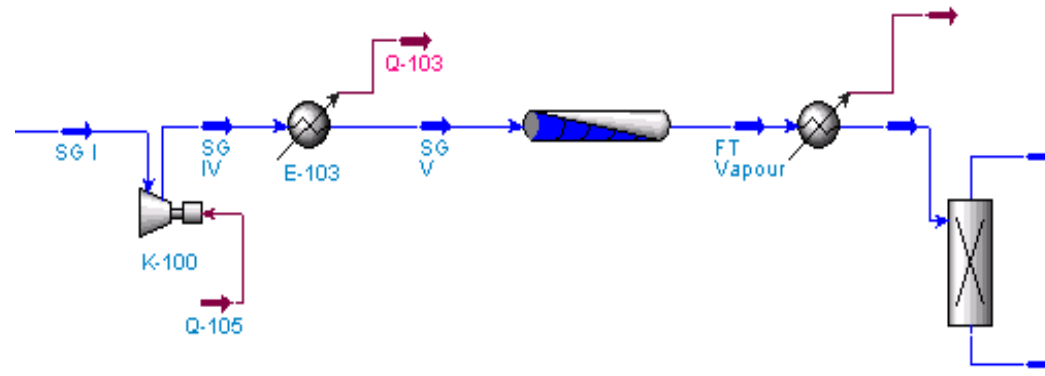
FIGURE 5.4 Simulated PFD of once-through FT reactor for the production of transportation fuel from synthesis gas (CASE A).

B. Two Series Fischer-Tropsch Reactors

Figure 5.5 presents the flowsheet of FTS using two series Fischer-Tropsch reactors as Case B. Each reactor applied same reaction and conditions were the same volume($0.25m^3$) and the total volume was kept the same as in case A.
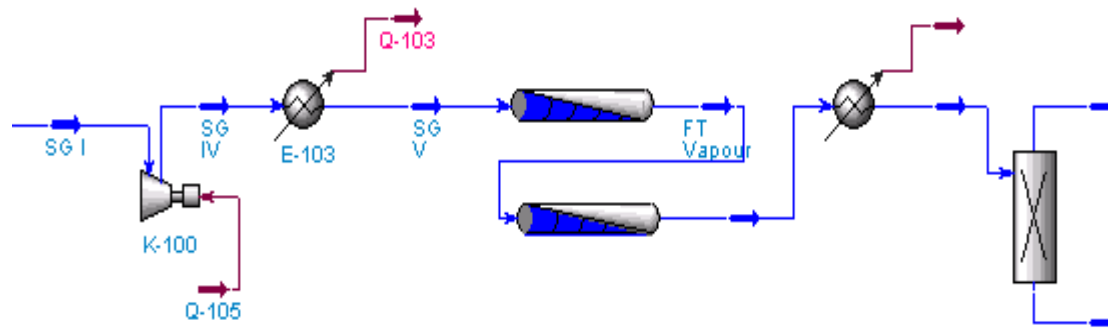
FIGURE 5.5 Simulated PFD of FTS used series Fischer-Tropsch reactor (CASE B).

C. Two Multi-stages Fischer-Tropsch Reactor

Figure 5.6 presents the flowsheet of FTS used two multi-stages Fischer-Tropsch reactors as Case C. The used reactors of same volume ($0.17m^3$) operated under the same reaction and conditions and also each FT reactor has separators in a stage.
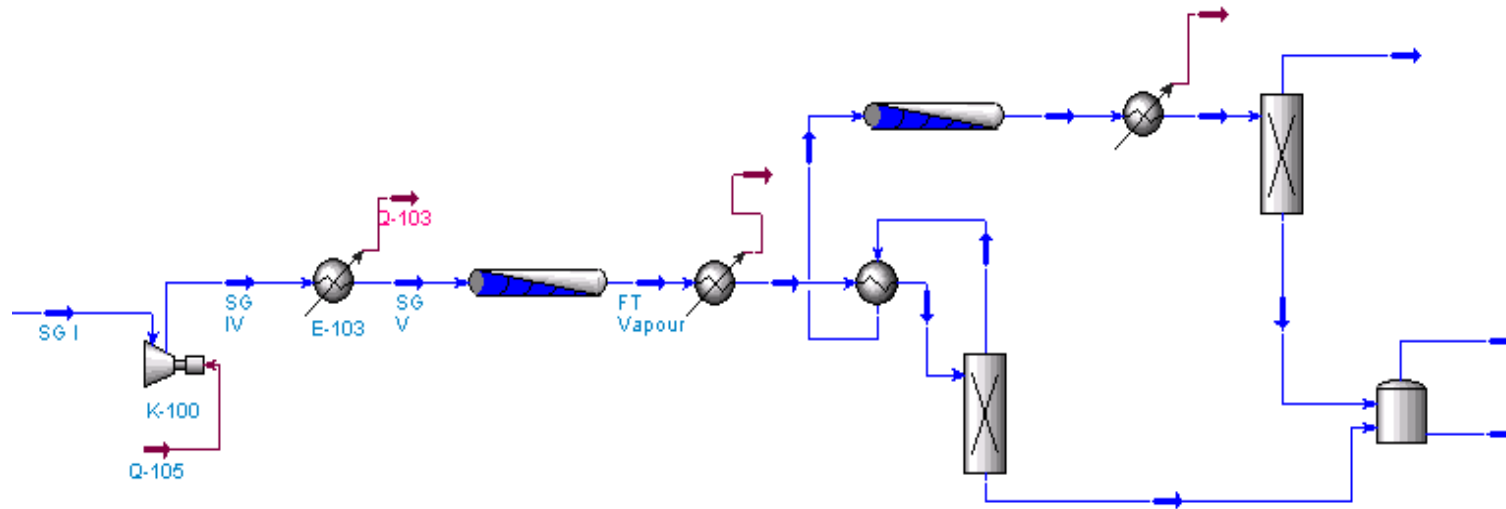
FIGURE 5.6 Simulated PFD of two multi-reactor stages for the production of transportation fuel from synthesis gas (CASE C).

D.   THREE MULTI-STAGES FT REACTOR WITH 3RD FRESH FEED

 The Figure 5.7 provided the three multi-stages FT separate process, respectively as mentioned in Section 2.4. The synthesis gas separates into first FT reactor and second FT reactor and the H_2/CO ratio are same. H_2/CO ratio of the 3rd FT reactor is same with 1st FT reactor.
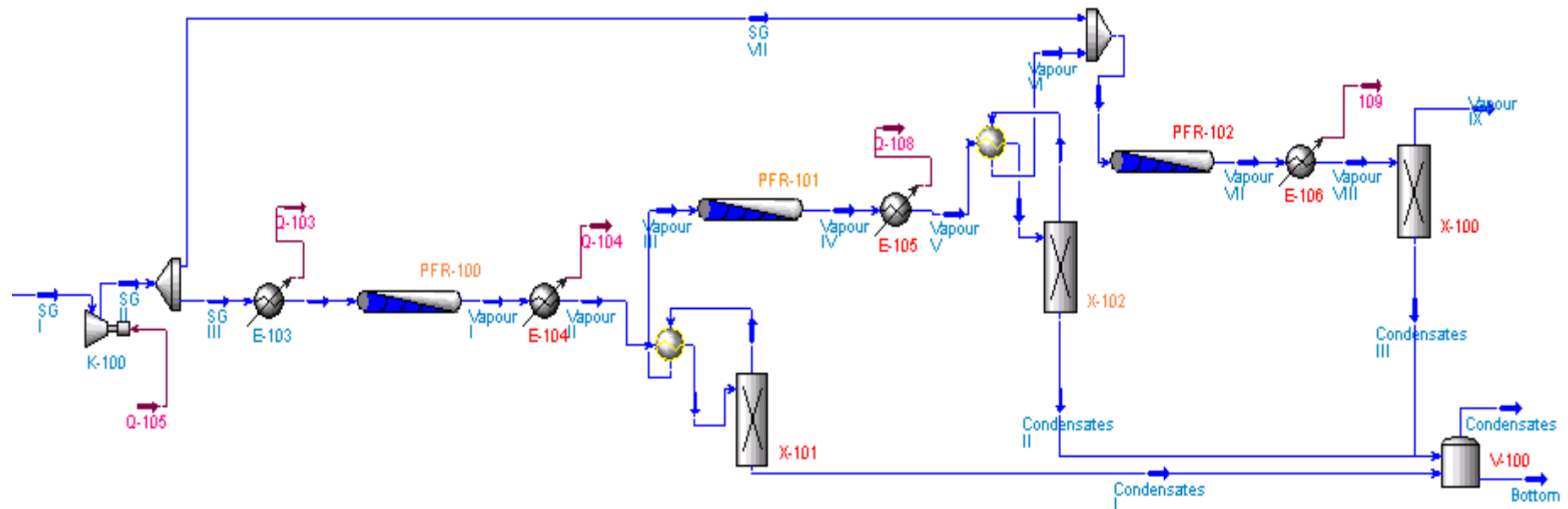
FIGURE 5.7 Simulated PFD of three multi-reactor stages with 3rd fresh synthesis gas feed for the production of transportation fuel from synthesis gas (CASE D).

E. THREE MULTI-STAGES FT REACTOR WITH 2ND AND 3RD FRESH FEED

The Case E is similar with Case D, however splitter included recycling and co-feeding process. The recycling products of unreacted synthesis gas go to POX reactor and the co-feeding products such as low hydrocarbons (C1-C4) go to FT reactor. H_2/CO ratio of both the 2nd and 3rd FT reactor is same with 1st FT reactor. The Figure 5.8 shows that each stages are included with FT reactor and separator.
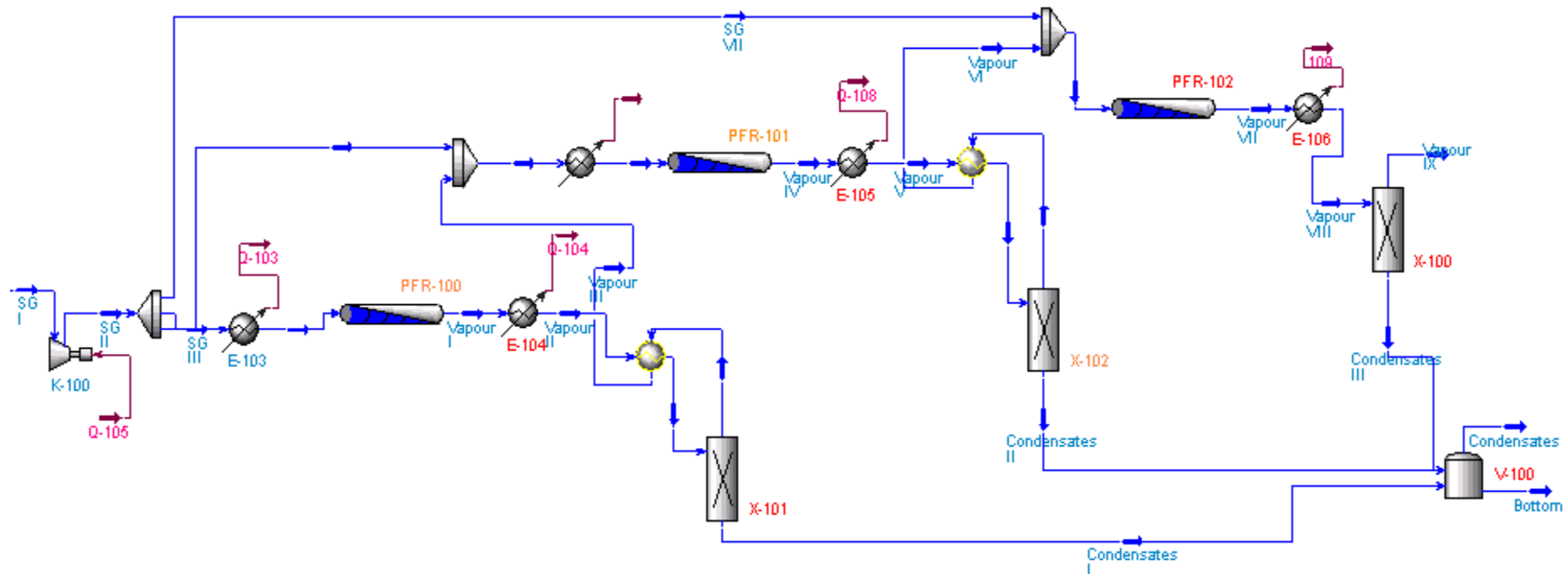
FIGURE 5.8 Simulated PFD of three multi-reactor stages with 2nd and 3rd fresh feed for the production of transportation fuel from synthesis gas (CASE E).

F. RECYCLING AND CO-FEEDING FISCHER-TROPSCH PLANT TO REFORMER

The Case F is includes recycling and co-feeding process. The recycling products of unreacted synthesis gas go to POX reactor and the co-feeding products such as low hydrocarbons (C1-C4) go to FT reactor. The Figure 5.9 shows that the simulated PFD of recycling & co-feeding to reformer.
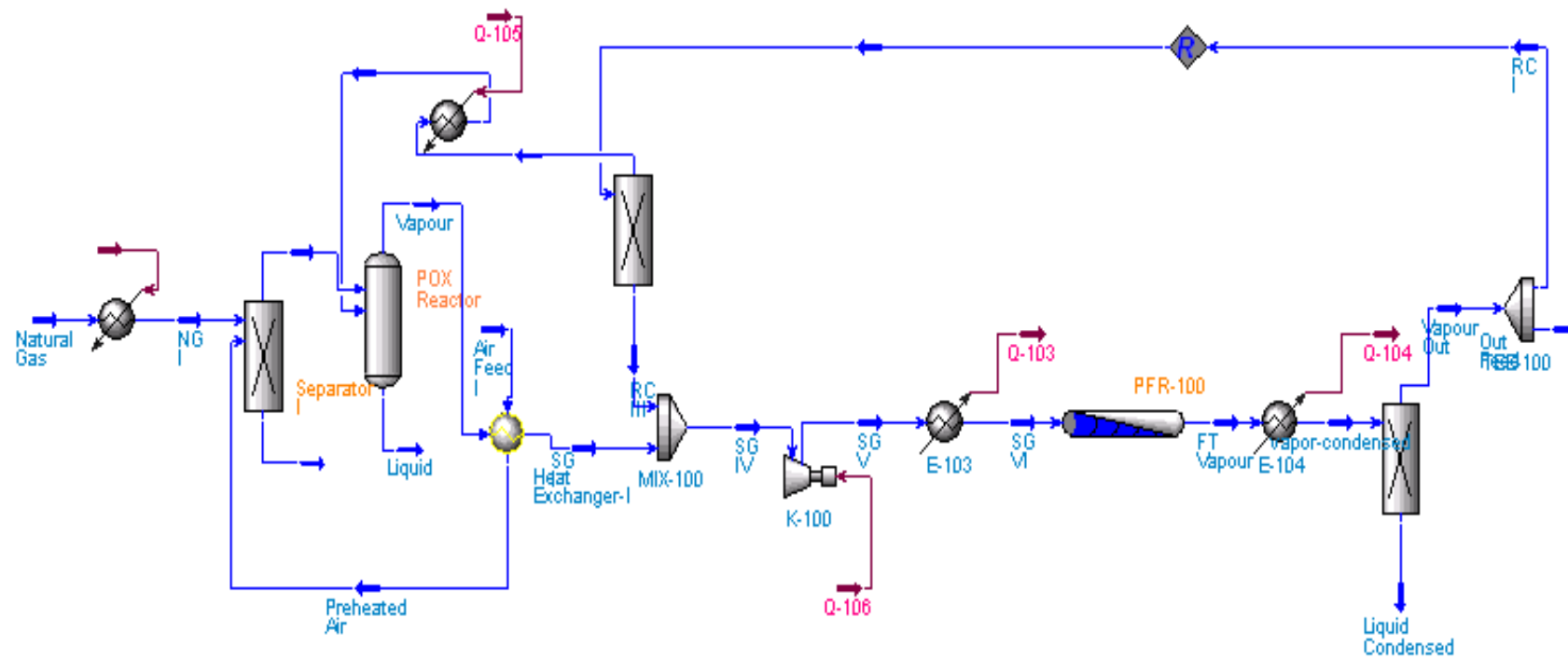
FIGURE 5.9 Simulated PFD of recycling & co-feeding for the production of transportation fuel from synthesis gas to reformer (CASE F).

G. RECYCLING AND CO-FEEDING FISCHER-TROPSCH PLANT TO REACTOR

The Case G is similar process with the Case E; however, the recycling feed goes to FT reactor like co-feeding products. Figure 5.10 shows the recycling and co-feeding FT process to FT reactor. The processes introduced recycling & co-feeding of unreacted synthesis gas and undesired compounds such as from C_1 to C_4 of paraffin and olefin and CO.
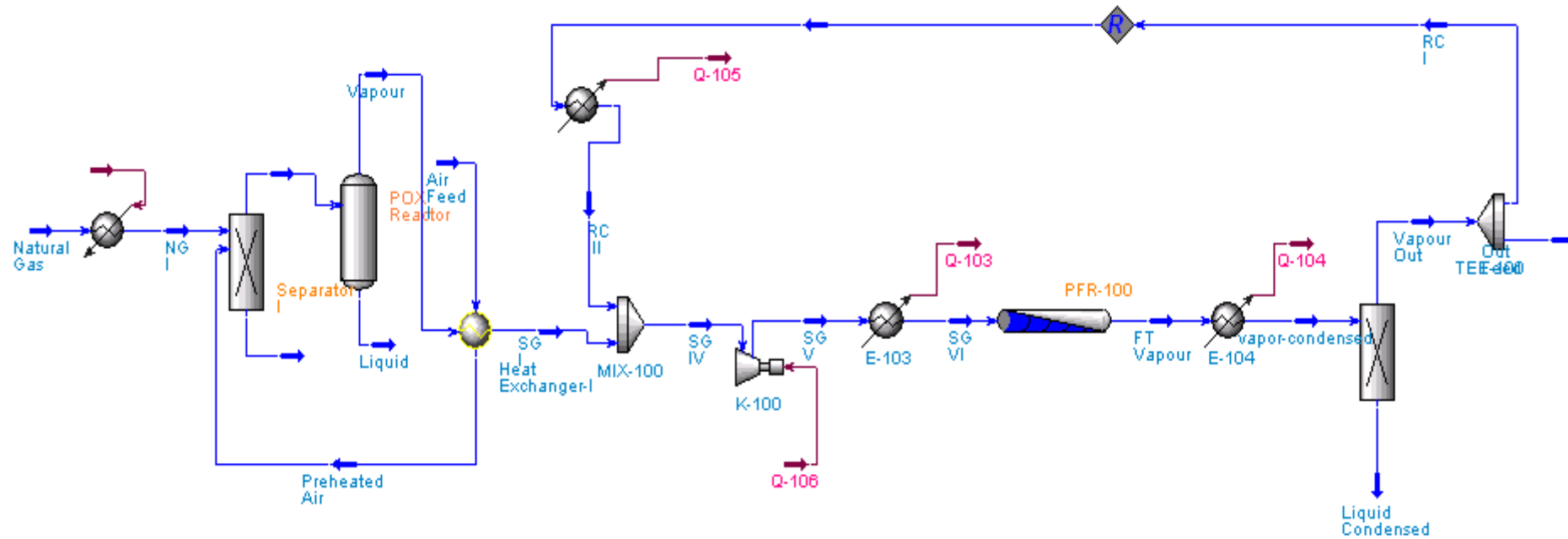
FIGURE 5.10 Simulated PFD of recycling & co-feeding for the production of transportation fuel from synthesis gas to FT reactor (CASE G).

H. METHANE PURGE AND RECYCLING AND CO-FEEDING TO FT REACTOR

Figure 5.11 shows that the seventh progress of FT plant was to purge light hydrocarbon in range of C_1 to C_3 to reformer and to recycling and co-feeding to FT reactor. The purged methane through POX reformer reacted with oxygen, and the synthesis gas was produced.
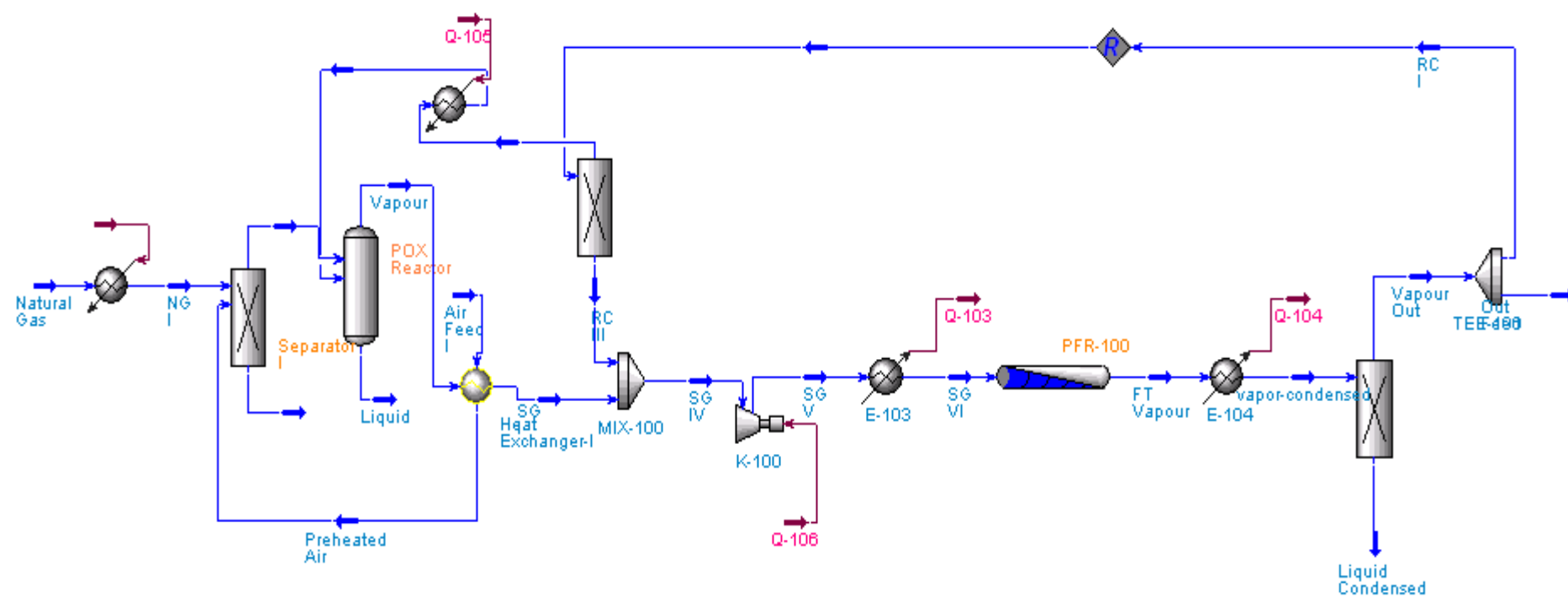
FIGURE 5.11 Simulated PFD of purging light hydrocarbons in Fischer-Tropsch plant (CASE H)

I. THE INTEGRATED FT REACTOR

The Figure 5.12 shows that the integrated FT reactor is designed as FT progress. The integrated FT reactor is directly connected to separator without cooler to decrease to set each operating temperature. The Case H is also included recycling and co-feeding process to reformer and to FT reactor, respectively.
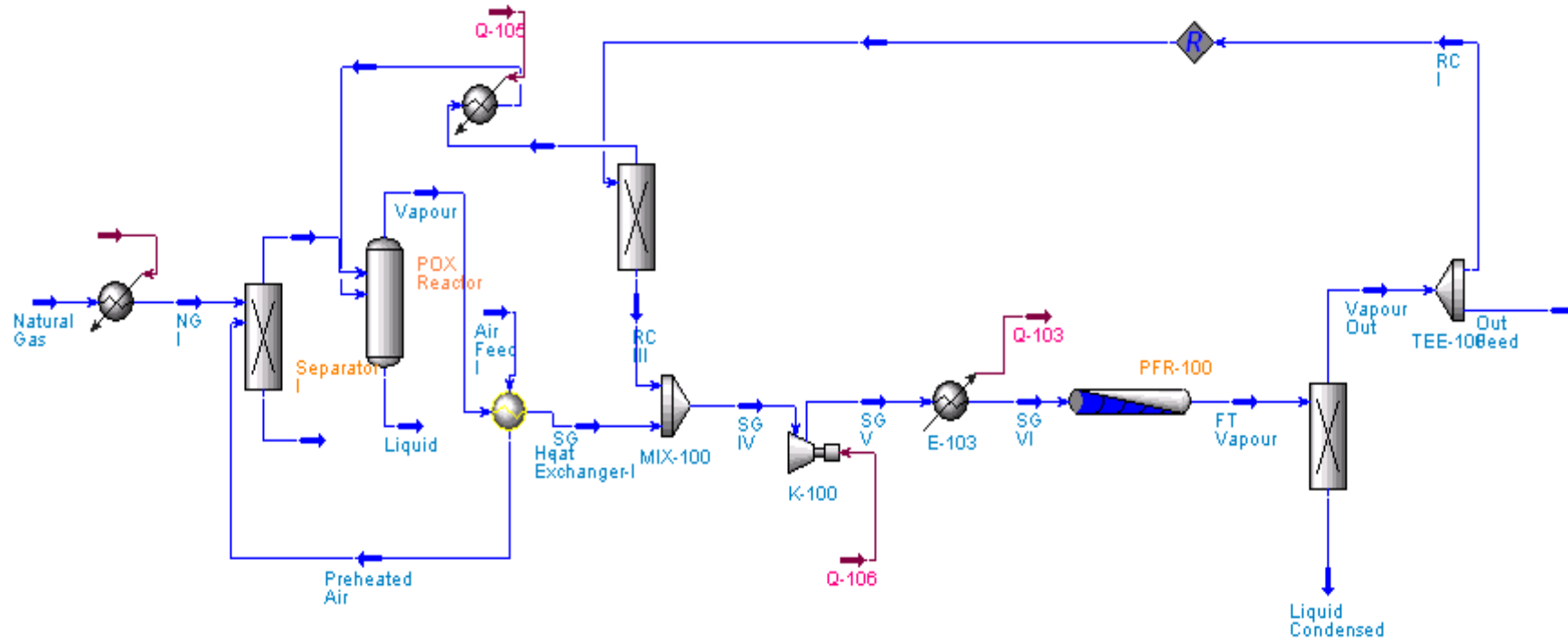
FIGURE 5.12 Simulated PFD of FTS used the integrated Fischer-Tropsch reactor (CASE I).

J. THE SERIES INTEGRATED FT REACTORS

The series integrated FT reactors process is provided in Figure 5.13. The integrated FT reactor was combined normal FT reactor with distillation column. However, the integrated FT reactor could not be indicated in ASPEN HYSYS, so cooler between the FT reactor and separator was removed to consider the integrated FT reactor. Here, product temperature is an important consideration. The temperature from reactor was high because of exothermic FT process.
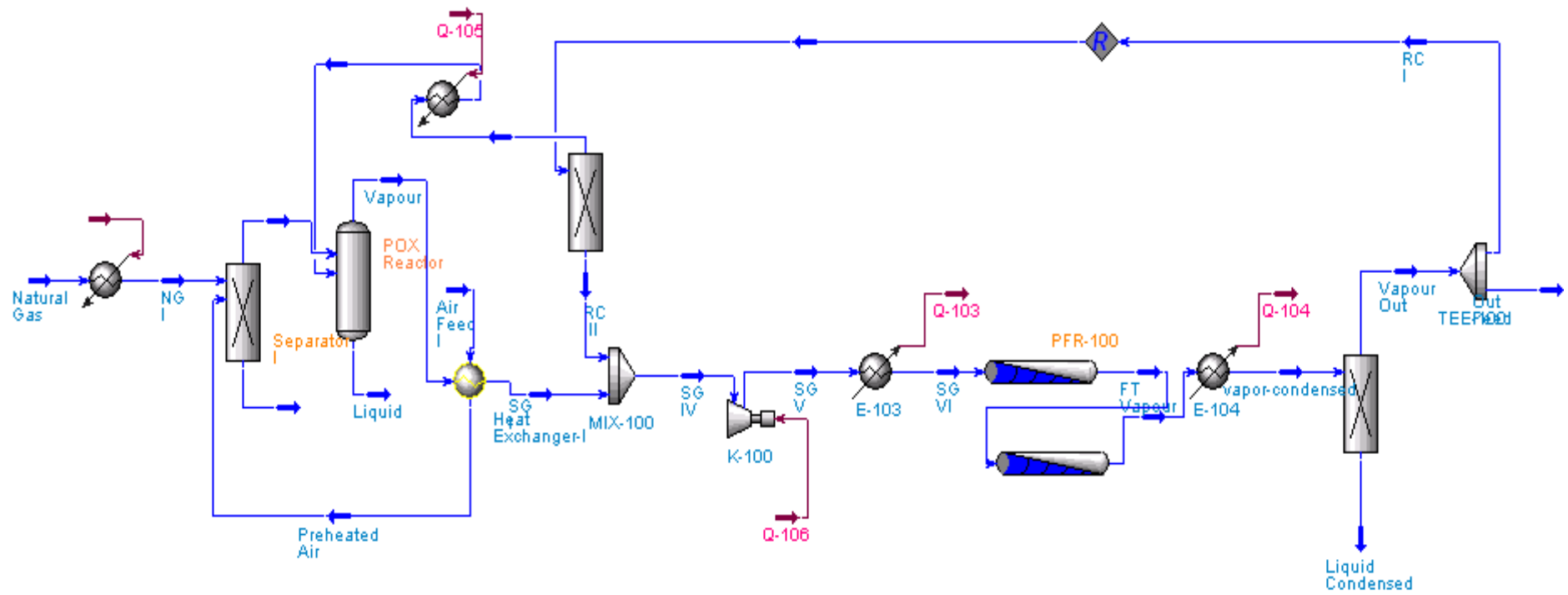
FIGURE 5.13 Simulated PFD of FTS used the series integrated Fischer-Tropsch reactor (CASE J).

For every flowsheet structure, the unreacted and unwanted compounds were recycled and Co-fed as much as possible to the reformer or FT reactor in order to maximize the overall synthesis gas conversion. Additionally, the result of the proposed FT plant including recycling & co-feeding and the integrated FT reactor was compared with the Base case model I and II that were performed using once-through process and normal FT reactor. Every flowsheet described above seven processes were analyzed for CO conversion, synthesis gas conversion and product distribution in order to be able to compare every flowsheet.

To compare the results for above cases, the CO_2 selectivity, hydrocarbon (HC) selectivity, CH_4 selectivity, C_2-C_4 selectivity and C_{5+} selectivity were calculated by using the following formulas:

$$CO_2 \text{ selectivity } [\%] = \frac{[CO_2]_{out}}{[CO]_{in} - [CO]_{out}} \times 100 \tag{5.1}$$

$$HC \text{ selectivity } [\%] = \frac{[CO]_{in} - [CO]_{out} - [CO_2]_{out}}{[CO]_{in} - [CO]_{out}} \times 100 \tag{5.2}$$

$$CH_4 \text{ selectivity } [\%] = \frac{[CH_4]_{out}}{[CO]_{in} - [CO]_{out} - [CO_2]_{out}} \times 100 \tag{5.3}$$

$$C2 - C4 \text{ selectivity } [\%] = \frac{\sum_{i=2}^{4} i(C_iH_{2i} + C_iH_{2i+2})_{out}}{[CO]_{in} - [CO]_{out} - [CO_2]_{out}} \times 100 \tag{5.4}$$

$$C5 + \text{ selectivity } [\%] = \frac{[HC]_{out} - [CH_4]_{out} - \sum_{i=2}^{4} i(C_iH_{2i} + C_iH_{2i+2})_{out}}{[HC]_{out}} \times 100 \tag{5.5}$$

5.2 RESULTS OF THE PROPOSED FT PLANT PROCESSES

The following were the results for both synthesis gas production and the nine proposed simulation progresses mentioned above.

The simulation of the partial oxidation of natural gas as the synthesis gas production was performed and a schematic process flowsheets of POX unit is shown in Figure 5.3. There were the main assumptions of perfect mixing of the reactants and ideal gas behaviour of the hot gases. Also, the reforming unit was only carried out under standard conditions (273K and 1MPa). When the POX reactor temperature was 1881K and pressure 1 MPa, complete equilibrium was assumed.

Partial oxidation of natural gas				
Stream		Natural Gas	Oxygen	Synthesis gas
Phase		Vapour	Vapour	Vapour
Mole Flow [kmol/h]		0.06233	2.5	188.8
Mass Flow[kg/h]		1	80	
CH_4		0.8	-	-
C_3H_8		0.1	-	-
CO_2		0.04	-	-
O_2		0.01	1	-
N_2		0.025	-	-
H_2S		0.025	-	-
CO		-	-	0.3333
H_2		-		0.6667
Temperature	[K]	298	1773	2061
Pressure	[MPa]	1	1	1

Table 5.1 General simulation results for the partial oxidation of natural gas

The mole fractions of the outlet feed from the POX were calculated. It can be seen from the data in Table 5.1, a complete report for the streams specifications was generated.

The rate constants calculated by the optimized kinetics model for both two-phase and three-phase reactor were used in each reaction of hydrocarbon, which are produced in FT synthesis. A first-order of CO and second-order of H_2 for two-phase model (2.46-48) provided in Section 2.2 were applied the hydrocarbons reactions, and for the three-phase model, first-order reactions of CO and H_2 were added to them in ASPEN HYSYS. The performance all flowsheet structures with full conversion concept differ slightly from each other. Especially, since a considerable amount of CO_2 is produced by using iron based catalyst due to its high activity in the water-gas-shift (WGS) reaction, CO_2 removal from the undesired products recycling & co-feeding improves either thermal or carbon efficiency. Significant improvement can be observed by comparing the Case A of once-through with the other cases (Case F, G and H) of recycling and co-feeding and by comparing the Case B of once-through series reactor with the Case J. For seperators of the recycling and co-feeding process, the boiling point ranges of the products in order to meet the specification are shown Table 5.2. The compositions of gasoline (C_5 to C_8) and diesel (C_{9-20}) are specified in British Standard BS2869:1998 and the boiling point ranges are 246 to 388℃.

The light hydrocarbons(C1-C4) were recycled to reformer(Case F) or FT reactor(Case G). In addition, the effect of multi-stages reactor can be analysed by comparing the Case C with Case D. Comparing the performance of the Case F with Case G shows that a small improvement can be achieved with the PFR reactor. The Case I and Case J can be compared the hydrocarbon amounts for integrated single reactor with series reactor of recycling and co-feeding process. In general, CO_2 removal from the FT tail gas recycling has a bigger influence on the energy efficiency of POX, which easily improves the overall efficiency.

	Boiling point[℃]	Pressure[MPa]		
		1	1.5	2.0
Methane	-167			
Ethane	-89			
Propane	-42			
Butane	-0.5			
Pentane	36	85℃	96℃	103℃
Hexane	69			
Heptane	98			
Octane	125			
Nonane	151	250℃	272℃	289℃
:				
Eicosane	343			

Table 5.2 The boiling point ranges of the gasoline and diesel for each pressure.

Figure 5.14 shows the comparison with paraffins and olefins distributions from the mathematic models and plant simulation models for once-through process. As be seen from the table, the paraffins and olefins distributions are same for FT reactor of Matlab and Aspen modelling.
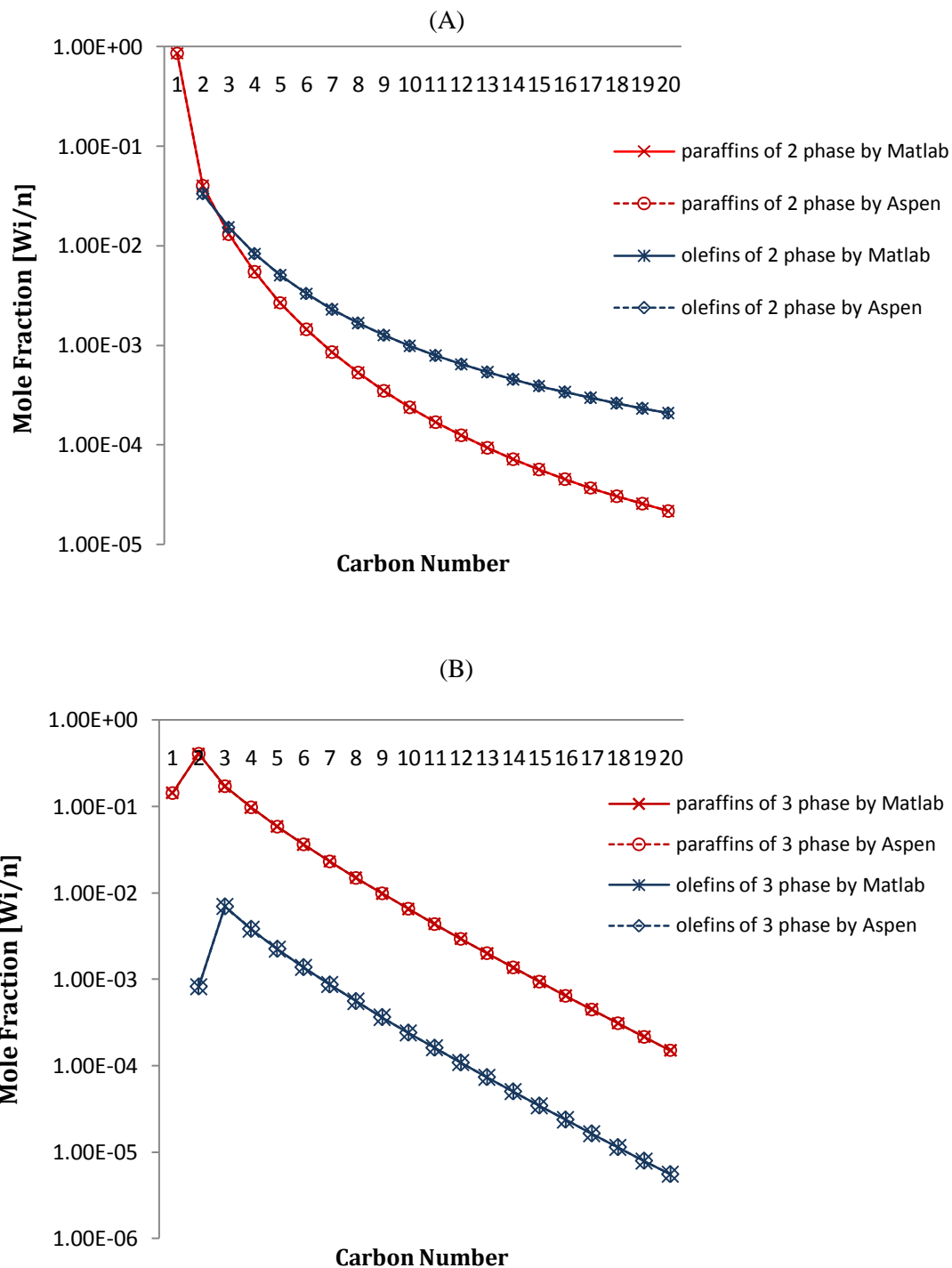
FIGURE 5.14 Comparison with hydrocarbon distributions from the mathematic models and plant simulation models for FT reactor; (A) 2-phase (B) 3-phase.

Firstly, in order to check the impact of polymerization, Table 5.3 and 5.4 show the selectivities of hydrocarbons for both two-phase by proposed Jun Yang et al. and three-phase FT plant by proposed AFN Fabiano. As be seen from the table, C5+ hydrocarbons of the three-phase model are lower and hydrocarbons of range from C_2 to C_4 also are higher amounts. This agrees that the three-phase model based on hydrocarbon rate expression by AFN Fabiano was not considered with re-adsorption of olefins. According to the results, three-phase model was considered with modification of Jun-Yang two-phase model.

CASE	CO conversion	Selectivity [%]				
		CO_2	HC	CH_4	C2-C4	C5+
A	80.89	4.71	95.29	0.03	49.81	50.159
B	80.70	0.56	99.44	0.01	49.82	50.172
C	80.53	0.42	99.58	0.00	49.83	50.173
D	80.85	0.70	99.30	0.00	49.82	50.176
E	80.31	1.10	98.90	0.01	49.82	50.170
F	100	0.23	99.77	0.00	43.29	56.71
G	100	0.23	99.77	0.00	42.95	57.05
H	100	0.30	99.70	0.00	42.52	57.48
I	100	0.20	99.80	0.00	42.85	57.15
J	100	2.71	97.29	0.00	44.07	55.93

Table 5.3 Performance of different cases of FT plant for two-phase reactor from Jun Yang et al.

*Note: **A** = once-through type with FT reactor; **B** = once-through type with two FT reactors series; **C** = two multi-reactor stages; **D** = three multi-reactor stages with 3rd fresh feed; **E** = three multi-reactor stages with 2nd and 3rd fresh feed; **F** = recycling and co-feeding of undesired products to the reactor and unreacted reactants to the reformer; **G** = recycling and co-feeding of undesired products and unreacted reactants to the FT reactor; **H** = methane purge and recycling & co-feeding undesired products; **I** = the integrated FT

reactor; **J** = the integrated FT reactor series; operating condition (510K, 2MPa, 2 H_2/CO ratio and reactor volume $0.5m^3$)

CASE	CO conversion	Selectivity [%]				
		CO_2	HC	CH_4	C2-C4	C5+
A	37.54	24.55	75.45	14.02	67.01	18.97
B	67.78	24.55	75.45	14.02	67.01	18.97
C	67.78	24.55	75.45	14.02	67.01	18.97
D	69.32	25.52	75.84	13.72	65.60	20.67
E	100	24.60	75.39	14.06	67.21	18.73
F	100	24.60	75.39	13.71	65.21	20.58
G	100	20.48	79.52	13.49	63.40	23.10
H	100	25.70	74.30	11.95	71.46	16.59
I	100	25.70	74.30	11.95	71.41	16.64
J	100	25.26	74.74	11.68	69.82	18.49

Table 5.4 Performance of different cases of FT plant for three-phase reactor from FN Fabiano.

*Note: **A** = once-through type with FT reactor; **B** = once-through type with two FT reactors series; **C** = two multi-reactor stages; **D** = three multi-reactor stages with 3rd fresh feed; **E** = three multi-reactor stages with 2nd and 3rd fresh feed; **F** = recycling and co-feeding of undesired products to the reactor and unreacted reactants to the reformer; **G** = recycling and co-feeding of undesired products and unreacted reactants to the FT reactor; **H** = methane purge and recycling & co-feeding undesired products; **I** = the integrated FT reactor; **J** = the integrated FT reactor series; operating condition (510K, 2MPa, 2 H_2/CO ratio)

From these results, the two-phase and three-phase models from Jun Yang et al. were considered and discussed about all the different cases A-J and the results are presented in Appendix C.

5.3 RESULTS AND DISCUSSION

The chapter provided the whole plant's simulation of proposed FT plant and also detailed the model development in ASPEN HYSYS. The established optimum FT conditions by using MATLAB in the Chapter 4 had application to FT part of the whole plant. The whole plant went through the ten simulation progresses. Firstly, the synthesis gas production was carried out from natural gas and Fischer-Tropsch synthesis both cases of once-through reactor and series reactors, and recycling & co-feeding were also performed. One of them, recycling & co-feeding process was considered both to reformer and to FT reactor, and furthermore, only methane was purged to reformer and other undesired compounds were recycling to FT reactor. Finally, the integrated Fischer-Tropsch reactor including reactive distillation was considered on the plant simulation both the Base case model I and II. The simulation results of the models will be presented and evaluated in next chapter.

The developed kinetics models were also described to find the effects of parameters such as temperature, pressure and H_2/CO ratio in order to apply to computer simulation of whole FT plant by ASPEN HYSYS. Each step of the proposed processes can be analyzed independently with ASPEN HYSYS to promote the investigation. Therefore, the performance of these models can be better understood. Subsequently, more process details of each progress such as compounds separator, heater, cooler and other process details are added to the each suitable flowsheets. The PFR models for FTS reactor are used in the simulation for analysis of the iron based catalyst FT process. The results of the ten proposed progresses for FT plant were presented and compared with the Fischer-Tropsch plant. In addition, the rate constants calculated by the optimized kinetics model for both two-phase and three-phase reactors were used in each reaction of hydrocarbon, which are produced in FT synthesis.

According to the FT plant model, the amounts of C5+ hydrocarbon for three-phase model are higher than two-phase model for once-through process (Case A-E). This means that the three-phase reactor is better than two-phase

reactor for productions of higher hydrocarbons and the consideration for re-adsorption of olefins affect to production of C5+ hydrocarbon. A comparison of the two results reveals that parafins amounts of the three-phase model are higher than those of two-phase model, while olefin amounts are lower at the three-phase model. It can therefore be observed that the olefins re-adsorption and secondary chain growth are more active at the three-phase reactor. In addition, hydrocarbon amounts of three-phase model were higher than those of two-phase model for recycling and co-feeding.

Case A and B displayed similar selectivity for two-phase and three-phase models. It is considered that the FT reaction is nearly finished at first FT reactor. The Case C and D gained little higher selectivity of higher hydrocarbon than case A and B. The reasons are that residence time of Case C and D were increased. The selectivity of hydrocarbon in Case E both two-phase and three-phase models were increased than those of Case C and D. Case E of three-phase reactor presents the effect of liquid feed to gain higher hydrocarbons. The higher hydrocarbon selectivities of three-phase reactor were higher than that of two-phase reactor for once-through process. This is in good agreement with Jun Yang et al. and AFN Fabiano. In addition, the models were undertaken to see the effect of undesired products in recycling and co-feeding to the FT reactor and each process is compared with the above cases both once-through FT plant and recycling and co-feeding to reformer. The recycling and co-feeding process of unreacted synthesis gas and light hydrocarbons (C1-C4) achieves the higher amounts of C5+ hydrocarbons. It seems possible that these results are due to higher chain growth probability and higher paraffin selectivity by the termination probability to olefin in recycling and co-feeding process. Also the mechanism for secondary reactions occurs by re-adsorption of olefins. For recycling and co-feeding to reformer, the best result of Case F was 69.23% and 87.42% for heavy hydrocarbons both two-phase and three-phase under conditions; 1MPa, $1H_2/CO$ ratio and 450K and 2MPa, $1H_2/CO$ ratio and 450K, respectively. The best results of recycling and co-feeding to FT reactors achieved higher selectivity of heavy hydrocarbons than case F, 68.94% and 99.9% both two-phase and three-phase reactors, respectively. Case H also

According to the results, recycling and co-feeding to FT reactor (Case G) was the best FT process to produce higher heavy hydrocarbons and the conditions was 2.0MPa, 1 H_2/CO ratio and 450K in three-phase model. The recycling and co-feeding to FT reactor is the best results to high selectivity of heavy hydrocarbons. There are several possible explanations for these results. Firstly, the results indicate that it is possible that hydrogenation increases with carbon number due to increased adsorption strength. The overall synthesis gas conversion of recycling and co-feeding are higher than those of once-through and the recycling process is to achieve higher reactor productivity. These results have a good agreement with Peter and Diane et al.(2006) and Gaube and Klein(2008). In addition, it agrees that low temperature leads to little lower light hydrocarbons and higher heavy hydrocarbons and olefins and high pressure leads to lower light hydrocarbons and higher heavy hydrcarbons. According to the results, a high H_2/CO ratio was little preferable for increased selectivity of hydrocarbons. This has a good agreement that H_2/CO ratio has a small influence for selectivity of hydrocarbons. The hydrocarbon products are increased in recycling & co-feeding.

Table 5.5 shows conversions and selectivities for compounds of the best results from each case under real plant feed both two-phase plant models. The feed gases, 1000 kg/h of natural gas and 80,000 kg/h of air were used to compare with real FT plant.

Case	Pressure	H_2/CO ratio	T[K]	Conversion[%]		Selectivity[%]			
				CO	CO_2	HC	CH_4	C2-C4	C5+
A	1MPa	1	450	38.83	0.00	100.00	0.00	49.81	50.19
B	1MPa	1	450	40.12	0.00	100.00	0.00	49.81	50.19
C	1MPa	1	450	40.53	0.58	99.42	0.51	49.56	49.93
D	1MPa	1	450	34.79	0.22	99.78	0.01	49.43	50.56
E	1MPa	1	450	38.40	0.00	100.00	0.00	49.44	50.56
F	1MPa	1	450	100	0.00	100.00	0.00	9.26	90.74
G	1MPa	1	450	100	0.00	100.00	0.00	4.15	95.85
H	2MPa	1	450	100	0.00	100.00	0.00	11.65	88.35
I	1MPa	1	450	100	0.00	100.00	0.00	10.88	89.12
J	1MPa	1	450	100	0.00	100.00	0.00	6.04	93.96

Table 5.5 Performance of different cases of FT plant for two-phase reactor under real conditions.

*Note: **A** = once-through type with FT reactor; **B** = once-through type with two FT reactors series; **C** = two multi-reactor stages; **D** = three multi-reactor stages with 3rd fresh feed; **E** = three multi-reactor stages with 2nd and 3rd fresh feed; **F** = recycling and co-feeding of undesired products to the reactor and unreacted reactants to the reformer; **G** = recycling and co-feeding of undesired products and unreacted reactants to the FT reactor; **H** = methane purge and recycling & co-feeding undesired products; **I** = the integrated FT reactor; **J** = the integrated FT reactor series.

Table 5.6 shows conversions and selectivities for compounds of the best results from each case under real plant feed both three-phase plant models. The feed gases, 1000 kg/h of natural gas and 80,000 kg/h of air were used to compare with real FT plant.

Case	Pressure	H_2/CO ratio	T [K]	Conversion[%]		Selectivity[%]			
				CO	CO_2	HC	CH_4	C2-C4	C5+
A	2MPa	2.00	450	86.94	0.00	100.00	0.00	17.36	82.64
B	2MPa	2.00	450	87.20	0.00	100.00	0.00	17.36	82.64
C	2MPa	2.00	450	89.10	0.00	100.00	0.00	17.36	82.64
D	2MPa	2.00	450	85.99	0.00	100.00	0.00	17.36	82.64
E	2MPa	2.00	450	87.99	0.00	100.00	0.00	17.36	82.64
F	2MPa	1.00	450	100	0.00	100.00	0.00	11.95	88.05
G	2MPa	1.00	450	100	0.00	100.00	0.00	11.93	88.07
H	2MPa	1.00	450	100	0.00	100.00	0.00	12.38	87.62
I	2MPa	1.00	450	100	0.00	100.00	0.00	11.94	88.06
J	2MPa	1.00	450	100	0.01	99.99	0.00	12.22	87.78

Table 5.6 Performance of different structures of FT plant for three-phase reactor of Jun Yang et al.

*Note: **A** = once-through type with FT reactor; **B** = once-through type with two FT reactors series; **C** = two multi-reactor stages; **D** = three multi-reactor stages with 3rd fresh feed; **E** = three multi-reactor stages with 2nd and 3rd fresh feed; **F** = recycling and co-feeding of undesired products to the reactor and unreacted reactants to the reformer; **G** = recycling and co-feeding of undesired products and unreacted reactants to the FT reactor; **H** = methane purge and recycling & co-feeding undesired products; **I** = the integrated FT reactor; **J** = the integrated FT reactor series.

The data for the process A-J were based on 1kg/h of natural gas and 80kg/h of air and the data of Table 5.5 and 5.6 results from 1000kg/h of natural gas and 80000kg/h of air. According to the results, The CO conversion for the individual cases was lower than that for increased space velocity. That means that the small flow conversions are much greater than the ones for higher flow because it is

possible to have more residence time in order to convert in the small flow. Furthermore, larger FT reactor may be used to increase CO conversion. Table 5.7 shows the impact of FT reactor size for per-pass of Case G. The CO conversion was increased with larger FT reactor for both two-phase and three-phase models and heavy hydrocarbon selectivity was decreased with larger FT reactor. The smaller reactor volume achieved the higher CO conversion as can be seen in the table and higher space velocity leads to lower selectivity of hydrocarbon and was showns the same trend for both two-phase and three-phase models. These are in good agreement with the data of the Figure 2.9.

Case G	P	H_2/CO ratio	Tem. [K]	Volume [m^3]	Conversion[%]			Selectivity[%]		
					CO	CO_2	HC	CH_4	C2-C4	C5+
2-phase	1MPa	1.0	450	1	44.80	0.00	100.0	0.00	8.75	91.25
				1.5	47.04	0.00	100.0	0.00	12.25	87.75
				2	48.92	0.00	100.0	0.00	14.67	85.33
				5	57.15	0.00	100.0	0.00	24.65	75.35
				50	64.03	0.00	100.0	0.00	30.79	69.21
				500	64.05	0.00	100.0	0.00	30.87	69.13
3-phase	2MPa	1.00	450	1	66.482	0.00	100.0	0.00	12.22	87.779
				1.5	66.528	0.00	100.0	0.00	12.23	87.775
				2	66.534	0.00	100.0	0.00	12.23	87.774
				5	66.536	0.00	100.0	0.00	12.23	87.773
				50	66.538	0.00	100.0	0.01	12.23	87.768
				500	66.557	0.02	99.98	0.01	12.23	87.767

Table 5.7 The impacts of the FT reactor volume for per-pass of Case G
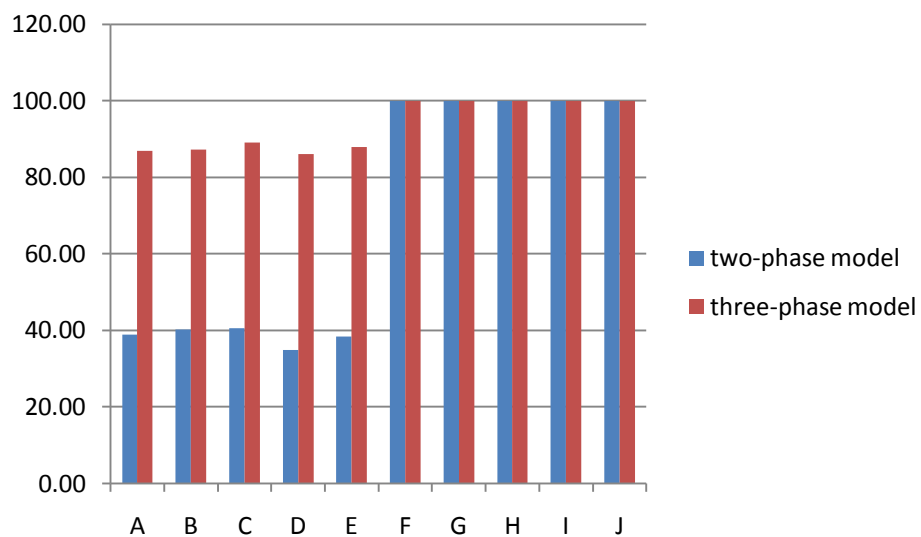
Figure 5.15 CO conversion for each case of both two-phase and three-phase models

Figure 5.15 shows the CO conversion for each case of both models. The CO conversion has usually 30-40% for two-phase reactor. The process from Raje and Davis was using more reactors rather than one large reactor because temperature control is better in smaller reactors and inter stage cooling can be used. Case C and D are multi-stage Fischer-Tropsch process. According to Arend and Joris (2007), the CO conversion should be at least 80%. This had also good agreement with result of the three-phase model. The process of the recycling unreacted compounds to reformer or FT reactor was more efficient than once-through processes and favourable to achieve high hydrocarbons. It is likely therefore that co-feeding of light hydrocarbons can be an effective way to achieve gasoline production proposed by Kuchar et al. comparing the results of ten cases, it can be seen that Case G process produced the highest selectivity of hydrocarbons. The Case G is the best to produce C5+ hydrocarbons because lowering the molecular weight of the hydrocarbon liquids inside the reactor increase the mass transfer and solubility, and diffusivity of the reactants in the hydrocarbons present as proposed by Rafael et al.(2003). As mentioned in introduction, to maximize profits, the plant is considered to produce gasoline and gas oil. The Case G process for both two-phase and three-phase models should be used to achieve the above products.

Table 5.8 shows the amounts of products such as gasoline and diesel for each case for both two-phase and three-phase models. As can seen the table, the amounts of three-phase model were higher than that of two-phase model and the diesel amount of three-phase model was lower than that of two-phase model.

Case	Two-phase		Three-phase	
	Gasoline	Diesel	Gasoline	Diesel
A	117.26	92.58	173.84	73.57
B	120.36	93.25	177.93	75.53
C	124.36	92.21	181.66	76.71
D	119.35	92.96	177.62	75.16
E	124.25	93.58	180.13	76.43
F	242.36	122.55	345.33	171.51
G	242.38	122.89	346.37	172.03
H	244.50	123.74	353.93	175.79
I	239.57	121.58	341.56	169.64
J	242.59	123.00	349.49	173.59

Table 5.8 Gasoline and Diesel amounts for each of the cases [kg/h]

Table 5.9 shows the impact of having water in the feeds to the reactors of per-pass for the best FT process, Case G that had the best results to produce heavy hydrocarbons. As can be seen from the table, two-phase reactor accomplished higher selectivity of heavy hydrocarbons with having water in feed to FT reactor while, three-phase reactor had no effect on including water in the feed. As mentioned section 3.4, the water production could increase the iron based catalyst choice and also increase the conditions: high temperature, high H_2/CO ratio and low pressure. The oxygen in feed to go through FT reactor was applied to consider and the CO conversion with oxygen was higher than that without oxygen, however C5+ selectivity was increased without oxygen in feed. In addition, the light

paraffins (C1-C3) were purged with same conditions. The CO conversion and C5+ selectivity with the light paraffins purging were higher than that without the light paraffins purging for both two-phase and three-phase models.

Case G	P MPa	H_2/CO ratio	Tem. [K]	H_2O	O_2	Light paraffins	Conversion[%]		Selectivity[%]			
							CO	CO_2	HC	CH_4	C2-C4	C5+
2-phase	1	1.0	450	X	O	X	42.09	0.00	100.00	0.00	12.31	87.69
				X	X	X	65.20	0.29	99.71	0.20	29.96	69.87
				X	X	O	65.57	0.69	99.31	0.26	24.84	74.60
3-phase	2	1.00	450	X	O	X	65.42	0.00	100.00	0.00	11.50	88.50
				X	X	X	71.11	6.55	93.45	0.04	13.12	86.84
				X	X	O	73.26	10.32	89.68	0.07	13.46	86.47

Table 5.9 The impacts of water and oxygen in the feeds to the FTreactors of per-pass for Case G

For Case G, the two-phase reactor accomplished higher selectivity (87.69%) of heavy hydrocarbons with having no water in feed to FT reactor while, three-phase reactor had no effect on including water in the feed. In addition, oxygen effect including feed to FT reactor was considered without water in feed. It is higher selectivity of C5+ hydrocarbon without oxygen in feed. Therefore, the recycling and co-feeding to FT reactor process was the best under condition; 2MPa, 1 H_2/CO ratio and 450K with including oxygen in feed for three-phase model.

6

Economic Evaluation
of the Fischer-Tropsch Plant

The economic evaluation of the proposed Fischer-Tropsch plant was carried out for the each case in this chapter. The approach being adopted for the economic evaluation involved the integration of the two-phase and three-phase models as mentioned in Chapter 6; Synthesis gas production, Fischer-Tropsch synthesis and Product upgrading. This analysis was done from the point of view of capital and operating costs as well as feedstock and product prices to ascertain the profitability of the project whilst focusing on the impact of cost escalation. The analysis has been taken into consideration, feedstock cost.

6.1   ECONOMIC ANALYSIS

There are five (Garrett 1989) main economic assumptions used in the model, namely total capital investment, tax rate, raw materials & utility costs, payback period and price parameters, however the thesis are considered two of them, capital investment and operating costs.

6.1.1   ECONOMIC ASSUMPTIONS

The plant economic analysis was based on the following assumptions:

The plant processes 100 MMSCF/day of natural gas and produce liquid FT products; namely a gasoline and gas oil. The plant uses all the by-product steam

and fuel gas to supply its internal electric power and heating requirements. The only materials delivered to the plant are natural gas and catalysts.

6.1.2 ESTIMATION OF TOTAL CAPITAL INVESTMENT

The total capital investment was calculated as the plant cost added to the working capital (Garrett 1989). The plant cost was the cost for installing all equipment including the cost for building offsite facilities and for start-up. For the optimized Fischer-Tropsch model, the processing equipments was estimated using CEPCI (Eq. 7.1) for three part of the process; Synthesis gas production, Fischer-Tropsch synthesis and product stream & upgrading. The equipment installation cost that consisted of the freight from the factory, the unloading and handling costs, foundations or supports, physically putting the equipment in place and securing it, and connecting it, was calculated by Eq. (7.2) using indicated installation factor in the book (Garrett 1989). Construction and engineering expense is for the detailed engineering required for the plant design, drawings, permits, and managing and supervising construction. Engineering and supervision is generally charged on a cost plus expenses and overhead basis, so it is quite variable, but is may be about 30% of the purchased equipment cost. The contractor's profit is usually from 10% of the equipment cost. The off-site might include assuming all of the cost of headquarters buildings, research and development facilities, engineering and plant technical service departments, power plant, shipping facilities and so on. The cost for these facilities may be estimated directly, usually as 0-30% of the total plant cost. Additional start-up costs were assumed about 5-10% of the total plant cost, even though the technology was assumed to be well established. The working capital were estimated to be 10-20% of plant cost (Garrett 1989). The estimated costs for plant capacity and time, which were calculated using the CEPCI as follows:

$$C_t = C_r \times \frac{CEPCI_t}{CEPCI_r}$$
(6.1)

Where

$C_{r,t}$ = reference or target year [=] $

$CEPCI_{r,t}$ = chemical engineering plant cost index for reference or target year

The ratio $\frac{CEPCI_2}{CEPCI_1}$ therefore, would be 1, if the reference year used was the same as the target year.

One of advantages is that it is easy to calculate the installation costs. While various authors have estimated the fraction of the purchased equipment cost, the book (Garrett 1989) generally introduced freight and shipping costs, foundations, mounting, and simple electric and piping connections, such as switch gear, starters, flange connections, and so on.

$$C_i = C_t \times i_f \tag{6.2}$$

Where

C_i = installed cost [=] \$

i_f = installation factor

A similar number that also includes all of the adjacent minor equipment and connections is sometimes listed in the literature (principally by Guthrie 1975 and Ulrich 1984) covering the cost of purchase and installation of the major equipment as well as all of the supporting equipment around each major unit (Garrett 1989). This is called the module factor, and when available is also listed under the charts as the range given by different authors and the average value.

$$C_{im} = C_t \times m_f \tag{6.3}$$

Where

C_{im} = cost of the installed module

m_f = module factor

Components		Total Capital Investment (basis Million $)[a]									
		A	B	C	D	E	F	G	H	I	J
Synthesis gas Production [b]											
POX reforming unit		49.4	49.4	49.4	49.4	49.4	38	38	38	38	38
Air separation unit		72.5	72.5	72.5	72.5	72.5	51.8	51.8	51.8	51.8	51.8
Fischer-Tropsch Synthesis [c]		0.3	0.6	3.1	5.9	5.9	0.3	1.1	0.3	0.3	0.6
Product Stream & separation [d]		1.8	1.7	7.0	8.1	8.3	7.3	8.3	5.7	8.9	8.9
Hydrocracking unit		4	4	4	4	4	-	-	-	-	-
Sub Total		127.8	128.1	135.8	139.8	140.0	97.0	98.8	95.4	98.6	98.9
Construction expense	30%(Cons. & Eng.)	38.4	38.5	40.8	42.0	42.0	29.1	29.7	28.7	29.6	29.7
	10%(Contractors fee)	12.8	12.9	13.6	14.0	14.0	9.7	9.9	9.5	9.9	9.9
Total onsite facilities		178.92	179.4	190.1	195.6	195.9	135.8	138.2	133.6	138.1	138.5
Offsite facilities	10% [e]	17.90	18.0	19.0	19.6	19.6	13.6	13.9	13.4	13.9	13.9
Start-up cost	5% [f]	9.0	9.0	9.5	9.8	9.8	6.8	6.9	6.7	6.9	7.0
Working Capital	15% [g]	26.84	26.90	28.5	29.4	29.4	20.4	20.8	20.1	20.8	20.8
Total Capital Investment		**232.59**	**233.12**	**247.05**	**254.3**	**254.7**	**176.6**	**179.7**	**173.6**	**179.5**	**180.0**

Table 6.1 Estimation of total capital investment for the Case A-I of the Fischer-Tropsch Process

*Note: **A** = once-through type with FT reactor; **B** = once-through type with two FT reactors series; **C** = two multi-reactor stages; **D** = three multi-reactor stages with 3rd FT reactor of fresh feed; **E** = three multi-reactor stages with 2nd and 3rd FT reactors of fresh feed; F = recycling and co-feeding of undesired products to FT reactor and unreacted reactants to the reformer; **G** = recycling and co-feeding of undesired products and unreacted reactants to the FT reactor; **H** = methane purge and recycling & co-feeding undesired products; **I** = the integrated FT reactor; **J** = the integrated FT reactor series.

[a] estimated using Chemical Engineering Plant Cost Index 2009

[b] Synthesis gas processing unit; POX reformer of 304 stainless st. and 1000gal, Heat exchanger of shell type of 16 fts tubes, Heaters, Storage Tank for Natural Gas of 304 stainless st. and horizontal type, Shift reactorof 304 stainless st. and volume of 1000 gal and Compressor of centrifugal type 150 horsepower.

[c] Fischer-Tropsch production unit; FT reactors of 304 stainless st. and volume of 1000 gal of PFR type.

[d] product stream & separation unit; coolers, Separator of 304 stainless st. and volume of 1000 gal, Storage Tanks of horizontal type. Hydrocracking unit: Capital cost will depend on feedstock and severity of operation besides location factor. It may range from US Dollars 3000 to US Dollars 6000 per bpsd (The technomanage group).

[e] The Offsite facilities was assumed to be 10% of plant cost.

[f] The start-up cost was assumed to be 5% of plant cost.

[g] The working capital was assumed to be 15% of plant cost.

Table 6.1 shows the capital cost for the proposed cases of Fischer-Tropsch plant. These equipments were involved Case A-J of the proposed Fischer-Tropsch plant. As shown in Table 5.25, C5+ selectivity was the highest for the process of recycling and co-feeding to FT reactor (Case G). The Case G was also second lowest capital cost. Therefore, the impact on capital cost of having the highest yield of the desired products without hydrocrackers unit. However, the case may need hydrogenation and isomerisation units for gasoline.

6.1.3   ESTIMATION OF OPERATING COST

Of equal importance to the capital cost estimate in an economic evaluation is the operating cost. The operating costs are generally broken down into two broad categories: variable costs and fixed costs. The operating cost consisted of six major items, namely feedstock costs, utility cost, sales related cost, capital related cost, and labour & labour related cost (Garrett 1989). The first four were considered to

be variable (i.e. vary according to the capacity), whereas the last two were considered to be fixed.

Firstly, the variable costs include raw material, utilities, labour and labour related cost, capital related cost, and sales related cost. The raw materials required by the process may be calculated from the stoichiometry and a material balance for the process with an allowance for extra materials because of the plant's inevitable inefficiencies and losses, estimated from laboratory or pilot plant data, prior experience, or related processes. Included with the raw materials should be all major additives, treating agents, catalyst, filter aids, and so forth that are required to complete the process. The cost of utilities has now become one of the larger segments of a chemical plant's operating cost, and where there is often the greatest potential to economize. The utilities needed in the plant were in the form of steam, water and electricity. The distribution of utility & raw materials costs for each unit was estimated according to US Energy Information Administration(2010) and the data of the book (Garrett 1989), respectively. These estimated electricity and raw materials costs of natural gas to transportation fuels plants are presented in Table 6.2.

Another operating cost that always must be itemized is the operating labour required to run the plant. In the factoring methods this does not include maintenance, supervision, analytical, clerical, or other types of totally necessary labour, since these staff costs will later be estimated from the operating labour or the plant capital cost. Also, it should involve a rotating shift arrangement, with some overtime or plant downtime with the four shift schedule to balance the total number of operating days each year. The pay is maintained at an assumed 40-hour work-week and the average salary for the production operators varies widely with the job skill, responsibility, and hazard, as well as the presence or absence of a union, the section of the country, and other factors. In 2008-2009, it averaed $49.04 per hour (Alberta Wage 2009) for the chemical engineering industry.

The annual capital related cost was estimated to be 21% of plant cost. It consisted of costs for depreciation and other capital related costs, namely maintenance, operating supplies, and plant overhead costs. The costs for taxes and

insurance as well as for environmental issues were ignored, since the plant is likely to receive support funding. In addition to this, as a Fischer-Tropsch plant, synthesis gas to transportation fuels is considered environmentally conscious; therefore, the cost for environmental treatment was considered very little. The depreciation used was the straight line method for ten year period and it was assumed that there was no salvage value. The depreciable capital investment was the plant cost; therefore, the rate of depreciation per year was 10% of the plant cost.

The sales related cost could be estimated 20% of sales. The cost for patents & royalties, packaging & storage, distribution & sales, administration, as well as for R&D was also considered to be insignificant.

Categories		A	B	C	D	E	F	G	H	I	J
Raw materials(NG)	22.562 $/BBL[a]										
two-phase		60.5	60.5	60.5	60.5	60.5	23	22	23.5	23.5	23.5
three-phase		60.5	60.5	60.5	60.5	60.5	14	14	14.1	13.9	13.7
Utility(Electricity)	0.0731$/KWh										
two-phase		3.2	3.2	3.2	3.2	3.2	3.2	3.2	5.1	3.2	3.2
three-phase		6.6	6.6	6.6	6.6	6.6	6.6	6.6	6.6	6.6	6.6
Labour and labour related cost											
Plant operator[b]	No. of workers	15	16	16	17	17	17	17	17	17	18
Overhead[c]		5	5	5	5	5	5	5	5	5	5
Total labour wages	49.04$/hour[d]	1.9	2.0	2.0	2.2	2.2	2.1	2.1	2.1	2.1	2.2
Labour related cost	60%[e]	1.15	1.2	1.2	1.25	1.25	1.25	1.25	1.25	1.25	1.3
Capital related cost											
Maintenance etc.	21%[f]	37.6	37.7	40.0	40.0	41.1	28.5	29.0	28.1	29.0	29.1
Depreciation	10%[g]	17.9	18.0	19.0	19.0	20.0	13.6	13.8	13.4	13.9	13.9
Sales related costs											
The two-phase	20%[h]	0.166	0.169	0.171	0.168	0.172	0.287	0.288	0.290	0.284	0.288
The three-phase		0.195	0.200	0.203	0.199	0.202	0.407	0.408	0.147	0.403	0.412
Total operating cost											
The two-phase		**122.30**	**122.58**	**125.90**	**127.92**	**128.01**	**71.54**	**71.32**	**71.45**	**72.84**	**73.12**
The three-phase		**125.73**	**126.01**	**129.34**	**131.36**	**131.45**	**66.36**	**67.10**	**65.79**	**66.93**	**67.04**

Table 6.2 Estimation of total operating cost for the Case A-I of the Fischer-Tropsch Process [basis: million$ per year]

*Note: **A** = once-through type with FT reactor; **B** = once-through type with two FT reactors series; **C** = two multi-reactor stages; **D** = three multi-reactor stages with 3rd FT reactor of fresh feed; **E** = three multi-reactor stages with 2nd and 3rd FT reactors of fresh feed; F = recycling and co-feeding of undesired products to FT reactor and unreacted reactants to the reformer; **G** = recycling and co-feeding of undesired products and unreacted reactants to the FT reactor; **H** = methane purge and recycling & co-feeding undesired products; **I** = the integrated FT reactor; **J** = the integrated FT reactor series.

[a] The price of natural gas was based on British Petroleum 2010.

[b] The technical and operating engineers are called as plant operator.

[c] The overhead involved director, secretary, security, drivers so on.

[d] According to the 2009 Alberta Wage and Salary Survey, Albertans in the Chemical Engineers occupational group earned from $25.00 to $96.88 an hour. The average wage was $ 49.04 an hour. Also the working time was assumed 40 hours per week and 4 weeks per year on holiday for workers.

[e] The labour related cost was assumed to be 60% of labour wages

[f] The maintenance, operating supplies, local taxes and insurance were assumed to be 21% of plant cost

[g] The depreciation was assumed to be 10% of plant cost

[h] The sales related cost was assumed to be 20% of sales cost

Table 6.2 presents the operating cost for the proposed cases of Fischer-Tropsch plant. As mentioned above, the five categories are listed detail and calculated based on the unit million $.

Table 6.3 is shown the costs gasoline and diesel that were calculated based on the current price; $54/BBL and $62/BBL, respectively. The total value of the gasoline and diesel sales was the best at case G for both two-phase and three-phase models.

Case	Two-phase		Three-phase	
	Gasoline	Diesel	Gasoline	Diesel
A	456.08	373.59	676.15	296.86
B	468.14	376.29	692.05	304.80
C	483.70	372.09	706.57	309.53
D	464.21	375.12	690.84	303.31
E	483.27	377.62	700.62	308.42
F	942.65	494.52	1343.17	692.12
G	942.73	495.90	1347.21	694.20
H	950.96	499.33	1376.63	709.36
I	931.79	490.61	1328.51	684.57
J	943.54	496.34	1359.34	700.45

Table 6.3 Sales income for each of the cases [basis million$ per yr]

Table 6.4 shows the economic outcomes in terms of annual profits. The investment can return after one year from the plant operating and the case H was the best FT plant with recycling and co-feeding as can be seen the Return of Investment which is calculated based on 1 years plant life. The heavy selectivity of case G was the best results however, the operating cost of Case G was higher than that of Case H and J.

Case	Operating Cost		Sale cost		Profit		ROI[9] [%]	
	Two	Three	Two	Three	Two	Three	Two	Three
A	122.30	125.73	829.67	973.01	707.37	847.28	294.13	354.28
B	122.58	126.01	844.43	996.85	721.85	870.84	299.65	363.56
C	125.90	129.34	855.79	1016.10	729.89	886.76	285.44	348.94
D	127.92	131.36	839.33	994.15	711.41	862.79	269.75	329.28
E	128.01	131.45	860.89	1009.04	732.88	877.59	277.74	334.56
F	71.54	66.36	1437.17	2035.29	1365.63	1968.93	763.29	1104.9
G	71.32	67.10	1438.63	2041.41	1367.31	1974.31	750.88	1088.7
H	71.45	65.79	1450.29	2085.99	1378.84	2020.20	784.26	1153.7
I	72.84	66.93	1422.40	2013.08	1349.56	1946.15	741.84	1074.2
J	73.12	67.04	1439.88	2059.79	1366.76	1992.75	749.31	1097.1

Table 6.4 Total economic outcomes for each of the cases [basis million$ per yr]

---

[9] **Return on Investment (ROI) analysis** is one of several commonly used approaches for evaluating the financial consequences of business investments, decisions, or actions

6.2 ECONOMIC EVALUATION

The economic results mentioned in Section 6.1 are evaluated in comparison with economic data from the once-through natural gas Fischer-Tropsch plant which, were developed by Bechtel in 1996. The plant is used advanced Fischer-Tropsch technology to produce high quality, liquid transportation fuels and natural gas was used as the feedstock (Choi et al. 1996). In addition, the product upgrading areas was also simplified to produce only FT liquids. The section describes the comparison of the results of both my study and the Bechtel study.

The plant proposed by Choi et al. consists of two main processing areas; synthesis preparation and once-through FT synthesis & product fractionation. The portion of the plant was simulated using Aspen HYSYS. The area of synthesis preparation consists of three major parts; air compression and separation, autothermal reforming (ATR), and CO_2 removal and recycling. In addition, the area of once-through FT synthesis & product fractionation consists of four plants; once-through FT synthesis, product separation, hydrogen recovery and wax hydrocracking. The conceptual plant cost estimates had developed producing about 8820BPD of FT liquids from 100 MMSCF/day of natural gas. The capital cost of plant was estimated to cost about $415 MM mid-1996 dollars. Table 6.5 shows a breakdown of the capital cost of the Fischer-Tropsch plant proposed by Choi et al. and they concluded that the estimated cost of the plant is about a third less than that of a FT plant of the same size using gas recycling to maximize liquid production (Choi et al. 1996).

Description	Cost (MM$)
Air Compression & Separation	70.4
Autothermal Reforming	22.8
CO_2 Removal and Recycling	13.4
Fischer-Tropsch Synthesis	35.8
Hydrogen Recovery	3.6
Product Fractionation	3.2
Wax Hydrocracking	11.8
Combined Cycle Plant	54.5
Total ISBL	215.5
Offsite	120.3
Subtotal:	335.8
HO Service/Fees & Contingency	79.4
Total Cost :	**415.2**

Table 6.5 Cost breakdown of the once-through BBL/Day FT liquefaction plant (Choi, Kramer et al. 1996)

Hamelinkck et al. (2003) investigated the Fischer-Tropsch plant and concluded that FT diesel derived from biomass via gasification is an attractive clean and carbon neutral transportation fuels. The Fischer-Tropsch plant using biomass as feedstock should be via gasification, so the FT plant is more expensive than those for natural gas and crude oil. In addition, they were considered for tar removal and cracking methods and the tars and BTX were removed by standard wet gas cleaning technologies. The CO conversion using large size of the FT reactor was about 70% because a higher conversion can be realised by a larger reactor. However, even though it is high CO conversion, this leads to higher capital costs and overall efficiencies for the best performing systems are 40-45% and FT liquids can be produced at 15€/GJ.

Gas utilization in Nigeria(2010) is also evaluated. The Fischer-Tropsch plant is included the product upgrading process. The hydrocarbons are upgraded by converting it into high quality diesel through hydrocracking and

hydroprocessing technology. Therefore, the high quality cleaner diesel fuels are produced and the fuels are more independent on crude oil imports like Nigeria is expected to rise. However, the total technical cost of $58.82/boe(train 7) for the overall project is rather very high when compared to the typical average FT project.

As mentioned above, Fischer-Tropsch processes are required to be operated on a large scale. Fischer-Tropsch(FT) process developers typically constructed FT plant costing in the order of $415M (Davis 2005). Anton C. Vosloo also pointed out that, in order to make the GTL technology more cost effective, the focus must be on reducing both the capital and operating cost of the Fischer-Tropsch plant (Vosloo 2001). Furthermore, Mordern Fischer-Tropsch plants are desired high alpha to produce higher hydrocarbons and then use hydrocracking to minimize methane formation.

As a result of the economic analysis it was concluded that Case H had overall cost advantage relative to base case by proposed Davis et al. The estimated cost is reduced about 30%, $145M. The benefit results from a lower total capital cost, higher C5+ selectivity and lower light hydrocarbon selectivity.

7

Conclusions and Recommendations

7.1 CONCLUSIONS

The work described in this thesis was focused on the development of alternative process in order to increase gasoline and gas oil and to reduce the overall production costs. The literature review indicated that there are ongoing debates on the reaction mechanism and FT plant process scheme. The proposed FT reaction mechanisms were not only interpreted qualitatively by Driving Force Analysis but also quantitatively via reactor modelling. Furthermore, there should be strategies for manipulating characteristics of FT plant, which consider economic aspects, along with technological feasibilities.

Fischer-Tropsch reaction mechanism

Several FT reaction mechanisms were evaluated in this study. In addition, the mechanisms were considered in adding the formation of alcohols and acids and for both primary and secondary reactions as polymerization, and modified with valuable components such as sizes of catalyst and reactor and three active sites on the catalyst in this study. The proposed mechanism includes the set of possible FT reactions; chain initiation, chain growth, termination and re-adsoprtion.

Driving Force Analysis

The proposed reaction mechanism was used to carry on Driving Force Analysis (DFA) as quantitative modelling that indicated analysis of each compounds' necessity for the Fischer-Tropsch reaction and mechanism, and understood the

influence of selectivity products on the reaction both two-phase and three-phase for the pure feed and co-feed.

The optimized Fischer-Tropsch kinetic modelling

The kinetics model for both two-phase and three-phase reactor were developed based on the proposed reaction mechanism and modified with some parameters such as size effects of catalyst and reactor and active sites on iron based catalysts to comprehend the effects of these parameters using MATLAB mathematics tool. In order to maximize hydrocarbon production requires pressure 2MPa and temperature 540K at a reaction. Also H_2/CO ratio=2 produces the desired hydrocarbon using iron-based catalyst. The effect of co-feeding on the iron-based catalyst was investigated in the two reactor types. It was found that co-feeding unwanted compounds to synthesis gas did increase the production of hydrocarbons. The recycling and co-feeding led to an increase in feed ratios of C_5^+ selectivity and a slight increase of low carbon hydrocarbons.

The modified Fischer-Tropsch kinetic modelling

The insertion of CO into a growing hydrocarbon chain formed alcohols and acids on the catalyst surface. The rate constants for these compounds were slower than the formation of both paraffins and olefins via insertion of CH_2 species with a growing hydrocarbon chain.

The optimization of Fischer-Tropsch Plant

The Fischer-Tropsch plant, including chemical reactions and heat/mass balance, was carried out with ASPEN HYSYS simulation tool. The kinetic parameters calculated by the optimized kinetic models were applied to plant flowsheets to simulate the ten cases of the Fischer-Tropsch plant. The optimizations to the process were found to be feasible. The results indicated that the series reactor with recycling and co-feeding achieved high yields of gasoline and gas oil. These results are good agreement, which recycling & co-feeding in Fischer-Tropsch process should be supported in the FT plant to increase the production of gasoline and gas

oil. The effects of temperature, pressure, and H_2/CO ratio on C5+ selectivity were discussed. According to simulation results, recycling and co-feeding to FT reactor, Case G was the best process and optimum operating parameters of the process were temperature of 450K, 1MPa and H_2/CO ratio of 1 and temperature of 450K, 2MPa and H_2/CO ratio of 1 for both two-phase and three-phase models.

Economic evaluations of the FT plants

The ten different Fischer-Tropsch plant designs based on Fischer-Tropsch reactor models were built in ASPEN HYSYS and validated with real FT plant data. The results of the simulation and optimization supported the proposed process plant changes suggested by qualitative analysis of the different components influence. The plants involving recycling and co-feeding were found to produce the highest quantities of gasoline and gas oil. The proposed ten FT processes were also evaluated the costs of capital and operating and compared with the real FT plant proposed by Gerard. The recycling and co-feeding to FT reactor plant was the best efficiency to produce both gasoline and gas oil and reduced capital cost 30% of the FT plant proposed by Gerard. Therefore, the proposed FT plant with recycling and co-feeding to FT reactor is considered to build up without additional upgrading units such as hydrocracking and hydroprocessing.

7.2 RECOMMENDATIONS

Future work in this field is recommended. This study's emphasis was on the feasibility analyses based on economic aspects. For further research, an inclusion of additional parameters relating to other aspects of sustainability (e.g. minimum environmental impact and product marketability) would be valuable.

The Fischer-Tropsch model developed in this study is based on iron catalyst. A wide variety of catalysts are active for the reaction, including cobalt, ruthenium and rhodium. It is not always clear whether a proposed mechanism on one type of catalyst is necessarily applicable to other catalysts. Further work should be done in order to study whether the same mechanisms and kinetic constant are applicable to other catalysts.

Moreover, there are other potential process modifications to the current Fischer-Tropsch processes that have not been observed. Conducting more modelling and simulations for natural gas would validate the previously proposed plant and furthermore, might lead to the discovery of general heuristics for Fischer-Tropsch process. In addition, it will be possible to modify the synthesis gas production unit from impure feed such as CO_2 and methane gas from landfills.

Sensitivity analysis modelling allowed the prediction of the composition of the Fischer-Tropsch product when the relative feed flow rates or reactor parameters were varied over a wide span, without real experimentation on the plant which could disturb production operation.

References

Achtsnit, H. S. a. D. (1977). Olefin Reactions During Fischer-Tropsch Synthesis Reactions. <u>Rev. Port. Quim.</u> **19**: 317.

Adrianus, H. (2001). A mechanistic study using transient isotopic tracing. Ph.D. dissertation.

Alberta Wage (2009) http://employment.alberta.ca/ accessed on 01 August, 2010

Anderson, R., Seligman, B. et al. (1952). "Fischer-Tropsch Synthesis: Some important Variables of the Synthesis on Iron catalysts." <u>Ind. Eng. Chem. Res.</u> **44**(2): 391.

Anderson, R., K. Griffin, et al. (2003). "Selective Oxidation of Alcohols to Carbonyl Compounds and Carboxylic Acids with Platinum Group Metal Catalysts." <u>Adv. Synth. Catal</u> **345**(4): 517-523.

Anderson, R. B. (1956). <u>Catalysts for the Fischer-Tropsch Synthesis</u>. In **Catalysis** Emmett, P. H. Ed.; Van Nostrand Reinhold, New York.

Anderson, R. B. (1984). <u>The Fischer-Tropsch Synthesis</u>. Academic Press, New York.

Arend, H. and R. T. Joris (2007). International Application Status Report. <u>Optimisation of a multi-stage Fischer-Tropsch synthesis process</u>. S. I. R. M. B.V.

Bai, L., Xiang H.-W., et al. (2002). "Slurry phase Fischer-Tropsch synthesis over managanese-promoted iron ultrafine particle catalyst." <u>Fuel</u> **81**: 1577-1581.

Bell, A. T. (1988). Surface chemistry of carbonaceous species, Structure and reactivity of surfaces, Elsevier Science Publishers B.V., Ed. Morterra, C., Amsterdam, 91-109

Bo-Tao, T., Jie C, Cheng-Hua Z et al. (2006). "A comprehensive kinetics model of Fischer-Tropsch synthesis over an industrial Fe-Mn catalyst." <u>Applied catalysis A</u> **301**: 39-50.

Bolian, X. and Yining F. (2005). "Pore diffusion simulation model of bimodal catalyst for Fischer-Tropsch synthesis." <u>AiChe J</u> **51**(7): 2068-2076.

Botes, F. G. (2007). "Proposal of a New product characterization model for the iron-based low-temperature Fischer-Tropsch synthesis." <u>Energy & Fuels</u> **21**: 1379-1389.

BP (2010). BP Statistical Review of World Energy.

Bub, G. and Baerns M. et al. (1980). "Prediction of the performance of catalytic fixed bed reactors for Fischer-Tropsch synthesis." <u>Chem. Eng. Technol.</u> **35**: 348-355.

Bukur, D., Nowicki L., et al. (1995). "Activation Studies with a Precipitated Iron Catalyst for Fischer-Tropsch Synthesis." <u>Journal of Catalysis</u> **155**: 366-375.

Bukur, D. B., Patel S. A., et al. (1990). "Fixed bed and slurry reactor studies of Fischer-Tropsch syntehsis on precipitated iron catalyst." Appl. Catal. A **61**(329).

Carlson and Daniel E. et al. (1989). Process for recyling and purifying condensate from a hydrocarbon or alcohol synthesis process. E. R. a. E. Company.

ChemicalEngineering (2010). Chemical Engineering Plant Cost Index (CEPCI). Chemical Engineering.

Choi, G. N., Kramer S. J., et al. (1996). "Design/Economics of a Once-Through Natural Gas Fischer-Tropsch Plant With Power Co-Production."

Clark, A. (Phillips Petroleum Co.) (1951). "Fischer-Tropsch Process for the Synthesis of Hydrocarbons." United States Patent 2564958.

CN, S. and H. Jr. et al. (1982). "Usefulness of a slurry-type Fischer-Tropsch reactor for processing synthesis gas of low hydrogen-carbon monoxide ratios." Can J. Chem. Eng. **60**: 159-162.

Curtis, C., J. W., et al. (1995). "Spillover in heterogeneous catalysts." Chem.Rev. **95**: 759-788.

Daniel, C. E. (1989). "Process for recycling and purifying condensate from a hydrocarbon or alcohol synthesis process." United States Patent 5053581.

Deckwer, W.-D., Burckhart, R., Zoll, G.(1974), "Mixing and mass transfer in tall bubble columns", Chem. Eng. Sci., 29: 2177-2188

Davis, B. H., B.; Jacobs, G.; Das, tk et al. (2005). "Fischer-Tropsch Synthesis : Process considerations based on performance of iron-based catalysts." Topics in Catalysis **32**(Nos. 3-4).

De Smet, C.R.H. (2000). Partial oxidation of methane to synthesis gas: Reaction kinetics and reactor modelling, Ph.D. dissertation, Eindhoven.

Dictor, R. A. and Bell A. T. (1986). "Fischer-Tropsch synthesis over reduced and unreduced iron oxide catalysts." J. Catal. **97**(121).

Donnelly, T.J. (1985). Product distributions of the Fischer-TRopsch synthesis, Massachusetts Institute of Technology. Phys. Chem. 89

Donnelly, T. J. and Satterfield C. N. (1989). "Product distributions of the Fischer-Tropsch synthesis on precipitated iron catalysts." Appl. Catal. **A**(52): 93-114.

Dry, M. E. (1976). Advances in Fischer-Tropsch chemisty, Ind. Eng. Chem. Prod **15**(282).

Dry, M. E. (1981). "The Fischer-Tropsch synthesis." Catalysis-Science and Technology **1**: 160-255.

Dry, M. E. (1982). "Catalytic aspects of industrial Fischer-Tropsch synthesis." J. Mol. Catal. **17**: 133-144.

Dry, M. E. (1990a). The Fischer-Tropsch process-commercial aspects. Catal. Today **6**(3): 183.

Dry, M. E. (1990b). "Firscher-Tropsch synthesis over iron catalysts." Catalysis Letters **7**: 241-252.

Dry, M. E. (1996). "Practical and theoretical aspects of the catalytic Fischer-Tropsch process." Appl. Catal. A **138**: 319-344.

Dry, M. E. (2001). "High quality diesel via the Fischer-Tropsch process - a review." Journal of Chemical Technology and Biotechnology **77**: 43-50.

Dwyer, D. and Somorjai G. (1979). "The role of re-adsorption in determining the product distribution uring CO hydrogenation over Fe single crystals." J Catal. **35**: 54.

Eliason, S.A. and Bartholomew C.H. (1999). "Reaction and deactivation kinetics for Fischer-Tropsch synthesis on unpromoted and potassium-promoted iron catalysts." Appl. Catal. A **186**: 229-243.

Exxon Research & Engineering Company (1990). Process for recycling and purfying condensate from hydrocarbon or alcohol synthesis process. United States Patent 5053581

Fischer.F and Tropsch H. (1923). Preparation of Synthetic Oil Mixtures (Synthol) From Carbon Monoxide and Hydrogen. Brennstoff-Chem **4**: 276-285.

Fernandes, A. F. N. (2005). "Polymerization Kinetics of Fischer-Tropsch Reaction on Iron Based Catalysts and Product Grade Optimization." Chem. Eng. Technol. **28**(No.8).

Field, R. W., Davidson, (1980), "Axial dispersion in bubble columns", Trans. IChemE, 58, : 228.

Garrett, D. E. (1989). Chemical Engineering Economics. New York. Springer

Gaube, J. and Klein H.-F. et al. (2008). "Studies on the reaction mechanism of the Fischer-Tropsch synthesis on iron and cobalt." Journal of Molecular Catalysis A **283**: 60-68.

G.D. Ulrich (1984), *A Guide* to *Chemical Engineering Process Design andEconomics,* Wiley, New York.

Gerard, P. V. d. L. (1999). "Kinetics and Selectivity of the Fischer-Tropsch Synthesis: A Literature Review." Catal. Rev. **41**(3 & 4): 255-318.

Graaf G.H., Stqamhuis E.J., and Beenackers A.A.C.M (1988), "Kinetics of low-pressure methanol synthesis," Chemical Engineering Science 43 3185-3195.

Giorgio Soave (1976), "Equilibrium constants from a modified Redlich-Kwong equation of state", Chemical Engineering Science, 27:1197-1203.

Greenwood NN and Earnshaw, A. (1997), Chemistry of the elements, Book(ISBN 0750633654) 2nd edition, Butterworth-Heinemann(Boston, Mass.)

Griboval-Constant A., Khodakov A.Y., Bechara R., Zholobenko V.L. (2002), "Support mesoporosity: a tool for better control of catalytic behavior of cobalt supported Fischer Tropsch catalysts", Characterization of porous solids VI, Eds.F.Rodriguez-Reinoso e.a., Amsterdam e.a., Stud.Surf.Sci.Catal.,v.144, 609-616.

Guo, X., Liu Y., Chang, J., Bai, L. and Xu, **Y**. et al. (2006). "Isothermal Kinetics Modelling of the Fischer-Tropsch Synthesis over the Spray-Dried Fe-Cu-K Catalyst." Journal of Natural Gas Chemistry **15**: 105-114.

Guthrie, R.I.L., and Cliff, R., and Henein, H. (1975), "Contacting problems associated with aluminum and ferro-alloy additions in steelmaking-hydrodynamic aspects", Metallurgical Transactions. Vol.6B:321-329.

Hamelinck, Carlo N., Faaij, Andre P. C., den Uil, Herman, Boerrigter, Harold (2004), "Production of FT transportation fuels from biomass; Technical options, process analysis and optimisation, and development potential", Energy 29:1743 – 1771.

Hanlon, R. T. and Satterfield C. N. (1988). "Reactions of selected 1-olefins and ethanol added during the Fischer-Tropsch synthesis." Energy & Fuels **2**: 196-204.

Henrici- Olivé G. and Olivé S. (1976) "Hydrogenation catalysts: A synthetic hydrogenase model", Journal of Molecular Catalysis, 1:121-135

Hilmen, A., Schanke D., et al. (1999). "Study of the effect of water on alumina supported cobalt Fischer-Tropsch catalysts." Applied catalysis A **186**: 169-188.

Hopper, J. R., Biava CG, Epstein WV (1982). "Design of multi-phase and catalytic chemical reactors: a simulation tool for pollution prevention" Clean Technologies and environmental policy **33**:92-103

Iglesia, E., Reyes S.C., et al. (1991). "Transport-enhanced alpha-olefin re-adsorption pathways Ru-catalyzed hydrocarbon synthesis." J. Catal. **129**(238).

Iglesia, E., Reyes S. C., et al. (1993). "Selectivity control and catlayst design in the Fischer-Tropsch synthesis : sites, pellets, and reactors." Advances in Catalysis **39**: 221-302.

Jager, B. (1997). "Developments in Fischer-Tropsch technology." Stud. Surf. Sci. Catal. **107**: 219-224.

Jess, A., Popp R., et al. (1999). "Fischer-Tropsch synthesis with nitrogen-rich syngas: Fundamentals and reactor design aspects." Appl. Catal. **A**(186): 321-342.

Ji, Y.-Y., H.-W. Xiang, et al. (2001). "Effect of reaction conditions on the product distribution during Fischer-Tropsch synthesis over an industrial Fe-Mn catalyst." Applied catalysis A **214**: 77-86.

Jie., C., Liang B., et al. (2007). "Kinetic modeling of Fischer-Tropsch synthesis over Fe-Cu-K-SiO2 catalyst in slurry phase reactor." Chemical Engineering Science **62**: 4983-4991.

Jordan, D.S. and Bell A.T. (1987). "The influence of propylene on CO hydrogenation over silica-supported ruthenium." J Catal. **107**: 338-350.

Joseph M. Fox III (1990), Slurry Reactor Design Studies DOE project No. DE-AC22-89PC89867, Bechtel Group Inc.

Kamm, G. R., Charleston S., et al. (1979). Integrated process for the partial oxidation-Thermal cracking of crude oil feedstocks. U. C. Corporation. United States Patent 4134824.

Kawagoe, Masaaki (1999) "Regional Dynamics in Japan: A Reexamination of Barro Regressions," Journal of the Japanese and International Economies, 13:61-72.

King, D., Cusumano J., et al. (1981). "A technological perspective for catalytic processes based on synthesis gas." Catalysis Reviews **23**(1-2): 233-263.

Klerk, A. d. (2006). "Distillate production by oligomerization of Fischer-Tropsch Olefins over Solid phosporic Acid." Energy & Fuels **20**: 439-445.

Kolbel, H., Ackermann, P., Ruschenburg, E., Langheim, R., Engelhardt, F. (1951), "Fischer-Tropsch Synthesis with iron catalysts. II. Conditioning and starting-up of iron catalysts, behavior during synthesis, and results obtained in various synthesis processes", Chem.-Ing.-Tech., 23:183-189.

Kolbel, H. and Ralek M. (1980). The Fischer-Tropsch Synthesis in Liquid Phase, Catal. Rev Sci Engng **21**: 225-74.

Kuchar, P., Bricker J., et al. (1993). "Paraffin isomerization innovations." Fuel Processing Technol. **35**: 183-200.

Laan, G. and Beenackers (1999). "Multicomponent reaction engineering model for Fe-catalyzed Fischer-Tropsch synthesis in commercial scale slurry bubble column reactors." Ind Engng Chem Res **38**: 1277.

Li, J., Z. Y, et al. (2002). "Fischer-Tropsch Synthesis: Effects of Water on the Deactivation of Pt Promoted Co/Al2O3 Catalyst." Appl. Catal. A **228**: 203.

Liu, Y., C.-H. Zhang, et al. (2008). "Effect of co-feeding carbon dioxide on Fischer-Tropsch synthesis over an iron-manganese catalyst in a spinning basket reactor." Fuel processing Technology **89**: 234-241.

Lox, E. et al. (1987). De Synthese van Koolwaterstoffen uit Koolmonoxide en Waterstof. Univ.of Ghent. Ph.D Dissertation.

Lox, E. and Marin G. (1988). "Characterization of a promoted precipitated iron catalyst for Fischer-Tropsch synthesis." Appl. Catal. A **40**: 197-218.

Lox, E. S. and Froment G. F. (1993). "Kinetics of the Fischer-Tropsch reaction on a precipitated promoted iron catalyst. Kinetic modeling." Ind. Eng. Chem. Res. **32**(71-82).

Madon, R. J., Reyes. S.C, et al. (1991). "Primary and secondary reaction pathways in ruthenium-catalyzed hydrocarbon synthesis." J. Phys. Chem. **95**: 7795-7804.

Mirzaei AA et al. (2009), "Fischer-Tropsch Synthesis over Iron Manganese Catalysts: Effect of Preparation and Operationg Conditions on Catalyst Performance" Advances in Physical Chemistry Vol. 2009:12

Mukoma P, Hildebrandt D et al. (2006), "A Process Synthesis Approach To Investigate the Effect of the Probability of Chain Growth on the Efficiency of Fischer-Tropsch Synthesis", Ind. Eng. Chem. Res. 45:5928-5935

Newsome, D. S. (1980). "The water-gas shift reaction." Catal. Rev. Sci. Eng. **21**: 275-318.

Nijs, H. H. and Jacobs P. A. (1980). "Metal Particle Size Distributions and Fischer-Tropsch Selectivity. An Extended Schulz-Flory Model." Journal of Catalysis **65**: 328-334.

Patzlaf, J., Y. Liu, et al. (2002). Interpretation and kinetic modeling of product distributions of cobalt catalyzed Fischer-Tropsch synthesis, Catal. Today **71**: 381-394.

P. Chaumette and Boucot P. et al. (1995), "Process for the conversion of natural gas into hydrocarbons", Fuel and Energy, 37:179.

Peter, M., Diane H., et al. (2006). "A Process Synthesis Approach to Investigate the Effect of the Probability of Chain Growth on the Efficiency of Fischer-Tropsch Synthesis." Ind. Eng.Chem. Res. **45**: 5928-5935.

Post, M., A. v. t. Hoog, et al. (1989). "Diffusion Limitations in Fischer-Tropsch Catalysts." AIChE J **35**(7): 1107-1114.

Pour, A., Zare M., et al. (2010). "Studies on product distribution of alkali promoted iron catalyst in Fischer-Tropsch synthesis." Journal of Natural Gas Chemistry **19**(1).

Rafael, L. E., W. H. A, et al. (2003). Recycling of low boiling point products to a Fischer-Tropsch reactor. C. Company. International Appl. no.: PCT/US2004/016133

Raje, A. and Inga J. R. (1997). "Fischer-Tropsch Synthesis: Process considerations based on performance of iron-based catalysts." Fuel **76**(Number 3) 273-280.

Raje, A. P. and Davis B. H. (1997). "Fischer-Tropsch synthesis over iron-based catalysts in a slurry reactor. Reaction rates, selectivities and implications for improving hydrocarbon productivity." Catalysis Today **36**: 335-345.

Raleigh, P. (June, 2010). Section: UK and International Plant Cost Indices. Process Engineering Magazine.

Rao, K., Huggins F., et al. (1995). "Mossbauer spectoscopy study of iron-based catalysts used in Fischer-Tropsch synthesis." Top. Catal. **2**: 71-78.

Rethwisch, D. G. and Dumesic J. A. (1986). "Adsorptive and catalytic properties of supported metal oxides.III. Water-gas shift over supported iron and zinc oxides." J. Catal. **101**(35-42).

Rideal, E. K. and Craxford, S. R (1939). A note on a simple molecular mechanism for heterogeneous catalytic reactions, J. Chem. Soc: 1604.

Rofer-De Poorter, C. K. Chem. Reu. (*1981),* "A comprehensive mechanism for the Fischer-Tropsch synthesis ", Chem. Rev. 81, 447

Towell, G. D., Ackermann, G. H.(1972), "Axial mixing of liquid and gas in large bubble reactors", Proc. 5th European-2nd Internation Symposium on Chemical Reaction Engineering, Amsterdam, B1.

Sachtler, W. M. H. (1984). Elementary steps in the catalyzed conversion of synthesis gas, Proc. 8th Int. Congr. Catal. 1: 151-173.

Satterfield C.N. and Huff G. (1982). "Usefulness of a slurry-type Fischer-Tropsch reactor for processing synthesis gas of low hydrogen-carbon monoxide ratios." Can J. Chem. Eng. **60**: 159-162.

Satterfield, C. N., Huff, G. A., Stenger, H. G., Carter, J. L., Madon, R. J.(1985), "A Comparison of Fischer-Tropsch Synthesis in a Fixed Bed Reactor and in a Slurry Reactor", Ind. Eng. Chem. Fund., 24: 450-454.

Schulz, H., Reidel Th., and Schaub G (1995). "Fischer-Tropsch principles of co-hydrogenation on iron catalysts." Topics in Catalysis **32**: 3-4.

Schulz, H., Beck K., et al. (1988). "Kinetics of Fischer-Tropsch selectivity." Fuel **18**: 293-304.

Schulz, H. P. a. H. (1970). "New insights in area of the synthesis of hydrocarbons from CO and H_2", Chem. Eng. Technol **42**: 1162.

Schweitzer, J. M. and Viguie J. C. (2009). "Reactor Modeling of a slurry bubble column for Fischer-Tropsch Synthesis." Oil & Gas Science and Technology **64**(No.1): 63-77.

Senzi Li, Sundaram Krishnamoorthy et al.(2002), "Promoted Iron-based catalysts for the Fischer-Tropsch synthesis: Design, Synthesis, Site Densities, and Catalytic Properties", Journal of Catalysis, 206:202-217

Seo, J., Oh M., et al. (2000). "Design Optimization of a Crude Oil Distillation Process." Chemical Engineering & Technology **23**(2): 157-164.

Shell (2001). "Shell middle destilate synthesis (Malaysia)." available online (www.shell.com.my/smds).

Sie, S. and Krishna R. (1999). "Fundamentals and selection of advanced Fisher-Tropsch reactors." Appl. Catal. A **186**: 55-70.

Sie, S. T. (1998). "Process development and scale up: IVCase history of the development of a Fischer-Tropsch synthesis process." Rev. Chem. Eng **14**: 109-157.

Spath, P. and Dayton D. (2003). Technical and Economic assessment of synthesis gas to fuels and chemicals with emphasis on the potential for biomass-derived syngas. National Renewable Energy Laboratory, NREL/TP-510-34929, December, 2003

Stella Madueme (2010), "Gas flaring activities of major oil companies in Nigeria: An economic investigation", International Journal of Engineering Science Technology Vol.2(4): 610-617

Steynberg, A. and Dry M. (2004). Fischer-Tropsch Technology, Publisher: Elsevier.

Storch, H. H., Columbic N., et al. (1984). The Fischer-Tropsch and Related Synthesis. NY.

Vandenbussche, K.M.; Froent, G.F.(1996), "A steady-state kinetic model for methanol synthesis and the water gas shift reaction on a commercial $Cu/ZnO/Al_2O_3$ catalyst", J. Catal. 161, 1-10

Venkataraman, V.K. and Driscoll, D.J. (2000). Natural gas-to-liquid advanced Fischer-Tropsch research program and commercialization strategy, AIChE Spring National Meeting, Atlanta, 2000, 97-103

Vosloo, A. C. (2001). "Fischer-Tropsch: a futuristic view." Fuel processing Technology **71**: 149-155.

Wall, K. and Sharratt P. N. (2003). Generating innovative process designs using limite data. Journal of Chemical Technology and Biotechnology 78:156-160

Wang, T. and Wang J. (2007). "Slurry Reactors for Gas-to-Liquid Processes: A Review." Ind Engng Chem Res **46**: 5824-5847.

Wang, Y.-N. and Ma W.P. (2003). "Kinetics modelling of Fischer-Tropsch synthesis over an industrial Fe-Cu-K catalyst." Fuel **82**: 195-213.

Wang, Y.-N., Xu Y.-Y., et al. (2003). "Heterogeneous modeling for fixed-bed Fischer-Tropsch synthesis reactor model and its applications." Chemical Engineering Science **58**: 867-875.

Wenping, M. and Edwin L. K. (2007). "Potassium Effects on Activated-Carbon-Supported Iron Catalysts for Fischer-Tropsch synthesis." Energy & Fuels **21**: 1832-1842.

Wendt, A. Steiff and Weinspach P.-M. (*1984*), "Liquid phase *dispersion* in bubble columns", Ger. chem. Engng 7, 267–273

Yang, J., Liu Y., Chang J. et al. (2004a). "Detailed kinetics of the Fischer-Tropsch synthesis over an industrial Fe-Mn catalyst during early period of reaction." www.chemistrymag.org **6**(No.1): 4.

Yang, J. (2004b). "A review of kinetics for Fischer-Tropsch synthesis." www.chemistrymag.org 6(No.4):27.

Yang, J., H.-J. Kim, et al. (2010). "Mass transfer limitations on fixed-bed reactor for Fiscer-Tropsch synthesis." Fuel processing Technology **91**: 285-289.

Yates, I. C. and Satterfield C. N. (1992). "Hydrocarbon Selectivity from Cobalt Fischer-Tropsch Catalysts." Energy & Fuels **6**: 308-314.

Zhan, H. and Schrader G. (1985). "Characterisation of a fused iron catalyst for Fischer-Tropsch synthesis by in situ laser Raman spectroscopy." J Catal. **95**: 325-332.

Zimmerman, W. H. and Bukur D. B. (1990). "Reaction kinetics over iron catalysts used for the fischer-tropsch synthesis" Can. J. Chem. Eng **68**(292).

Appendix A

CHEMICAL ENGINEERING PLANT COST INDICES

The Chemical Engineering Plant Cost Index (CEPCI) is used as an inflation indicator made specifically for the chemical industry to correct the cost of each piece of equipment to the date of my estimate, by the relationship

$$euipment\ cost\ at\ my\ date = chart\ cost\ \times \frac{CE\ Index, my\ date}{CE\ Index, chart} \tag{A.1}$$

There are a fairly wide variety of inflation cost indicators that could be used to provide a measure of how the costs of labour, material, supplies, and equipment increase each year. Any one of the factors could be used to update the equipment cost charts. The one specifically designed for chemical plants that many chemical engineers prefer to use is the Chemical Engineering Plant Cost Index, called the CE Index. Both are listed each month, along with a 10 year notation of past yearly indexes (See Table A.1), in the magazine Chemical Engineering. The CE Index is composed of four components, weighted as follows: equipment, machinery, and supports, 61%; erection and installation labour, 22%; buildings, material, and labour, 7%; and engineering and supervision, 10% (See Table A.2). It mentions that a survey is taken each month of selected manufacturers and contractors in the industry, and the price increases averaged and tabulated to form the index. The yearly index is established as the average value for that year (Garrett 1989).

Chemical Engineering Plant Cost Index, Annual Averages (1957-1959=100)					
Year	CEPI	Year	CEPI	Year	CEPI
1992	358.2	1998	389.5	2004	444.2
1993	359.2	1999	390.6	2005	468.2
1994	368.1	2000	394.1	2006	499.6
1995	381.1	2001	394.3	2007	525.4
1996	381.7	2002	395.6	2008	575.4
1997	386.5	2003	402.0	2009	548.4
2010					

Table A.1 Plant inflation cost indicators (Raleigh June, 2010)

CE Plant Cost Index (1957-59 = 100)	Oct. '09 Prelim. 527.9	Sep. '09 Final 525.7	Oct. '08 Final 592.2
Equipment	623.6	621.5	720.0
Heat exchangers & tanks	567.0	563.4	711.7
Process machinery	605.7	604.0	664.7
Pipe, valves & fittings	768.9	768.3	864.0
Process instruments	409.8	409.7	439.0
Pumps & compressors	896.3	895.9	893.0
Electrical equipment	464.2	464.7	471.9
Structural supports & misc	636.5	632.5	771.8
Construction labor	331.4	327.5	326.2
Buildings	495.4	493.2	522.8
Engineering & supervision	344.6	345.4	351.3

Table A.2 CE Plant Cost Index 2009 (ChemicalEngineering 2010)

Appendix B

MATLAB CODES

The codes in this Appendix B are developed to generate model carbon number distributions using mathematic computer tool, MATLAB. The first and second codes are based on two-phase and three-phase reactor model of both once-through and recycling & co-feeding and required the values of operation conditions and sizes of catalyst and reactor as input. The third and fourth programmes are calculated carbon number distributions based on both two reactors with recycling process.

(A) OPTIMIZED TWO-PHASE MODEL

TITLE : Carbon number distributions for two-phase based on Jun Yang model

```
function [R_c]=twooptimizedkk2(t,y)

global P_t p2

p = zeros(size(y));
%% Arrhenius eq ; k = A*exp(-Ea/RT) ; Rate constant
R = 8.314 ; % The gas constant; [J/molK]

T=p2(1,1);
P_t=p2(2,1);
ratio=p2(3,1);
P_r=p2(4,1);
R_d=p2(5,1);
U_G=p2(6,1);

Ea_ch = p2(7) ; % The activation energy of the chain growth, [J/mol]
Ea_m = p2(8) ; % The activation energy of the methane formation, [J/mol]
Ea_p = p2(9) ; % The activation energy of the paraffins formation, [J/mol]
Ea_o = p2(10) ; % The activation energy of the olefins formation, [J/mol]
%T = 585 ; % Temperature in Kelvin, [K];

%% parameters reaction-rate constant
k_5 = p2(11) * exp(-Ea_ch/(R*T)) ; % rate constant of chain growth, [mol/g s
bar]
k_7_m =p2(12) * exp(-Ea_m/(R*T)) ; % rate constant of methane formation,
[mol/g s bar]
k_7 = p2(13) * exp(-Ea_p/(R*T)) ; % rate constant of paraffin formation,
[mol/g s bar]
k_8_p =p2(14) * exp(-Ea_o/(R*T)); % rate constant of olefin formation, [mol/g
s]
k_8_m = p2(15) * exp(-Ea_o/(R*T)) ; % rate constant of olefin readsorption
reaction, [mol/g s bar]

% van't Hoff equation
% the enthalpy change of reaction is assumed to be constant with temperature
K_1 = p2(16)*exp((1/R)*(1/556-1/T)) ; % equilibrium constant of the elementary
reaction 1 for FTS, [1/bar]
K_2 = p2(17) *exp((1/R)*(1/556-1/T)) ; % equilibrium constant of the
elementary reaction 2 for FTS,[1/bar]
K_3_a = p2(18)*exp((1/R)*(1/556-1/T)); % equilibrium constant of the
elementary reaction 3 for FTS,[]
K_4 = p2(19)*exp((1/R)*(1/556-1/T)) ; % equilibrium constant of the elementary
reaction 4 for FTS,[1/bar]
K_6 = p2(20)*exp((1/R)*(1/556-1/T)) ; % equilibrium constant of the elementary
reaction 6 for FTS,[]


%Reactor Sizing Consideration : Superficial flow rate

% Effects of Space velocity, Superficial velocity and Residence time
% R_d = 0.012 ; % Reactor diameter, [m]
% H_r = 1 ; % Reactor hight, [m]
% V_r = 10^-3 ; % 3.14 * D_r^2 * H_r ; % Reactor volume, [m^3]
% V_o = 2 ; % Flow rate, [m^3/h]
% SV = GHSV/3600 * T/273 * 101.3/P ; gas volumetric flow rate
% SV = 7000; % Space Velocity, SV [1/h]
% R_T = 0.1 ; % Residence Time
% U_G = 0.0016  ; % V_o/(3.14 * (D_r)^2) ; % Superficial velocity [m/h]
% U_G = SV * H_r ; % by Space Velocity
% U_G = 1/R_T * H_r; % by Residence Time
```

```matlab
% Gas phase dispersion coefficient
D_G = 20.0 * (R_d/2)^2 * U_G ; % Gas Phase Dispersion Coefficient

% Effective Dispersion coefficient
H = 1282.05 * exp(500 * (1/T - 1/298)) * 0.0099 ; % Solubility, Henry's
D_disp = D_G + 1/(1+(1/(H^2))); % Effective Dispersion coefficient

%% Catalyst Particle Sizing consideration: Diffusion Limitations effect
%P_r = 0.0003 ; % Catalyst particle Radius, [m]

D_diff = R * T / (6 * pi *P_r) ; % Diffusion constant, [m^2/h]

Pe = R_d * U_G / D_disp ; % Peclet Number

De = D_diff * (1 + (1/192) * Pe^2); % Effective Diffusivity

M_t = (P_r/3)*((k_7/De)^(1/2)) ; % Thiele Modulus

n_t_s = 42 ; % total number of species

% Define Partial Pressure of CO, H2, H2O

P_p =  zeros(size(y));

P_p(1) = (y(1)/sum(y)) * P_t;  % Partial Pressure of CO
P_p(2) = (y(2)/sum(y)) * P_t;  % Partial Pressure of H2
P_p(3) = (y(3)/sum(y)) * P_t;  % Partial Pressure of H2O

for z=4:42
    P_p(z) = (y(z)/sum(y)) * P_t ;
end

%% Define alpha, beta, alpha_A

alpha = zeros(n_t_s,1);
beta = zeros(n_t_s,1);
alpha_A = 0;

sdiff=10;
s1=1;

while (sdiff>1e-6)

p=P_p;

%% alpha_A

c1= k_5 * K_3_a * (p(1) * p(2)^2 / p(3)) * s1;
c2= k_7 * K_6 * K_4 * p(2) * s1 + k_8_p;

alpha_A = c1 / (c1 + c2) ;

%% beta_sum

for n=24:42
   n2=n-24+2;
   beta_sum=0;

   for i=2:n2
    beta_sum = alpha_A^(i-2)*p(n-i+2)+ beta_sum;
   end

   a1= k_8_m/k_8_p ;
   a2= K_3_a * p(1) * p(2)^2/p(3);
```

```matlab
    a3= (k_5 * K_3_a * (p(1) * p(2)^2/p(3)) * s1); %changed so now multiplied
by s1 and not divided
    a4= k_7 * K_6 * K_4 * p(2) * s1 + k_8_p;

    beta(n2) = a1*(p(n)/(alpha_A^(n2-1) * a2 + (k_8_m/(a3 + a4)) * beta_sum));
end

%% alpha_sum
alpha_sum=0;

for n=1:20

    b1= k_5*K_3_a*(p(2)^2*p(1)/p(3));
    b2= k_7*K_6*K_4*p(2);
    b3= k_8_p*(1- beta(n))/s1; %k_8_p*(1- beta_sum)/s1;

    alpha(n) =  b1 / (b1 + b2 + b3);
end

alp=0;
for i=2:n
    if (i==2)
        alp=alpha(i);
    else
        alp=alp*alpha(i);
    end
    alpha1(i)=alp;
end

for i=2:n
    alpha_sum(i)=0;
    if (i==2)
        alpha_sum(i)=alpha1(i);
    else
        alpha_sum(i)=alpha_sum(i-1)+alpha1(i);
        alpha_sum(i)=alp;
    end
end

%S1
 z1= 1+(sqrt(K_4*p(2)))+K_1*p(1) + K_3_a*(p(2)^2*p(1)/p(3));
 z2= K_1*K_2*p(1)*p(2) + K_6*(K_4^0.5)*K_3_a*(p(2)^2.5*p(1)/p(3));
 z3=
K_3_a*(p(2)^2*p(1)/p(3))*(alpha_sum(20)+K_6*(K_4^0.5)*K_3_a*(p(2)^2.5*p(1)/p(3
)*(alpha_sum(20))));
%
 s11=1/(z1+z2+z3);

 sdiff=abs(log(s1)-log(s11))
 s1=s11

end

%% Define rate expression
R_c=zeros(n_t_s,1);

    g1= k_7_m*K_4*K_6*K_3_a*(p(2)^3*p(1)/p(3));
    g2= 1+(sqrt(K_4*p(2)))+K_1*p(1) + K_3_a*(p(2)^2*p(1)/p(3));
    g3= K_1*K_2*p(1)*p(2) + K_6*(K_4^0.5)*K_3_a*(p(2)^2.5*p(1)/p(3));
    g4= K_3_a*(p(2)^2*p(1)/p(3))*(1+K_6*(sqrt(K_4*p(2)))* (alpha_sum(1)));

    R_c(4) = E_f*g1 /((g2 + g3 + g4)^2);
%end
```

```matlab
%% Paraffins formation
for n=5:23
     na=n-3;

    e1= k_7 * K_4 * K_6 * K_3_a * (p(2)^3 * p(1) / p(3)) * (alpha1(na));
    e2= 1 + (sqrt(K_4 * p(2))) + K_1 * p(1) + K_3_a * (p(2)^2 * p(1) / p(3));
    e3= K_1 * K_2 * p(1) * p(2) + K_6 * K_4^0.5 * K_3_a * (p(2)^2.5 * p(1) /
p(3));
    e4= K_3_a * (p(2)^2 * p(1) / p(3)) * (1 + K_6 * (sqrt(K_4 * p(2))) *
(alpha_sum(na)));

   R_c(n) = E_f*e1  / ((e2 + e3 + e4)^2) ;
end
%% Olefins formation
for n=24:42
       na=n-22;

    f1= k_8_p*(1-beta(na))*K_3_a*p(2)^2*p(1)/p(3)*(alpha1(na));
    f2= 1 + sqrt(K_4*p(2))+K_1*p(1) + K_3_a*(p(2)^2*p(1)/p(3));
    f3= K_1*K_2*p(1)*p(2) + (K_6*(K_4^0.5)*K_3_a*(p(2)^2.5)*p(1)/p(3));
    f4= K_3_a*(p(2)^2*p(1)/p(3))*(1+K_6*(sqrt(K_4*p(2)))* (alpha_sum(na)));

    R_c(n) = E_f*f1 / ((f2 + f3 + f4)^1.5);
end

dydt(1) =0;
dydt(2) =0;
dydt(3) =0;

for n=4:23
    dydt(1) = dydt(1) - ((n-3)*R_c(n));
    dydt(2) = dydt(2) - ((2*n-5)*R_c(n));
    dydt(3) = dydt(3) + ((n-3)*R_c(n));
end
for n=24:42
    dydt(1) = dydt(1) - ((n-22)*R_c(n));
    dydt(2) = dydt(2) - ((2*n-44)*R_c(n));
    dydt(3) = dydt(3) + ((n-22)*R_c(n));
end

R_c(1)= E_f*dydt(1);
R_c(2)= E_f*dydt(2);
R_c(3)= E_f*dydt(3);
```

TITLE : Plot code of Carbon number distributions for two-phase based on Jun Yang model

```matlab
global p2

p2(1,1)=510; %T
p2(2,1)=1; %Ptotal
p2(3,1)=1.0; %H2/CO Ratio
p2(4,1)=0.00001; %P_r
p2(5,1)=0.2; %R_d
p2(6,1)=0.4; %U_G

p2(7,1)= 75520 ; % The activation energy of the chain growth, [J/mol]
p2(8,1)= 97390 ; % The activation energy of the methane formation, [J/mol]
p2(9,1)=111480 ; % The activation energy of the paraffins formation, [J/mol]
p2(10,1)=97370 ; % The activation energy of the olefins formation, [J/mol]

p2(11,1)=0.000001364181837*1.0e+018;
p2(12,1)=   0.398896536543344*1.0e+018;
p2(13,1)=   2.777585121892731*1.0e+018;
```

```matlab
p2(14,1)=   0.000124521184151*1.0e+018;
p2(15,1)=   0.000000000152423*1.0e+018;


p2(16,1)=2.59 ; % equilibrium constant of the elementary reaction 1 for FTS, [1/bar]
p2(17,1)=1.67 ; % equilibrium constant of the elementary reaction 2 for FTS,[1/bar]
p2(18,1)=8.34; % equilibrium constant of the elementary reaction 3 for FTS,[]
p2(19,1)=1.21 ; % equilibrium constant of the elementary reaction 4 for FTS,[1/bar]
p2(20,1)=0.10 ; % equilibrium constant of the elementary reaction 6 for FTS,[]
p2(21,1)=1;

yo=zeros(1,42);
yo(1)=1;
yo(2)=1.0;
yo(3)=0.000000001;
[t,y] = ode15s('Yang_op2',[0:1000],yo);
length(t);
size(y);

ratio=p2(3,1);

a1=y(1001,4:23);
b1=y(1001,24:42);

totmol=0;

for i=1:42
    totmol=totmol+y(1001,i);
end

for i=1:20
    a1(1,i)=a1(1,i)/totmol;
    if (i<20)
    b1(1,i)=b1(1,i)/totmol;
    end
end

% Plot carbon number vs intensity, paraffins

semilogy([1:20],a1,'r-');hold on
xlabel('Carbon Number');
ylabel('Mole Fraction [Wi/n]');

% Plot carbon number vs intensity, olefins

semilogy([2:20],b1,'b-');hold on
xlabel('Carbon Number');
ylabel('Mole Fraction [Wi/n]');
```

(B) OPTIMIZED THREE-PHASE MODEL

TITLE: Carbon number distribution for three-phase based on Jung Yang model

```
function [R_c]=Yang_3(t,y)

global P_t p2

p = zeros(size(y));

%% Arrhenius eq ; k = A*exp(-Ea/RT) ; Rate constant
R = 8.314 ; % The gas constant; [J/molK]

T=p2(1,1);
P_t=p2(2,1);
ratio=p2(3,1);
P_r=p2(4,1);
R_d=p2(5,1);
U_G=p2(6,1);

Ea_5 = 79900 ; % The activation energy of the chain growth, [J/mol]
Ea_11_1 = 86800 ; % The activation energy of the methane formation, [J/mol]
Ea_11 = 94500 ; % The activation energy of the paraffins formation, [J/mol]
Ea_12 = 87600 ; % The activation energy of the olefins formation, [J/mol]
Ea_9 = 94700 ; % The activation energy of the formation of alcohols, [J/mol]
Ea_10 = 108000 ; % The activation energy of the formation of acids, [J/mol]

%T = 573 ; % Temperature in Kelvin, [K];

%% parameters reaction-rate constant
k_5 = 24612257957042.72 * exp(-Ea_5/(R*T)) ; %1.26*10^6, rate constant of chain growth, [mol/Kg s]
k_9 = 8980561052534628 * exp(-Ea_9/(R*T));%2.09*10^7, rate constant of the formation of alcohols,
[mol/Kg s]
k_10 = 477982965388627800 * exp(-Ea_10/(R*T)); %6.82*10^7, rate constant of the formation of acids,
[mol/Kg s]
k_11 = 1957123125672729.5 * exp(-Ea_11/(R*T)); %4.75*10^6,rate constant of the formation of paraffins,
[mol/Kg s]
k_11_1= 21605864674392337 * exp(-Ea_11_1/(R*T)); %2.64*10^6, rate constant of the formation of
methane, [mol/Kg s]
k_12_p= 65440257383761.66 * exp(-Ea_12/(R*T)); %6.76*10^6, rate constant of the formation of olefins,
[mol/Kg s]
k_12_m= 2100.670984064538 * exp(-Ea_12/(R*T)); %2.17*10^-7, rate constant of the readsorption reaction,
[mol/Kg s bar]

% k_5 = 7089784320041.31*3600 * exp(-Ea_5/(R*T)) ; %1.26*10^6, rate constant of chain growth, [mol/Kg s]
% k_9 = 5973282653827673*3600 * exp(-Ea_9/(R*T));%2.09*10^7, rate constant of the formation of
alcohols, [mol/Kg s]
% k_10 = 300227740893521900*3600 * exp(-Ea_10/(R*T)); %6.82*10^7, rate constant of the formation of
acids, [mol/Kg s]
% k_11 = 1302871991282259.2*3600 * exp(-Ea_11/(R*T)); %4.75*10^6,rate constant of the formation of
paraffins, [mol/Kg s]
% k_11_1= 148680620517824.84*3600 * exp(-Ea_11_1/(R*T)); %2.64*10^6, rate constant of the formation
of methane, [mol/Kg s]
% k_12_p= 44877814621239.76*3600 * exp(-Ea_12/(R*T)); %6.76*10^6, rate constant of the formation of
olefins, [mol/Kg s]
% k_12_m= 14.406044042616905*3600 * exp(-Ea_12/(R*T)); %2.17*10^-7, rate constant of the readsorption
reaction, [mol/Kg s bar]

% van't Hoff equation
% the enthalpy change of reaction is assumed to be constant with temperature
% K_1 = 0.199;%*exp((1/R)*(1/556-1/T)) ; % equilibrium constant of the elementary reaction 1 for FTS,
[1/bar]
```

```matlab
% K_2 = 0.203; %*exp((1/R)*(1/556-1/T)) ; % equilibrium constant of the elementary reaction 2 for
FTS,[1/bar]
% K_3 = 0.407;%*exp((1/R)*(1/556-1/T)); % equilibrium constant of the elementary reaction 3 for FTS,[]
% K_4 = 0.804;%*exp((1/R)*(1/556-1/T)) ; % equilibrium constant of the elementary reaction 4 for
FTS,[1/bar]
% K_6 = 0.182;%*exp((1/R)*(1/556-1/T)) ; % equilibrium constant of the elementary reaction 6 for FTS,[]
% K_7 = 3.55*10^-2 ; % equilibrium constant of the elementary reaction 7 for FTS,[]
% K_8 = 0.102 ; % equilibrium constant of the elementary reaction 8 for FTS,[]

K_1 = p2(16)*exp((1/R)*(1/556-1/T)) ; % equilibrium constant of the elementary reaction 1 for FTS, [1/bar]
K_2 = p2(17) *exp((1/R)*(1/556-1/T)) ; % equilibrium constant of the elementary reaction 2 for FTS,[1/bar]
K_3 = p2(18)*exp((1/R)*(1/556-1/T)); % equilibrium constant of the elementary reaction 3 for FTS,[]
K_4 = p2(19)*exp((1/R)*(1/556-1/T)) ; % equilibrium constant of the elementary reaction 4 for FTS,[1/bar]
K_6 = p2(20)*exp((1/R)*(1/556-1/T)) ; % equilibrium constant of the elementary reaction 6 for FTS,[]
K_7 = p2(22)*exp((1/R)*(1/556-1/T)) ; % 3.55*10^-2 ; % equilibrium constant of the elementary reaction 7
for FTS,[]
K_8 = p2(23)*exp((1/R)*(1/556-1/T)) ; % 0.102 ; % equilibrium constant of the elementary reaction 8 for
FTS,[]

%% Reactor Sizing Consideration : Superficial flow rate

% Effects of Space velocity, Superficial velocity and Residence time
%R_d = 0.012 ; % Reactor diameter, [m]
% H_r = 1 ; % Reactor hight, [m]
% V_r = 10^-3 ; % 3.14 * D_r^2 * H_r ; % Reactor volume, [m^3]
% V_o = 2 ; % Flow rate, [m^3/h]
% SV = GHSV/3600 * T/273 * 101.3/P ; gas volumetric flow rate
% SV = 7000; % Space Velocity, SV [1/h]
% R_T = 0.1 ; % Residence Time

%U_G = 0.0016  ; % V_o/(3.14 * (D_r)^2) ; % Superficial velocity [m/h]
% U_G = SV * H_r ; % by Space Velocity
% U_G = 1/R_T * H_r; % by Residence Time

% Gas phase dispersion coefficient
D_G = 20.0 * (R_d/2)^2 * U_G ; % Gas Phase Dispersion Coefficient

% Effective Dispersion coefficient
H = 1282.05 * exp(500 * (1/T - 1/298)) * 0.0099 ; % Solubility, Henry's
D_disp = D_G + 1/(1+(1/(H^2))); % Effective Dispersion coefficient

%% Catalyst Particle Sizing consideration: Diffusion Limitations effect
%P_r = 0.0003 ; % Catalyst particle Radius, [m]

D_diff = R * T / (6 * pi *P_r) ; % Diffusion constant, [m^2/h]

Pe = R_d * U_G / D_disp ; % Peclet Number

De = D_diff * (1 + (1/192) * Pe^2); % Effective Diffusivity

M_t = (P_r/3)*((k_5/De)^(1/2)) ; % Thiele Modulus

if (M_t<0.00001)
   E_f=1;
else
   E_f = 3/(M_t)* (1/(tanh(M_t))- 1/M_t )  ; % Effectiveness Factor
end

E_f=E_f*p2(21,1);

%%
n_t_s = 42 ; % total number of species
```

```matlab
% ptot = sum(y)*R*T/1000;

%P_t = 3.02 ;% ptot ;% Total Pressure, [MPa] originally 0.5

% Define Partial Pressure of CO, H2, H2O

P_p =  zeros(size(y));

P_p(1) = (y(1)/sum(y)) * P_t;  % Partial Pressure of CO
P_p(2) = (y(2)/sum(y)) * P_t;  % Partial Pressure of H2
P_p(3) = (y(3)/sum(y)) * P_t;  % Partial Pressure of H2O

for z=4:42
   P_p(z) = (y(z)/sum(y)) * P_t ;
end

%%% Define alpha, beta, alpha_A

alpha = zeros(n_t_s,1);
beta = zeros(n_t_s,1);
alpha_A = 0;

sdiff=10;
s1=1;

while (sdiff>1e-6)

p=P_p;

A=sqrt(K_4*p(2))*s1; % H-s
B=p(3)/K_6*A *s1; % OH-s
C=K_1*K_2*K_4*K_6*p(2)*p(1)/p(3)*s1; %C-s
D=K_1*K_2*K_3*K_4*K_6*p(2)^2*p(1)/p(3)*s1; % CH2-s
alpha_1=k_5*D/(k_5*D+k_9*K_1*K_7*K_8*p(2)*p(1)*A+k_11*A);

%%% alpha_A

c1= k_5*D;
c2= c1+ k_9*K_1*K_7*K_8*p(1)*p(2)*A + k_10*K_1*K_7*p(1)*B+k_11*A+k_12_p;

alpha_A = c1 / c2 ;

%%% Bn

for i=1:20

c1= k_12_m *p(i+22)*A;
c2= k_5*D+k_9*K_1*K_7*K_8*p(1)*p(2)*A + k_10*K_1*K_7*p(1)*B+k_11*A+k_12_p;

bn(i) = c1 / c2 ;
end

%%% beta_sum

for n=24:42
  n2=n-24+2;
  beta_sum=0;

  for i=2:n2
  beta_sum = alpha_A^(n2-i)*p(i)+ beta_sum;
  end

  a1= k_12_m/k_12_p ;
```

```matlab
    Z=p(n2)*A;
    b1=(alpha_A^(n-1))*alpha_1*A;
    b2=bn(n2)*beta_sum;

    beta(n2) = a1*Z/(b1+b2);
end


%% alpha_sum
alpha_sum=0;

for n=2:20

    b1= k_5*D;
    b2= k_9*K_1*K_7*K_8*p(2)*p(1)*A;
    b3= k_10*K_1*K_7*p(1)*B+k_11*A+k_12_p*(1- beta(n));

    alpha(n) =  b1 / (b1 + b2 + b3);

end

alp=0;
for i=2:n
    if (i==2)
        alp=alpha(i);
    else
        alp=alp*alpha(i);
    end
    alpha1(i)=alp;
end

for i=2:n
    alpha_sum(i)=0;
    if (i==2)
        alpha_sum(i)=alpha1(i);
    else
        alpha_sum(i)=alpha_sum(i-1)+alpha1(i);
        alpha_sum(i)=alp;
    end
end
%% Define rate expression
R_c=zeros(n_t_s,1);

%S1
z1= 1+(sqrt(K_4*p(2)))+K_1*p(1) + K_1*K_7*(p(1)*sqrt(K_4*p(2)));
z2= K_1*K_7*K_8*p(1)*p(2)*sqrt(K_4*p(2)) + K_1*K_2*K_4*K_6*p(2)*p(1)/p(3) +
K_1*K_2*K_3*K_4*(p(2)^2*p(1)/p(3));
z3= p(3)/(K_6*sqrt(K_4*p(2)));
z4= (alpha_sum(20)*(1+K_1*K_7*K_8*p(1)*p(2)*sqrt(K_4*p(2)) +
K_1*K_7*p(1)*sqrt(K_4*p(2)))*sqrt(K_4*p(2)));
%
s11=1/(z1+z2+z3+z4);

sdiff=abs(log(s1)-log(s11))
s1=s11

end

%% methane formation
for na=1:20

    alpha_1=k_5*D/(k_5*D+K_1*K_7*K_8*p(2)*p(1)*A+k_11*A);
```

```
  R_c(4)= E_f*k_11_1*alpha_1*K_2*p(2)*s1^2;

end

 %% Paraffins formation
for n=5:23
  na=n-3;

  d1= k_5*D;
  d2= k_9*K_1*K_7*K_8*p(2)*p(1)*A;
  d3= k_10*K_1*K_7*p(1)*B+k_11*A+k_12_p*(1- beta(na));

  alpha(na) = d1 / (d1 + d2 + d3);


  R_c(n) = E_f*k_11*K_4*p(2)*s1^2*(alpha1(na)) ;
end
%% Olefins formation
for n=24:42
   na=n-22;
   n2=n-2;

  d1= k_5*D;
  d2= k_9*K_1*K_7*K_8*p(2)*p(1)*A;
  d3= k_10*K_1*K_7*p(1)*B+k_11*A+k_12_p*(1- beta(na));

  alpha(na) = d1 / (d1 + d2 + d3);


  R_c(n) = E_f*k_12_p*sqrt(K_4*p(2))*s1^2*(alpha1(na))*(1-beta(n2));

end

dydt(1) =0;
dydt(2) =0;
dydt(3) =0;

for n=4:23
  dydt(1) = dydt(1) - ((n-3)*R_c(n));
  dydt(2) = dydt(2) - ((2*n-5)*R_c(n));
  dydt(3) = dydt(3) + ((n-3)*R_c(n));
end
for n=24:42
  dydt(1) = dydt(1) - ((n-22)*R_c(n));
  dydt(2) = dydt(2) - ((2*n-44)*R_c(n));
  dydt(3) = dydt(3) + ((n-22)*R_c(n));
end

R_c(1)= E_f*dydt(1);
R_c(2)= E_f*dydt(2);
R_c(3)= E_f*dydt(3);
```

TITLE : Plot code of Carbon number distributions for three-phase based on Fernandes model

```
close all,  clc, clear all
global p2

p2(1,1)=540; %T
```

```matlab
p2(2,1)=2; %Ptotal
p2(3,1)=3; %H2/CO Ratio
p2(4,1)=0.00001; %P_r
p2(5,1)=0.2; %R_d
p2(6,1)=0.4; %U_G

p2(16,1)=1.99 ; % equilibrium constant of the elementary reaction 1 for FTS,
[1/bar]
p2(17,1)=2.03 ; % equilibrium constant of the elementary reaction 2 for
FTS,[1/bar]
p2(18,1)=4.07; % equilibrium constant of the elementary reaction 3 for FTS,[]
p2(19,1)=8.04 ; % equilibrium constant of the elementary reaction 4 for
FTS,[1/bar]
p2(20,1)=1.82 ; % equilibrium constant of the elementary reaction 6 for FTS,[]
p2(21,1)=1;
p2(22,1)=3.55;
p2(23,1)=1.02;

yo=zeros(1,42);
yo(1)=1;
yo(2)=2.51;
yo(3)=0.000000001;
[t,y] = ode15s('Yang_3',[0:1000],yo);
length(t);
size(y);

ratio=p2(3,1);

a1=y(1001,4:23);
b1=y(1001,24:42);

totmol=0;

for i=1:42
    totmol=totmol+y(1001,i);
end

for i=1:20
    a1(1,i)=a1(1,i)/totmol;
    if (i<20)
    b1(1,i)=b1(1,i)/totmol;
    end
end

% Plot carbon number vs intensity, paraffins

semilogy([1:20],a1,'r-');hold on
xlabel('Carbon Number');
ylabel('Mole Fraction [Wi/n]');

% Plot carbon number vs intensity, olefins
semilogy([2:20],b1,'b-')
xlabel('Carbon Number');
ylabel('Mole Fraction [Wi/n]');
```

Appendix C

THE RESULTS OF TEN CASES FISCHER-TROPSCH PROCESSES

CASE A OF TWO-PHASE MODEL

The Case A for once-through FT process of two-phase reactor achieved the best results under conditions; 1MPa, 1 H_2/CO ratio and 450K. The result is good agreement with Matlab results of the highest carbon distribution of two-phase reactor under same conditions shown in Figure 4.8-4.10. In addition, the result is satisfied with two-phase reactor of FT process accomplished higher hydrocarbon at same conditions. CO conversion and CO_2 selectivity were increased with higher temperature and pressure, while hydrocarbon selectivity was decreased.

P [Mpa]	H_2/CO ratio	T [K]		M/F[kgmole/h]		Conversion[%]			Selectivity[%]		
		In	Out	In	Out	CO	CO_2	HC	CH_4	C2-C4	C5+
1		450	609.92	0.66589	0.62954	40.04	0.01	99.99	0.00	49.82	**50.184**
	1.0	510	668.65	0.66589	0.62953	40.08	0.08	99.92	0.00	49.82	50.181
		600	757.49	0.66589	0.62938	40.65	1.08	98.92	0.00	49.82	50.180
		450	720.01	0.69957	0.63523	60.87	0.03	99.97	0.00	49.82	50.180
	1.5	510	777.87	0.69957	0.63519	61.03	0.22	99.78	0.00	49.82	50.179
		600	867.07	0.69957	0.6347	62.64	2.05	97.95	0.01	49.82	50.176
		450	845.48	0.74227	0.6422	80.11	0.68	99.32	0.00	49.82	50.175
	2.0	510	902.11	0.74227	0.64231	80.50	0.39	99.61	0.01	49.82	50.175
		600	992.11	0.74227	0.64134	83.27	2.75	97.25	0.02	49.81	50.166
1.5		450	609.68	0.66589	0.62954	40.03	0.01	99.99	0.00	49.82	50.178
	1.0	510	668.52	0.66589	0.62952	40.10	0.12	99.88	0.00	49.82	50.178
		600	757.87	0.66589	0.62931	40.93	1.56	98.44	0.00	49.82	50.179
		450	719.74	0.69957	0.63523	60.88	0.05	99.95	0.00	49.82	50.180
	1.5	510	777.82	0.69957	0.63516	61.12	0.32	99.68	0.00	49.82	50.177
		600	868.4	0.69957	0.63446	63.44	2.92	97.08	0.01	49.82	50.173
		450	844.82	0.74227	0.64243	80.17	0.10	99.90	0.00	49.82	50.177
	2.0	510	902.27	0.74227	0.64224	80.70	0.56	99.44	0.01	49.82	50.171
		600	994.52	0.74227	0.64088	84.57	3.80	96.20	0.03	49.81	50.162
2		450	609.45	0.66589	0.62954	40.04	0.02	99.98	0.00	49.82	50.176
	1.0	510	668.39	0.66589	0.62952	40.12	0.15	99.85	0.00	49.82	50.176
		600	758.21	0.66589	0.62924	41.20	2.02	97.98	0.00	49.82	50.176
		450	719.47	0.69957	0.63523	60.89	0.06	99.94	0.00	49.83	50.174
	1.5	510	777.76	0.69957	0.63514	61.20	0.41	99.59	0.00	49.83	50.174
		600	869.65	0.69957	0.63423	64.20	3.73	96.27	0.01	49.82	50.171
		450	844.56	0.74227	0.64242	80.21	0.13	99.87	0.00	49.83	50.175
	2.0	510	902.41	0.74227	0.64218	80.89	0.73	99.27	0.01	49.82	50.168
		600	996.66	0.74227	0.64047	85.73	4.71	95.29	0.03	49.81	50.159

TABLE A.3 Selectivities of modified two phase model for the Case A.

CASE A OF THREE-PHASE MODEL

Higher hydrocarbon selectivity of three-phase reactor is the best results of the conditions; 2MPa, 2 H_2/CO ratio and 450K. This result had good agreement with Matlab result shown in Figure 4.21-4.22. Firstly, distribution of paraffins was increased with higher temperature, while that of olefins was decreased. However, distribution of paraffins was even higher than that of paraffins. Next, effects of pressure and H_2/CO ratio were the highest 2MPa and 2 H_2/CO ratio. Therefore, the best result was satisfied with the results in Table A.3 for once-through process.

CO conversion and CO_2 selectivity were increased with higher temperature and pressure, while hydrocarbon selectivity was decreased.

P [Mpa]	H_2/CO ratio	T [K] In	T [K] Out	M/F[kgmole/h] In	M/F[kgmole/h] Out	Conversion[%] CO	Conversion[%] CO_2	HC	Selectivity[%] CH_4	Selectivity[%] C2-C4	Selectivity[%] C5+
1		450	614.79	0.66589	0.6261	43.91	0.11	99.89	0.02	21.86	78.11
	1.0	510	673.86	0.66589	0.6263	44.13	1.18	98.82	0.01	25.16	74.83
		600	776.84	0.66589	0.6241	53.25	13.63	86.37	0.01	28.91	71.08
		450	723.66	0.69807	0.6286	66.32	0.32	99.68	0.01	20.81	79.18
	1.5	510	783.76	0.69807	0.6287	67.63	2.39	97.61	0.00	24.04	75.96
		600	899.17	0.69807	0.6241	83.89	16.13	83.87	0.00	27.79	72.21
		450	857.19	0.74227	0.6321	88.79	0.48	99.52	0.00	20.25	79.75
	2.0	510	917.67	0.74227	0.6322	90.78	2.71	97.29	0.00	23.44	76.56
		600	1014.4	0.74227	0.6326	99.04	17.15	82.85	0.00	26.45	73.55
1.5		450	614.99	0.66589	0.6258	44.25	0.11	99.89	0.03	19.67	80.30
	1.0	510	674.15	0.66589	0.6260	44.49	1.18	98.82	0.00	22.81	77.19
		600	777.62	0.66589	0.6237	53.90	13.56	86.44	0.01	26.47	73.52
		450	723.96	0.69807	0.6282	66.76	0.32	99.68	0.01	18.87	81.12
	1.5	510	784.1	0.69807	0.6282	68.07	2.36	97.64	0.01	21.98	78.02
		600	899.18	0.69807	0.6237	84.08	15.86	84.14	0.00	25.67	74.32
		450	857.54	0.74227	0.6314	89.30	0.45	99.55	0.00	18.48	81.52
	2.0	510	917.78	0.74227	0.6315	91.14	2.54	97.46	0.00	21.51	78.49
		600	1015.8	0.74227	0.6295	99.02	16.74	83.26	0.00	24.74	75.26
2		450	615.01	0.66589	0.6256	44.43	0.11	99.89	0.03	18.48	81.49
	1.0	510	674.19	0.66589	0.6258	44.66	1.18	98.82	0.00	21.51	78.48
		600	777.87	0.66589	0.6236	53.78	13.49	86.51	0.02	25.20	74.78
		450	723.96	0.69807	0.6279	66.99	0.30	99.70	0.01	17.84	82.15
	1.5	510	784.98	0.69807	0.6280	68.19	2.23	97.77	0.01	20.84	79.15
		600	899.28	0.69807	0.6237	83.47	15.24	84.76	0.01	24.50	75.50
		450	857.65	0.74227	0.6310	89.63	0.40	99.60	0.00	17.36	**82.64**
	2.0	510	917.88	0.74227	0.6313	91.18	2.34	97.66	0.00	20.49	79.51
		600	1016.1	0.74227	0.6293	98.87	15.38	84.62	0.00	23.64	76.36

TABLE A.4 Selectivities of modified three phase model for the Case A.

CASE B OF TWO-PHASE MODEL

CO conversion and CO_2 selectivity were increased with higher temperature and pressure, while hydrocarbon selectivity was decreased. In addition, C5+ selectivity also was decreased with increasing temperature and pressure. The best result for higher selectivity of C5+ was the conditions; 1MPa, 1 H_2/CO ratio and 510K.

P [Mpa]	H_2/CO ratio	T [K] In	T [K] Out	M/F[kgmole/h] In	M/F[kgmole/h] Out	Conversion[%] CO	Conversion[%] CO_2	Selectivity[%] HC	Selectivity[%] CH_4	Selectivity[%] C2-C4	Selectivity[%] C5+
1		450	609.91	0.6659	0.6295	40.04	0.01	99.99	0.00	49.81	**50.186**
	1.0	510	668.65	0.6659	0.6295	40.08	0.08	99.92	0.00	49.82	50.182
		600	757.49	0.6659	0.6294	40.65	1.08	98.92	0.00	49.82	50.182
		450	715.35	0.6981	0.6350	60.07	0.03	99.97	0.00	49.82	50.184
	1.5	510	773.22	0.6981	0.6349	60.22	0.21	99.79	0.00	49.82	50.177
		600	862.38	0.6981	0.6345	61.77	1.99	98.01	0.00	49.82	50.174
		450	846.49	0.7423	0.6422	80.82	0.67	99.33	0.00	49.82	50.177
	2.00	510	902.12	0.7423	0.6423	80.50	0.39	99.61	0.01	49.82	50.175
		600	992.13	0.7423	0.6413	83.27	2.75	97.25	0.02	49.81	50.168
1.5		450	609.68	0.66589	0.6295	40.04	0.01	99.99	0.00	49.82	50.181
	1.0	510	668.53	0.66589	0.6295	40.10	0.12	99.88	0.00	49.82	50.179
		600	757.88	0.66589	0.6293	40.94	1.56	98.44	0.00	49.82	50.178
		450	715.01	0.69807	0.6350	60.07	0.04	99.96	0.00	49.82	50.182
	1.5	510	773.18	0.69807	0.6349	60.31	0.30	99.70	0.00	49.82	50.180
		600	931.72	0.69807	0.6240	61.88	2.48	97.52	0.00	49.82	50.175
		450	844.81	0.74227	0.6424	80.17	0.10	99.90	0.00	49.82	50.174
	2.00	510	902.27	0.74227	0.6422	80.70	0.56	99.44	0.01	49.82	50.172
		600	994.56	0.74227	0.6409	84.58	3.81	96.19	0.02	49.81	50.164
2		450	609.46	0.66589	0.6295	40.04	0.02	99.98	0.00	49.82	50.180
	1.0	510	668.4	0.66589	0.6295	40.12	0.15	99.85	0.00	49.82	50.177
		600	758.24	0.66589	0.6292	41.21	2.02	97.98	0.00	49.82	50.176
		450	714.72	0.69807	0.6350	60.08	0.06	99.94	0.00	49.83	50.174
	1.5	510	773.11	0.69807	0.6349	60.38	0.39	99.61	0.00	49.82	50.177
		600	864.84	0.69807	0.6340	63.27	3.64	96.36	0.01	49.82	50.171
		450	844.56	0.74227	0.6424	80.20	0.13	99.87	0.00	49.83	50.171
	2.00	510	902.42	0.74227	0.6422	80.88	0.73	99.27	0.01	49.82	50.169
		600	996.7	0.74227	0.6405	85.74	4.72	95.28	0.03	49.81	50.160

TABLE A.5 Selectivities of modified two phase model for the Case B.

CASE B OF THREE-PHASE MODEL

CO conversion and CO_2 selectivity were increased with higher temperature and pressure, while hydrocarbon selectivity was decreased. In addition, C5+ selectivity also was decreased with increasing temperature and pressure. The best result for higher selectivity of C5+ was the conditions; 2MPa, 2 H_2/CO ratio and 450K.

P [Mpa]	H_2/CO ratio	T [K] In	T [K] Out	M/F[kgmole/h] In	M/F[kgmole/h] Out	Conversion[%] CO	Conversion[%] CO_2	HC	Selectivity[%] CH_4	Selectivity[%] C2-C4	Selectivity[%] C5+
1		450	614.81	0.66589	0.62606	43.92	0.11	99.89	0.03	21.87	78.10
	1.0	510	673.85	0.66589	0.62629	44.13	1.18	98.82	0.01	25.16	74.83
		600	776.86	0.66589	0.62412	53.26	13.64	86.36	0.00	28.91	71.09
		450	723.66	0.69807	0.62862	66.32	0.32	99.68	0.00	20.81	79.19
	1.5	510	783.76	0.69807	0.62871	67.63	2.39	97.61	0.00	24.04	75.96
		600	899.35	0.69807	0.62411	83.99	16.19	83.81	0.00	27.79	72.21
		450	857.19	0.74227	0.6321	88.79	0.48	99.52	0.01	20.25	79.75
	2.0	510	917.68	0.74227	0.63216	90.79	2.72	97.28	0.00	23.44	76.56
		600	1018.6	0.74227	0.62994	99.12	9.10	90.90	0.00	27.19	72.81
1.5		450	615.01	0.66589	0.62576	44.25	0.11	99.89	0.04	19.67	80.29
	1.0	510	674.15	0.66589	0.62598	44.49	1.17	98.83	0.01	22.80	77.19
		600	777.64	0.66589	0.62374	53.91	13.59	86.41	0.02	26.47	73.51
		450	723.95	0.69807	0.62815	66.76	0.32	99.68	0.00	18.87	81.12
	1.5	510	784.11	0.69807	0.62825	68.07	2.36	97.64	0.01	21.98	78.02
		600	899.45	0.69807	0.62371	84.18	15.92	84.08	0.00	25.67	74.33
		450	857.55	0.74227	0.63144	89.30	0.45	99.55	0.01	18.48	81.51
	2.0	510	917.79	0.74227	0.63153	91.15	2.55	97.45	0.00	21.51	78.49
		600	1018	0.74227	0.62946	99.10	8.69	91.31	0.00	25.20	74.79
2		450	615.02	0.66589	0.62559	44.44	0.11	99.89	0.04	18.48	81.49
	1.0	510	674.19	0.66589	0.62581	44.66	1.16	98.84	0.01	21.51	78.48
		600	777.23	0.66589	0.62364	53.79	13.50	86.50	0.02	25.20	74.78
		450	723.96	0.69807	0.6279	66.99	0.30	99.70	0.00	17.84	82.16
	1.5	510	784.74	0.69807	0.62802	68.19	2.23	97.77	0.00	20.84	79.15
		600	919.54	0.69807	0.62371	83.56	15.30	84.70	0.00	24.50	75.50
		450	857.64	0.74227	0.63099	89.63	0.40	99.60	0.00	17.35	**82.64**
	2.0	510	917.85	0.74227	0.63159	90.29	2.22	97.78	0.00	20.61	79.39
		600	1018	0.74227	0.62924	98.94	8.36	91.64	0.00	24.08	75.91

TABLE A.6 Selectivities of modified three phase model for the Case B.

CO conversion and CO_2 selectivity were increased with higher temperature and pressure, while hydrocarbon selectivity was decreased. In addition, C5+ selectivity also was decreased with increasing temperature and pressure. The best result for higher selectivity of C5+ was the conditions; 1MPa, 1 H_2/CO ratio and 450K.

P [MPa]	H_2/CO ratio	T [K] In	Out[1]	Out[2]	M/F[kgmole/h] In	Out[1]	Out[2]	Conversion[%] CO	CO_2	Selectivity[%] HC	CH_4	C2-C4	C5+
1		450	609.91	450.00	0.66589	0.6295	0.0544	40.04	0.01	99.99	0.00	49.81	**50.189**
	1.0	510	668.61	511.99	0.66589	0.6295	0.0544	40.17	0.25	99.75	0.00	49.82	50.181
		600	756.96	771.42	0.66589	0.6295	0.0513	51.83	1.63	98.37	0.00	49.82	50.180
		450	715.32	450.00	0.69807	0.6350	0.0682	60.06	0.02	99.98	0.00	49.82	50.184
	1.5	510	773.05	511.01	0.69807	0.6350	0.0682	60.20	0.19	99.81	0.00	49.82	50.178
		600	860.82	640.23	0.69807	0.6347	0.0667	63.51	2.24	97.76	0.00	49.82	50.176
		450	845.70	450.05	0.74227	0.6423	0.0869	80.11	0.03	99.97	0.00	49.82	50.180
	2.00	510	901.67	510.06	0.74227	0.6424	0.0870	80.31	0.22	99.78	0.00	49.82	50.179
		600	989.06	611.27	0.74227	0.6419	0.0855	82.71	2.28	97.72	0.02	49.81	50.168
1.5		450	609.68	450.00	0.66589	0.6295	0.0544	40.04	0.02	99.98	0.00	49.81	50.186
	1.0	510	668.46	512.92	0.66589	0.6295	0.0544	40.24	0.37	99.63	0.00	49.82	50.178
		600	756.87	772.38	0.66589	0.6294	0.0513	52.05	1.64	98.36	0.00	49.82	50.176
		450	715.01	450.00	0.69807	0.6350	0.0682	60.06	0.03	99.97	0.00	49.82	50.182
	1.5	510	772.92	511.46	0.69807	0.6350	0.0681	60.28	0.28	99.72	0.00	49.82	50.177
		600	860.40	669.79	0.69807	0.6346	0.0658	66.79	2.57	97.43	0.01	49.82	50.174
		450	844.70	450.00	0.74227	0.6424	0.0872	80.12	0.05	99.95	0.00	49.82	50.177
	2.00	510	901.63	510.05	0.74227	0.6424	0.0869	80.43	0.32	99.68	0.00	49.82	50.176
		600	988.95	611.04	0.74227	0.6416	0.0848	83.87	3.24	96.76	0.02	49.81	50.164
2		450	609.45	450.00	0.66589	0.6295	0.0544	40.04	0.03	99.97	0.00	49.82	50.179
	1.0	510	668.32	513.82	0.66589	0.6295	0.0544	40.31	0.49	99.51	0.00	49.82	50.176
		600	757.24	772.49	0.66589	0.6294	0.0513	52.15	1.66	98.34	0.00	49.82	50.174
		450	714.72	450.00	0.69807	0.6350	0.0682	60.07	0.04	99.96	0.00	49.82	50.177
	1.5	510	772.79	511.89	0.69807	0.6349	0.0681	60.35	0.36	99.64	0.00	49.82	50.175
		600	860.20	718.74	0.69807	0.6345	0.0643	71.17	2.98	97.02	0.01	49.82	50.171
		450	844.41	450.00	0.74227	0.6424	0.0871	80.13	0.07	99.93	0.00	49.83	50.174
	2.00	510	901.59	510.12	0.74227	0.6423	0.0868	80.53	0.42	99.58	0.00	49.83	50.173
		600	987.89	611.03	0.74227	0.6414	0.0841	84.96	4.11	95.89	0.03	49.81	50.160

TABLE A.7 Selectivities of modified two phase model for the Case C.

CASE C OF THREE-PHASE MODEL

CO conversion and CO$_2$ selectivity were increased with higher temperature and pressure, while hydrocarbon selectivity was decreased. In addition, C5+ selectivity also was decreased with increasing temperature and pressure. The best result for higher selectivity of C5+ was the conditions; 2MPa, 2 H$_2$/CO ratio and 450K.

P [MPa]	H$_2$/CO ratio	T [K]			M/F[kgmole/h]			Conversion[%]		Selectivity[%]			
		In	Out[1]	Out[2]	In	Out[1]	Out[2]	CO	CO$_2$	HC	CH$_4$	C2-C4	C5+
1		450	614.75	451.45	0.66589	0.6261	4.97E-02	43.97	0.20	99.80	0.01	21.88	78.11
	1.0	510	673.22	516.15	0.66589	0.6264	4.85E-02	49.75	1.12	98.88	0.00	23.18	76.82
		600	768.46	617.98	0.66589	0.6255	3.37E-02	59.34	3.04	96.96	0.02	30.16	69.83
		450	723.37	450.00	0.69807	0.6287	5.96E-02	66.21	0.22	99.78	0.00	20.81	79.19
	1.5	510	781.65	531.94	0.69807	0.6291	5.95E-02	67.88	3.76	96.24	0.00	24.32	75.68
		600	884.56	630.26	0.69807	0.6267	4.66E-02	71.74	5.41	94.59	0.00	30.80	69.20
		450	856.58	450.00	0.74227	0.6322	7.32E-02	88.51	0.25	99.75	0.00	20.25	79.75
	2.00	510	914.40	514.46	0.74227	0.6328	7.34E-02	89.46	1.72	98.28	0.00	23.44	76.56
		600	1013.27	638.43	0.74227	0.6310	6.75E-02	99.24	9.17	90.83	0.00	27.19	72.81
1.5		450	614.94	451.91	0.66589	0.6258	4.93E-02	44.32	0.19	99.81	0.01	19.67	80.32
	1.0	510	673.49	516.25	0.66589	0.6261	4.72E-02	51.02	1.70	98.30	0.00	21.20	78.80
		600	769.00	618.28	0.66589	0.6252	3.33E-02	63.46	2.84	97.16	0.02	25.98	74.00
		450	723.66	450.00	0.69807	0.6282	5.90E-02	66.65	0.21	99.79	0.00	18.87	81.12
	1.5	510	781.99	532.59	0.69807	0.6286	5.89E-02	68.35	2.64	97.36	0.00	21.98	78.02
		600	884.68	631.26	0.69807	0.6263	4.60E-02	73.06	4.80	95.20	0.00	27.89	72.11
		450	856.97	450.00	0.74227	0.6315	7.23E-02	89.03	0.24	99.76	0.00	18.48	81.52
	2.00	510	914.69	514.54	0.74227	0.6321	7.25E-02	89.90	1.61	98.39	0.00	21.51	78.48
		600	1013.35	638.70	0.74227	0.6305	6.70E-02	99.24	8.77	91.23	0.00	25.20	74.79
2		450	614.95	451.87	0.66589	0.6256	4.91E-02	44.50	0.16	99.84	0.01	18.47	81.52
	1.0	510	673.54	516.35	0.66589	0.6259	4.72E-02	52.44	1.31	98.69	0.00	19.33	80.67
		600	769.24	618.29	0.66589	0.6250	3.31E-02	66.08	2.64	97.36	0.02	23.70	76.28
		450	723.69	450.00	0.69807	0.6279	5.87E-02	66.88	0.19	99.81	0.00	17.84	82.16
	1.5	510	781.99	532.68	0.69807	0.6284	5.86E-02	68.45	2.48	97.52	0.00	20.84	79.15
		600	884.79	631.65	0.69807	0.6262	4.59E-02	75.85	4.20	95.80	0.00	25.54	74.46
		450	857.12	450.00	0.74227	0.6311	7.17E-02	89.38	0.21	99.79	0.00	17.36	**82.64**
	2.00	510	914.75	514.68	0.74227	0.6318	7.21E-02	90.03	1.48	98.52	0.00	20.49	79.51
		600	1013.37	640.43	0.74227	0.6303	6.68E-02	99.13	8.48	91.52	0.00	24.08	75.91

TABLE A.8 Selectivities of modified three phase model for the Case C.

CASE D OF TWO-PHASE MODEL

CO conversion and CO_2 selectivity were increased with higher temperature and pressure, while hydrocarbon selectivity was decreased. In addition, C5+ selectivity also was decreased with increasing temperature and pressure. The best result for higher selectivity of C5+ was the conditions; 1MPa, 1 H_2/CO ratio and 450K.

P [MPa]	H_2/CO ratio	T [K] In	Out[1]	Out[2]	Out[3]	M/F[kgmole/h] In	Out[1]	Out[2]	Out[3]	Conversion[%] CO	CO2	HC	Selectivity[%] CH4	C2-C4	C5+
1		450	609.53	450.00	594.14	0.66747	0.3156	0.0272	0.3428	40.04	0.02	99.98	0.00	49.81	**50.189**
	1	510	668.24	512.73	652.83	0.66747	0.3156	0.0272	0.3427	40.17	0.25	99.75	0.00	49.82	50.182
		600	756.78	660.20	746.58	0.66747	0.3155	0.0195	0.3254	69.91	1.79	98.21	0.00	49.82	50.181
		450	714.70	450.00	681.62	0.69966	0.3183	0.0341	0.3524	60.07	0.03	99.97	0.00	49.82	50.184
	1.5	510	772.51	511.37	739.30	0.69966	0.3183	0.0341	0.3523	60.28	0.28	99.72	0.00	49.82	50.178
		600	860.76	662.91	829.63	0.69966	0.3181	0.0330	0.3500	64.35	2.77	97.23	0.00	49.82	50.176
		450	845.12	450.05	782.84	0.74386	0.3219	0.0434	0.3653	80.73	0.08	99.92	0.00	49.82	50.181
	2	510	900.98	510.04	837.86	0.74386	0.3220	0.0435	0.3654	80.48	0.37	99.63	0.00	49.82	50.179
		600	989.30	615.13	927.72	0.74386	0.3216	0.0425	0.3635	83.76	3.15	96.85	0.02	49.82	50.168
1.5		450	609.30	450.00	593.84	0.66747	0.3156	0.0272	0.3428	40.04	0.02	99.98	0.00	49.81	50.187
	1	510	668.10	514.05	652.67	0.66747	0.3156	0.0272	0.3427	40.23	0.36	99.64	0.00	49.82	50.179
		600	756.74	662.85	746.83	0.66747	0.3155	0.0194	0.3252	70.35	1.82	98.18	0.00	49.82	50.178
		450	714.41	450.00	681.18	0.69966	0.3183	0.0341	0.3524	60.08	0.05	99.95	0.00	49.82	50.183
	1.5	510	772.41	511.99	739.18	0.69966	0.3183	0.0340	0.3523	60.39	0.41	99.59	0.00	49.82	50.179
		600	860.88	735.11	829.54	0.69966	0.3180	0.0319	0.3477	64.35	2.77	97.23	0.00	49.82	50.176
		450	843.89	450.00	780.98	0.74386	0.3220	0.0436	0.3656	80.16	0.09	99.91	0.00	49.82	50.179
	2	510	900.15	511.24	837.85	0.74386	0.3220	0.0434	0.3653	80.67	0.54	99.46	0.00	49.82	50.176
		600	989.32	622.28	927.18	0.74386	0.3215	0.0420	0.3627	85.25	4.34	95.66	0.02	49.82	50.165
2		450	609.07	450.00	593.55	0.66747	0.3156	0.0272	0.3428	40.04	0.03	99.97	0.00	49.82	50.181
	1	510	667.98	517.06	652.48	0.66747	0.3156	0.0272	0.3427	40.27	0.50	99.50	0.00	49.82	50.179
		600	756.26	665.57	746.33	0.66747	0.3155	0.0193	0.3252	70.46	2.01	97.99	0.00	49.82	50.178
		450	714.16	450.00	680.84	0.69966	0.3183	0.0341	0.3524	60.09	0.06	99.94	0.00	49.82	50.179
	1.5	510	772.29	512.58	739.06	0.69966	0.3183	0.0340	0.3522	60.49	0.53	99.47	0.00	49.82	50.178
		600	860.26	929.05	829.41	0.69966	0.3180	0.0292	0.3418	76.67	3.08	96.92	0.00	49.82	50.173
		450	843.61	450.00	780.21	0.74386	0.3220	0.0436	0.3656	80.17	0.10	99.90	0.00	49.82	50.178
	2	510	900.01	510.94	837.82	0.74386	0.3219	0.0434	0.3652	80.85	0.70	99.30	0.00	49.82	50.176
		600	989.17	628.84	927.01	0.74386	0.3213	0.0416	0.3619	86.55	5.35	94.65	0.02	49.82	50.163

TABLE A.9 Selectivities of modified two phase model for the Case D.

CASE D OF THREE-PHASE MODEL

CO conversion and CO₂ selectivity were increased with higher temperature and pressure, while hydrocarbon selectivity was decreased. In addition, C5+ selectivity also was decreased with increasing temperature and pressure. The best result for higher selectivity of C5+ was the conditions; 2MPa, 2 H₂/CO ratio and 450K.

P [MPa]	H₂/CO ratio	T [K] In	Out[1]	Out[2]	Out[3]	M/F[kgmole/h] In	Out[1]	Out[2]	Out[3]	Con. [%] CO	CO₂	Selectivity[%] HC	CH4	C2-C4	C5+
1		450	578.37	416.26	564.45	0.66747	0.31382	2.48E-02	3.39E-01	43.99	0.23	99.77	0.00	20.87	79.12
	1	510	637.05	524.85	629.06	0.66747	0.31397	1.73E-02	3.22E-01	72.00	2.77	97.23	0.01	21.72	78.27
		600	735.01	763.84	728.16	0.66747	0.3133	1.66E-02	3.22E-01	75.87	3.04	96.96	0.01	22.44	77.55
		450	686.85	415.11	658.45	0.69966	0.31512	2.98E-02	3.45E-01	66.38	0.38	99.62	0.00	20.81	79.19
	1.5	510	745.76	507.98	719.48	0.69966	0.31527	2.95E-02	3.44E-01	68.94	2.85	97.15	0.00	21.65	78.35
		600	853.54	671.81	831.08	0.69966	0.31366	2.27E-02	0.331927	90.92	3.28	96.72	0.00	22.26	77.74
		450	819.92	414.00	734.99	0.74386	0.31688	3.66E-02	0.35337	88.78	0.46	99.54	0.00	20.25	79.75
	2	510	878.72	479.34	827.12	0.74386	0.31707	3.64E-02	0.353062	90.89	4.43	95.57	0.00	23.84	76.16
		600	978.25	590.53	922.54	0.74386	0.31603	3.34E-02	0.348878	98.99	9.02	90.98	0.00	27.19	72.81
1.5		450	578.57	416.61	564.79	0.66747	0.31367	2.46E-02	0.338278	44.34	0.21	99.79	0.00	19.67	80.33
	1	510	637.33	524.96	629.63	0.66747	0.31382	1.71E-02	0.321873	72.19	2.74	97.26	0.01	20.10	79.89
		600	735.63	764.12	729.33	0.66747	0.31313	1.63E-02	0.321188	76.23	3.03	96.97	0.01	21.18	78.81
		450	687.14	415.14	659.11	0.69966	0.31489	2.95E-02	0.344315	66.82	0.37	99.63	0.01	19.75	80.25
	1.5	510	746.01	509.46	720.34	0.69966	0.31504	2.92E-02	0.343472	69.41	2.83	97.17	0.00	20.95	79.05
		600	853.58	677.28	846.23	0.69966	0.31346	2.58E-02	0.336874	86.47	3.26	96.74	0.00	21.93	78.06
		450	820.3	414.02	735.26	0.74386	0.31655	3.61E-02	0.352638	89.18	0.35	99.65	0.00	18.48	81.51
	2	510	878.94	479.65	827.23	0.74386	0.31675	3.60E-02	0.352322	91.27	4.40	95.60	0.00	21.91	78.09
		600	978.43	590.94	923.35	0.74386	0.31578	3.31E-02	0.348348	99.00	8.63	91.37	0.00	25.20	74.79
2		450	578.58	416.68	564.81	0.66747	0.31359	2.45E-02	0.338083	44.85	0.19	99.81	0.01	18.38	81.61
	1	510	637.38	525.13	629.82	0.66747	0.31374	1.70E-02	0.321701	72.90	27.64	72.36	0.01	19.33	80.65
		600	735.93	764.23	729.65	0.66747	0.31307	1.63E-02	0.321035	76.22	2.92	97.08	0.01	20.75	79.24
		450	687.16	415.23	659.52	0.69966	0.31476	2.93E-02	0.344047	66.99	0.30	99.70	0.01	19.27	80.72
	1.5	510	746.06	510.95	720.59	0.69966	0.31492	2.90E-02	0.343268	69.45	2.81	97.19	0.00	20.71	79.29
		600	853.62	679.27	846.35	0.69966	0.31343	2.24E-02	0.331359	90.83	3.24	96.76	0.00	21.08	78.92
		450	820.44	414.03	735.35	0.74386	0.31632	3.58E-02	0.352153	89.47	0.28	99.72	0.00	17.36	**82.64**
	2	510	879.01	479.85	827.35	0.74386	0.3166	3.58E-02	0.352017	91.32	4.37	95.63	0.00	20.91	79.09
		600	978.62	593.45	923.55	0.74386	0.31569	3.30E-02	0.348102	98.89	8.33	91.67	0.00	24.08	75.91

TABLE A.10 Selectivities of modified three phase model for the Case D.

CASE E OF TWO-PHASE MODEL

CO conversion and CO_2 selectivity were increased with higher temperature and pressure, while hydrocarbon selectivity was decreased. In addition, C5+ selectivity also was decreased with increasing temperature and pressure. The best result for higher selectivity of C5+ was the conditions; 1MPa, 1 H_2/CO ratio and 450K.

P [MPa]	H_2/CO ratio	T [K]				M/F [kgmole/h]				Conversion [%]			Selectivity [%]		
		In	Out[1]	Out[2]	Out[3]	In	Out[1]	Out[2]	Out[3]	CO	CO2	HC	CH4	C2-C4	C5+
1		450	609.53	594.55	581.16	0.66747	0.20827	2.33E-01	2.45E-01	40.04	0.02	99.98	0.00	49.82	**50.182**
	1	510	668.27	653.28	639.93	0.66747	0.20827	2.33E-01	2.45E-01	40.15	0.21	99.79	0.00	49.82	50.181
		600	757.14	743.43	731.44	0.66747	0.20822	2.32E-01	2.44E-01	41.76	2.95	97.05	0.00	49.82	50.180
		450	714.71	682.48	655.44	0.69966	0.21007	2.39E-01	2.56E-01	60.09	0.06	99.94	0.00	49.82	50.180
	1.5	510	772.63	740.34	713.31	0.69966	0.21005	2.39E-01	2.56E-01	60.40	0.42	99.58	0.00	49.82	50.179
		600	861.84	832.21	806.84	0.69966	0.2099	2.38E-01	0.253944	63.85	4.25	95.75	0.00	49.82	50.178
		450	845.66	785.04	734.85	0.74386	0.21245	2.47E-01	0.270285	81.13	0.94	99.06	0.00	49.82	50.178
	2	510	901.29	839.83	792.16	0.74386	0.21249	2.48E-01	0.270542	80.74	0.60	99.40	0.00	49.82	50.176
		600	991.38	932.14	885.04	0.74386	0.21216	2.46E-01	0.267798	85.25	4.35	95.65	0.01	49.81	50.171
1.5		450	609.3	594.26	580.82	0.66747	0.20827	2.33E-01	0.244748	40.04	0.03	99.97	0.00	49.82	50.179
	1	510	668.14	653.15	639.95	0.66747	0.20827	0.232526	0.244686	40.20	0.31	99.69	0.00	49.82	50.178
		600	757.11	743.32	733.1	0.66747	0.2082	0.232165	0.24374	42.55	4.22	95.78	0.00	49.82	50.178
		450	714.5	682.21	655.45	0.69966	0.21006	0.238936	0.255748	60.14	0.12	99.88	0.00	49.82	50.182
	1.5	510	772.57	740.32	713.31	0.69966	0.21004	0.238847	0.255543	60.56	0.61	99.39	0.00	49.82	50.177
		600	863.13	834.62	810.38	0.69966	0.20982	0.237823	0.253132	65.51	5.08	94.92	0.00	49.82	50.176
		450	843.98	782.63	734.98	0.74386	0.21253	0.247703	0.270861	80.22	0.14	99.86	0.00	49.82	50.177
	2	510	901.1	839.78	792.23	0.74386	0.21246	0.247456	0.270359	81.04	0.86	99.14	0.01	49.82	50.173
		600	991.32	932.01	888.46	0.74386	0.21201	0.245629	0.266629	87.13	5.79	94.21	0.02	49.82	50.168
2		450	609.07	593.96	580.24	0.66747	0.20827	0.23255	0.244749	40.04	0.03	99.97	0.00	49.82	50.176
	1	510	668.01	653.02	640.14	0.66747	0.20827	0.232517	0.244664	40.26	0.40	99.60	0.00	49.82	50.176
		600	757.01	745.24	734.82	0.66747	0.20817	0.232048	0.243434	43.30	5.39	94.61	0.00	49.82	50.177
		450	714.19	681.82	655.54	0.69966	0.21007	0.23894	0.255756	60.13	0.10	99.90	0.00	49.83	50.174
	1.5	510	772.51	740.27	713.35	0.69966	0.21004	0.238813	0.255468	60.72	0.79	99.21	0.00	49.83	50.174
		600	864.34	834.52	813.57	0.69966	0.20975	0.237495	0.252374	67.05	6.20	93.80	0.00	49.83	50.166
		450	843.72	764.07	735.12	0.74386	0.21252	0.247694	0.270855	80.22	0.14	99.86	0.00	49.83	50.174
	2	510	900.89	839.71	792.3	0.74386	0.21244	0.24737	0.270186	81.31	1.10	98.90	0.01	49.82	50.170
		600	990.99	931.97	891.16	0.74386	0.21187	0.245115	0.265649	88.68	6.93	93.07	0.02	49.82	50.165

TABLE A.11 Selectivities of modified two phase model for the Case E.

CO conversion and CO_2 selectivity were increased with higher temperature and pressure, while hydrocarbon selectivity was decreased. In addition, C5+ selectivity also was decreased with increasing temperature and pressure. The best result for higher selectivity of C5+ was the conditions; 2MPa, 2 H_2/CO ratio and 450K.

P [MPa]	H_2/CO ratio	T [K]				M/F[kgmole/h]				Conversion[%]		Selectivity [%]			
		In	Out[1]	Out[2]	Out[3]	In	Out[1]	Out[2]	Out[3]	CO	CO2	HC	CH4	C2-C4	C5+
1	1	450	614.42	600.9	588.52	0.66747	0.20712	2.30E-01	2.40E-01	44.03	0.28	99.72	0.01	20.87	79.115
		510	673.48	661.34	650.26	0.66747	0.2072	2.30E-01	2.40E-01	45.37	3.32	96.68	0.00	21.21	78.783
		600	776.75	788.04	798.94	0.66747	0.20647	0.22588	2.30E-01	70.96	6.30	93.70	0.01	22.31	77.680
	1.5	450	723.7	696.13	673.04	0.69966	0.20812	0.234081	2.48E-01	67.65	0.61	99.39	0.00	20.51	79.488
		510	783.21	758.78	737.01	0.69966	0.208	0.233507	2.46E-01	70.38	4.74	95.26	0.00	21.05	78.949
		600	898.75	891.14	869.59	0.69966	0.20647	0.227168	2.34E-01	94.80	6.43	93.57	0.00	22.00	77.996
	2	450	856.34	772.85	763.46	0.74386	0.20912	0.239467	2.58E-01	89.19	0.78	99.22	0.00	20.25	79.750
		510	916.92	867.36	825.01	0.74386	0.20913	0.238963	2.56E-01	92.75	4.87	95.13	0.00	20.72	79.282
		600	1017	962.92	916.7	0.74386	0.20841	2.37E-01	0.252541	99.64	9.41	90.59	0.00	21.15	78.852
1.5	1	450	614.61	601.24	588.97	0.66747	0.20702	0.229553	2.40E-01	44.38	0.25	99.75	0.00	19.67	80.327
		510	673.78	661.92	651.27	0.66747	0.2071	0.22957	0.239714	45.86	3.26	96.74	0.01	20.83	79.157
		600	777.53	789.25	801.78	0.66747	0.20634	0.225472	0.228959	72.16	6.25	93.75	0.01	21.69	78.303
	1.5	450	723.85	696.21	673.05	0.69966	0.20782	0.233512	0.247128	67.10	0.51	99.49	0.00	18.84	81.153
		510	783.55	759.6	738.28	0.69966	0.20784	0.23313	0.245789	70.84	4.64	95.36	0.00	20.77	79.228
		600	898.85	891.66	870.66	0.69966	0.20633	0.226854	0.233231	94.97	6.32	93.68	0.00	21.37	78.630
	2	450	856.7	773.72	763.85	0.74386	0.2089	0.238994	0.257148	89.36	0.69	99.31	0.00	18.52	81.476
		510	917.02	868.44	826.44	0.74386	0.20893	0.23849	0.255643	93.06	4.65	95.35	0.00	19.71	80.291
		600	1017	963.52	917.95	0.74386	0.20825	0.236163	0.251999	99.65	9.02	90.98	0.00	20.17	79.829
2	1	450	614.62	601.27	589.15	0.66747	0.20697	2.29E-01	0.239822	44.49	0.19	99.81	0.00	18.48	81.512
		510	673.82	661.96	651.35	0.66747	0.20704	0.22944	0.239515	46.00	3.17	96.83	0.00	20.53	79.472
		600	777.98	789.06	801.88	0.66747	0.20631	0.225447	0.228986	71.75	6.21	93.79	0.01	21.21	78.780
	1.5	450	723.92	696.32	673.09	0.69966	0.20773	0.233337	0.24691	67.14	0.45	99.55	0.00	17.84	82.156
		510	783.65	759.78	738.3	0.69966	0.20777	0.232978	0.245586	70.84	4.55	95.45	0.00	20.52	79.478
		600	898.95	891.99	870.67	0.69966	0.20633	0.226911	0.233287	94.56	6.05	93.95	0.00	20.86	79.133
	2	450	856.8	774.54	763.99	0.74386	0.20875	0.238681	0.256703	89.24	0.58	99.42	0.00	17.46	**82.541**
		510	917.52	868.65	826.45	0.74386	0.20883	0.238309	0.255398	93.01	4.49	95.51	0.00	18.87	81.131
		600	1017.3	963.69	918.43	0.74386	0.20818	0.236004	0.251736	99.59	8.76	91.24	0.00	19.23	80.770

TABLE A.12 Selectivities of modified three phase model for the Case E.

CASE F OF TWO-PHASE MODEL

CO conversion and CO_2 selectivity were increased with higher temperature however, they were decreased with increasing pressure, In addition, hydrocarbon selectivity was decreased and C5+ selectivity also was decreased with increasing temperature and increased with increaseing pressure. The best result for higher selectivity of C5+ was the conditions; 2MPa, 1 H_2/CO ratio and 450K.

P [MPa]	H_2/CO ratio	T [K]		M/F[kgmole/h]		Conversion[%]		Selectivity [%]			
		In	Out	In	Out	CO	CO2	HC	CH4	C2-C4	C5+
1	1	450	586.60	1.1070	1.0573	100	0.00	100.00	0.00	30.98	69.02
		510	645.18	1.1013	1.0575	100	0.03	99.97	0.00	31.56	68.44
		600	733.82	1.1097	1.0570	100	0.42	99.58	0.00	31.81	68.19
	1.5	450	657.95	1.1514	1.0678	100	0.01	99.99	0.00	39.69	60.31
		510	715.83	1.1513	1.0677	100	0.04	99.96	0.00	40.43	59.57
		600	800.08	0.0683	1.0669	100	0.53	99.47	0.00	41.27	58.73
	1.77	450	692.73	1.17321	1.07336	100	0.02	99.98	0.00	42.65	57.34
		510	749.95	1.17325	1.07342	100	0.13	99.87	0.00	42.82	57.18
		600	837.15	1.17278	1.07265	100	0.71	99.29	0.00	43.12	56.88
1.5	1	450	586.39	1.10977	1.05722	100	0.01	99.99	0.00	30.87	69.13
		510	645.18	1.1098	1.05725	100	0.05	99.95	0.00	31.01	68.99
		600	733.78	1.10951	1.05676	100	0.65	99.35	0.00	31.53	68.47
	1.5	450	657.66	1.15134	1.06775	100	0.01	99.99	0.00	39.30	60.70
		510	712.29	1.14948	1.06735	100	0.09	99.91	0.00	39.96	60.04
		600	799.98	1.14897	1.06648	100	1.09	98.91	0.00	40.15	59.84
	1.77	450	692.22	1.1733	1.07349	100	0.04	99.96	0.00	42.76	57.24
		510	749.78	1.17322	1.07337	100	0.18	99.82	0.00	43.00	57.00
		600	836.95	1.1706	1.07208	100	1.18	98.82	0.01	43.67	56.33
2	1	450	586.09	1.10993	1.05738	100	0.01	99.99	0.00	30.77	**69.23**
		510	645.06	1.10973	1.05717	100	0.07	99.93	0.00	31.43	68.57
		600	734.06	1.10974	1.05693	100	0.82	99.18	0.00	31.72	68.28
	1.5	450	653.96	1.14955	1.06745	100	0.03	99.97	0.00	38.93	61.07
		510	712.12	1.14947	1.06734	100	0.11	99.89	0.00	39.59	60.40
		600	799.87	1.1487	1.0661	100	1.74	98.26	0.02	41.21	58.77
	1.77	450	691.91	1.17329	1.07348	100	0.05	99.95	0.00	42.99	57.01
		510	749.57	1.1732	1.07334	100	0.23	99.77	0.00	43.29	56.71
		600	836.65	1.17282	1.07242	100	1.39	98.61	0.00	44.36	55.64

TABLE A.13 Selectivities of modified two phase model for the Case F.

CASE F OF THREE-PHASE MODEL

For recycling and co-feeding to reformer, the best result of Case F was 86.70% for heavy hydrocarbons both three-phase under condition; 2MPa, 1H$_2$/CO ratio and 450K, respectively.

CO conversion and CO$_2$ selectivity were increased with higher temperature and pressure, In addition, hydrocarbon selectivity was decreased.

P [MPa]	H$_2$/CO ratio	T [K] In	T [K] Out	M/F[kgmole/h] In	M/F[kgmole/h] Out	Conversion[%] CO	Conversion[%] CO2	Selectivity [%] HC	Selectivity [%] CH4	Selectivity [%] C2-C4	Selectivity [%] C5+
1	1	450	589.02	1.1040	1.0476	100	0.04	99.96	0.01	14.54	85.46
		510	647.46	1.1044	1.0485	100	0.51	99.49	0.00	16.60	83.40
		600	736.33	1.1009	1.0461	100	6.02	93.98	0.00	20.12	79.88
	1.5	450	656.77	1.1384	1.0513	100	0.08	99.92	0.00	17.11	82.89
		510	710.75	1.1373	1.0525	100	0.63	99.37	0.01	20.11	79.88
		600	798.77	1.1330	1.0497	100	6.13	93.87	0.00	23.95	76.05
	1.77	450	703.96	1.16406	1.05408	100	0.11	99.89	0.00	18.62	81.38
		510	760.5	1.16484	1.05575	100	0.75	99.25	0.00	21.58	78.42
		600	851.57	1.16444	1.05453	100	6.29	93.71	0.00	26.37	73.63
1.5	1	450	589.26	1.10367	1.04688	100	0.06	99.94	0.01	13.32	86.67
		510	647.79	1.10407	1.04773	100	0.55	99.45	0.00	15.43	84.57
		600	736.93	1.10056	1.04523	100	6.18	93.82	0.00	18.55	81.44
	1.5	450	656.99	1.13977	1.05052	100	0.09	99.91	0.00	16.02	83.97
		510	712.58	1.1386	1.05163	100	0.72	99.28	0.01	18.56	81.44
		600	802.56	1.13424	1.04881	100	6.29	93.71	0.00	22.34	77.66
	1.77	450	704.54	1.16345	1.0528	100	0.18	99.82	0.00	17.08	82.92
		510	761.15	1.1642	1.05444	100	0.82	99.18	0.00	19.90	80.10
		600	851.84	1.16162	1.05298	100	6.42	93.58	0.00	24.30	75.70
2	1	450	592.13	1.10478	1.04654	100	0.07	99.93	0.01	12.57	**87.42**
		510	650.71	1.10517	1.04737	100	0.60	99.40	0.00	14.62	85.38
		600	742.66	1.10292	1.04492	100	6.24	93.76	0.00	18.07	81.93
	1.5	450	657.22	1.13765	1.04969	100	0.10	99.90	0.00	15.00	85.00
		510	714.84	1.13829	1.051	100	0.86	99.14	0.01	17.62	82.37
		600	802.26	1.13406	1.04847	100	6.48	93.52	0.00	21.46	78.54
	1.77	450	704.82	1.16307	1.05195	100	0.24	99.76	0.00	16.60	83.40
		510	761.34	1.16388	1.05377	100	0.92	99.08	0.01	18.68	81.31
		600	852.02	1.16378	1.05305	100	6.63	93.37	0.00	22.60	77.40

TABLE A.14 Selectivities of modified three phase model for the Case F.

CASE G FOR TWO-PHASE MODEL

CO conversion and CO_2 selectivity were increased with higher temperature however, they were decreased with increasing pressure. In addition, hydrocarbon selectivity was decreased. C5+ selectivity also was decreased with increasing temperature and increased with increaseing pressure. The best result for higher selectivity of C5+ was the conditions; 1MPa, 1 H_2/CO ratio and 450K.

P [MPa]	H_2/CO ratio	T [K] In	T [K] Out	M/F[kgmole/h] In	M/F[kgmole/h] Out	Conversion[%] CO	Conversion[%] CO2	Selectivity [%] HC	Selectivity [%] CH4	Selectivity [%] C2-C4	Selectivity [%] C5+
1	1	450	586.608	1.110	1.057	100	0.01	99.99	0.00	31.07	**68.93**
		510	645.264	1.110	1.057	100	0.03	99.97	0.00	31.09	68.91
		600	731.027	1.109	1.057	100	0.47	99.53	0.00	31.65	68.35
	1.5	450	654.554	1.150	1.067	100	0.01	99.99	0.00	39.30	60.70
		510	712.328	1.150	1.068	100	0.06	99.94	0.00	39.64	60.36
		600	799.941	1.150	1.067	100	0.68	99.32	0.00	39.90	60.10
	1.77	450	692.731	1.173	1.073	100	0.02	99.98	0.00	41.78	58.22
		510	749.953	1.173	1.073	100	0.13	99.87	0.00	42.82	57.18
		600	836.908	1.173	1.073	100	0.76	99.24	0.00	43.26	56.73
1.5	1	450	586.341	1.110	1.057	100	0.01	99.99	0.00	31.34	68.66
		510	642.413	1.109	1.057	100	0.04	99.96	0.00	31.36	68.64
		600	730.851	1.110	1.057	100	0.61	99.39	0.00	31.75	68.25
	1.5	450	654.417	1.150	1.068	100	0.01	99.99	0.00	39.27	60.73
		510	712.287	1.149	1.067	100	0.09	99.91	0.00	39.30	60.70
		600	799.719	1.149	1.067	100	0.98	99.02	0.00	40.18	59.81
	1.77	450	691.658	1.173	1.073	100	0.03	99.97	0.00	42.76	57.24
		510	749.780	1.173	1.073	100	0.18	99.82	0.00	42.88	57.11
		600	835.467	1.172	1.072	100	1.17	98.83	0.01	43.44	56.56
2	1	450	586.122	1.110	1.057	100	0.01	99.99	0.00	31.45	68.55
		510	642.382	1.110	1.057	100	0.06	99.94	0.00	31.83	68.17
		600	730.786	1.109	1.057	100	0.80	99.20	0.00	32.15	67.85
	1.5	450	653.963	1.150	1.067	100	0.03	99.97	0.00	39.33	60.67
		510	712.123	1.149	1.067	100	0.11	99.89	0.00	39.38	60.62
		600	799.688	1.149	1.066	100	1.31	98.69	0.00	40.06	59.93
	1.77	450	691.523	1.173	1.073	100	0.05	99.95	0.00	42.80	57.20
		510	749.569	1.173	1.073	100	0.23	99.77	0.00	42.95	57.05
		600	835.325	1.172	1.072	100	1.30	98.70	0.00	43.40	56.60

TABLE A.15 Selectivities of modified two phase model for the Case G.

CASE G FOR THREE-PHASE MODEL

CO conversion and CO_2 selectivity were increased with higher temperature and pressure. In addition, hydrocarbon selectivity was decreased. C5+ selectivity also was decreased with increasing temperature and increased with increasing pressure.

Case H gained higher selectivity of hydrocarbons and the best conditions were 2.0MPa, 1 H_2/CO ratio and 450K.

P [Mpa]	H_2/CO ratio	T [K] In	T [K] Out	M/F[kgmole/h] In	M/F[kgmole/h] Out	Conversion [%] CO	Conversion [%] CO_2	Selectivity[%] HC	Selectivity[%] CH4	Selectivity[%] C2-C4	Selectivity[%] C5+
1		450	586.23	1.10269	1.04752	100	0.04	99.96	0.01	2.40	97.59
	1.0	510	647.42	1.10449	1.04858	100	0.53	99.47	0.00	2.54	97.46
		600	737.76	1.10159	1.04611	100	6.10	93.90	0.00	2.66	97.33
		450	660	1.14032	1.05167	100	0.05	99.95	0.00	3.02	96.98
	1.5	510	720.93	1.14288	1.05327	100	0.63	99.37	0.00	3.17	96.83
		600	802.13	1.13476	1.04985	100	6.50	93.50	0.00	3.35	96.65
		450	703.96	1.16406	1.05408	100	0.07	99.93	0.00	3.23	96.77
	2.0	510	760.5	1.16484	1.05575	100	0.75	99.25	0.00	3.42	96.58
		600	851.57	1.16444	1.05453	100	13.89	86.11	0.00	4.04	95.96
1.5		450	592.07	1.105	1.04699	100	0.05	99.95	0.01	2.37	99.90
	1.0	510	647.83	1.10402	1.04768	100	0.53	99.47	0.00	2.45	99.90
		600	739.74	1.1018	1.04524	100	6.37	93.63	0.00	2.55	99.88
		450	661.04	1.13797	1.05033	100	0.07	99.93	0.00	2.85	99.85
	1.5	510	721.26	1.13858	1.05161	100	0.72	99.28	0.01	3.03	99.84
		600	803.25	1.13253	1.04866	100	6.64	93.36	0.00	3.09	99.83
		450	704.25	1.16347	1.05284	100	0.07	99.93	0.00	3.08	99.82
	2.0	510	761.15	1.1642	1.05444	100	0.83	99.17	0.00	3.30	99.80
		600	852.18	1.16274	1.05319	100	14.14	85.86	0.00	3.45	99.76
2		450	592.13	1.10478	1.04654	100	0.06	99.94	0.01	2.27	**99.90**
	1.0	510	650.71	1.10517	1.04737	100	0.54	99.46	0.00	2.43	99.90
		600	739.87	1.10161	1.04487	100	6.65	93.35	0.00	2.55	99.88
		450	661.16	1.13769	1.04973	100	0.08	99.92	0.00	2.78	99.85
	1.5	510	721.69	1.13829	1.051	100	0.86	99.14	0.01	2.98	99.84
		600	803.25	1.13406	1.04847	100	6.73	93.27	0.00	3.08	99.83
		450	704.82	1.16307	1.05195	100	0.09	99.91	0.00	2.97	99.82
	2.0	510	761.25	1.16417	1.05405	100	0.99	99.01	0.00	3.20	99.81
		600	852.84	1.16247	1.05268	100	15.55	84.45	0.00	3.41	99.76

TABLE A.16 Selectivities of modified three phase model for the Case G.

Case H for Two-phase Model

CO conversion and CO_2 selectivity were increased with higher temperature and pressure. In addition, hydrocarbon selectivity was decreased. C5+ selectivity also was decreased with increasing temperature and increased with increasing pressure.

Case H gained higher selectivity of hydrocarbons and the best conditions were 2.0MPa, 1 H_2/CO ratio and 600K.

P [MPa]	H_2/CO ratio	T [K] In	T [K] Out	M/F[kgmole/h] In	M/F[kgmole/h] Out	Conversion[%] CO	Conversion[%] CO2	Selectivity [%] HC	CH4	C2-C4	C5+
		450	586.60	1.1098	1.0573	100	0.00	100.00	0.00	31.09	68.91
	1	510	645.35	1.1097	1.0571	100	0.05	99.95	0.00	31.00	69.00
		600	733.86	1.1096	1.0569	100	0.42	99.58	0.00	30.91	69.09
		450	654.56	1.1495	1.0674	100	0.01	99.99	0.00	38.98	61.02
1	1.5	510	712.33	1.1497	1.0676	100	0.06	99.94	0.00	38.85	61.15
		600	798.40	1.1484	1.0668	100	0.77	99.23	0.00	38.78	61.22
		450	692.74	1.1732	1.0734	100	0.03	99.97	0.00	42.88	57.12
	1.77	510	749.96	1.1733	1.0734	100	0.13	99.87	0.00	42.82	57.18
		600	836.93	1.1729	1.0727	100	1.02	98.98	0.00	42.47	57.52
		450	586.39	1.1098	1.0572	100	0.01	99.99	0.00	31.01	68.99
	1	510	645.19	1.1098	1.0572	100	0.05	99.95	0.00	30.97	69.03
		600	733.82	1.1092	1.0566	100	0.65	99.35	0.00	30.92	69.08
		450	654.4	1.1493	1.0672	100	0.02	99.98	0.00	38.89	61.11
1.5	1.5	510	712.29	1.1495	1.0674	100	0.09	99.91	0.00	38.72	61.28
		600	798.34	1.1492	1.0667	100	0.97	99.03	0.00	38.63	61.37
		450	692.22	1.1733	1.0735	100	0.04	99.96	0.00	42.76	57.24
	1.77	510	749.79	1.1732	1.0734	100	0.18	99.82	0.00	42.68	57.32
		600	836.87	1.1727	1.0724	100	1.44	98.56	0.00	42.08	57.92
		450	645.01	1.1097	1.0572	100	0.02	99.98	0.00	30.91	69.09
	1	510	645.06	1.1097	1.0572	100	0.07	99.93	0.00	30.88	69.12
		600	733.78	1.1095	1.0567	100	0.84	99.16	0.00	30.87	**69.13**
		450	653.96	1.1496	1.0675	100	0.03	99.97	0.00	38.76	61.24
2	1.5	510	712.12	1.1495	1.0673	100	0.11	99.89	0.00	38.68	61.32
		600	798.25	1.1490	1.0664	100	1.43	98.57	0.00	38.58	61.42
		450	691.9	1.1733	1.0735	100	0.05	99.95	0.00	42.61	57.39
	1.77	510	749.61	1.1731	1.0732	100	0.30	99.70	0.00	42.52	57.48
		600	836.79	1.1727	1.0723	100	1.49	98.51	0.00	41.60	58.40

TABLE A.17 Selectivities of modified two phase model for the Case H.

CASE H FOR THREE-PHASE MODEL

CO conversion and CO_2 selectivity were increased with higher temperature and pressure. In addition, hydrocarbon selectivity was decreased. C5+ selectivity also was decreased with increasing temperature and increased with increasing pressure.

The condition for the best results 87.42% was 2.0MPa, 1 H_2/CO ratio and 450K.

P [Mpa]	H_2/CO ratio	T [K] In	T [K] Out	M/F[kgmole/h] In	M/F[kgmole/h] Out	Conversion [%] CO	Conversion [%] CO_2	HC	Selectivity[%] CH_4	Selectivity[%] C2-C4	Selectivity[%] C5+
1		450	588.97	1.10406	1.0477	100	0.05	99.95	0.01	14.72	85.27
	1.0	510	650.22	1.10582	1.04871	100	0.53	99.47	0.00	16.93	83.07
		600	739.08	1.10248	1.04639	100	6.26	93.74	0.00	20.98	79.01
		450	656.6	1.13851	1.05145	100	0.09	99.91	0.00	17.49	82.51
	1.5	510	714.16	1.13917	1.05277	100	0.68	99.32	0.00	20.04	79.96
		600	802.05	1.13479	1.04989	100	6.42	93.58	0.00	24.23	75.77
		450	703.96	1.16406	1.05408	100	0.12	99.88	0.00	19.47	80.53
	2.0	510	760.51	1.16484	1.05575	100	0.75	99.25	0.00	22.25	77.75
		600	851.77	1.16479	1.0548	100	6.67	93.33	0.00	26.55	73.45
1.5		450	592.05	1.10511	1.04711	100	0.05	99.95	0.01	13.50	86.49
	1.0	510	650.6	1.1054	1.04785	100	0.55	99.45	0.00	15.45	84.55
		600	739.99	1.1018	1.04523	100	6.31	93.69	0.00	18.86	81.13
		450	656.98	1.13859	1.05161	100	0.11	99.89	0.00	15.09	84.91
	1.5	510	714.69	1.13859	1.05161	100	0.72	99.28	0.00	18.50	81.49
		600	802.52	1.13426	1.04883	100	6.52	93.48	0.00	22.43	77.57
		450	704.54	1.16346	1.0528	100	0.13	99.87	0.00	18.74	81.26
	2.0	510	761.06	1.16449	1.05473	100	0.79	99.21	0.00	20.92	79.08
		600	851.92	1.16387	1.0534	100	6.76	93.24	0.00	24.75	75.25
2		450	597.58	1.10476	1.04648	100	0.06	99.94	0.01	12.57	**87.42**
	1.0	510	650.71	1.10517	1.04737	100	0.56	99.44	0.00	14.61	85.38
		600	740.58	1.10038	1.04487	100	6.48	93.52	0.01	17.51	82.49
		450	658.84	1.13767	1.04972	100	0.12	99.88	0.00	14.08	85.92
	1.5	510	714.85	1.13829	1.051	100	0.77	99.23	0.00	17.60	82.39
		600	802.96	1.13229	1.04825	100	6.71	93.29	0.00	20.84	79.16
		450	704.82	1.16307	1.05195	100	0.14	99.86	0.00	16.91	83.09
	2.0	510	761.25	1.1641	1.05399	100	0.85	99.15	0.00	19.22	80.78
		600	851.96	1.16396	1.05317	100	6.83	93.17	0.00	23.73	76.27

TABLE A.18 Selectivities of modified three phase model for the Case H.

CASE I FOR TWO-PHASE MODEL

CO conversion and CO_2 selectivity were increased with higher temperature while, CO conversion was decreased with increasing pressure. In addition, hydrocarbon selectivity was decreased. C5+ selectivity also was decreased with increasing temperature and increased with increasing pressure.

The condition for the best results 87.42% was 2.0MPa, 1 H_2/CO ratio and 450K.

P [MPa]	H_2/CO ratio	T [K] In	T [K] Out	M/F[kgmole/h] In	M/F[kgmole/h] Out	Conversion[%] CO	Conversion[%] CO_2	Selectivity[%] HC	Selectivity[%] CH_4	Selectivity[%] C2-C4	Selectivity[%] C5+
		450	586.55	1.1099	1.0574	100	0.00	100.00	0.00	31.23	68.77
	1	510	645.26	1.1100	1.0574	100	0.04	99.96	0.00	31.25	68.75
		600	733.75	1.1098	1.0571	100	0.47	99.53	0.00	31.43	68.57
		450	654.57	1.1495	1.0674	100	0.01	99.99	0.00	39.27	60.73
1	1.5	510	712.41	1.1496	1.0675	100	0.06	99.94	0.00	39.43	60.57
		600	798.45	1.1484	1.0668	100	0.66	99.34	0.00	39.46	60.54
		450	692.71	1.1732	1.073356	100	0.14	99.86	0.00	42.81	57.19
	1.77	510	749.95	1.17323	1.0734	100	0.09	99.91	0.00	42.78	57.22
		600	836.93	1.17295	1.0728	100	0.82	99.18	0.00	43.16	56.84
		450	586.34	1.10986	1.057317	100	0.01	99.99	0.00	31.21	68.79
	1	510	645.16	1.10986	1.057305	100	0.05	99.95	0.00	31.14	68.86
		600	733.64	1.10968	1.056924	100	0.63	99.37	0.00	31.25	68.75
		450	654.32	1.14942	1.067322	100	0.01	99.99	0.00	39.11	60.89
1.5	1.5	510	712.29	1.14948	1.067353	100	0.09	99.91	0.00	39.30	60.70
		600	798.36	1.14923	1.066742	100	0.96	99.04	0.00	39.66	60.34
		450	692.23	1.17326	1.073446	100	0.02	99.98	0.00	42.75	57.25
	1.77	510	749.74	1.17321	1.073359	100	0.13	99.87	0.00	42.80	57.20
		600	836.85	1.17282	1.072554	100	1.17	98.83	0.00	43.34	56.66
		450	586.26	1.10985	371.9534	100	0.02	99.98	0.00	31.09	**68.91**
	1	510	645.01	1.10984	1.057281	100	0.06	99.94	0.00	31.11	68.89
		600	733.51	1.10963	1.056818	100	0.82	99.18	0.00	31.32	68.68
		450	653.97	1.14952	1.067424	100	0.02	99.98	0.00	39.28	60.72
2	1.5	510	712.12	1.14947	1.067338	100	0.11	99.89	0.00	39.31	60.69
		600	798.27	1.14908	1.06647	100	1.32	98.68	0.00	39.79	60.21
		450	691.91	1.17325	1.073442	100	0.03	99.97	0.00	42.75	57.25
	1.77	510	749.59	1.17315	1.073286	100	0.20	99.80	0.00	42.85	57.15
		600	836.74	1.17278	1.072382	100	1.37	98.63	0.00	43.37	56.63

TABLE A.19 Selectivities of modified two phase model for the Case I.

CASE I FOR THREE-PHASE MODEL

CO conversion and CO_2 selectivity were increased with higher temperature and pressure. In addition, hydrocarbon selectivity was decreased. C5+ selectivity also was decreased with increasing temperature and increased with increasing pressure.

The condition for the best results 87.31% was 2.0MPa, 1 H_2/CO ratio and 450K.

P [Mpa]	H_2/CO ratio	T [K] In	T [K] Out	M/F[kgmole/h] In	M/F[kgmole/h] Out	Conversion [%] CO	Conversion [%] CO_2	Selectivity[%] HC	Selectivity[%] CH_4	Selectivity[%] C2-C4	Selectivity[%] C5+
1		450	591.8	1.1054	1.04782	100	0.05	99.95	0.00	14.78	85.22
	1.0	510	650.22	1.10582	1.04871	100	0.53	99.47	0.00	16.93	83.07
		600	739.29	1.10236	1.04625	100	5.96	94.04	0.00	20.21	79.79
		450	656.65	1.13847	1.05141	100	0.08	99.92	0.00	17.37	82.63
	1.5	510	713.2	1.13914	1.05274	100	0.57	99.43	0.00	18.74	81.26
		600	800.58	1.13383	1.04969	100	6.40	93.60	0.00	23.91	76.09
		450	703.96	1.16406	1.05408	100	0.11	99.89	0.00	18.77	81.23
	2.0	510	760.51	1.16484	1.05575	100	0.75	99.25	0.00	21.58	78.42
		600	851.7	1.16468	1.05467	100	6.95	93.05	0.00	26.41	73.59
1.5		450	592.09	1.105	1.04699	100	0.06	99.94	0.00	13.41	86.58
	1.0	510	650.6	1.1054	1.04784	100	0.55	99.45	0.00	15.45	84.55
		600	739.86	1.10191	1.04533	100	6.10	93.90	0.00	18.71	81.29
		450	657.09	1.13794	1.05031	100	0.08	99.92	0.00	15.85	84.15
	1.5	510	713.06	1.13769	1.0515	100	0.64	99.36	0.00	17.96	82.03
		600	802.66	1.13416	1.04872	100	6.68	93.32	0.00	22.29	77.71
		450	704.54	1.16345	1.0528	100	0.12	99.88	0.00	17.07	82.93
	2.0	510	761.52	1.16469	1.05525	100	0.88	99.12	0.00	21.36	78.63
		600	851.9	1.17282	1.07255	100	7.12	92.88	0.00	25.37	74.63
2		450	592.8	1.10476	1.04648	100	0.08	99.92	0.00	12.68	**87.31**
	1.0	510	650.71	1.10517	1.04737	100	0.56	99.44	0.00	14.61	85.38
		600	739.99	1.10172	1.04497	100	6.17	93.83	0.00	17.87	82.13
		450	657.18	1.13767	1.04972	100	0.08	99.92	0.00	15.06	84.94
	1.5	510	714.89	1.13828	1.05099	100	0.70	99.30	0.01	17.27	82.73
		600	802.99	1.13225	1.04821	100	6.88	93.12	0.00	20.85	79.15
		450	704.82	1.16307	1.05195	100	0.13	99.87	0.00	16.08	83.92
	2.0	510	761.65	1.16389	1.05377	100	0.98	99.02	0.00	18.94	81.06
		600	852.1	1.16383	1.05303	100	4.25	95.75	0.00	22.89	77.11

TABLE A.20 Selectivities of modified three phase model for the Case I.

CASE J FOR TWO-PHASE MODEL

CO conversion and CO_2 selectivity were increased with higher temperature while, CO conversion was decreased with increasing pressure. In addition, hydrocarbon selectivity was decreased. C5+ selectivity also was decreased with increasing temperature and increased with increasing pressure.

The condition for the best results 68.91% was 2.0MPa, 1 H_2/CO ratio and 450K.

P [MPa]	H_2/CO ratio	T [K] In	T [K] Out	M/F[kgmole/h] In	M/F[kgmole/h] Out	Conversion[%] CO	Conversion[%] CO_2	Selectivity[%] HC	Selectivity[%] CH_4	Selectivity[%] C2-C4	Selectivity[%] C5+
		450	586.55	1.1099	1.0574	100	0.00	100.00	0.00	31.23	68.77
	1	510	645.26	1.1100	1.0574	100	0.04	99.96	0.00	31.25	68.75
		600	733.75	1.1098	1.0571	100	0.47	99.53	0.00	31.43	68.57
		450	654.57	1.1495	1.0674	100	0.01	99.99	0.00	39.27	60.73
1	1.5	510	712.41	1.1496	1.0675	100	0.06	99.94	0.00	39.43	60.57
		600	798.45	1.1484	1.0668	100	0.66	99.34	0.00	39.46	60.54
		450	692.71	1.1732	1.0734	100	0.14	99.86	0.00	42.81	57.19
	1.77	510	749.95	1.17323	1.0734	100	0.09	99.91	0.00	42.78	57.22
		600	836.93	1.17295	1.0728	100	0.82	99.18	0.00	43.16	56.84
		450	586.34	1.10986	1.057317	100	0.01	99.99	0.00	31.21	68.79
	1	510	645.16	1.10986	1.057305	100	0.05	99.95	0.00	31.14	68.86
		600	733.64	1.10968	1.056924	100	0.63	99.37	0.00	31.25	68.75
		450	654.32	1.14942	1.067322	100	0.01	99.99	0.00	39.11	60.89
1.5	1.5	510	712.29	1.14948	1.067353	100	0.09	99.91	0.00	39.30	60.70
		600	798.36	1.14923	1.066742	100	0.96	99.04	0.00	39.66	60.34
		450	692.23	1.17326	1.073446	100	0.02	99.98	0.00	42.75	57.25
	1.77	510	749.74	1.17321	1.073359	100	0.13	99.87	0.00	42.80	57.20
		600	836.85	1.17282	1.072554	100	1.17	98.83	0.00	43.34	56.66
		450	586.26	1.10985	371.9534	100	0.02	99.98	0.00	31.09	**68.91**
	1	510	645.01	1.10984	1.057281	100	0.06	99.94	0.00	31.11	68.89
		600	733.51	1.10963	1.056818	100	0.82	99.18	0.00	31.32	68.68
		450	653.97	1.14952	1.067424	100	0.02	99.98	0.00	39.28	60.72
2	1.5	510	712.12	1.14947	1.067338	100	0.11	99.89	0.00	39.31	60.69
		600	798.27	1.14908	1.06647	100	1.32	98.68	0.00	39.79	60.21
		450	691.91	1.17325	1.073442	100	0.03	99.97	0.00	42.75	57.25
	1.77	510	749.59	1.17315	1.073286	100	0.20	99.80	0.00	42.85	57.15
		600	836.74	1.17278	1.072382	100	1.37	98.63	0.00	43.37	56.63

TABLE A.21 Selectivities of modified two phase model for the Case J.

CASE J FOR THREE-PHASE MODEL

CO conversion and CO_2 selectivity were increased with higher temperature and pressure. In addition, hydrocarbon selectivity was decreased. C5+ selectivity also was decreased with increasing temperature and increased with increasing pressure.

The condition for the best results 87.31% was 2.0MPa, 1 H_2/CO ratio and 450K.

P [Mpa]	H_2/CO ratio	T [K] In	T [K] Out	M/F[kgmole/h] In	M/F[kgmole/h] Out	Conversion [%] CO	Conversion [%] CO_2	HC	Selectivity[%] CH_4	Selectivity[%] C2-C4	Selectivity[%] C5+
1		450	591.8	1.1054	1.04782	100	0.05	99.95	0.00	14.78	85.22
	1.0	510	650.22	1.10582	1.04871	100	0.53	99.47	0.00	16.93	83.07
		600	739.29	1.10236	1.04625	100	5.96	94.04	0.00	20.21	79.79
		450	656.65	1.13847	1.05141	100	0.08	99.92	0.00	17.37	82.63
	1.5	510	713.2	1.13914	1.05274	100	0.57	99.43	0.00	18.74	81.26
		600	800.58	1.13383	1.04969	100	6.40	93.60	0.00	23.91	76.09
		450	703.96	1.16406	1.05408	100	0.11	99.89	0.00	18.77	81.23
	2.0	510	760.51	1.16484	1.05575	100	0.75	99.25	0.00	21.58	78.42
		600	851.7	1.16468	1.05467	100	6.95	93.05	0.00	26.41	73.59
1.5		450	592.09	1.105	1.04699	100	0.06	99.94	0.00	13.41	86.58
	1.0	510	650.6	1.1054	1.04784	100	0.55	99.45	0.00	15.45	84.55
		600	739.86	1.10191	1.04533	100	6.10	93.90	0.00	18.71	81.29
		450	657.09	1.13794	1.05031	100	0.08	99.92	0.00	15.85	84.15
	1.5	510	713.06	1.13769	1.0515	100	0.64	99.36	0.00	17.96	82.03
		600	802.66	1.13416	1.04872	100	6.68	93.32	0.00	22.29	77.71
		450	704.54	1.16345	1.0528	100	0.12	99.88	0.00	17.07	82.93
	2.0	510	761.52	1.16469	1.05525	100	0.88	99.12	0.00	21.36	78.63
		600	851.9	1.17282	1.07255	100	7.12	92.88	0.00	25.37	74.63
2		450	592.8	1.10476	1.04648	100	0.08	99.92	0.00	12.68	**87.31**
	1.0	510	650.71	1.10517	1.04737	100	0.56	99.44	0.00	14.61	85.38
		600	739.99	1.10172	1.04497	100	6.17	93.83	0.00	17.87	82.13
		450	657.18	1.13767	1.04972	100	0.08	99.92	0.00	15.06	84.94
	1.5	510	714.89	1.13828	1.05099	100	0.70	99.30	0.01	17.27	82.73
		600	802.99	1.13225	1.04821	100	6.88	93.12	0.00	20.85	79.15
		450	704.82	1.16307	1.05195	100	0.13	99.87	0.00	16.08	83.92
	2.0	510	761.65	1.16389	1.05377	100	0.98	99.02	0.00	18.94	81.06
		600	852.1	1.16383	1.05303	100	4.25	95.75	0.00	22.89	77.11

TABLE A.22 Selectivities of modified three phase model for the Case J

Appendix D

CAPITAL INVESTMENT OF CASE G

	Specific Itemised	Unit factor	Installation Ct	if	'1987 index Ci	'2010 Ci
Syntheis Gas production						
POX Reformer	304 stainless st, 1000 gal		10000	1.7	17000	29150
Heat Exchanger	Shell, tube 150psig, 16 ft tubes		900	1.61	1449	2484
Heater I	stainless st	1.62	170	1.52	418.6	718
Storage Tank (NG)	stainless, horizontal, 150psi	2	52	1.88	195.5	336
Separator I	304 stainless st, 1000 gal		100	1.7	170	292
Fischer-Tropsch Synthesis						
Cooler I	stainless st	1.62	170	1.52	418.6	718
F-T reactor PFR	304 stainless st, 1000 gal		100	1.7	170	292
Compressor K-100	centrifugal, 150 horsepower	2.6	600	1.49	2324	3984
Product Stream & Upgrading						
Mixer	MFG		100	1.12	112	192
Spliter TEE-100	MFG		100	1.12	112	192
Cooler II	stainless st	1.62	170	1.52	418.6	718
Cooler III	stainless st	1.62	170	1.52	418.6	718
Separator II	304 stainless st, 1000 gal		100	1.7	170	292
Storage Tank (Liquid concensed)	Mild st. 30Kgal	2	250	1.88	940	1611
Storage Tank (Out Feed I)	Mild st. 30Kgal	2	250	1.88	940	1611
Storage Tank (Out Feed II)	Mild st. 30Kgal	2	250	1.88	940	1611
Storage Tank (Water)	Mild st. 30Kgal	2	250	1.88	940	1611
Total						**46600**
Construction expense	Construction, engineering	30%				14000
	Contractors fee	10%				4660
Total						**65110**
Total onsite facilities						65110
Offsite facilities		10%				6511
Start-up cost		5%				3256
Working Capital		15%				9767
Total Capital Investment						**84650**

A.23 Capital cost of the Case G